

Plankton Dynamics and Distribution in the Eastern Mediterranean Sea

Dissertation
zur Erlangung des Doktorgrades
der Mathematisch-Naturwissenschaftlichen Fakultät
der Christian-Albrechts-Universität
zu Kiel

vorgelegt von
Georgia Assimakopoulou

Kiel 2011

Referent: Prof. Dr. Franciscus Colijn

Korreferent: Prof. Dr. Ulrich Sommer

Tag der mündlichen Prüfung, 18 Oktober 2011

Zum Druck genehmigt Kiel, 10 Dezember 2011

Der Dekan

Δίνει ο μαΐστρος το πανί
Στη θάλασσα
Τα χάδια των μαλλιών
Στην ξεγνοιασιά του ονείρου του
Δροσιά-

*The northwest wind bestows the sail
To the sea
The hair's caress
In the insouciance of its dream
Dew – cool –*

*From Orientations (1940)
By **Odysseus Elytis***

Table of Contents

Chapter 1: General introduction	11
1.1. Theoretical background	11
1.2. Phytoplankton	12
1.3. Fronts	14
1.4. Role of autotrophic picoplankton	16
1.5. Study areas-General	18
1.5.1. North Aegean Sea	20
1.5.2. Saronikos Gulf	22
1.6. Thesis Objectives	24
1.6.1. Chapter 3	24
1.6.2. Chapter 4	24
1.6.3. Chapter 5	24
Chapter 2: Material and Methods	27
2.1. Sampling and Hydrography	27
2.2. Nutrients	27
2.3. Total and size fractionated chlorophyll α	28
2.4. Total and size fractionated primary production	29
2.5. Qualitative and quantitative analysis of phytoplankton	30
2.6. Flow cytometric analysis - Autotrophic picoeukaryotes	31
2.7. Population and biomass estimations	34
2.8. Biomass-specific primary productivity (P/B)	34
2.9. Growth rate	35
2.10. Data analysis	36
2.10.1. Statistical analysis	37
2.10.2. Multivariate analysis	38

Chapter 3: Seasonal differences in chlorophyll distribution and phytoplankton composition in a frontal region of the oligotrophic North Aegean Sea (Eastern Mediterranean) 41

Abstract 41

3.1. Introduction 42

3.2. Material and methods 43

3.2.1. Study area and sampling 43

3.2.2. Nutrients 44

3.2.3. Phytoplankton chlorophyll α 45

3.2.4. Phytoplankton populations 45

3.2.5. Integrated values calculations 45

3.2.6. Statistical analysis 46

3.3. Results 47

3.3.1. Physical, chemical and biological characteristics 47

3.3.2. Nutrient and phytoplanktonic biomass distribution 49

3.3.3. Nutrient ratios 49

3.3.4. Phytoplanktonic biomass 50

3.3.5. Phytoplankton community structure 52

3.4. Discussion 55

3.4.1. Hydrology 55

3.4.2. Nutrient distribution 55

3.4.3. Phytoplankton biomass distribution in relation to the frontal structure 56

Chapter 4: Dynamics of autotrophic picoplankton in the N. Aegean Sea 75

Abstract 75

4.1. Introduction 76

4.1.1. Study periods 79

4.2. Material and methods 79

4.2.1. Study area 79

4.2.2. Field sampling 79

4.2.3. Total and size fractionated chlorophyll α 81

4.2.4. Total and size fractionated primary production 81

4.2.5. Microplankton stock measurements 82

4.2.6. Biomass-specific primary productivity (P/B)	82
4.2.7. Growth rate calculations	82
4.2.8. Flow cytometry	83
4.2.9. Plankton conversion to biomass	83
4.2.10. Statistical analysis	83
4.3. Results	84
4.3.1. Hydrography	84
4.3.2. Nutrients	86
4.3.3. Size-fractionated chlorophyll α	87
4.3.4. Size-fractionated primary production	89
4.3.5. Picoplankton abundances	91
4.3.6. Phytoplankton community composition based on light microscopy	93
4.3.7. Autotrophic carbon biomass	94
4.3.8. Total and size fractionated C:Chl α –ratios	94
4.3.9. Phytoplankton growth rates	95
4.3.10. Carbon standing-stocks and production of autotrophic picophytoplankton	96
4.4. Discussion	96
4.4.1. Seasonal variability of Chl α concentration	96

**Chapter 5: Seasonal variability of autotrophic picoplankton
in the Saronikos**

	123
Abstract	123
5.1. Introduction	123
5.2. Material and methods	126
5.2.1. Study area	126
5.2.2. Field sampling	128
5.2.3. Total and size fractionated chlorophyll α	128
5.2.4. Flow cytometry	129
5.2.5. Plankton conversion to biomass	129
5.2.6. Statistical analysis	130
5.3. Results	130
5.3.1. Hydrography	130
5.3.2. Nutrients	132

5.3.3. Size-fractionated chlorophyll α	132
5.3.4. Picoplankton abundances	133
5.3.5. Biomass distribution over size classes	136
5.4. Discussion	137
Chapter 6: Conclusions	157
Chapter 7: References	161
CHAPTER 8: Zusammenfassung	177
CURRICULUM VITAE	181
ACKNOWLEDGEMENTS	185
ERKLÄRUNG	187

CHAPTER 1: General introduction

1.1 Theoretical background

Biological activity is closely linked to dynamical processes, which regulate the vertical supply of nutrients, and the movements of phytoplanktonic cells in the euphotic layer. Thus far the study of marine plankton has largely focused on growth rates of ecosystem components and how they affect biogeochemical cycles. In the ocean, intense primary production is usually coupled to hydrodynamic features that favour the replenishment of nutrients in the photic layer. For example, phytoplankton biomass often develops and accumulates in density fronts where nutrient enrichment of the surface layer may result either from tidal mixing (tidal fronts) or from the interaction between wind stress and internal tides (shelf-break fronts) (see reviews by Holligan 1981, Loder & Platt 1984, Lefèvre 1986, Legendre *et al.*, 1986). The breaking of large eddies can also inject nutrients from the mixed to the stratified side of these fronts (Bowman & Iverson 1978, Loder & Platt 1984, Lefèvre 1986).

Analysis of the functioning of ocean ecosystems requires an understanding of how the structure of the ecosystem is determined by interactions between physical, chemical and biological processes. Such analysis needs to consider the interactions across a wide range of spatial (approx. 10m–10000km) and temporal (minutes to centuries) scales, and across all trophic levels (primary producers to top predators; Murphy *et al.*, 1988; Angel, 1994). There are, however, few areas of the global ocean where there is sufficient knowledge to achieve such an integrated analysis (de Young *et al.*, 2004). Circulation patterns of the major ocean gyres, involve movement of water masses through very different climatic regimes which favour distinctly different groups of organisms (Longhurst 1998). Generating comprehensive views of the operation of oceanic ecosystems is complicated as a result of such heterogeneity in species distribution and ecosystem structure (Murphy *et al.*, 1988; Levin 1990; Longhurst 1998).

The upper water layers of the open oligotrophic ocean sustain plankton communities whose structure and functioning depend on complex interactions between physical, geochemical and biological processes. In particular, mesoscale hydrodynamic structures such as fronts, eddies and gyres control the biomass and primary production (McGillicuddy *et al.*, 1998) as well as phytoplankton composition (e.g. Rodriguez *et al.*, 2001; Vidussi *et al.*, 2001). Hydrodynamic structures and circulation can influence directly via vertical motion the phytoplankton size structure (Rodriguez *et al.*, 2001). At the same time hydrodynamic structures drive nutrients or modify the light environment and thus indirectly control phytoplankton biomass and composition (Vidussi *et al.*, 2001). We examined the distribution and the dynamic of picophytoplankton in contrasting oceanic and coastal ecosystems, and the seasonal changes of the pattern.

1.2. Phytoplankton

Pelagic microbial food web structure and functioning is to a large extent determined by the dominating primary producers. For example, in a system dominated by diatoms a large part of the primary production is channelled through the classical food web or lost from the system through sedimentation (Wassmann 1993; Heiskanen and Kononen 1994). Contrary, in systems dominated by unicellular cyanobacteria a large part of the energy and carbon will be processed within the microbial food web and recycled in the photic zone (Smetacek, 1985, 2002). The fate of the primary production (grazing, exudation, aggregate formation, sedimentation) seems to a large extent depend on cell size. In general high concentrations of micro sized plankton are connected to turbulent waters e.g. upwelling areas, fronts or spring and autumn mixed waters, while pico- and nanoplankton dominate in stagnant waters e.g. open sea areas or stratified waters during summer period stratification (Kjørboe 1993). Well mixed waters are characterized by high input of “new” nutrients resulting in high nutrient concentrations, while stratified water usually are characterized by regenerated nutrients and low nutrient concentrations (Legendre and Rassoulzadegan, 1995). If more nutrients are added to the system, the growth rate of small algae will increase until nutrient concentrations equal saturation levels. Still higher nutrient concentrations will allow large cells to be established. At saturated nutrient concentrations uptake is proportional to cell surface and there is no advantage in being small. The phytoplankton community

composition is also influenced by the elementary composition of the water. The size and activity of biological organisms are controlled through the availability of nitrogen and phosphorus. For the major elements C, N, and P, it is defined by the Redfield ratio: C:N:P = 106:16:1 (Redfield *et al.*, 1963). The transformations of the nutrients exerted by biological processes differ vertically in the ocean. Species with special requirements such as diatoms need a Si:N relationship of 1:1 (e.g. Harris 1986). A ratio > 25:1 is, however, needed for diatoms to be favoured over other algae (Sommer 1994).

Within the pelagic system prokaryotic and eukaryotic algae are the main primary producers. These phytoplankton vary more than 100-times in cell size from small picoplankton (0.2-2 μm) and nanoplankton (2-20 μm) to large microplankton (20-200 μm). The picoplankton fraction mainly consists of prokaryotes (unicellular cyanobacteria and *Prochlorococcus*), but also eukaryotes are included. In the nanoplankton fraction flagellates are common, while diatoms and dinoflagellates usually dominate the microplankton fraction. Biological activity is closely linked to dynamical processes, which regulate the vertical supply of nutrients, and the movements of phytoplanktonic cells in the euphotic layer. Thus far the study of marine plankton ecology has largely focussed on growth rates of ecosystem components and how they affect biogeochemical cycles.

Phytoplankton composition is considered as a natural bioindicator because of its complex and rapid responses to fluctuations of environmental conditions (Livingston, 2001). Major factors influencing phytoplankton production include light and nutrient availability (Underwood and Kromkamp, 1999). The limitation of light penetration by turbidity has been frequently cited as a factor controlling primary production (Pennock, 1985; Lehman, 1992). Recent attention has focused on regional climate and weather patterns that produce variation in nutrient concentrations, dissolved organic Matter (DOM) and suspended particulate matter (SPM) traceable to freshwater flow (Najar, 1999). Plankton has been used recently as an indicator to observe and understand global change because it seems to be strongly influenced by climatic features (Li *et al.*, 2000). Physical and other chemical factors such as temperature, salinity and the concentration of inorganic mineral nutrients (PO_4^{3-} , NO_3^-) are also involved in the modulation of chlorophyll and primary production (Cunha *et al.*, 2000). Unstable periods, which are represented by a situation of mixing of the water

column, cause an increase of nutrients, either by sediment resuspension or riverine water input (dependent on the seasonal cycle). The subsequent stratification period presents the necessary conditions to start phytoplankton growth. Variability is associated with frontal features and tide (Cloern *et al.*, 1984; Hood *et al.*, 1999); lateral gradients are driven by circulation (Malone *et al.*, 1986) and cause individual bloom forming species (Tyler *et al.*, 1982). The measurement of chlorophyll α is one of the methods for estimation of phytoplanktonic biomass.

It is well known that phytoplankton size distributions are related to phytoplankton biomass and the structure of food chains in the ocean (Kiørboe, 1990). For this reason, phytoplankton size distributions, and factors affecting the size distributions, such as variation in upwelling and nutrient levels, need to be studied and understood. It is seen that large phytoplankton dominates in areas of high and variable nutrient levels and high phytoplankton biomass, and smaller phytoplankton dominates in areas of lower and stable nutrient levels (Varela 1987; Morris 1980). Therefore, in open ocean conditions, smaller phytoplankton is usually prevalent, while in neritic waters, larger species make up a greater fraction of the phytoplankton population (Malone *et al.*, 1993).

1.3. Fronts

Frontal systems occur at a point where a stratified and mixed body of water meet. The resulting density gradient between the two bodies of water means that a flux of nutrients occurs from the mixed water mass to the nutrient-depleted upper stratified waters of the adjacent water mass.

Over the world ocean, frontal zones are always the areas of productivity and phytoplankton biomass enhancements (Franks, 1992). Oceanic fronts are complex fluid structures often characterized by sharp sea-surface gradients in density, temperature, and/or salinity. Frontal phenomena include, but are not limited to, boundaries between different water masses. Distributed throughout the world's oceans, fronts occur at multiple spatial scales and have highly variable kinematics and flow fields (Fedorov, 1986). Oceanic fronts support high levels of biotic activity across a wide range of trophic levels (reviewed by Lefèvre, 1986, Olson *et*

al., 1994). Frontal enrichment or concentration has been documented in a wide variety of marine plankton, including microbes (e.g. Floodgate *et al.*, 1981, Fernandez *et al.*, 1994), phytoplankton (e.g. Iverson *et al.*, 1979, Franks 1992a, Laubscher *et al.*, 1993, Yoder *et al.*, 1993), and zooplankton (e.g. Smith *et al.* 1986, Epifanio 1987).

A biological feature associated with many fronts in the ocean is a subsurface patch of enhanced chlorophyll biomass on the stratified side of the front. Such features have been seen at tidal fronts (e.g., Holligan, 1981; Pingree *et al.*, 1978), shelf-break fronts (e.g., Houghton and Marra, 1983); wind-driven upwelling fronts (e.g., Traganza *et al.*, 1987; Small and Menzies, 1981), eastern boundary currents (e.g., Hood *et al.*, 1991; Washburn *et al.*, 1991); western boundary currents (e.g., Lohrenz *et al.*, 1993; Hitchcock *et al.*, 1993) and the Almeria-Oran front of the Mediterranean (Claustre *et al.*, 1994a, b; Prieur and Sournia, 1994). The processes invoked to account for the formation and maintenance of such patches are diverse, and include: subduction of surface populations (Hood *et al.*, 1991; Claustre *et al.*, 1994; Lohrenz *et al.*, 1993; Washburn *et al.*, 1991); physical accumulation (e.g., Boucher *et al.*, 1987; Franks, 1992b); enhanced growth in response to diapycnal or isopycnal nutrient fluxes (Yentsch, 1974; Hitchcock *et al.* 1993; Holligan *et al.*, 1984; Traganza *et al.*, 1987); photoadaptation (Hood *et al.*, 1991; Claustre *et al.*, 1994b); and reduced grazing stress (e.g., Holligan *et al.*, 1984; Mitchell-Innes and Walker, 1991).

Numerous factors controlling phytoplankton blooms in the frontal zones have been considered: strong water stratification due to the cross-frontal circulation (Laubscher *et al.*, 1993; Bradford-Grieve *et al.*, 1997; Strass *et al.*, 2002), passive transport of cells (Van Ballegooyen *et al.*, 1994), transport of nutrients into the surrounding environment by eddies moving across fronts (Froneman *et al.*, 1999; Read *et al.*, 2000).

However, due to the complexity of frontal physics, spatial and temporal variability in phytoplankton community abundance and biomass size structure may occur. In contrast to microphytoplankton responsible for large accumulation of biomass during austral summer, the biomass of picoplankton and nanoplankton fluctuates slightly during the year. The dominance of pico- and nano sized phytoplankton in the different frontal zones of the South Ocean has been documented for spring and winter (Laubscher *et al.*, 1993; Bradford-Grieve

et al., 1997; Fiala *et al.*, 1998 a, b; Froneman *et al.*, 1999). Autotrophic cyanobacteria belonging to the genera *Synechococcus* and *Prochlorococcus* are an important component of the marine plankton. Picoplankton communities are most efficiently enumerated by flow cytometry. *Synechococcus* and *Prochlorococcus* which have different pigment compositions are distinguished by their fluorescence and light scatter signatures. Knowledge of the relative contribution of different size fractions to the total biomass and primary production is of great importance for understanding the trophic organization and community structure of pelagic ecosystems.

A finding common to all physical-biological studies of fronts is that phytoplankton production is strongly linked to physical forcing at time scales of weeks to months (e.g., Gulf Stream meanders, Hitchcock *et al.*, 1993; Lohrenz *et al.*, 1993; and by jets of the coastal transition zone, (Washburn *et al.*, 1991; Hood *et al.*, 1991). However, the importance of transient events (days) to the phytoplankton dynamics at fronts is beginning to be recognized (e.g., Claustre *et al.*, 1994b). Short time and space scale physical processes, for example wind events, can excite nonlinear phenomena which decouple biological trophic interactions. Such decouplings may lead to transient states in which the phytoplankton can show unusually high net production rates, leading to an amplification of phytoplankton patchiness at fronts.

1.4. Role of autotrophic picoplankton

In recent years, existing views on the structure and function of pelagic ecosystems have been changing profoundly mainly because of the recent discovery of picoplankton (Johnson and Sieburth, 1979; Waterbury *et al.*, 1979) and its importance in the pelagic food web (Gomes *et al.*, 1992) of the oceans (Azam *et al.*, 1983; Li and Platt, 1987; Shapiro and Guillard, 1987; Stockner, 1988). Picoplankton is composed of organisms between 0.2-2 μ m, including Archaea, Bacteria, *Synechococcus sp.*, *Prochlorococcus sp.* and other picophytoplankton. Nanoplankton (2-20 μ m) includes autotrophic Nano-Flagellates (ANF) and Heterotrophic Nano-Flagellates (HNF). Microplankton (20-200 μ m) includes Centric or Pennate Diatoms, autotrophic-, and heterotrophic microflagellates. These groups are major components of the microbial loop at the base of the food chain. Bacteria can account for

30% of total production. Photosynthetic picoplankton can account for >50% of primary production and may dominate biomass. Picoplankton can cycle nutrients and carbon at fast rates (e.g. cycling amino acid pools in a few hours). Photosynthetic prokaryotes evolving oxygen are a major component of oceanic (Partensky *et al.*, 1999) ecosystems. The diversity of these micro-organisms in the picoplanktonic fraction of open oceans appears to be very limited, since they are represented almost exclusively by two genera: *Synechococcus* and *Prochlorococcus*. *Synechococcus* is virtually ubiquitous in all marine environments. It is much more abundant in nutrient-rich than in oligotrophic areas and its distribution is generally restricted to the upper well-illuminated layer. *Synechococcus* has also been reported at fairly high abundances from environments with low salinities and (or) low temperatures. In contrast *Prochlorococcus* appears to be less ubiquitous. However it is by far the most abundant group in the central oligotrophic part of oceans. Moreover, these organisms are generally restricted to oligotrophic areas, but can be found in mesotrophic conditions as well. Another peculiarity of this organism is its ability to colonize the water column to depths of 150-200m, which are reached by less than 0.1% of the surface irradiance. Thus, although *Synechococcus* and *Prochlorococcus* often co-occur, they have different types of adaptation with regard to biogeochemical conditions. *Synechococcus* is easily distinguishable by fluorescence techniques due to the intense orange fluorescence emitted by its phycoerythrin under blue light (Waterbury *et al.*, 1979; Murphy & Haugen, 1985; Olson *et al.*, 1988). *Prochlorococcus* differs from *Synechococcus* by virtue of its smaller size and very low or lack of orange fluorescence (Chisholm *et al.*, 1988, 1992; Hess *et al.*, 1996). Planktonic cyanobacteria (*Synechococcus sp.*) are known to be major contributors of photosynthetic biomass (Agawin & Agustí, 1997) in the open sea (Waterbury *et al.*, 1979; Glover *et al.*, 1985), especially in the more oligotrophic regions (Stockner, 1988) such as the Mediterranean Sea (cf. Magazzu and Decembrini, 1995). Their distribution is associated with water column stratification, being most abundant at the beginning or during the summer stratification and sparse during the rest of the year, when the water column is not strongly stratified (Ferrier-Pages and Rassoulzadegan, 1994; Bustillos-Guzman *et al.*, 1995). At a coastal station in the Ligurian Sea (NW Mediterranean) (Bustillos-Guzman *et al.*, 1995) and in the Eastern Mediterranean Sea (Li *et al.*, 1993), cyanobacterial abundance was found to be highest in the upper surface waters. In oceanic stations in the NW Mediterranean (along a transect from Barcelona to the Balearic Islands), the abundance of cyanobacteria (*Synechococcus sp.*)

during summer, when a stable thermocline results in the occurrence of a subsurface (50-70 m) chlorophyll α maximum (hereafter DCM; Estrada *et al.*, 1993), is generally higher in the DCM than in the upper layers (Delgado *et al.*, 1992; Latasa *et al.*, 1992), although this pattern may not be consistent between years (Algarra and Vaque, 1989). Prochlorophytes, which have recently been reported to contribute equally to the total winter prokaryotic phytoplankton biomass in the NW Mediterranean as cyanobacteria (Vaulot *et al.*, 1990), are closely associated with stratified waters and accumulate at the bottom of the photic zone in coastal waters (Bustillos-Guzman *et al.*, 1995), although they are also present during well-mixed conditions (Vaulot *et al.*, 1990). However, they occur only in a site south of these stations in the NW Mediterranean (off Blanes Bay, NE Spain).

1.5. Study areas-General

The Mediterranean is an ideal region to study physical-biological relationships as different hydrodynamic structures (mesoscale of 10-100 km) occur at relative small scales which can be simultaneously sampled for physical and biological parameters (Claustre *et al.*, 1994; Rodriguez *et al.*, 2001; Vidussi *et al.*, 2001). The general Mediterranean circulation is characterized by an inflow of Atlantic Water (AW) at the surface and a non return westward deeper flow of the dominant water mass of the Mediterranean, the Levantine Intermediate Water (LIW), into the Atlantic Ocean.

As a consequence the Mediterranean is potentially oligotrophic because of the inflow of generally nutrient poor Atlantic surface waters. However, the LIW is known to play an important role in transporting inorganic nutrients around the basin and further on in the Atlantic Ocean (Béthoux, 1979). In fact the LIW affects winter time dense water formation processes both in the eastern and western basin (Schlitzer *et al.*, 1991; Leaman and Schott, 1991), creating conditions of vertical transfer of nutrient rich intermediate/deep waters close to the surface for the biological consumption. This is the case for example in the north western Mediterranean where deep convection occurs during winter followed by spring phytoplankton bloom and further by oligotrophy in summer (Marty *et al.*, 2002). At the same time, in the eastern Mediterranean the thermohaline circulation and physical processes establish conditions of low nutrient content and low primary production (Azov,

1986, Psara *et al.*, 2000; Tselepides *et al.*, 2000). Thus the Mediterranean is considered as ultra-oligotrophic or mesotrophic system, depending on the studied area and the season (Berman *et al.*, 1984; Minas *et al.*, 1988; Conan *et al.*, 1998, Krom *et al.*, 2003, 2005). The high saline water of Mediterranean origin may affect water formation processes, variability, and even the stability of the global thermohaline equilibrium state. The Mediterranean circulation is forced by water exchange through the various straits, by wind stress, and by buoyancy flux at the surface due to freshwater and heat fluxes. The general circulation in the Mediterranean Sea is complex, and composed of three predominant and interacting spatial scales: basin scale (including the thermohaline (vertical) circulation), sub-basin scale, and mesoscale. In many previous studies, the extremely low nutrient levels (Betoux, 1989; Salihoglou *et al.*, 1990; Krom, Kress, Brenner & Gordon, 1991; Souvermezoglou, Pavlidou & Georgakopoulou, 1996); the low primary production, and impoverished phytoplankton populations (Berman, Azov, Schneller, Walline & Towensend, 1986; Dowidar, 1984; Kimor, Berman & Schneller, 1987); and low zooplankton standing stock (Pancucci-Papadopoulou *et al.*, 1992, Siokou-Frangou *et al.*, 2002, Theocharis & Georgopoulos, 1992) are mentioned. This marine area exhibits a strong seasonality, in its prevailing hydrographic and biological characteristics. A period of vertical mixing lasts approximately from October to April, and is followed by a period between late spring and early autumn of stratification of the water column, that is associated closely with the formation of a nitracline. In general, the upper part of the euphotic zone receives high irradiance, but is very poor in nutrients; in the deeper waters, nutrients are available but illumination is poor (Gotsis *et al.*, 1999). One of the most typical features of the phytoplankton distribution in the Mediterranean is the occurrence of a Deep Chlorophyll Maximum (DCM) during a large part of the year, when there is a certain degree of stratification of the water column. This DCM results from the accumulation of actively growing biomass and increased pigment content per cell due to photoacclimation (Estrada, 1985b). These maxima usually form at the top of the nitracline (depth in which nutrients become available and light, although generally of the order of 1% that at surface, is still sufficient for growth) and well below the zone of the maximum vertical gradient of the thermocline, or the pycnocline, which acts as a barrier to the supply of nutrients from the deeper to the upper water (Oszoy, Hecht & Unluata, 1989). The reduced diffusion losses at the pycnocline contribute to the maintenance of the biomass peak. The presence of the DCM accentuates the strong vertical differentiation of the pelagic ecosystem

into a light- sufficient but nutrient-limited upper layer, based mainly on recycled production, and a nutrient sufficient but light-limited lower layer, where new production takes place (Herbland and Voituriez, 1979). These vertical patterns affect the structure of the trophic links among the diverse plankton components and are accompanied by changes in the relative importance of the microbial versus the classical, zooplankton-based, food web. In addition, sporadic enrichment events at the nutricline level may superimpose considerable horizontal patchiness on the elevated phytoplankton concentration background of the DCM (Estrada, 1985a; Latasa *et al.*, 1992). For example, in the summer of 1983, the phytoplankton of the DCM contributed up to 30% of the total primary production in the water column of the Catalano-Balearic Sea (Estrada, 1985a) and Eastern Mediterranean Sea (Gotsis-Skretas, Pagou, Christaki & Akepsimaidis, 1993a; Ediger & Yilmaz, 1996).

The Eastern Mediterranean (including the Aegean), is one of the world' s poorest seas (Ignatiades *et al.*, 2002) characterized by Azov (1991) as a “marine desert”, a concept based on the impoverished phytoplankton biomass and productivity levels mainly due to phosphorus deficiency (Berland *et al.*, 1980; Krom *et al.*, 1991). Investigations in the Mediterranean Sea (Dolan, 2000; Christaki *et al.*, 2001; Pitta *et al.*, 2001; Van Wambeke *et al.*, 2002) demonstrated a distinct longitudinal gradient of increasing oligotrophy from west to east (Ignatiades, 1969; Moutin and Raimbault, 2002) in terms of the biomass and production of bacteria, autotrophic picoplankton and nanoplankton as well as the standing stocks of ciliate communities. In the Eastern Mediterranean Sea, unlike in other ocean basins, phosphates, as opposite to nitrates, are considered to be the factor limiting phytoplankton growth (Berland *et al.*, 1980; Krom *et al.*, 1991, 1992; Tselepides *et al.*, 2000; Ignatiades *et al.*, 2002).

1.5.1. North Aegean Sea

The North Aegean Sea is a highly dynamic region because of the interaction of different water types. The N. Aegean Sea has large brackish water influences from adjacent inland seas (Black Sea) and circulation patterns with north flowing surface currents. It has a freshwater input from rivers and deep basins (1100m in the N. Aegean). Low salinity surface waters and the circulation patterns lead to deep plankton maxima (70-80m in the Aegean).Corresponding maximum nutrient values for the N. Aegean are $3.5 \mu\text{mol N l}^{-1}$ and

0.15 $\mu\text{mol P l}^{-1}$. Nevertheless the N. Aegean is the most nutrient rich area of the Aegean Sea. In summer phosphate values are usually undetectable in the N. Aegean and this is expected to lead to major differences in processes and fluxes between the two areas (North and South Aegean), such as primary production and vertical flux rates of particulate material to the benthic systems and nutrient cycling within the sediment. The North Aegean Sea (Fig.3.1) is connected through the Dardanelles Strait and, hence, through the Bosphorus strait, to the Black Sea. The Aegean Sea is connected with the Mediterranean Sea to the South, through the passages between Crete-Carpathos-Rhodos-Turkey (southeast) and Crete-Kithira-Peloponnesos (southwest) (Poulos *et al.*, 1977). The outflow of Black Sea Water (BSW) from the Dardanelles follows the periphery of the cyclonic gyre existing in the N. Aegean, deflecting branches in the Samothraki and Thermaikos plateau. During winter BSW flows westward mostly along the northern coast of Limnos island, where it then bifurcates to the south and north. During warm periods BSW after passing Dardanelles flows southward and its core appears south of Limnos Island. The result is a winter-spring distribution of colder brackish waters in the Northern and Western parts and warm higher salinity water (Levantine Water) in the south east (off Limnos). The intermediate and deep waters of the Aegean Sea are characterized by the lowest concentrations of nutrients and the highest concentration of oxygen when compared with those of the other main Mediterranean basins (Souvermezoglou, 1989). The salinity of the N. Aegean is between 34 and 38. The N. Aegean has clear water with extremely low attenuation coefficient. It is thus likely that not only primary production processes will be different but also behavioural differences. The N. Aegean has a high content of calcareous material, which is expected to lead to different rates and processes of nutrient recycling, and erosion, transport, deposition, accumulation of particulate matter and trace substances. Thus, the processes and rates of mineralization and material burial will vary. Recent developments in the field of deep-water formation in the eastern Mediterranean Sea have shown that water masses (the Cretan Intermediate Water), being formed in the southern Aegean Sea, leave through the Cretan Straits and sink in the deep layers of the adjacent south-eastern Ionian and north-western Levantine Seas (Theocharis *et al.*, 1992). In the northern Aegean, general circulation is cyclonic, (Georgopoulos *et al.*, 1992). The chlorophyll maximum at typical stations in the N. Aegean is at 70-80 m depth in summer with concentrations of only around 0.3-1 mg.l^{-1} (largest recorded value: 1.6 mg.l^{-1}) (Pagou *et al.*, 1998). During summer the water systems are

dominated by flagellates (small dinoflagellates and other flagellates) (Pagou *et al.*, 1988), whereas during spring the phytoplankton is dominated by small sized diatoms.

1.5.2. Saronikos Gulf

The Saronikos Gulf (Athina) receives primary treated wastewater of the central sewage outfall of Athens through a deep underwater outlet situated on Psittalia Island, at the inner part of Saronikos Gulf (Fig. 5.1), discharging primarily treated urban sewage. The disposal of the untreated domestic effluents from the Athens metropolitan area (5 million inhabitants) since 1950's has led to eutrophication phenomena in the naturally oligotrophic waters. Since 1994, with the construction of the sewage treatment plant on the small island of Psittalia, the effluents are subjected to a primary treatment and are disposed ($16 \text{ m}^3/\text{sec}$) through a V-shape duct situated at $\sim 63 \text{ m}$ depth below the sea surface. Since then the effects of the Psittalia sea outfalls on the ecosystem have been monitored regularly by the Hellenic Centre for Marine Research (HCMR) (Siokou-Fragou *et al.*, 1999, 2003). Saronikos Gulf is the marine gateway of the Athens metropolitan area and covers a total surface area of 1117 km^2 (Fig. 5.1). The gulf is separated into two basins by a shallow zone (inner Saronikos, depth $<100\text{m}$); the western basin with depths exceeding 400m and the eastern basin with depths around 100 and 200m . Furthermore, the Elefsis Bay situated to the north is separated from the gulf by two shallow sills. This bottom morphology influences the general water circulation. A considerable short-term variability has been observed in the circulation of the Saronikos gulf (Kontoyannis and Papadopoulos, 1999). The disposal of domestic sewage without visible effects into coastal waters is more difficult in the Mediterranean Sea than in most other seas as a result of the extreme oligotrophy found in the former. The Saronikos Gulf represents, in many ways, an excellent case for investigations of the effects of urban waste disposal into an oligotrophic marine environment. The untreated sewage effluent of Athens in the Keratsini Bay and the urbanization and industrial development of the area has affected the marine ecosystem of the Saronikos Gulf. Since 1968, we have investigated the effects of urban pollution on the eutrophication of this naturally oligotrophic marine ecosystem.

The Saronikos Gulf, which is taken to include Elefsis Bay, occupies an area of about 3000 km^2 , between the latitudes $37^{\circ}30'$ and $38^{\circ}05'N$ and longitudes $23^{\circ}00'$ and $24^{\circ}00'E$. It is divided into two parts by the Methanon Peninsula and the islands of Salamis and Aegina.

The deep waters to the east and west of this division are connected by shallower channels between the islands. There is a distinct change in sea bed level between the Inner and Outer areas of the eastern Gulf. Depths in the Outer Gulf are usually between 150 and 300 m, whereas those in the Inner Gulf are mostly 60-90 m. Previous work using hydrographic data (Coachman & Hopkins, 1975; Coachman *et al.*, 1976) or a wind driven model (Hopkins & Coachman, 1975) revealed the water masses and the circulation pattern in the Saronikos Gulf. Its flow field is wind driven and there are no appreciable tidal effects. The winds develop two circulation patterns, cyclonic and anticyclonic. During cyclonic circulation, the Aegean oligotrophic (Outer Gulf) water enters from the eastern side of Aegina, mixes with the water between Aegina and Salamis islands, exposes this mixture to the outfall effluents and moves it out to the southeast. The opposite occurs during anticyclonic circulation. Coachman & Hopkins (1975) and Friligos (1984a) reported that the upper waters in the Inner Saronikos Gulf underwent a well defined annual cycle of thermal stratification. From a minimum average temperature of about 14⁰C in February and March, the temperature rose to a maximum in July and August of about 25⁰C. The same authors indicated that the temperature of the deeper waters also increased to a maximum of about 16-18⁰C in October. Peak summer temperatures of the near surface waters of the Inner Saronikos Gulf recorded during the summer 1982 cruises again reached 26⁰C. On the other hand Saronikos Gulf is the marine area located between Attiki and Peloponissos and its southern border is positioned in the northern part of Saronikos Gulf; the semi-enclosed shallow area is connected with Saronikos Gulf through the eastern channel (12m depth) and the western channel (8m depth). The imaginary line between Salamina and Aigina islands divides the Western from the Eastern basin of Saronikos Gulf. The latter basin is divided in the inner Saronikos (above the imaginary line Aigina-Fleves) and outer Saronikos, which is in open connection with the Aegean Sea. Saronikos Gulf can be divided into four sampling areas: Elefsis Bay, Keratsini bay, Western basin, Inner Saronikos Gulf and Outer Saronikos Gulf. The differentiation between Elefsis bay and Keratsini bay, but also the oligotrophic conditions of the southern inner Saronikos gulf and the western basin, are in agreement with recent studies (Pagou & Assimakopoulou, 1999). Another interesting feature is that usually maximum chlorophyll α concentrations in the western and inner Saronikos gulf were recorded below 10m depth (Pagou, 1988). Saronikos gulf is a system that behaves as the open oligotrophic Aegean Sea.

1.6. Thesis Objectives

The main objective of this study is to analyze the dynamics of the phytoplankton in Eastern Mediterranean Sea. The goal is to identify patterns in phytoplankton biomass and community structure and to relate those patterns with changes in different water mass. Specifically, the aim of this study is to evaluate the phytoplankton dynamics and the environmental variability and to investigate the main environmental factors affecting phytoplankton structure. The main objective is divided into three different chapters:

1.6.1. Chapter 3

The aim of this work was: (1) to identify whether the hydrographic properties of the water column (stratification or frontal conditions) can be related to vertical and horizontal distribution of nutrients, chlorophyll α and phytoplankton populations, (2) to assess the spatial and seasonal variation of the biological parameters in a region of complex hydrography and to gather further insight into qualitative and quantitative changes in chlorophyll and phytoplankton standing stock in the upper water column, (3) to examine the ratios between nitrate, phosphate and silicate and their possible role as limiting factor for phytoplanktonic biomass.

1.6.2. Chapter 4

The aim of the present paper was to investigate the temporal and spatial distribution patterns of picophytoplankton species in a frontal area in northeast Aegean Sea. Chapter 4 focuses on the two most important periods of the pelagic cycle in temperate areas: the spring bloom and late summer. The spring bloom represents the most intense period with new production, while the late summer is the culmination of the pelagic cycle with a peak in zooplankton biomass often co-occurring with blooms of large dinoflagellates. We assess population dynamics of picophytoplankton groups (<2 μ m diameter; *Prochlorococcus*, *Synechococcus*, and picoeukaryotes).

1.6.3. Chapter 5

In this chapter the contribution of picophytoplankton to phytoplankton community structure in the Saronikos Gulf (Eastern Mediterranean Sea) is studied according to the work content

of the “Monitoring of the Saronikos Gulf ecosystem affected by the Psittalia Sea Outfalls” project. Furthermore, this chapter examines the dynamics of autotrophic picoplankton in a coastal system and the influence and consequences of enhanced anthropogenic nutrient emission to the coastal zone (anthropogenic eutrophication).

CHAPTER 2: Material and Methods

2.1. Sampling and hydrography

Based on the water mass classification given in the different chapters, the geographic distributions of the various surface layer water masses were determined for the purpose of relating phytoplankton features to water mass characteristics. Vertical profiles of temperature, pressure, conductivity salinity and *in-situ* fluorescence were performed using a SeaBird Electronics SBE 9/11+CTD-General Oceanics Rosette assembly with 10-l Niskin bottles. Water samples for nutrient analyses and biochemical measurements were collected from six depths corresponding to 100%, 46%, 38%, 13%, 5% and 0.6% of surface irradiance.

2.2. Nutrients

For the determination of dissolved inorganic nutrient concentrations (NO_2^- , NO_3^- , SiO_4^{4-} and PO_4^{3-}) samples were collected with the rosette from standard depths, in the whole water column. Samples for the determination of nutrients were collected in 100 ml polyethylene bottles and kept continuously under deep freeze (-20°C), until their analysis in the laboratory by an ALPEKEM Flow Solution III, autoanalyser. The methods described by (Strickland and Parsons (1968) and Bendschneider & Robinson (1952) for nitrate and nitrite concentrations ($[\text{NO}_3+\text{NO}_2]$) and Mullin and Riley (1955) for silicate (SiO_4^{4-}) were employed. The phosphates (PO_4^{3-}) were measured on board, with a Perkin Elmer Lambda 2S UV/VIS Spectrometer, according to the methods of Murphy and Riley (1962) and Koroleff (1969). The precision is estimated at $\pm 0.02\mu\text{M}$ for phosphate and $\pm 0.1\mu\text{M}$ for nitrate and silicate. For simplicity, in the text we will refer to nitrate+nitrite as nitrate. N/P ratios were calculated from ($\text{NO}_3^-+\text{NO}_2^-$)-N and PO_4^{3-} -P values. Nitracline depth was defined as the depth at which $[\text{NO}_3+\text{NO}_2]$ equals $0.1\mu\text{M}$ (Borgne *et al.*, 2002) and was used as an index inferring nitrate availability to

phytoplankton in upper water. It represents not only stock abundance of surface nitrate, but also the upward diffusion potential of deep nitrate.

2.3. Total and size fractionated chlorophyll α

Chlorophyll α concentration indicates the trophic level of the pelagic ecosystem. It is also a measure of the phytoplankton production potential. Though all autotrophic algae contain chlorophyll, the chlorophyll concentration need not be directly correlated with biomass; their relationship is affected, for instance, by illumination, nutrient concentrations and the species composition of the phytoplankton assemblage.

Size fractionation has been used by ecologists to describe, in relative terms, the distribution and structure of marine organisms in pelagic ecosystems. Sieburth *et al.*, 1978 used this approach to sort plankton into size categories dividing numerous trophic compartments of plankton by using a spectrum of size classes. We adapted the terminology of Sieburth to our sizes classes, namely, picoplankton (0.2 to 1.2 μ m), nanoplankton (1.2 to 3 μ m), and microplankton (>5 μ m). For chlorophyll α analysis, 1-2 liters of water collected from each sampling depth was filtered through polycarbonate Millipore filters were size fractionated with separate filtration through polycarbonate Millipore filters having porosities 0.2 μ m (total stock), 1.2 μ m and 3.0 μ m. The filters were stored at -20 $^{\circ}$ C until analysis in the laboratory by using the fluorometric method of Holm-Hansen *et al.*, (1965), EPA Method 445).

Chl α extraction was carried out by placing 10 ml of 90% acetone (Parsons *et al.*, 1984) and grinding until all pigments were extracted, and then centrifuged at 3600 rpm for 5 minutes. The supernatant is measured in a TURNER 00-AU-10 fluorometer (Holm-Hansen *et al.*, 1965), then acidified with 1 N HCl and remeasured to determine the phaeophytin concentrations (degradation product). The concentration in the natural water sample is reported in μ g/L. The calibration was conducted using pure chlorophyll α (Sigma) as a standard. Samples obtained at most of the stations and fluorescence data derived from the CTD were used to depict a more precise distribution of total integrated chlorophyll over the euphotic zone. Terminology used in this study regarding the chlorophyll α , primary production and phytoplankton population fractions, is as follows: total population: retention on the 0.2 μ m

porosity filter; picophytoplankton (0.2-1.2 μm retention on the 1.2 μm porosity filter; and nanophytoplankton (1.2-3.0 μm): retention on the 3.0 μm porosity filter. For some data analyses, phytoplankton size structure was further simplified into <3 μm and >3 μm size classes by combining measurements 0.2 and 3.0 μm filters (<3 μm) and the 2.0 and 3.0 μm filters (>3 μm). The results are expressed as mg m^{-3} (for each depth zone) and mg m^{-2} (integrated for the entire water column). Water-column integrated chl α was calculated down to 1% of photosynthetic irradiance depth through trapezoidal integration. The trapezoidal integration is based on the approximation of the area by looking at trapezoids associated with portions of the area (O'Reilly and Zetlin 1998). The vertical profiles of chlorophyll α pigment were vertically integrated over the water column to a depth of ~120 m (or bottom if <120m) to yield $\text{mg Chl } \alpha \text{ m}^{-2}$.

2.4. Total and size fractionated primary production

Phytoplankton primary production was estimated using the standard ^{14}C technique (Steemann-Nielsen, 1952) which has been modified according to Ignatiades (1988). The Underwater light attenuation was measured with a LI-COR 1800 Underwater Spectroradiometer down to 100-120m, which determines directly photosynthetically available radiation (PAR 400-720 nm) at different depths (depends from station depth) in the euphotic layer of water column (defined as 1% of surface PAR). Photosynthetically available radiation is defined as the quantum energy flux from the sun in the spectral range of 400-700 nm. It is expressed in $\mu\text{Einstein.m}^{-2}.\text{s}^{-1}$. The water samples of the ^{14}C incubation experiments were collected at depths, which corresponding to 100, 50, 25, 10, 5 and 1% of photosynthetic irradiance received at the surface To avoid light shock to the phytoplankton, water samples were kept in the dark and, following addition of tracer. Water from each sampled depth was transferred into 250 ml clear polycarbonate bottles (three lights and one dark for each depth); all bottles were cleaned following JGOFS protocols (IOC, 1994) to reduce trace metal contamination. Each bottle was inoculated with 1ml of 5 μCi (148 kBq) of $\text{NaH}^{14}\text{CO}_3$ (sodium bicarbonate, Amersham), and incubated *in situ* using a free-floating buoyed which allowed incubation at the depth from which samples were taken. The incubation rig was deployed at midday and recovered after ~ 2 hours. At the end of the incubations samples were fractionated by filtration through separate 3 μm , 1.2 μm and 0.2 μm

polycarbonate Millipore filters under low-vacuum pressure (<100mmHg). This filter type was chosen because the water passage is faster and the holes do not have sharp edges, which reduces cell damage during the filtration. Filters were placed in scintillation vials, acidified with 0.5N HCL to remove dissolved ^{14}C (inorganic C). Upon evaporation of the acid, 15ml liquid scintillation cocktail was added. The mixtures were refrigerated until analysis. Radiation of ^{14}C - taken up by phytoplankton was measured in a scintillation counter (Beckman Liquid Scintillation Counter, BECKMAN LS 6500), that used an internal standard for quenching. The conversion of radioactive counts to carbon turnover followed the method described by Steemann Nielsen (1952). Depth-integrated production was calculated by trapezoidal integration of the entire euphotic zone (0.6-100% surface irradiance) for the primary production (IPP) and expressed as ($\text{mgC}\cdot\text{m}^{-2}\cdot\text{day}^{-1}$). Daily production rates were calculated by extrapolating 2-h incubation rates to 24-h rates. The measured hourly carbon fixation rates were extrapolated to daily rates by assuming an effective day length of 12 h. For the calculation of primary production, two estimation procedures were used: first, the direct conversion of the values obtained from the measurement into the amount of carbon produced per hour and volume ($\text{mg C m}^{-3}\text{h}^{-1}$) and second, the conversion of these values into the daily production ($\text{mg C m}^{-3} \text{d}^{-1}$) by a factor of 24 assuming a constant production rate during day and night (Bienfang *et al.*, 1984).

2.5. Qualitative and quantitative analysis of phytoplankton

Water-column samples for microscopy were collected at various depths in the upper 100m from rosette bottles during standard hydrographic casts. Microscopic counts were conducted according to the sedimentation chamber technique (Utermöhl, 1958), using an inverted microscope. The Utermöhl technique is restricted to larger phytoplankton (cells >10 μm). Smaller cells will not settle quantitatively in the settling chambers because their specific weight, even after Lugol's iodine addition, is not sufficient. The assembly sedimentation chambers (10 and 25ml) (Utermöhl, 1958) are allowed to stay for 24 hrs on a levelled surface. During this time, larger phytoplankton cells sediment to the bottom of the assembly. From each sampling depth 100ml of seawater will be required for autotrophic nanoplankton and microplankton. Organisms were counted at magnifications of 200-640 according to the size of the organisms examined. The samples were viewed at 200 or 400X

magnification with an Olympus IX70 inverted microscope for the identification and enumeration of diatoms, dinoflagellates and autotrophic nanoflagellates species (Tomas, 1997). Cell abundances were determined under the inverted light microscope on 100ml settled volumes. Each sample was examined until at least 400 cells had been counted. Cell sizes of species were measured and their biovolume calculated from equivalent geometrical shapes (Edler 1979). Length and width measurements are be converted to biomass by applying appropriate geometric shapes and the most recent carbon conversion factors (e.g., Menden-Deur & Lessard 2000).

2.6. Flow cytometric analysis - Autotrophic picoeukaryotes

Flow cytometry (Fig. 2.1) was originally used to distinguish certain cells in liquid suspension without probes and now offers excellent counting statistics (Mackey *et al.*, 2002; Olson *et al.*, 1989; Veldhuis and Kraay 1990; Veldhuis and Kraay 2000). Identification of a cell is based on its visual characteristics. FCM measures cells in liquid suspension. Cells, are aligned by a fluid (sheath fluid) into a stream (Reckermann, M., personal communications; Marie *et al.*, 2005), onto which one or several light sources (laser) are focused. Cell abundances, taxonomic diversity and fluorescence signatures can be estimated. For these data we have directly related forward light scattering to cell size using empirically determined calibrations. In addition to cell size, forward light scattering is also influenced by cell refractive index and cell shape. For laboratory cultures of reasonably spherically shaped cells a strong correlation between FLS and cell size (Olson *et al.*, 1989; DuRand, 1995), despite small changes in refractive index (DuRand and Olson, 1998) has been observed (Fig.2.2). Each time a particle passes through the beam, it scatters light; angular intensity depends on the refractive index, size and shape of the particles. Moreover, if the particle contains a fluorescent compound whose absorption spectrum corresponds to the excitation source (e.g., blue light for chlorophyll), it emits fluorescence at a higher wavelength (e.g., red light for chlorophyll). These light pulses are detected by photodiodes or more often by photomultipliers and then converted to digital signals that are processed by a computer. Measurements rates vary between 10 and 10000 events per second. Chlorophyll α emits fluorescence light in far red (>630nm) end of the visible light spectrum, when excited by blue light (450-490nm). The photomultipliers were set up to quantify: the red fluorescence (RF) from Chl α

(wavelength>650nm), the orange fluorescence (OF) from phycoerythrin PE (564-606nm), and the green fluorescence (GF) from phycourobilin PUB (515-545nm), following Wood *et al.*, (1985) and Olson *et al.*, (1988). Basic components of a flow cytometer are the fluidic system, which carries the cell one by one to the illumination point; the excitation optics (lasers, mirrors, prisms and focussing lenses), which illuminates the cells as they pass the laser intercept point; the emission optics, which collects the specific fluorescent colours and light scatter signals emitted by the cells; and finally the electronic data processing, which allows the light pulses which are converted to voltages in the photomultipliers, for detection of forward scattered light according to population fluorescence and light scatter characteristics following Vaulot *et al.*, (1990) to be analyzed and processed by special software (Reckermann *et al.*, 1997, 2000)

Excitation optics: a laser, lenses to shape and focus the laser beam.

Collection optics: Collection lens to collect light emitted from the particle-laser beam interaction; system of optical mirror and filters.

8 Optical filters: FSC (488nm), SSC (488nm), FI1 (530nm), FL2 (575nm), FL3 (675nm), FL4 (660nm, Helium-Neon Laser), FL5 (630nm=SSC of 633nm-laser).

Lasers: Helium neon; air cooled; emits at 633nm in the red region; the argon laser was turned (emitted) at 488nm at power-15mW to excite the pigments of autotrophic cells.

Beads: Polymer Microspheres, Beads 0.961µm ø red fluorescing for 488nm excitation (blue Laser); Molecular Probes Beads 2.5µm ø for 633nm excitation (red Laser).

Thus, a characteristic combination of optical properties can be recorded for every individual cell. Each of the recorded optical properties stands for a characteristic quality of the cell, e.g. FSC is correlated with cell size, SSC more to surface and internal structure (granularity). Flow cytometers are equipped with a sheath liquid (buffer, distilled water, seawater) that carries the cells through the instrument; another tank collects the waste fluid. When a cell or particles passes through a forward laser beam, laser light is scattered in all directions. The light that scatters axially to the laser beam is called Forward scatter (FSC-180⁰), it represents differences in size of the cells or particles. The light that scatters perpendicularly to the laser beam is called side scatter (SSC-90⁰) and represents differences in internal complexity or granularity of the cells or particles. Both parameters are related to cell size, but the side

scatter is more influenced by the cell surface and internal cellular structure (Morel, 1991, Green *et al.*, 2003). The single cell analysis was run with a FACScan flow cytometry (Becton-Dickinson) equipped with argon laser and photomultipliers. The argon laser was turned (emitted) at 488nm at power-15mW to excite the pigments of autotrophic cells (Gasol and del Giorgio, 2000). Cell populations (*Prochlorococcus*, *Synechococcus*, picoeukaryotic algae) were distinguished by differences in forward-angle light scatter (FSC) and fluorescence emission. *Prochlorococcus* (*Pro*) showed small size (FSC) and red fluorescence. *Prochlorococcus* have a lower FL3 signal and no FL2 signal (Fig. 2.3). *Synechococcus* spp. (*Syn*) was identified based on orange fluorescence and small size. *Synechococcus* cells were detected by their signature in a plot of orange fluorescence (FL2) versus red fluorescence (FL3). Larger photosynthetic eukaryotes (*Peuks*) displayed greater light-scatter and red fluorescence. Autotrophic picoeukaryotes have higher FL3 signals and no FL2 signal. Running time of samples on FCM was about 5 to 10 minutes (flow mode and time depending on the abundance of the cells analyzed). Digital data are transmitted to a computer that displays and records the results. Data can be further processed to discriminate specific cell populations and estimate their cell concentration and average cellular parameters using software provided with programs such as the Windows Multiple Document Interface software (WinMDI) (freeware) designed by J. Trotter (1993-1998) to analyse flow cytometric listmode data files. For each cell, five signals (Blanchot *et al.*, 1996) were recorded on 4-decade logarithmic scales: two light scatter (side scatter, SSC, and forward light scatter, FLS), and three fluorescences.

Flow cytometric cell abundances were estimated using a Becton Dickinson FACS flow cytometer (FTZ, Reckermann, pers. communication). The combination of fluorescence signals (phycoerythrin and chl α) with measurements of forward- and side-light scatter, allowed the enumeration of cyanobacteria (*Synechococcus*) and eukaryotic phytoplankton (Chisholm *et al.*, 1988; Olson *et al.*, 1990; Li *et al.*, 1992). The latter was sub-divided into two size classes by attractors, where the smaller cells were classified as picoplankton and the bigger cells were referred to as nanoplankton. Each individual signal was stored in 'list mode' and analyzed with WinMidi software (Reckermann *et al.*, 1997, 2000).

2.7. Population and biomass estimations

Phytoplankton biomass and primary production are commonly used to indicate trophic status. Total phytoplankton biomass was determined by chlorophyll α concentration in samples. To compare autotrophic pico- and phytoplankton biomass (APP) biomass with autotrophic primary productivity in similar units it was necessary to also determine APP biomass in terms of organic carbon content.

In the study of pelagic ecosystems, the carbon (C) biomass of the assemblage as a whole, or of individual trophic levels, is frequently of interest (Montagnes *et al.*, 1994). The use of microscope analysis in combination with published C:volume relationships is a common method of determining the C biomass of phytoplankton or other microbial organisms from field samples, and is the only method that can resolve biomass estimates to species level (Montagnes *et al.*, 1994). The cell biovolume of each species was also estimated from the appropriate equations for cell shape according to the method of Hillebrand (Hillebrand *et al.*, 1999) and converted to biomass by applying the most recent carbon conversion factors (e.g., Menden-Deur & Lessard 2000).

Cell biovolume (BV, μm^3) was converted to cellular carbon content through recommended carbon conversion equations using the following carbon to volume relationships (Menden-Deur & Lessard 2000): for small diatoms ($<3000\mu\text{m}^3$), $\text{C.cell}^{-1}=0.288\times\text{BV}^{0.811}$, for large diatoms ($>3000\mu\text{m}^3$), $\text{C.cell}^{-1}=0.117\times\text{V}^{0.881}$, for prymnesiophytes; $\text{C.cell}^{-1}=0.228\times\text{V}^{0.899}$; for dinoflagellates, $\text{C.cell}^{-1}=0.444\times\text{BV}^{0.864}$ and for chrysophytes, $\text{C.cell}^{-1}=0.020\times\text{BV}^{1.218}$; with BV representing total cell volume (μm^3) and C the estimated cellular carbon content (pg). *Prochlorococcus*, *Synechococcus*, photosynthetic eukaryotes (*Peuks*) cell numbers were directly converted to biomass with conversion factors (53 fg C cell⁻¹, 250 fg C cell⁻¹ and 2100 fg C.cell⁻¹, respectively) (Kana and Glibert, 1987; Campbell *et al.*, 1994).

2.8. Biomass-specific primary productivity (P/B)

The Chl α :C ratio is used for convert chlorophyll α biomass into phytoplankton carbon. This ratio is known (Fahnenstiel *et al.*, 1989; Geider, 1987) to vary as a function of the light climate (algal cells contain less chlorophyll a in high light conditions, i.e. Chl α :C is high), and

can be influenced by nutrient, especially N, availability. The biomass-specific primary productivity (P/B , $\mu\text{g C } (\mu\text{g Chl } \alpha)^{-1} \text{ h}^{-1}$) was calculated as the carbon fixation (P) per unit of chlorophyll α biomass (B). The calculated chlorophyll α concentrations were used to normalize the values of primary production to formulate the ratio of photosynthetic rate (*carbon uptake*) per unit volume to chlorophyll concentration. This is called the assimilation number. Under conditions of balanced community growth, the rate of ^{14}C incorporation into chl α equals the rate of C incorporation into total community biomass (i.e. the C-specific growth rate). Measurements with phytoplankton grown in culture show that $\text{Chl}\alpha:\text{C}$ is highly variable, ranging from 0.003 (Falkowski *et al.*, 1985) to $>0.1 \text{ mg Chl}\alpha (\text{mgC})^{-1}$ (Geider, 1987). This variability includes adaptive responses to ambient light, temperature, and nutrient conditions. Although $\text{Chl}\alpha:\text{C}$ is a sensitive indicator of algal physiological condition and growth rate in the laboratory, there is no unique relation between growth rate and $\text{Chl}\alpha:\text{C}$. For example, Laws and Bannister (1980) demonstrated that different functional relations exist between $\text{Chl}\alpha:\text{C}$ and growth rate, depending on whether phytoplankton are grown under conditions of nutrient limitation. The use of Chl α and C content estimates are dependent on conversion factors. These conversion factors vary with different studies (Riemann *et al.*, 1990). Total autotrophic biomass was derived from chlorophyll concentrations by assuming a carbon to chlorophyll a conversion factor ($\text{Chl}\alpha:\text{C}$) of 50. A similar factor has been widely used by many authors (e.g., Li *et al.*, 1992; Gasol *et al.*, 1997; Bode *et al.*, 2001), although it probably represents a minimum threshold, since the ratio may be close to 100 in oligotrophic open-ocean systems (Welschmeyer and Lorenzen, 1984; Hewes *et al.*, 1990; Verity *et al.*, 1996; Buck *et al.*, 1996).

2.9. Growth rate

A fundamental aim in biological oceanography is to predict the abundance of organisms and their temporal change (Banse, 2002). Many direct and indirect methodologies of varying accuracy have been used to estimate phytoplankton growth rate, μ (day^{-1}). According to Kirchman (2002), the most appropriate approach for estimating μ of microbial assemblages is the simplest, that is, dividing the production rate by the biomass estimate (B). This ratio called the “*specific uptake rate*” is a carbon (C) based measurement of μ corresponding to the cell specific or biomass specific uptake of C (Lipschultz, 1995; Dickson and Wheeler,

1995; Ducklow, 2000). The specific growth rate of phytoplankton (μ) is hard to measure *in situ*. Conceptually, it is the biomass-normalized, instantaneous rate of biomass increase of a species or assemblage in the absence of losses. Phyto- and picoplankton growth rates (μ) were estimated using the primary production data (in $\mu\text{gC l}^{-1} \text{d}^{-1}$) and the phyto- and picoplankton biomass values (in $\mu\text{gC l}^{-1} \text{d}^{-1}$) derived from the chlorophyll concentration and the carbon to chlorophyll conversion factors. Transformation of productivity and biomass into population growth rate requires a conversion factor between these different units of measurement—the cellular ratio of chlorophyll α to carbon, Chl α :C by various autotrophic biomass (AB) estimators such as chlorophyll α (Chl α), carbon content using microscopy or flow cytometry measurements (Eppley, 1972; Vadstein *et al.*, 1988; Malone *et al.*, 1993; Marañon *et al.*, 2000, 2005; Moreira-Turcq, 2001).

In order to estimate the specific growth rate (μ) of phytoplankton in the study area, we combined the measurements of primary productivity and chlorophyll α integrated over the top 100m. The first step was to convert the chlorophyll α measurements into estimates of algal biomass using a carbon to chlorophyll (Chl α :C) ratio. Productivity was then divided by the standing stock of algal carbon to yield a μ expressed in units of h^{-1} or day^{-1} . Picophytoplankton specific growth rate (μ , day^{-1}) averaged for the euphotic layer were calculated from integrated primary production and biomass values (Morán, 2007). Combining C uptake rates with size fractionations, we determined the specific uptake rate in three size fractions corresponding to picophytoplankton and nano-microphytoplankton (0.2–2; 2–5 and $>5 \mu\text{m}$, respectively). Phytoplankton μ estimates vary widely from values of around $0.1\text{--}0.3 \text{d}^{-1}$ (Letelier *et al.*, 1996; Marañon *et al.*, 2000, 2005) to $1\text{--}2 \text{d}^{-1}$ (Laws *et al.*, 1987; Quevedo and Anadon, 2001).

2.10. Data analysis

Maps and hydrographic charts were performed with SURFERv7 and GRAPHERV7. All the statistical analyses were carried out using Statgraphics Centurion XV. With the exception of the percentages of picoplankton, all variables (phyto, pico abundances) were log-transformed in order to attain normality and homogeneity of variables. To normalize distributions and eliminate zero values, biomass values were transformed using the log

factor $\log_{10}(x+1)$. The flow cytometry data were analyzed with WinMidi software (FTZ, Reckermann, personal communications). The whole integrated values were calculated according to the classical trapezoidal method. All data were reported as means \pm SD.

2.10.1 Statistical analysis

Statistical analysis of research data often rests on assumptions about data measurement properties and the normality of data distributions, and many other features. These assumptions must be satisfied to make the data analysis legitimate. By contrast, nonparametric, or distribution-free, statistical methods can be used to evaluate group differences or the correlations among variables when research measurements are in the form of categories or ranks. All calculations were performed after adequate transformation (logarithmic) of the data in order to obtain approximate normal distributions.

Differences between average concentrations found at various stations were detected by 1-way ANOVA if the data passed normality test. In that case, average concentrations are the arithmetic means (Sokal & Rohlf 1995). However, the majority of data was not distributed normally and therefore variances were analyzed by Kruskal-Wallis 1-way analysis on ranks. Hence, the medians serve as average values. High values of the test statistics F from 1-way ANOVA and H of Kruskal-Wallis ANOVA on ranks indicate differences in average values across stations. A critical p-value of <0.05 was always applied. The all pair wise multiple comparison Student-Newman-Keuls method was used to isolate the significantly differing values. Data were arcsin- or square root-transformed as necessary prior to analysis.

Correlation analyses among the variables were performed according to Pearson's product-moment correlation coefficients. A one way ANOVA test was used to test for statistical differences in the measured physical and chemical variables and the monthly average phytoplankton biomass among sampling dates and stations. Two way analysis of variance was performed to test the effects of season and stations on the biomass. Multiple regressions were used for evaluating the relationships between the abundance of the most dominant phytoplankton species, environmental and nutrient variables and examine spatio-temporal relationships among water quality parameters at each collection site.

Pearson product-moment correlation was used to determine the degree of association between variables. Linear regressions were used to estimate the relationship of one variable to another. The simple Pearson correlation coefficient was used to test the effects of environmental parameters (temperature, salinity, and chlorophyll α) on primary production. This is a parametric measure of association, ranging from + 1 to -1 for two continuous random variables.

2.10.2. Multivariate analysis

The multivariate statistical analysis was performed with the PRIMERv5 (Plymouth Routines in Multivariate Ecological Research) program developed at the Plymouth Marine Laboratory. Cluster analysis was performed in order to explore similarities between the sampled stations and groups. Hierarchical agglomerative clustering was applied to differentiate the phytoplankton communities using the Bray-Curtis Index. The complete linkage method was used to obtain strong separations of the groupings. Distinct station groups were identified in a dendrogram. To show differences in the vertical composition of the phytoplankton among normalized sample profiles a non-metric multi-dimensional scaling plot (MDS) was created from a similarity matrix. All depth strata from the sampling profiles of the stations with phytoplankton counts were included. Cluster analysis using single linkage and the Euclidean distance metric (Wilkinson, 1993), was performed in order to explore similarities between the sampled stations, depths and phytoplankton groups.



Figure 2.1.: Becton Dickinson FacsVantage (Flowcytometer) in **Research and Technology Centre (FTZ), Working Group Applied Physics/ Marine Technology (APM)**. The specification of the system: Argon ion plasma laser (488 nm) and an HeNe-Laser (633 nm) for the excitation, 3 scatter and 4 fluorescence detectors on the emission side, sort head implemented.

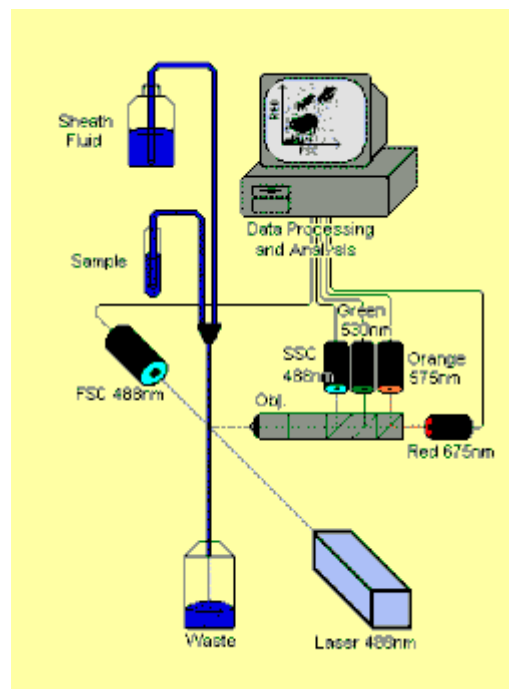


Figure 2.2.: Sketch of a standard flow cytometer with its principal components. (according Reckermann, 2000). Reckermann M. (2000): Flow sorting in aquatic ecology. In *Aquatic flow cytometry: Achievements and Prospects*, Reckermann M. and Colijn F. (eds.), *SCI. MAR.* 64 (2): Pages 235-246.

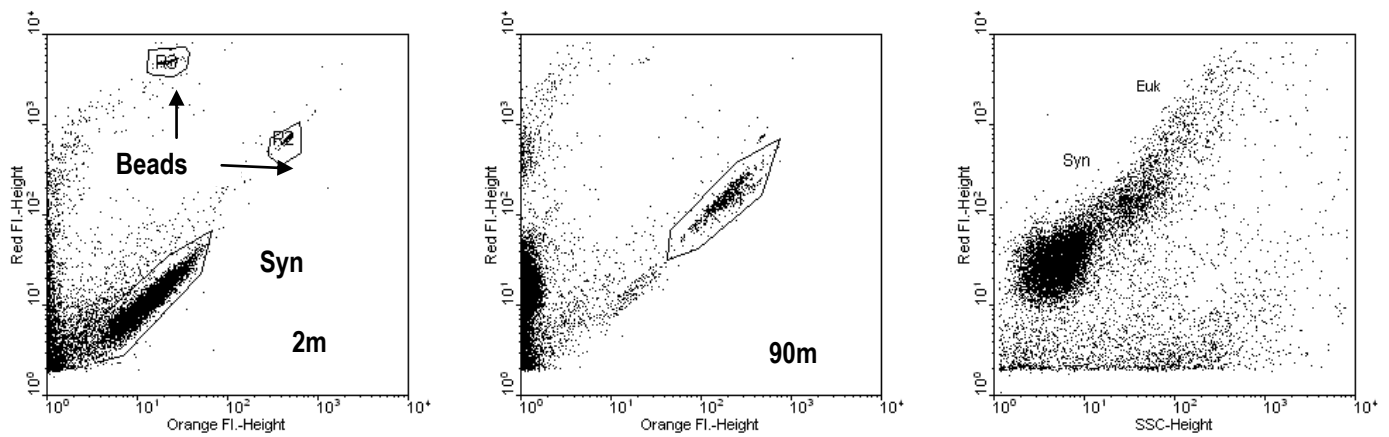


Figure 2.3.: Characteristic of flow cytometric signatures of the main groups of *Synechococcus* and eukaryotes (pico- and nanoplankton) in samples collected in the Aegean Sea (at different depths) analyzed using a FACSBeeton flow cytometer. The *Synechococcus* (*Syn*) group was discriminated using its high phycoerythrin orange autofluorescence. The eukaryotes groups were enumerated using a scatter plot of chlorophyll red autofluorescence versus side scatter. Beads 0.5 μm diameter, were used as an internal standard and these are shown. Arrows and polygon regions indicate the beads and dominant groups that were enumerated.

CHAPTER 3: Seasonal differences in chlorophyll distribution and phytoplankton composition in a frontal region of the oligotrophic North Aegean Sea (Eastern Mediterranean)

Assimakopoulou G.¹, Krasakopoulou, E.¹, K. Pagou.¹, Zervakis V.³, Georgopoulos D. ¹, Colijn F. ²

¹Institute of Oceanography, National Centre for Marine Research, P.O. Box 712, Anavyssos 19013, Greece

²Research- and Technology Centre Westcoast of Christian-Albrechts-University at Kiel, Germany

Abstract

The hydrography and plankton community structure was investigated in the North Aegean Sea. Variations in phytoplankton pigments and community composition were examined in relationship to water mass properties, characterised by the influence of the Black Sea waters and by the thermal stratification. Two cruises were conducted in 1998 with R/V *Aegeao* during June (spring) and September (late summer). Sampling was performed along a transect perpendicular to the shelf break, from the coast across the shelf into deep water. Chlorophyll α and nutrients were measured in the North Aegean Sea, during the INTERREG project "Infrastructure development for the monitoring of interregional pollution in the North Aegean Sea". The Aegean Sea constitutes an important area within the Mediterranean Sea due to its geographical position between the Black Sea and the main Eastern Mediterranean basin. The North Aegean receives large amounts of brackish water from the Black Sea, as well as the fresh waters from many of the rivers draining the Balkan Peninsula. Furthermore, the area consists of two shelf areas and discrete basins. Two chlorophyll maxima were observed, one in the upper 20m near the Dardanelles (well correlated to the Black Sea water), and a second deep chlorophyll maximum (DCM) at depths from 50 to 75m. The pattern of vertical distribution of chlorophyll was related to patterns of the physical

structure and nutrient concentrations during the beginning and the end of the warm period. Based on chlorophyll α data, a general oligotrophic character could be attributed to the area.

Keywords: Aegean Sea; Eastern Mediterranean; phytoplankton; chlorophyll; salinity; front

3.1 Introduction

The Aegean Sea is the north-eastern extension of the Mediterranean Sea and highly dynamic region, due to the interaction of different water masses. The hydrological characteristics of the North Aegean Sea have been described in detail by a number of investigators (Theocharis and Georgopoulos, 1993; Zervakis *et al.*, 2000). The north Aegean is characterized by an alternation of deep trenches and troughs, shallow shelves and sills. It receives the freshwater inputs from major rivers (Evros, Strymon, Nestos) discharging along the Greek and Turkish coastlines (Poulos *et al.*, 1997). The surface water circulation pattern of the Aegean Sea is not simple and regular, but changes temporally and seasonally due to many factors, such as: the high variability of the wind regime, the geomorphological configuration of the Aegean Sea basin, inflow of the lower temperature and salinity Black Sea Waters and rivers outflows (Poulos *et al.*, 1997). However, the most active dynamic features of the Aegean are the mesoscale cyclonic and anticyclonic eddies (Fig. 3.2). The most pronounced characteristic of the circulation in the North Aegean is the spreading of the BSW inflow from the Dardanelles (Zodiatis, 1994). A simple description of the BSW surface water route after exiting the Dardanelles is show in Figure 3.2. During the transitional period (spring) it follows a north-westward route and most of the BSW is captured by the permanent anticyclone that dominates the eastern part of the Sea of Thrace, and flows around the island of Samothraki (Fig. 3.2A). Whereas during stratification period (summer) a large portion of BSW flows south-westward and a significant proportion flows to the north of Limnos, follows a south-westward route along the western shores of Aegean and move cyclonically towards the South (Theocharis and Georgopoulos, 1993; Zervakis and Georgopoulos, 2002; Vlasenko *et al.*, 1996). A surface layer of light, brackish ($S \sim 30$) water is formed in the northeast Aegean by the inflow of modified Black Sea Water through the Dardanelles Straits; this water mass affects the uppermost (20-30m) layer of the North Aegean Sea (Theocharis and Georgopoulos, 1993). Thus, the North Aegean, and

especially the surroundings of the island of Limnos, is a region characterized by very strong thermohaline fronts and related jets, resulting in a clear pronounced heterogeneity of its ecological characters. The north Aegean Sea has been characterised oligotrophic, in terms of both primary productivity (Ignatiades *et al.*, 2002; Siokou *et al.*, 2002) and chlorophyll α concentrations. It exhibits significant horizontal variability in nutrient, chlorophyll concentrations and phytoplankton abundances. The Black Sea outflow in the north Aegean Sea has been found to be enriched in dissolved organic carbon and dissolved organic nitrogen (Polat and Turgul, 1996). The pattern of vertical distribution of chlorophyll was close to uniform throughout the basin, with a prominent deep chlorophyll maximum (DCM), which is characteristic of the oligotrophic Aegean Sea Water (of Levantine origin).

Moreover, at the stations near Dardanelles a small surface chlorophyll maximum was observed at 20m depth, well correlated with Black Sea waters, in agreement with the findings of the study of the physical characteristics (Zervakis & Georgopoulos, 2002). Deep chlorophyll maxima are characteristic features in the summer (Gotsis-Skretas, Pagou, Christaki & Akepsimaidis, 1993a; Ediger & Yilmaz, 1996). These maxima usually form at the top of nitracline and well below the zone of the maximum vertical gradient of the thermocline, or the pycnocline, which act as a barrier to the supply of nutrients from the deeper to the upper water (Oszoy, Hecht & Unluata, 1989). In some cases it has been reported, that changes in the composition of the planktonic communities occurring in the DCM and the upper layers (Cullen, 1982).

3.2 Material and methods

3.2.1. Study area and sampling

Based on the simultaneously acquired hydrological information and in order to achieve the objectives of this work, sea water sampling was performed during two oceanographic cruises undertaken in the north-eastern Aegean sea during two periods of: (a) relatively well mixed (spring) water column conditions, June 1998); (b) strong stratification (late summer-early autumn)-September 1998) on board of the R/V *Aegeao*. Samples were taken on selected transects crossing the frontal structures in the NE Aegean Sea, in the framework of the INTERREG project. To simplify analysis and to identify overall trends, sampling stations were

grouped according to the above hydrographic properties of the area, to represent the shelf water stations with a weak pycnocline receiving the freshwater outflows from various rivers, where more or less mixed conditions were expected (IR09, IR16, MNB6, MNB1) and oceanic (O-stations) waters which presented weak or no pycnocline (IR72, IR88), as well as the frontal area (F-stations), influenced from BSW (IR30, IR36, MNB5, IR43, IR50, MNB4, IR64), with strong pycnocline and separating shelf from oceanic waters (Fig. 3.1, Tab. 3.1). The maximum depth sampled for the most of the stations was ~ 100m and ~ 50m for stations IR09 and IR16.

Integrated values of physical, chemical and biological properties were estimated for the layers: 2-10m, 20-50m and 50-100m. The selection of the 0-20 m layer was based on the hydrological state of the Dardanelles outflow (BSW) which is characterized by a 20 km wide - 20m deep jet (Zervakis *et al.*, 1998). Hence, the 0-20m layer represented communities affected mostly by BSW. The spring sampling of June 1998 corresponds to an intermediate climatic situation, whereas the sampling of September 1998 corresponds to the hot summer season Poulos *et al.*, (1997). The methodological approach used for this study included the sampling of the following parameters:

- a. Measurements of hydrological parameters (temperature, salinity and nutrients concentrations).
- b. Phytoplankton chlorophyll α concentrations
- c. Estimation of phytoplankton abundance (cells.l⁻¹)

Vertical profiles of temperature, pressure, conductivity salinity and in-situ fluorescence were performed using Seabird Electronics SBE 9/11 CTD-General Oceanic Rosette assembly with 12 Niskin bottles with a volume of 8 liters.

3.2.2. Nutrients

For the determination of nutrient concentrations (NO_2^- , NO_3^- , SiO_4^{4-} and PO_4^{3-}), samples were collected with the rosette from standard depths, in the whole water column. Samples for the determination of nutrients were collected in 100 ml polyethylene bottles and kept continuously under deep freeze (-20°C), until their analysis in the laboratory by an ALPEKEM

Flow Solution III, autoanalyser. The methods described by Strickland and Parsons (1968) and Bendschneider & Robinson (1952) for nitrite and nitrate and Mullin and Riley (1955) for silicate were employed. The phosphates were measured on board, with a Perkin Elmer Lambda 2S UV/VIS Spectrometer, according to the methods of Murphy and Riley (1962) and Koroleff (1969). The precision is estimated at $\pm 0.02 \mu\text{M}$ for phosphate and $\pm 0.1 \mu\text{M}$ for nitrate and silicate. For simplicity, in the text we will refer to nitrate+nitrite as nitrate. N/P ratios were calculated from $(\text{NO}_3^- + \text{NO}_2^-)\text{-N}$ and $\text{PO}_4^{3-}\text{-P}$ values.

3.2.3. Phytoplankton chlorophyll α

Water samples for the determination of chlorophyll α were collected during routine, using a CTD rosette sampler, from standard depths (2, 10, 20, 50, 75, 100m) in the euphotic zone. Each station was initially surveyed by an in situ fluorometer (AQUATRACKA III CHELSEA Instruments) fitted on the CTD. Maximum fluorescence peaks from this profile were used to determine the sampling depths closest to the chlorophyll maxima, so that samples were always collected from these depths.

The relative fluorescence values were calibrated using the discrete water samples taken with the rosette and filtered through GF/F filters. There was a good linear correlation (June 1998 data set: $r^2=0.68$, $n=130$; September 1998 data set: $r^2=0.72$, $n=224$) between the fluorometer-determined chlorophyll fluorescence *in situ* and the chlorophyll α determined in the laboratory. For chlorophyll α analysis one or two liters of sea water from each sampling depth was filtered under a vacuum $<10\text{cmHg}$ through Whatman GF/F fibre filters ($\emptyset 47$ mm diameter). The filters were kept deep frozen at -20°C . Filters were ground in 90% acetone and extracted for 24h in the dark at 4°C . Fluorescence was measured in the laboratory with a TURNER 00-AU-10 fluorometer that had been calibrated with Sigma Chlorophyll α according to Holm-Hansen *et al.*, 1965 without acidification.

3.2.4. Phytoplankton populations

Samples for phytoplankton analysis (100ml) were preserved by adding Lugol and stored in dark bottles. The samples were kept in refrigerator until analysis, which was performed in sedimentation counting chambers of 25 ml, where each sample remained for 24 or 48 hours.

Phytoplankton analysis was carried out following the Utermöhl method (Utermöhl, 1958), using an inverted microscope (OLYMPUS) at X300 magnification. The samples were analyzed qualitatively (species/liter), and quantitatively (cells/liter) for the determination of following groups: diatoms, dinoflagellates, coccolithophores and silicoflagellates, “other groups”. All these groups together constitute the total microplankton (groups with cell diameter larger than 5µm). The group named “other groups” is constituted from specimen of Cryptophyceae, Haptophyceae, Chrysophyceae, etc., whose identification was possible. As a reference book for identification of the phytoplankton mainly Tomas (1997) was used.

3.2.5. Integrated values calculations

From the hydrographical casts of the sampled stations, vertically integrated chlorophyll α (total budget) or “mean integrated chlorophyll α ” concentrations, nutrients concentrations and phytoplankton abundances are given as depth-weighted averages (calculated by dividing the trapezoidal integration of measured values for each variable by the maximum sampling depth at each sampling location) according to Riley (1957) for comparison among stations.

3.2.6. Statistical analysis

The model of a one-way analysis of variance (ANOVA) was performed to test the significance of differences in abiotic and biotic variables among seasons, stations and layers followed by a pair-wise multiple comparison test (Kruskal-Wallis-test) to identify which groups were significantly different from the others. The significance level chosen (p) was 0.05. We used Pearson's correlation in order to examine the spatio-temporal relationships among environmental variables salinity, nitrate, phosphate, chlorophyll α , and phytoplankton. Pearson's correlation (r) measures the correlation between two environmental variables and reflects the degree of linear relationship between those two variables. Cluster analysis was performed in order to explore similarities between the sampled stations, depths and phytoplankton taxa. The analysis was performed with the PRIMER5 (Plymouth Routines in Multivariate Ecological Research) program developed at the Plymouth Marine Laboratory. MDS (multidimensional scaling) was used to analyze how sampling layers were similar in relation with the phytoplankton characteristics.

3.3. Results

3.3.1. Physical, chemical and biological characteristics

The hydrographic properties of the waters across the transect are shown in the following θ/S diagram: Figure 3.3 displays a typical T/S diagram with data collected across the transect throughout both cruises in the North Aegean, in spring (June 1998) and late summer (September 1998). Three water masses of the study area are shown in the T-S diagram (Fig. 3.3). Each type of water mass is characterised, with a characteristic temperature; salinity and density (Table 3.2). We see that there is a very strong change of density and T-S properties across the front, located in the neighbourhood of stations IR64, IR50, MNB4 and IR43.

The density of the surface layers varies from less than 23 kg m^{-3} north of the island of Limnos, to more than 28 kg m^{-3} at the southeast of the island. The southernmost part of transect is characterized by almost vertically homogeneous salinity, with high values (>39) characteristic of the South Aegean, while the northern part exhibits very low salinities (<32) indicating a large amount of water from the Black Sea at the surface. The deeper layers display very little horizontal variability, constituted mostly by water from the Levantine region (Zervakis and Georgopoulos, 2002). Criteria for location of the front were based on temperature and salinity characteristics of the upper 100m. Contour maps of horizontal distribution (Fig. 3.4 and 3.5) of salinity, temperature and chlorophyll distribution at surface and at depth of 50m represent descriptions of the dynamic characteristics of the region during both cruises. From detailed analyses of the parameters it can be seen that seasonality is evident in the physical characteristics of the means of temperatures and salinities in the upper 100m. The lowest water temperatures were observed in early spring and highest in summer. In the euphotic zone, the highest temperatures (19.44°C) were measured in September 1998 in the northern part of the transect (S-stations) (Fig. 3.4, Tab. 3.1), while lowest (17.15°C) were measured also at S-stations in June 1998 (Fig. 3.3, Tab. 3.1). In the euphotic zone, during spring, mean salinity varied from 36.04 (S-stations) to 38.72 (O-stations). Analysis of variance showed that all the considered environmental variables were statistically different between the stations ($P<0.05$) (Table 3.2).

Nitrate concentrations above $2.0\mu\text{mol/L}$ (Tab. 1), were encountered during spring at shelf stations, which situated either on the Samothraki or the Limnos Plateau. On the contrary in late summer nitrate concentrations do not exceed $1\mu\text{mol/L}$ and were generally lower at the frontal stations. Very low phosphate concentrations ($<0.08\mu\text{mol/L}$) were observed at all stations at both seasons, with irregular variations and a poorly defined seasonal cycle. Silicate values ranged from $2.13\mu\text{mol/L}$ (F-stations) in late summer, to maxima of $3.11\mu\text{mol/L}$ (S-stations) in June 1998. During both cruises, this band of relatively low salinity waters (<35) had intruded down to a depth of approximately 20m in the northern-eastern part of the transect, indicating a large amount of water from the Black Sea (Fig. 3.4 and 3.5) and from the various rivers.

A synthesis of the conditions in the area is given in Table 3.2, which reports the integrated values of the parameters analyzed along the transect in the three different layers 0-20m, 20-50m and 50-100m in the euphotic zone. Mean values of surface salinity during June 1998 ranged from 20.08 (F-stations) to 21.29 (S-stations) and in September ranged from 22.05 (O-stations) to 23.35 (S-stations). Throughout the area, in intermediate and mixed layers at all stations, water masses were characterized in both seasons by an almost homogeneous salinity with high values (>37) and lower temperature ($<17^{\circ}\text{C}$). During the second survey (Fig. 3.8), summer, the influence of the low-salinity water was detected down to 30-50m. The lowest salinity values and highest temperature values in spring and summer were observed in a layer of 2-50m mainly at the northern part (S-stations) of Limnos island. Figure 3.8 and 3.9 also shows the progressive change in frontal structure with the depth, in which the frontal isohalines were displaced towards the coast concomitantly with a decrease in their intersection with the bottom. Temperature and salinity below 50m was almost constant around >38 and $\leq 16^{\circ}\text{C}$, respectively, due to Mediterranean waters (Fig. 3.9). The deeper layer displayed very little horizontal variability and was constituted mostly by water from Levantine origin (LIW). One-way ANOVA analysis between these groups in both seasons, concerning salinity values, showed statistically significant differences between the three types of stations and all layers ($p<0.05$), but no significant differences between the seasons (ANOVA, $p>0.05$) were found. On the other hand temperature values differentiated significantly between seasons and layers ($p<0.05$), but no statistically significant differences were found between the shelf-, front- and oceanic stations (ANOVA, $p>0.05$).

3.3.2. Nutrient and phytoplanktonic biomass distribution

Nutrients ranges and mean concentrations for both seasons are presented in Table 3.2. In general higher nutrients values were recorded during the June 1998 cruise than in September. The differences in nutrients concentrations among stations and depth are large and responsible for the relatively high standard deviations. Although high nitrate+nitrite concentrations of ($3.30\mu\text{mol/L}$) were observed during June 1998, at the 2-20m layer of shelf stations, suggesting nitrogen inputs in shelf zone due to the freshwater inflow, it a gradual decrease was observed at the deeper layers ($1.80\mu\text{mol/L}$), which is probably regenerated from the sediments. Regarding the stations in the frontal area (F-stations) the nitrate concentrations were quite high in the 2-20m layer in the range of $0.66\mu\text{mol/L}$, while in the 20-50m and 50-100m layers they were more homogeneous and lower (Fig. 3.8). All layers at the stations far from the frontal structure (O-stations) were presented a uniform nitrate distribution (mean value $0.80\mu\text{mol/L}$) (Tab. 3.2). When the research was conducted during September the nitrate concentrations were lower than in June (Fig. 3.8). The highest nitrate values were observed at surface layers in the northern stations ($1.00\mu\text{mol/L}$, S-stations) and at F-stations in the mixed layer ($0.60\mu\text{mol/L}$) (Tab. 3.2, Fig. 3.9). The oceanic stations, far from the frontal structure, presented high nitrate concentrations, increasing with depth ($1.15\mu\text{mol/L}$) (Tab. 3.2). During spring phosphate concentrations were generally lower at all stations and layers below and near detection limit in the surface waters, and rose to about $0.09\mu\text{mol/L}$ in the intermediate layer (20-50m) of offshore stations (O-stations) (Fig. 3.8). The same pattern was observed in late summer (September 1998), without strong fluctuations and lower values, uniformly distributed along the transect (Tab. 3.2 and Fig. 3.9). The highest dissolved silicate concentrations were recorded in northern S-stations in intermediate layer (mean: $3.33\mu\text{mol/L}$ and $2.85\mu\text{mol/L}$, respectively), in spring and summer (Tab. 3.2).

3.3.3. Nutrient ratios

In order to compare nutrient availability and possible effects of phytoplankton utilization on nutrient ratios, we calculated nitrate, phosphate, and silicate integrated over the euphotic zone of the transect. The elemental ratios differed not greatly among seasons and layers. Nitrate versus phosphate plots were examined to determine limiting nutrients in surface

water. The linear regression of integrated nitrate versus phosphate in spring (June 1998), in the different stations groups, showed that N:P ratios were above the normal value of 16:1 in the shelf stations. However the other groups of stations were below the Redfield ratio. In September the highest N:P ratio was found at the front stations, but still below the Redfield ratio. The linear regression for integrated nitrate versus silicate showed that these two nutrients were used in approximately equal proportions (i.e. slopes close to 1, Fig.3.6). During September, when nitrite was completely depleted from the euphotic zone, there was 0.45 $\mu\text{mol/L}$ residual silicate. In contrast, during June 1998, nitrate and silicate were depleted at approximately the same time as indicated by an intercept of 0.2 $\mu\text{mol/L}$. The regressions between nitrite+nitrate (N), phosphate (P) and silicate (Si) were calculated (Tab. 3.3) for the upper part of the water column of the study area. We looked at the N:P ratios, with slope of N vs. P. Figures 3.6 and 3.7 showed the N vs. P plot, obtained for both cruises. During both sampling periods the nitrite+nitrate versus phosphate ratios were similar (9.82 and 9.20) and significantly lower than the Redfield ratio, indicating a severe nitrate deficiency in the upper layer of the North Aegean Sea. However, the y-intercepts indicate that 0.20 and 0.34 $\mu\text{mol/L}$ of nitrite+nitrate remained in the water column when phosphate was depleted during June and September 1998, respectively. The slope of the nitrite+nitrate versus silicate plots suggest that there is a nitrate deficiency relative to silicate during both seasons, being more pronounced during September 1998. During June the intercept shows that nitrate was depleted prior to silicate, while during September the intercept was close to zero indicating that nitrate and silicate are depleted in parallel. During June the silicate versus phosphate ratio appears slightly inferior to the theoretical Redfield ratio, indicating a lack of silicate relative to phosphate. In contrast during September a strong phosphate deficiency relative to silicate is observed (stations).

3.3.4. Phytoplanktonic biomass

The range and median concentrations of the phytoplanktonic biomass measured in the three water masses present, during the two seasons, are presented in Table 3.1. The lowest chlorophyll α concentration was observed in early spring (0.031 $\text{mg}\cdot\text{m}^{-3}$) at the stations far from the frontal area (O—stations) and the highest at the front stations (0.119 $\text{mg}\cdot\text{m}^{-3}$) in September 1998. Highest chlorophyll α values (0.119 $\text{mg}\cdot\text{m}^{-3}$) occurred in late summer, at the

frontal stations. The horizontal distribution of chlorophyll α concentration at surface layer at the 50m depth, are presented in Fig. 3.4 and 3.5, and seems to confirm the above mentioned hydrographic observations in the area. In Table 3.2 the range and median concentrations (integral means over depth) of the phytoplanktonic biomass are presented measured in the three water layers present, during the two seasons.

Typical vertical profiles of chlorophyll, at shelf and pelagic stations are shown in Figure 3.8 and 3.9 with discrete chlorophyll samples. The chlorophyll α concentrations were relatively high and uniformly distributed across the euphotic zone, showing some seasonality. Surface chlorophyll maximum was observed during June in the S-stations, northern part of the transect, as well at the stations in the frontal area (F-stations) at intermediate layer with concentrations $0.130\text{mg}\cdot\text{m}^{-3}$ and $0.117\text{mg}\cdot\text{m}^{-3}$, respectively (Tab. 3.2). This maximum is well correlated with Black Sea Waters. In the O-stations chlorophyll α concentrations were generally low at all stations and layers without strong fluctuations. During late summer (September 1998), chlorophyll values at all stations and layers showed an increase with depth (Fig. 3.8). The F-stations, situated at the vicinity of Dardanelles straits, presented the highest biomass values in comparison with the other stations. A surface chlorophyll maximum ($0.113\text{mg}\cdot\text{m}^{-3}$) was observed at the mixed layer (20-50m), well correlated with the presence of the modified BSW (Tab. 3.2), in agreement with the findings of the study of the physical characteristics (Zervakis & Georgopoulos, 1998). However, during stratification period (late summer), a second chlorophyll maximum ($0.171\text{mg}\cdot\text{m}^{-3}$) was recorded at deeper layers (50-100m). This second chlorophyll maximum (Deep Chlorophyll Maximum, DCM), is attributed to the influence of the oligotrophic S. Aegean Sea (Zervakis & Georgopoulos, 2000). This chlorophyll maximum, at about 75-100m depth (Fig. 3.9) was located either below the thermocline and coincided approximately with the nitracline. The maximum concentrations measured at these depths were approximately 2 or 3 times higher than the surface values and are more pronounced at the stations neighbouring the Dardanelles (IR43 and IR50). An almost homogeneous water column was observed at the southern part of the transect (no BSW was found). The stations located south of Limnos (oceanic stations) presented the lowest chlorophyll concentrations and low vertical variability, with highest values at the deeper layers ($0.083\text{mg}\cdot\text{m}^{-3}$). From Figure 3.9, it is obvious that along the transect the detected chlorophyll maxima remained at depths

between 50 and 100m unaffected by the position of the jet of the Black Sea Waters. However higher biomass correlated well with surface salinity minima. Despite this hydrographic variability, chlorophyll decreases offshore, and the highest values were associated with the areas of low salinity. Surface chlorophyll tended to increase northeast of Limnos in spring (Fig. 3.8) and southeast of Limnos island in summer (Fig. 3.9). Chlorophyll concentrations showed statistically significant differences between seasons, layers and stations types (ANOVA, $p > 0.05$).

3.3.5. Phytoplankton community structure

The analysis of micro-phytoplankton community structure involved identification of dinoflagellates, diatoms, and coccolithophorids. The seasonal variation of cell abundance (mean cell densities over depth) of the major groups is presented in Table 3.4. There was no distinctive or consistent pattern of the vertical distribution of phytoplankton cells between the stations. For example, in June, maximum abundances were recorded either at 20m or at 50m depth (Tab. 3.4). In September the phytoplankton maximum was usually deeper at either 50 or 75m. The depths of chlorophyll maximum and maximum of cell abundances coincided in half of the profiles; in the other half, the phytoplankton maximum occurred at shallower depths than the chlorophyll maximum. However, the maxima for both parameters were consistently either at the top of, or above the nitracline. Vertical profiles of total phytoplankton, diatoms and dinoflagellates for the entire periods are presented in Fig. 3.8 and 3.9. High values of phytoplankton were recorded at surface layer (2-20m) and intermediate layer (20-50m) of all stations in the area, during both seasons. Thus, in June 1998 abundance values ranged from $98.50 \times 10^3 \text{ cells.l}^{-1}$ (S-stations, 20-50m) to $201.50 \times 10^3 \text{ cells.l}^{-1}$ (F-stations, 2-20m). While in late summer the abundances of total phytoplankton ranged from $2.00 \times 10^3 \text{ cells.l}^{-1}$ (O-stations, 50-100m) to $54.00 \times 10^3 \text{ cells.l}^{-1}$ (F-stations, 2-20m). During June diatoms occurred in high numbers in the 2-20m layer of F-stations $169.00 \times 10^3 \text{ cells.l}^{-1}$ and their minima were found in S-stations $34.50 \times 10^3 \text{ cells.l}^{-1}$ in the 20-50m layer (Fig. 3.8, Tab. 3.5). Dinoflagellates ranged from $6.00 \times 10^3 \text{ cells.l}^{-1}$ in the intermediate layer of F-stations to $6.00 \times 10^3 \text{ cells.l}^{-1}$ in surface layer of oceanic stations. During summer, diatoms occurred in low numbers in S-, F- and S-stations (maximum value: $4.15 \times 10^3 \text{ cells.l}^{-1}$) at surface layer (Tab. 3.5).

Dinoflagellates, were more abundant in F-stations (2-20m) and varied between $0.03 \times 10^3 \text{ cells.l}^{-1}$ and to $0.80 \times 10^3 \text{ cells.l}^{-1}$ at surface layers in F-stations (Tab. 3.5). Comparison between the two cruises regarding biomass and abundances showed that there is a significant difference from one season to the other (ANOVA, $p < 0.05$). It was revealed that the mean biomass in September was higher than in June, whereas the opposite happened with the abundance values. Generally, highest densities of phytoplankton in terms of biomass and abundance occurred in the upper 50m in both seasons and for the most of the stations, followed by a sharp reduction with depth especially below 50m. The most significant feature of the vertical distribution of phytoplankton biomass in spring at S-stations (salinity less than 35) was the influence of thermal stratification. The maximum densities were observed in the region of the halocline (2-40m) (Fig. 3.10). Stations with salinity between 35 and 37 showed higher values also at surface layer (2-20m). The O-stations (salinity > 37) presented similar pattern with the previous, where phytoplankton concentrated mainly at the surface layer. The vertical distribution of phytoplankton in September didn't show any clear pattern in relation with salinity minima and halocline. Other phytoplankton groups, Chrysophyceae, Dictyochophyceae always have low density values. Silicoflagellates occurred with negligible numbers and very scattered distributions throughout the study area and the water column. Density of phytoplankton varied significantly among the sampling stations (shelf-, front- and oceanic stations) and the different layers (ANOVA, $p < 0.05$), but not among seasons (ANOVA, $p > 0.05$).

Phytoplankton assemblages are characterized by the dominance of the species *Nitzschia seriata*, *Nitzschia closterium*, *Nitzschia longissima*, *Rhizosolenia fragilissima*, *Leptocylindrus minimus*, *Leptocylindrus danicus*, *Skeletonema costatum*, *Cryptomonas acuta* (data not shown). Based on both dendrogram classification (not presented here) and MDS ordination, the abundance of each group and species in both cruises showed a positioning of stations according to geographical and hydrographic information of each area indicating similarities or dissimilarities between them. A clear differentiation between surface and intermediate layer (0-20, 20-50 m) and mixed, deeper layer (50-100 m) was evident. This ordination reveals a close relation with the hydrological state of the area in the following way: (i) stations close to the Dardanelles Straits (IR30, IR36, IR43, IR50, MNB4, MNB5), (ii) stations

influenced by modified BSW (MNB6, IR09, MNB1), and (iii) stations influenced by LW, southern stations (Fig. 3.10, Fig. 3.11).

In June, the stations separated in two major groups. The samples of the surface layer (2-20m) comprised the first group of F- and S-stations (Fig. 3.10A), whereas the second group consists of O-stations. In mixed layer (50-75m) the ordination of stations is similar to the previous one where it's more clear the differentiation of the F-stations from S- and O-stations (Fig. 3.11B). In general, the S-stations and F-stations differentiated from of O-stations. Thus, they appeared to be positioned along a gradient from lower to higher salinity, with the north-eastern stations which are influenced by the Black Sea Water on one side and the west-southern where the influence of BSW is very low or insignificant, on the other. In September the ordination is based mainly on geographical position of the stations but also according to the salinity pattern of area. The stations situated at the vicinity of Dardanelles Straits and the northern stations located in the region of BSW presented lower salinity differentiated from the stations, that are influenced by Levantine Water (LIW) (Fig. 3.11 A, B). Correlation analysis was carried out between the physical, chemical and biological variables measured in the water column shows remarkable levels of correlation with both positive and negative values among different variable pairs. In June 1998 (Table 3.6) the correlation analysis, at a significance level of $p < 0.05$, revealed strong positive relationships between salinity and chlorophyll α ($r=0.62$), temperature and diatoms ($r=0.64$) and total phytoplankton ($r=0.52$) and strong negative relationships between salinity and temperature ($r=-0.71$) and temperature and chlorophyll ($r=-0.76$). During September 1998 (Table 3.7) salinity and temperature showed a strong negative correlation ($r=-0.68$), as well temperature and chlorophyll α ($r=-0.81$) and positive correlations between salinity and chlorophyll α ($r=0.51$), salinity and nitrate ($r=0.43$). The correlation analysis provides information on direct relationships among variables. The correlation between chlorophyll, salinity, temperature and nitrate during both seasons may be an indication that these factors control the chlorophyll stock. The strong positive correlation between total phytoplankton and diatoms in spring and summer ($r=0.88$ and $r=0.94$, respectively) due to the dominance of the diatoms species.

3.4 Discussion

3.4.1. Hydrology

The water-column structure of the N. Aegean represents the transition zone of different water masses influenced by the input of brackish waters from the Black Sea through the Dardanelles generating strong salinity stratification in the upper layers during both seasons. A second water mass LIW (Levantine Intermediate Water) and a third one NADW (North Aegean Deep Waters). The enhanced biomass and abundance of phytoplankton appeared to be connected with the permanent hydrographic front. Relatively higher nutrient concentrations are recorded at the near surface layer of the stations close to the Dardanelles. The vertical distribution of chlorophyll and nutrients determined during this study indicates that the water masses in North Aegean Sea are characterized by the depletion of nutrients in the euphotic zone and the development of a DCM, closely associated with the nutricline, within the density stratification layer. Nutrient levels, according to Ignatiades (1992), fell within the range characteristic of oligotrophic environments, and concentrations were often below the detection limits, especially for phosphate. Nutrient concentrations in the upper layers of the water column ranged from low to almost non-detectable. From recent studies undertaken in the area (Siokou-Frangou *et al.*, 2002), it has been shown that the trophic levels of the North Aegean are low (phosphates 0.02-0.08 μ M; nitrates 0.05-1.6 μ M in the 0-200m layer), comparable to those of other parts of the Mediterranean; likewise, that the inflow of BSW contributes to the carbon pool, rather than to inorganic nutrients (Polat and Turgul, 1996).

3.4.2. Nutrient distribution

In general higher nutrient values were recorded during spring in comparison with summer period. The values of the N/Si and Si/P ratios during September imply that silicate is rather more abundant in the upper layer of the system in relation to the other nutrients, suggesting a decreased uptake of this element from the phytoplankton and/or the predominance of non siliceous species relative to June. The N:P ratio of Redfield has long been used as a predictor of phytoplankton nutrient limitation in aquatic ecosystems. Fiocca, *et al.* (1996) showed that the dissolved inorganic nitrogen and dissolved inorganic phosphorus availability leads to a

seasonal change in N:P ratio, high in winter and low in summer. The N:P ratio in North Aegean Sea, during spring and late summer, was below ratio of 16:1. These results indicate that limiting factors didn't show seasonal variability. The great scatter of the data points results in the correlations that are observed, and suggests patchiness in the distribution of nitrate, silicate and phosphate, probably related to their different sources and/or the differential rates of utilization in the upper part of the water column by the phytoplanktonic organisms.

Our analysis of nutrient depth profiles clearly shows that of the three macronutrients (nitrate, phosphate and silicate) utilized by phytoplankton in these waters, nitrate was the most limiting nutrient in the euphotic zone. The higher nitrate concentrations at the deeper layers of the northern stations during June 1998 are probably regenerated from the sediments. The values of the nitrite+nitrate versus phosphate ratios during both sampling periods were significantly lower than the Redfield ratio, indicating a severe nitrate deficiency in the upper layer of the North Aegean Sea. Both intercepts suggest P limitation due to the slight excess of N over P. Furthermore, the decrease of the concentrations of the inorganic nutrients is assumed to be associated with an increase of the particulate organic matter and of dissolved organic nutrients; with these modified chemical properties the BSW leaves the Marmara basin and enters the Aegean Sea. These processes in the area provoke the dominance of phytoplanktonic groups like diatoms and dinoflagellates.

3.4.3. Phytoplankton biomass distribution in relation to the frontal structure

Three distinct water masses were sampled during the survey, as previously described for the area [e.g. (Zervakis, 2002)]: Both phytoplankton biomass and community structure exhibited very little difference between front locations. Total phytoplankton biomass, measured as chl α was not significantly higher in front than at the shelf or oceanic stations. In June, patches of higher Chl α concentration ($\text{mg}\cdot\text{m}^{-3}$) were observed northeast of Limnos island which seem to be related to the general circulation pattern that exists during this period at the area, since the major part of the Dardanelle's outflow follows a northwest direction (Zervakis *et al.*, 1998). In September, it is evident the substantial influences of the circulation on phytoplankton distribution occur during this period as well. The very low chlorophyll

concentrations in the Aegean Sea can be comparable with those observed in the eastern Ionian Sea (0.06-0.26 mg.m⁻³, Gotsis-Skretas *et al.*, 1993a), offshore Israeli waters (0.06-0.12 mg.m⁻³, Berman *et al.*, 1986), offshore Egyptian waters (0.09-0.79 mg.m⁻³, (Dowidar, 1984), the NW Levantine Sea (0.10-0.47 mg.m⁻³, (Ediger & Yilmaz, 1996) and in the core of the Cyprus eddy (0.16-0.23 mg.m⁻³), (Krom, Brenner, Kress, Neori & Gordon, 1993).

The vertical distribution of chlorophyll α , during the stratification period (September 1998) revealed the existence of a very characteristic Deep Chlorophyll Maximum (DCM) at a depth of 75-100m. Water column stability induced by surface heating, as well as the lack of nutrients in the upper layer, led to the formation of a deep chlorophyll maximum, in correspondence with the nutricline. The observed DCM became more pronounced in an offshore direction (as the system became more oligotrophic). This summer picture represented a typical feature of an oligotrophic system. This occurs for example in the western Mediterranean Sea (Estrada, 1985; Raimbault *et al.*, 1993), in the major gyres of the Atlantic and Pacific Oceans (Gieskes *et al.*, 1978; Eppley *et al.*, 1988; Strass and Woods, 1991) and being pronounced in the extremely oligotrophic waters of the Eastern Mediterranean Sea (Berman *et al.*, 1984; Yacobi *et al.*, 1995). Light adaptation leading to a higher cellular content of chlorophyll at the DCM, than in the overlying water could explain the high chlorophyll maximum records from other oligotrophic oceans (e.g. Beers *et al.*, 1982; Cullen, 1982; Olson *et al.*, 1990; Li *et al.*, 1992a).

Another mechanism for the DCM formation may be a summer sinking of epipelagic species, composed of small cells and many dinoflagellates down to deeper levels, when the surface layer is warming up (Kimor, 1990) causing a decrease in water density. Among seasons, environmental parameters, which affect chlorophyll variability and phytoplankton composition (temperature and nutrients), showed statistically significant differences.

Cluster and MDS analysis showed the geographical distribution of the phytoplankton groups and species separating the whole area. In both cruises, the stations reflecting the abundance and species composition grouped according to the salinity gradient. We must notice that the nutrient content of the Black Sea surface waters is modified by biochemical processes, before these waters reach the Dardanelles. The inorganic nutrients of the BSW are

consumed in the basin of Marmara and accordingly their concentrations in the out flowing jet of BSW towards the Aegean Sea are much lower than those of the Black Sea inflow to the Marmara Sea. Furthermore, the decrease of the concentrations of the inorganic nutrients is assumed to be associated with an increase of the particulate organic matter and of dissolved organic nutrients; with these modified chemical properties the BSW leaves the Marmara basin and enters the Aegean Sea (Zervoudaki *et al.*, 1999). For years it was considered that the higher phytoplankton and zooplankton assemblages observed in the area close to Dardanelles were associated with the influence of the nutrient-rich BSW out flowing through the Dardanelles (Pagou & Gotsis-Skretas, 1989; Siokou-Frangou *et al.*, 1999). Although recent chemical observations in the area did not show any persistent nutrient signal of Black Sea Water in the surface water (Souvermezoglou & Krasakopoulou, 1999), it is interesting to estimate the importance of the advective import of nutrients through the Dardanelles in relation to their inputs from the atmosphere and the rivers and their possible internal sources and sinks.

In conclusion, it can be assumed that the chlorophyll and phytoplankton dynamics in the area are mainly driven by: (1) the presence of Black Sea Waters, which probably enhances the growth of phytoplankton in the area; the nutrient content in these waters favours larger phytoplankton like diatoms, which are able to exert “new production” processes in the upper layer. (2) the vertical stability in summer, with inorganic nutrient depletion in the upper warmer layer which leads to low phytoplankton biomass; (3) the summer DCM formation at the nutricline (75 or 100m depth) typical of an oligotrophic system. The results clearly demonstrate a link between phytoplankton abundance and composition and physical features of their environment such as a hydrographic heterogeneity; extension of the continental shelf and the presence of a hydrographic front. However, long-term multidisciplinary studies are required to understand fully the interaction between physical and biological processes in N. Aegean.

CHAPTER 3: Seasonal differences in chlorophyll distribution and phytoplankton composition in a frontal region of the oligotrophic North Aegean Sea (Eastern Mediterranean)

Table 3.1.: Averaged values of the water column integrated salinity [ISal], temperature [ITemp] ($^{\circ}\text{C}$), chlorophyll α (IChl α , $\text{mg}\cdot\text{mg}^{-3}$), nitrate concentration [INO₃] (μM), phosphate concentration [IPO₄] (μM), silicate concentration [ISiO₃] (μM) at the different stations types (S-Shelf, F-Front and O-oceanic stations), during June 1998 and September 1998.

June 1998	S-stations		F-stations		O-stations	
	mean \pm SD	ranges	mean \pm SD	ranges	mean \pm SD	ranges
Salinity	36.04 \pm 1.43	35.22-37.60	36.13 \pm 1.27	36.13-38.19	38.72 \pm 0.1	38.62-38.81
Temperature ($^{\circ}\text{C}$)	17.15 \pm 1.54	15.73-18.29	17.61 \pm 1.35	16.47-18.69	17.52 \pm 1.2	16.44-18.71
Phosphate (μM)	0.080 \pm 0.01	0.063-0.093	0.075 \pm 0.12	0.064-0.088	0.092 \pm 0.01	0.084-0.105
Nitrate (μM)	2.070 \pm 0.83	1.755-3.154	0.614 \pm 0.12	0.482-0.793	0.780 \pm 0.12	0.713-0.930
Silicate (μM)	3.117 \pm 0.50	2.626-3.608	2.674 \pm 0.49	2.327-3.099	2.467 \pm 0.16	2.341-2.641
Chl α ($\mu\text{g}\cdot\text{l}^{-1}$)	0.098 \pm 0.04	0.057-0.169	0.107 \pm 0.04	0.072-0.146	0.031 \pm 0.01	0.023-0.042

September 1998	S-stations		F-stations		O-stations	
	mean \pm SD	ranges	mean \pm SD	ranges	mean \pm SD	ranges
Salinity	36.77 \pm 0.64	36.32-37.31	37.23 \pm 0.91	36.33-38.10	39.02 \pm 0.07	38.96-39.07
Temperature ($^{\circ}\text{C}$)	19.44 \pm 1.02	18.61-20.14	18.93 \pm 1.33	17.80-20.24	19.03 \pm 1.37	17.58-20.44
Phosphate (μM)	0.048 \pm 0.01	0.033-0.063	0.034 \pm 0.01	0.023-0.043	0.032 \pm 0.01	0.022-0.040
Nitrate (μM)	0.896 \pm 0.21	0.651-1.135	0.449 \pm 0.11	0.288-0.579	0.778 \pm 0.24	0.579-1.026
Silicate (μM)	2.391 \pm 0.63	1.906-2.885	2.131 \pm 0.50	1.721-2.566	2.523 \pm 0.443	2.213-2.865
Chl α ($\mu\text{g}\cdot\text{l}^{-1}$)	0.077 \pm 0.03	0.056-0.096	0.119 \pm 0.05	0.083-0.153	0.058 \pm 0.02	0.034-0.069

Table 3.2.: Averaged values of the water column integrated salinity [ISal], temperature [ITemp] ($^{\circ}\text{C}$), chlorophyll α (IChl α , $\text{mg}\cdot\text{mg}^{-3}$), nitrate concentration [INO₃](μM), phosphate concentration [IPO₄] (μM), silicate concentration [ISiO₄] (μM) at the different stations types (S-Shelf, F-Front and O-oceanic stations), during June 1998 and September 1998.

June 1998	Shelf stations			Front stations			Oceanic stations		
	Layer: 2-20m	Layer: 20-50m	Layer: 50-100m	Layer: 2-20m	Layer: 20-50m	Layer: 50-100m	Layer: 2-20m	Layer: 20-50m	Layer: 50-100m
Salinity	31.84±1.60	37.37±1.55	38.92±0.10	34.74±1.40	37.91±1.33	38.89±0.07	38.60±0.03	38.66±0.15	38.89±0.16
Temperature ($^{\circ}\text{C}$)	21.29±0.60	15.51±0.80	14.65±0.10	20.08±1.50	17.37±1.15	15.39±0.34	20.21±0.90	17.15±2.48	15.21±0.25
Phosphate (μM)	0.078±0.01	0.083±0.01	0.080±0.01	0.079±0.00	0.074±0.01	0.072±0.01	0.091±0.00	0.093±0.00	0.090±0.02
Nitrate (μM)	3.295±1.60	2.433±0.45	1.803±0.30	0.663±0.08	0.503±0.06	0.676±0.20	0.809±0.01	0.740±0.08	0.790±0.26
Silicate (μM)	2.986±0.40	3.334±0.50	3.030±0.60	2.794±0.63	2.744±0.60	2.485±0.25	2.471±0.06	2.487±0.14	2.443±0.28
Chl α ($\text{mg}\cdot\text{m}^{-3}$)	0.092±0.05	0.130±0.05	0.073±0.05	0.096±0.03	0.117±0.03	0.108±0.04	0.023±0.00	0.038±0.01	0.033±0.02

September 1998	Shelf stations			Front stations			Oceanic stations		
	Layer: 2-20m	Layer: 20-50m	Layer: 50-100m	Layer: 2-20m	Layer: 20-50m	Layer: 50-100m	Layer: 2-20m	Layer: 20-50m	Layer: 50-100m
Salinity	34.28±0.91	37.01±0.92	39.01±0.07	35.01±1.23	37.75±1.45	38.93±0.04	38.98±0.05	38.99±0.14	39.10±0.01
Temperature ($^{\circ}\text{C}$)	23.35±0.70	19.41±2.18	15.55±0.17	22.22±0.74	18.73±3.11	15.85±0.14	22.05±0.91	18.99±1.83	16.05±0.36
Phosphate (μM)	0.039±0.02	0.054±0.02	0.044±0.00	0.035±0.01	0.025±0.00	0.041±0.012	0.031±0.00	0.031±0.02	0.033±0.00
Nitrate (μM)	1.021±0.10	0.825±0.25	0.842±0.28	0.388±0.08	0.330±0.08	0.630±0.15	0.536±0.23	0.656±0.30	1.142±0.18
Silicate (μM)	2.037±0.78	2.858±0.72	2.278±0.39	2.037±0.78	1.969±0.34	2.386±0.34	2.632±0.81	2.364±0.34	2.572±0.17
Chl α ($\text{mg}\cdot\text{m}^{-3}$)	0.048±0.00	0.077±0.03	0.106±0.05	0.072±0.02	0.113±0.04	0.171±0.07	0.029±0.00	0.047±0.01	0.083±0.04

CHAPTER 3: Seasonal differences in chlorophyll distribution and phytoplankton composition in a frontal region of the oligotrophic North Aegean Sea (Eastern Mediterranean)

Table 3.3.: Linear regression of N vs. P, of N vs. Si and of Si vs. P for the upper part of the water column in N.Aegean Sea during June and September 1998.

	N/P	N/Si	Si/P
June 1998			
Slope	9.825	0.679	11.44
Intercept	0.198	-0.870	1.827
r ²	0.166	0.308	0.336
September 1998			
Slope	9.202	0.258	22.53
Intercept	0.342	0.077	1.466
r ²	0.206	0.348	0.238

Table 3.4.: Mean and SD values **10⁴ cells/l** of hydrographic and chemical variables during June and September 1998.

June 1998	Shelf stations		Front stations		Oceanic stations	
Variable	Mean±SD	Range	Mean±SD	Range	Mean±SD	Range
Diatoms	61.00±6.00	44.00-81.00	97.00±6.00	90.00-172.00	67.00±1.00	47.00-91.00
Dinoflagellates	9.00±2.00	6.00-9.00	7.00±6.00	3.00-12.00	39.00±1.00	27.00-57.00
Coccolithophores			5.00±7.00	1.50-12.00	13.00±6.00	8.00-16.00
Silicoflagellates	20.00±7.80	16.50-27.50	9.00		9.50±1.00	2.00-10.00
Other groups	25.00±5.00	4.00-25.00	22.00±6.00	13.00-51.00	21.50±7.00	12.70-65.00
Total phytoplankton	115.00±22.51	9.00-61.00	140.00±39.14	5.00-97.00	150.00±23.62	9.50-67.00

September 1998	Shelf stations		Front stations		Oceanic stations	
Variable	Mean±SD	Range	Mean±SD	Range	Mean±SD	Range
Diatoms	3.00±3.00	2.00-6.00	3.00±3.00	2.00-5.00	1.00±1.00	0.50-1.00
Dinoflagellates	5.00±5.00	3.00-11.00	13.00±13.00	9.00-19.00	3.00±3.00	1.00-5.00
Coccolithophores	10.00±10.00	2.00-21.00	1.00±1.00	0.50-2.00	0.50±0.50	0.20-1.00
Silicoflagellates			4.00±4.00	0.50-6.00		
Other groups	3.00±3.00	2.00-4.00	4.00±4.00	2.00-6.00	3.00±3.00	1.50-4.00
Total phytoplankton	21.00±3.30	3.00-10.00	25.00±4.64	1.00-13.00	7.50±1.31	0.50-3.00

Table 3.5.: Statistics for phytoplankton groups values (10^4 cells.l⁻¹) at the stations sampled the both cruises.

Shelf stations	June 1998						September 1998					
	Layer: 2-20m	range	Layer: 20-50m	range	Layer: 50-100m	range	Layer: 2-20m	range	Layer: 20-50m	range	Layer: 50-100m	range
Diatoms	90.00±7.00	85.00-95.00	34.50±17.00	28.50-52.50	91.00±40.00	66.00-118.00	2.00±1.00	1.00-3.00	17.00±7.00	1.00-44.00	1.00±0.50	0.50-1.00
Dinoflagellates	12.00±3.00	10.00-14.00	12.00±0.60	11.00-12.00	45.00±11.00	23.00-67.50	5.00±0.10	4.00-5.00	4.00±1.00	1.00-6.00	5.00±1.00	1.00-5.00
Coccolithophores					17.00±6.00	4.00-17.00	1.50±0.30	1.00-2.00	1.00±0.20	0.20-2.00	0.50±0.10	0.20-1.00
Silicoflagellates			17.00±1.00		0.10±0.10	0.10-0.10						
Other groups	4.00±0.20	3.00-4.00	35.00±10.00	5.00-48.00			2.00±1.00	1.00-3.00	2.00±1.00	3.00	1.50±0.50	1.50-4.00
Total	106.00±47.51	4.00-90.00	98.50±11.87	12.00-35.00	153.10±39.73	0.10-91.00	10.50±1.60	1.50-5.00	24.00±7.44	1.00-17.00	8.00±2.04	0.50-5.00
Front stations												
Diatoms	169.00±7.00	85.00-95.00	81.00±40.00	97.00-192.00	63.00±0.80	62.00-63.00	41.50±15.00	3.00-80.00	18.00±5.00	.00-114.00	1.00±0.50	0.50-1.00
Dinoflagellates	15.50±10.00	6.00-32.50	9.00±3.00	2.00-8.00	39.00±11.00	32.00-47.00	8.00±0.50	2.00-15.00	5.00±3.00	1.00-32.00	1.00±0.10	1.00-1.50
Coccolithophores	4.00±1.00	2.00-6.00	2.00±0.30	1.00-2.00	8.00±5.00	4.00-11.00	1.50±0.50	1.00-2.00	1.00±0.10	0.20-3.00	0.50±0.10	0.20-0.50
Silicoflagellates	2.00±0.60	1.00-3.50	3.00±0.60	1.00-4.00	0.10±0.10	0.10-0.10						
Other groups	11.00±9.00	5.00-26.00	30.00±2.00	3.00-7.00	13.00±0.20	12.00-13.00	3.00±1.00	1.50-4.00	21.00±7.00	3.00-107.50	1.00±0.50	0.50-1.50
Total	201.50±72.15	2.00-169.00	125.00±33.28	2.00-81.00	123.10±25.94	0.10-63.00	54.00±18.87	1.50-41.50	45.00±9.74	1.00-21.00	3.50±0.25	0.50-1.00
Oceanic stations												
Diatoms	43.50±21.10	29.00-58.00	61.00±18.00	47.00-82.00	47.00±21.00	32.50-62.00	1.50±0.50	1.50-4.00	4.00±1.00	1.00-7.00	1.00±0.50	0.00-1.00
Dinoflagellates	7.00±5.00	4.00-11.00	6.00±4.00	3.00-11.50	27.00±6.00	23.00-32.00	1.00±0.10	0.20-2.00	0.30±0.10	0.20-2.00	1.00±0.50	1.00-1.00
Coccolithophores			6.00±0.30	1.00-12.00	13.00±3.50	11.00-16.00	1.00±0.30	0.00-1.50	0.50±0.10	0.50-2.00	0.00-0.00	0.00-0.00
Silicoflagellates	22.00±8.00	16.50-27.50	3.00±1.00	1.00-4.50	0.10±10.00	5.00-7.00						
Other groups	46.00±3.00	44.00-48.00	25.00±7.00	26.00-67.00	39.00±17.00	13.00-65.00	4.50±2.00	3.00-6.00	6.00±6.00	5.00-14.00	0.00-0.00	0.00-0.00
Total	118.50±18.54	7.00-46.00	101.00±24.43	3.00-61.00	126.10±19.02	0.10-47.00	8.00±1.68	1.00-4.50	10.80±2.78	0.30-6.00	2.00±0.00	1.00-1.00

CHAPTER 3: Seasonal differences in chlorophyll distribution and phytoplankton composition in a frontal region of the oligotrophic North Aegean Sea (Eastern Mediterranean)

Table 3.6.: Spearman rank order correlations between physical (temperature [°C], salinity) and chemical variables (nitrate [$\mu\text{mol l}^{-1}$], phosphate and silicate), as well as chlorophyll α concentrations [mgm^{-3}] and the abundance of phytoplanktonic groups ($\times 10^4 \text{ cells.l}^{-1}$) during June 1998.

Variable	salinity	temperature	phosphate	nitrate	Chlorophyll α	Diatoms
temperature	-0.7152					
phosphate	-0.0867	0.1998				
nitrate	-0.0939	-0.3274	0.1661			
Chlorophyll α	0.6176	-0.7625	-0.2590	0.0229		
Diatoms	-0.5327	0.6417	0.3169	-0.2481	0.4222	
Phytoplankton	-0.4306	0.5114	0.2577	-0.2149	0.3713	0.8813

(Correlation coefficient in bold, significant, $p > 0.05$)

Table 3.7.: Spearman rank order correlations between physical (temperature [°C], salinity) and chemical variables (nitrate [$\mu\text{mol l}^{-1}$], phosphate and silicate), as well as chlorophyll α concentrations [mgm^{-3}] and the abundance of phytoplanktonic groups ($\times 10^4 \text{ cells.l}^{-1}$) during September 1998.

Variable	salinity	temperature	phosphate	nitrate	Chlorophyll α	Diatoms
temperature	-0.6858					
phosphate	0.0268	-0.1912				
nitrate	0.4319	-0.2069	0.1805			
Chlorophyll α	0.5074	-0.8150	0.0992	0.0416		
Diatoms	-0.3607	0.2156	0.1054	0.0011	0.1748	
Phytoplankton	-0.4193	0.2278	0.1204	-0.0362	0.2203	0.9424

(Correlation coefficient in bold, significant, $p > 0.05$)

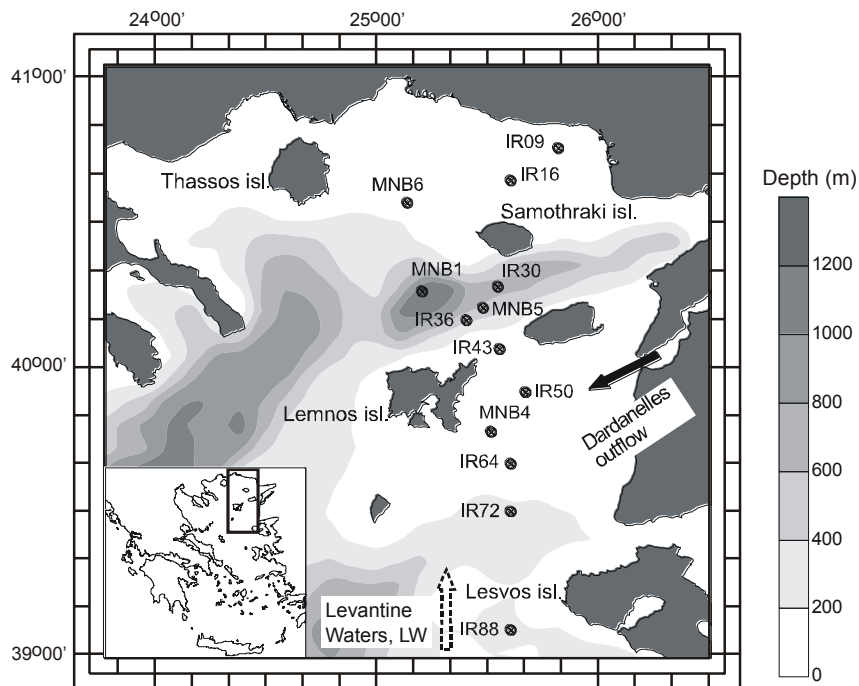


Figure 3.1.: Map of the North Aegean Sea showing the sampling stations during June and September 1998. Stations codes: shelf (S-more or less mixed conditions IR09, IR16, MNB6, MNB1), front (F-weak pycnocline IR30, IR36, MNB5, IR43, IR50, MNB4, IR64), oceanic (O-weak or no pycnocline IR72, IR88).

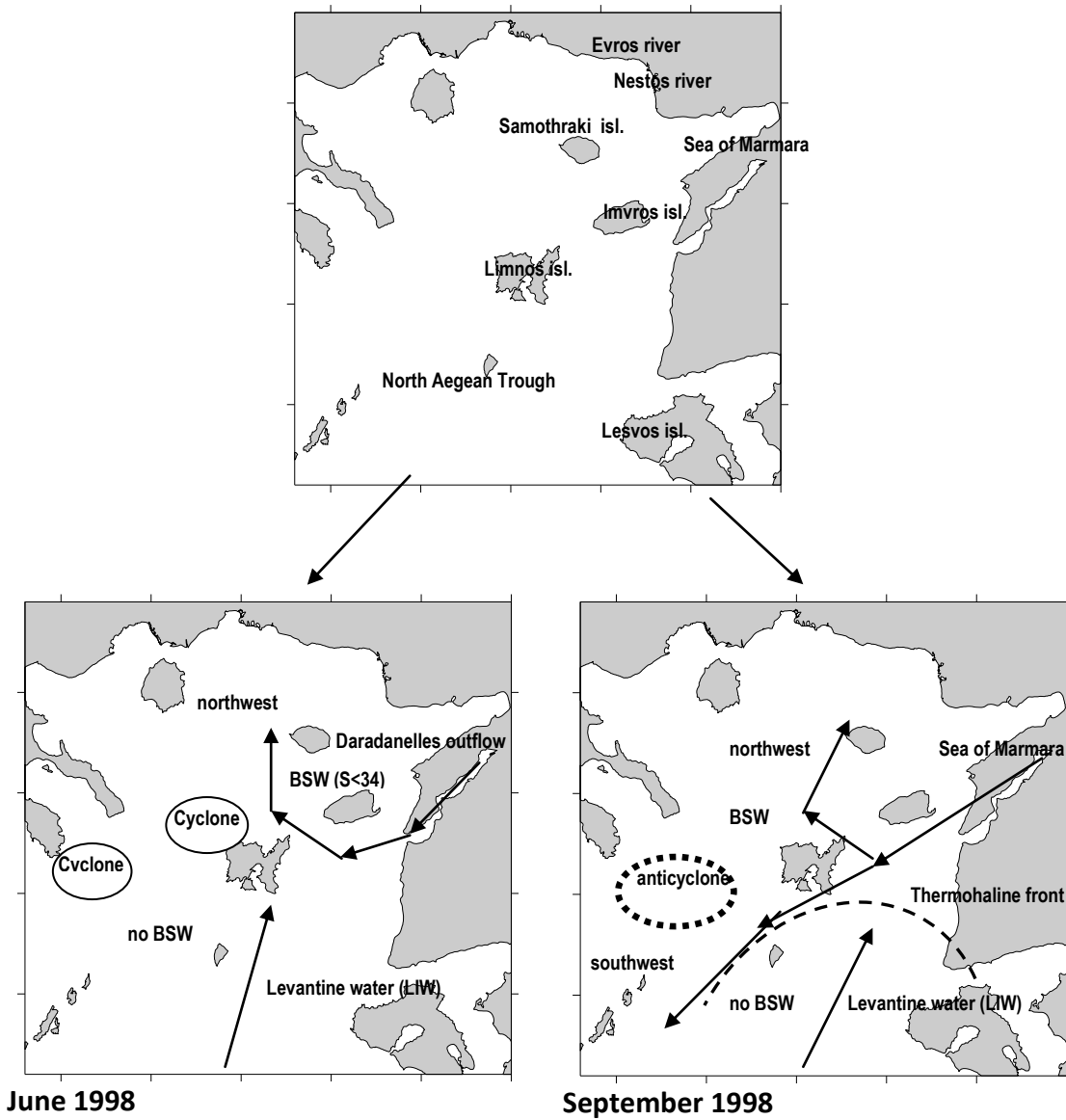


Figure 3.2.: Typical surface spring and summer circulation of North Aegean Sea (according to Zervakis and Georgopoulos, 2002).

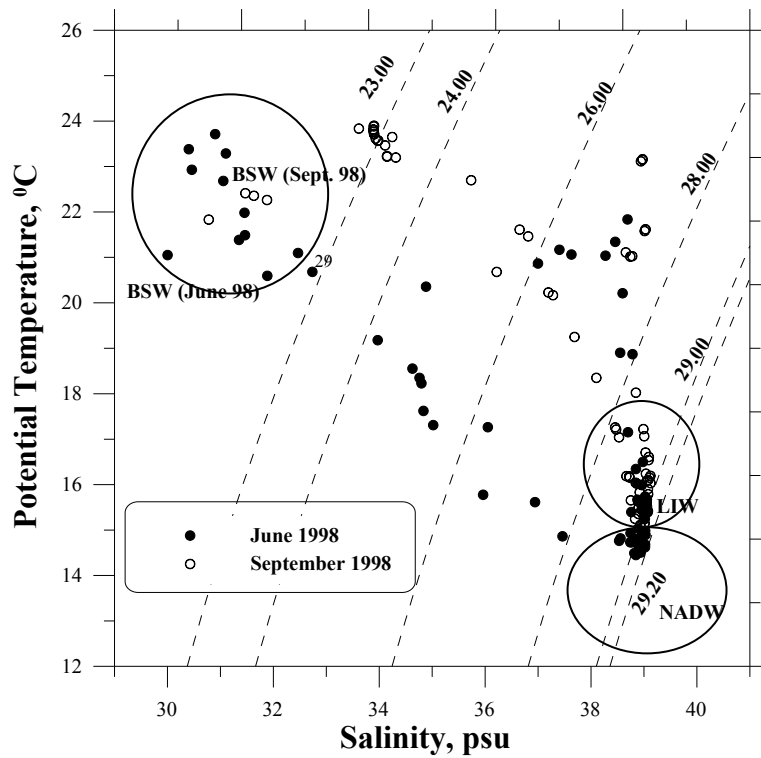


Figure 3.3.: Temperature–salinity plot θ/S (diagram) corresponding to CTD casts performed during the two cruises in spring and late summer conditions. Lines within the plot represent pycnocline limits of water masses: BSW, Black Sea water (density<28); LIW, Levantine intermediate waters (density>28-29.2), NADW, North Aegean Deep Waters (density>29.2).

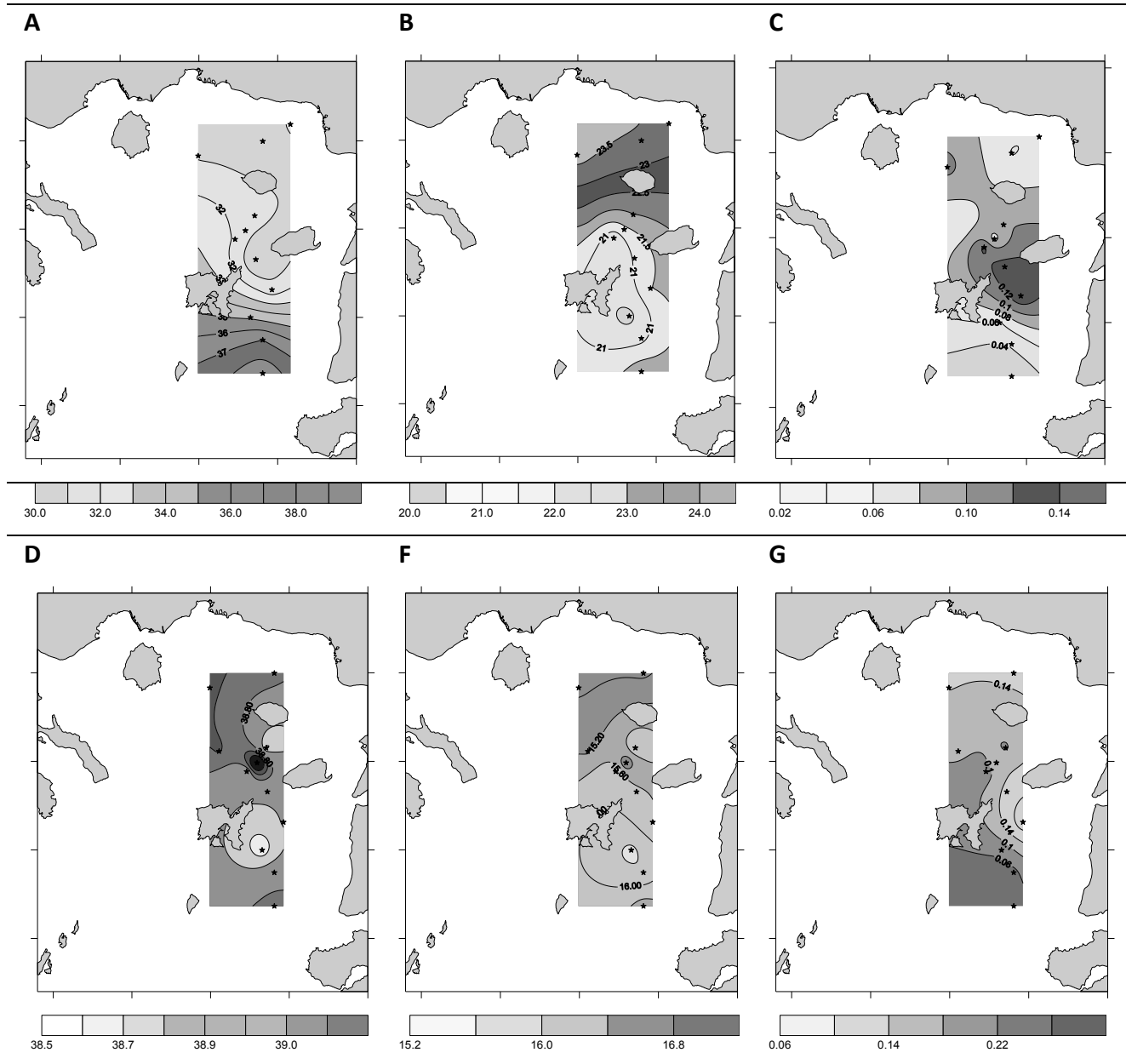


Figure 3.4.: Contour plots showing the distribution of salinity (A), temperature (B) and chlorophyll α (C) at the surface and salinity (D), temperature (E) and chlorophyll α (F) at 50m depth during June 1998.

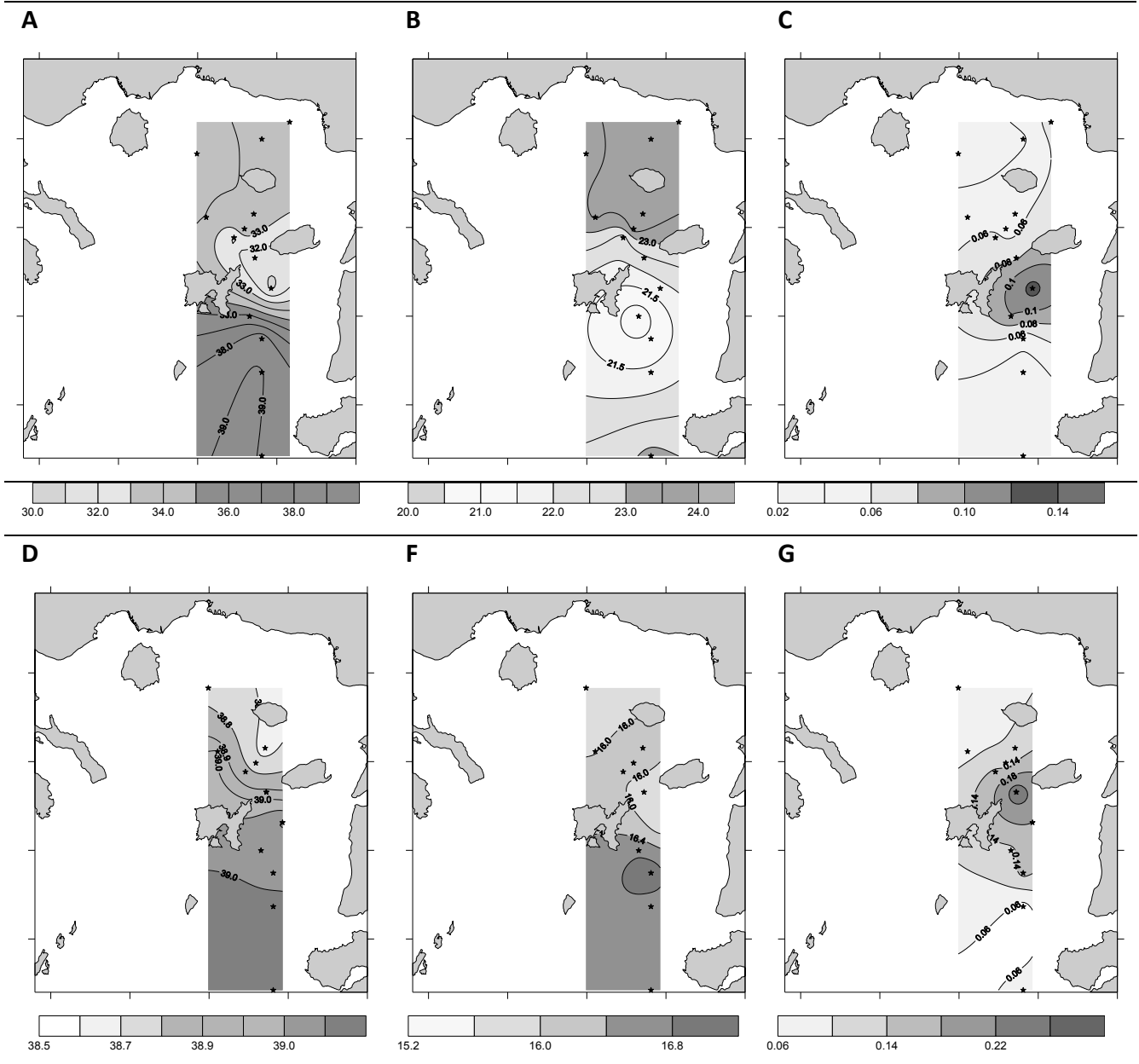


Figure 3.5.: Contour plot describing the distribution of salinity (A), temperature (B) and chlorophyll α (C) at the surface and salinity (D), temperature (E) and chlorophyll α (F) at 50m depth during September 1998.

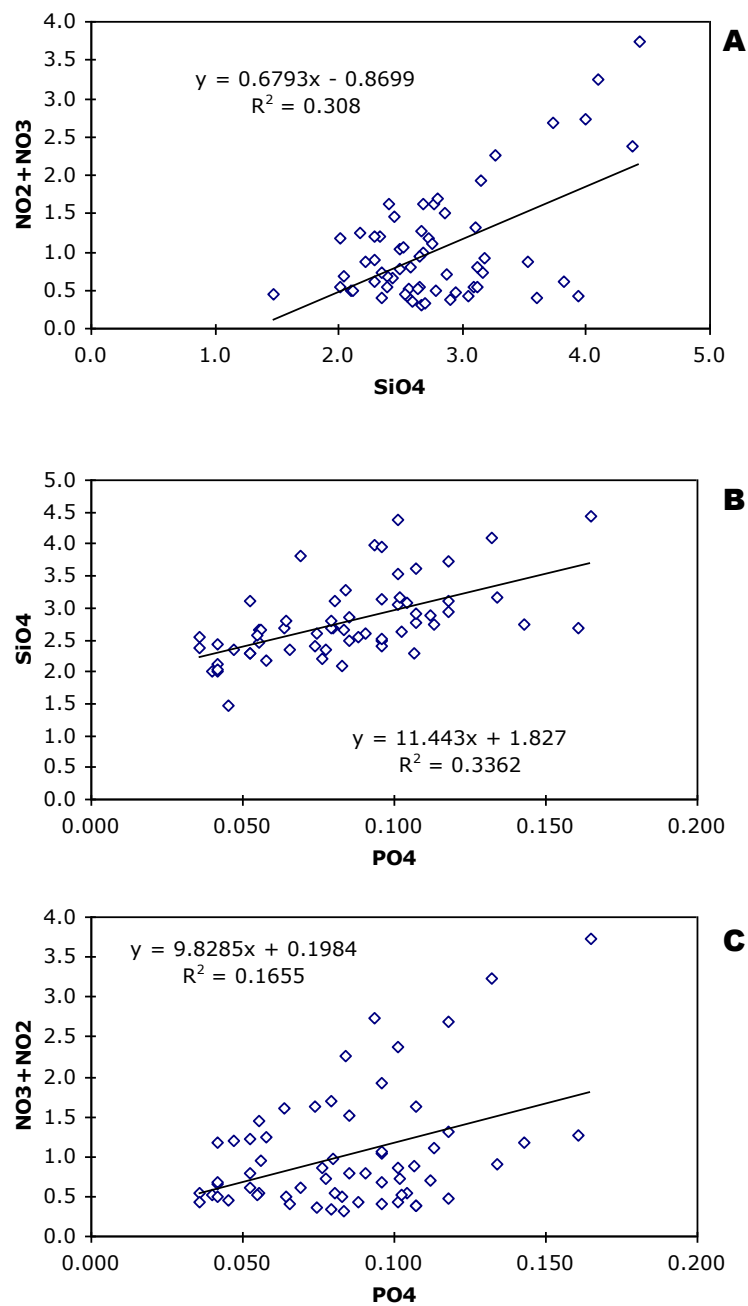


Figure 3.6.: Nitrate vs. silicate (A), Silicate vs. phosphate (B) and Nitrate vs. phosphate (C), linear plot for June 1998.

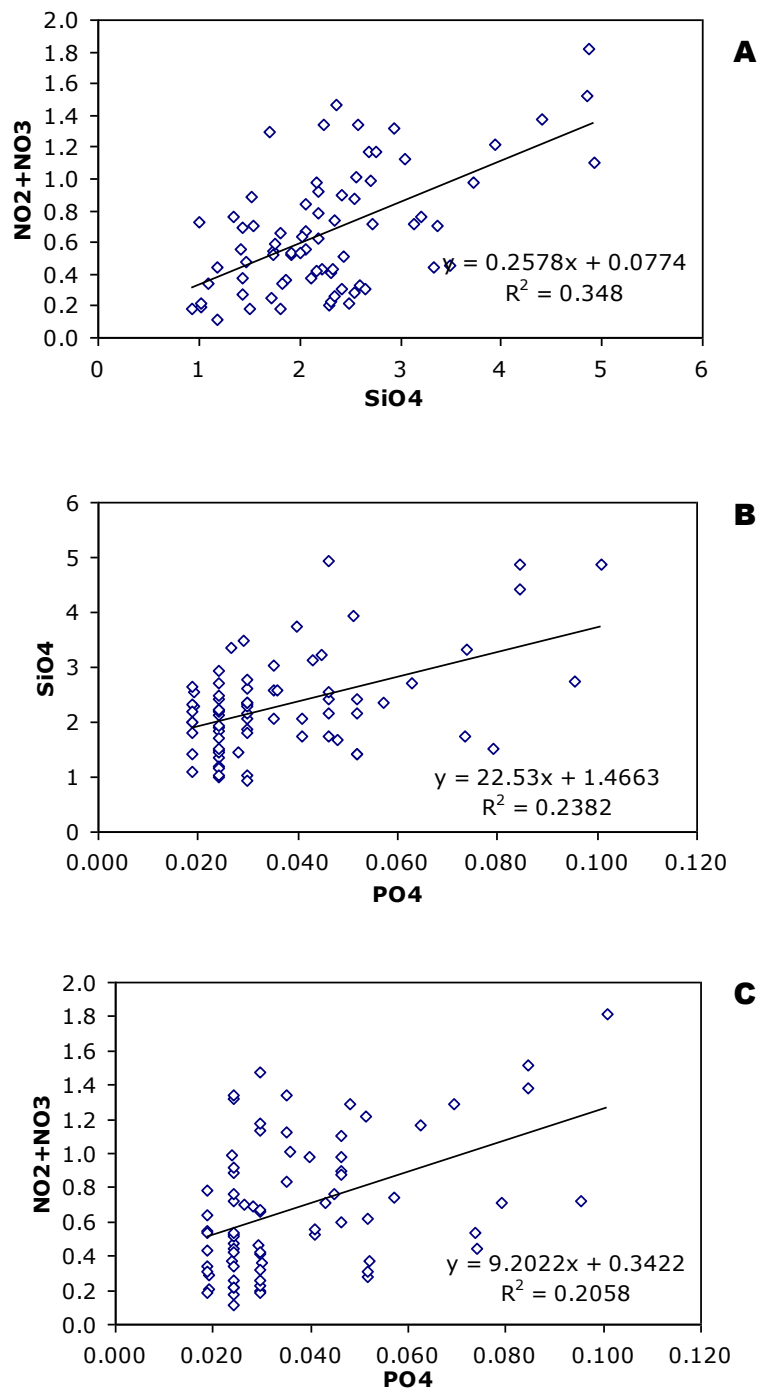


Figure 3.7.: Nitrate vs. silicate (A), Silicate vs. phosphate (B) and Nitrate vs. phosphate (C), linear plot for September 1998.

CHAPTER 3: Seasonal differences in chlorophyll distribution and phytoplankton composition in a frontal region of the oligotrophic North Aegean Sea (Eastern Mediterranean)

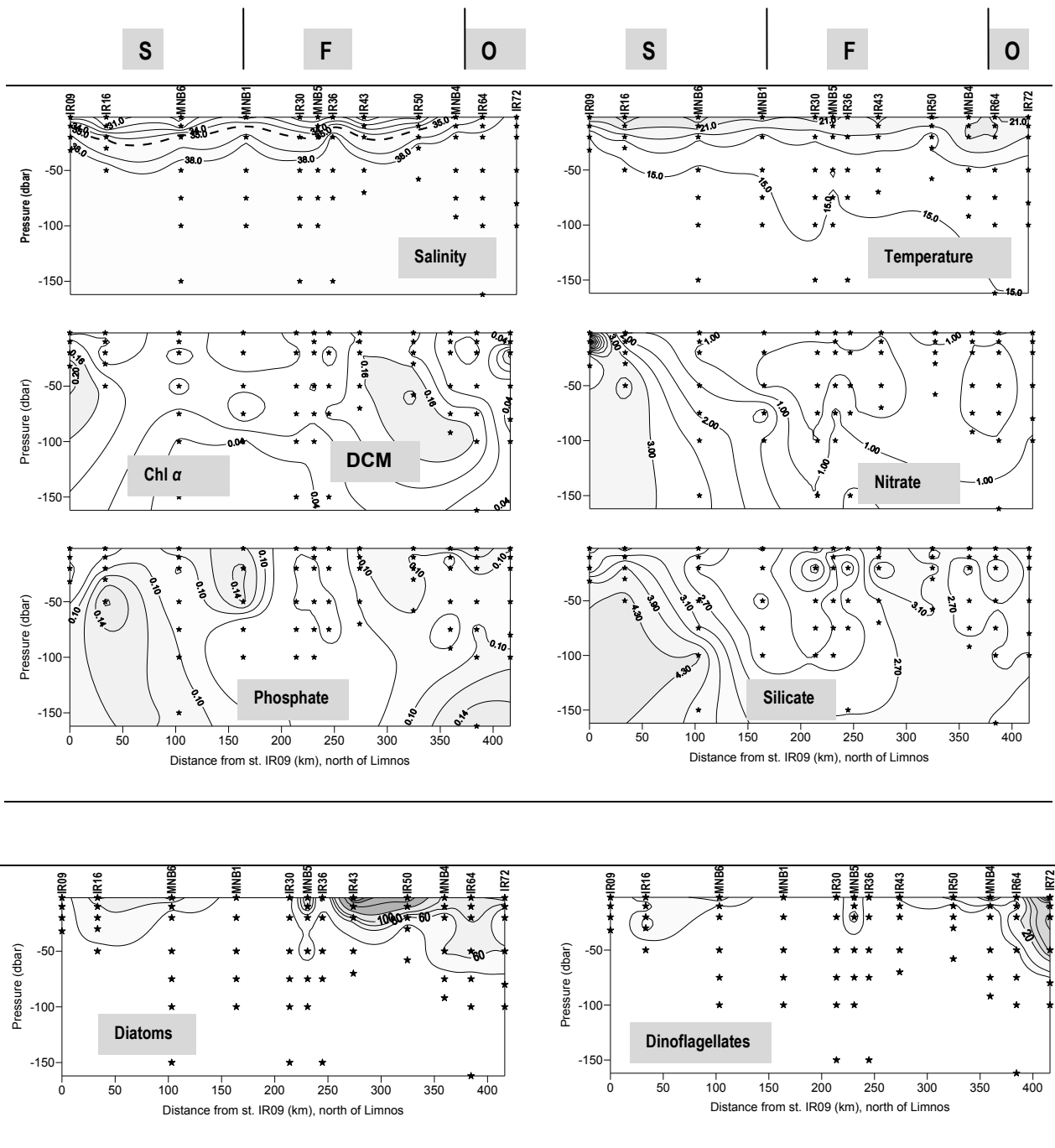


Figure 3.8.: Vertical distribution of temperature ($^{\circ}\text{C}$), salinity, phosphate, nitrate and silicate concentrations ($\mu\text{M l}^{-1}$), chlorophyll α concentration ($\mu\text{g l}^{-1}$) and the dominant phytoplankton groups diatoms and dinoflagellates abundance ($\times 10^4 \text{ cells.l}^{-1}$) at the section east of Limnos in June 1998. (S=Shelf stations, F=Front stations and O=oceanic stations). Dashed line represents the less saline Black sea waters in the upper layer).

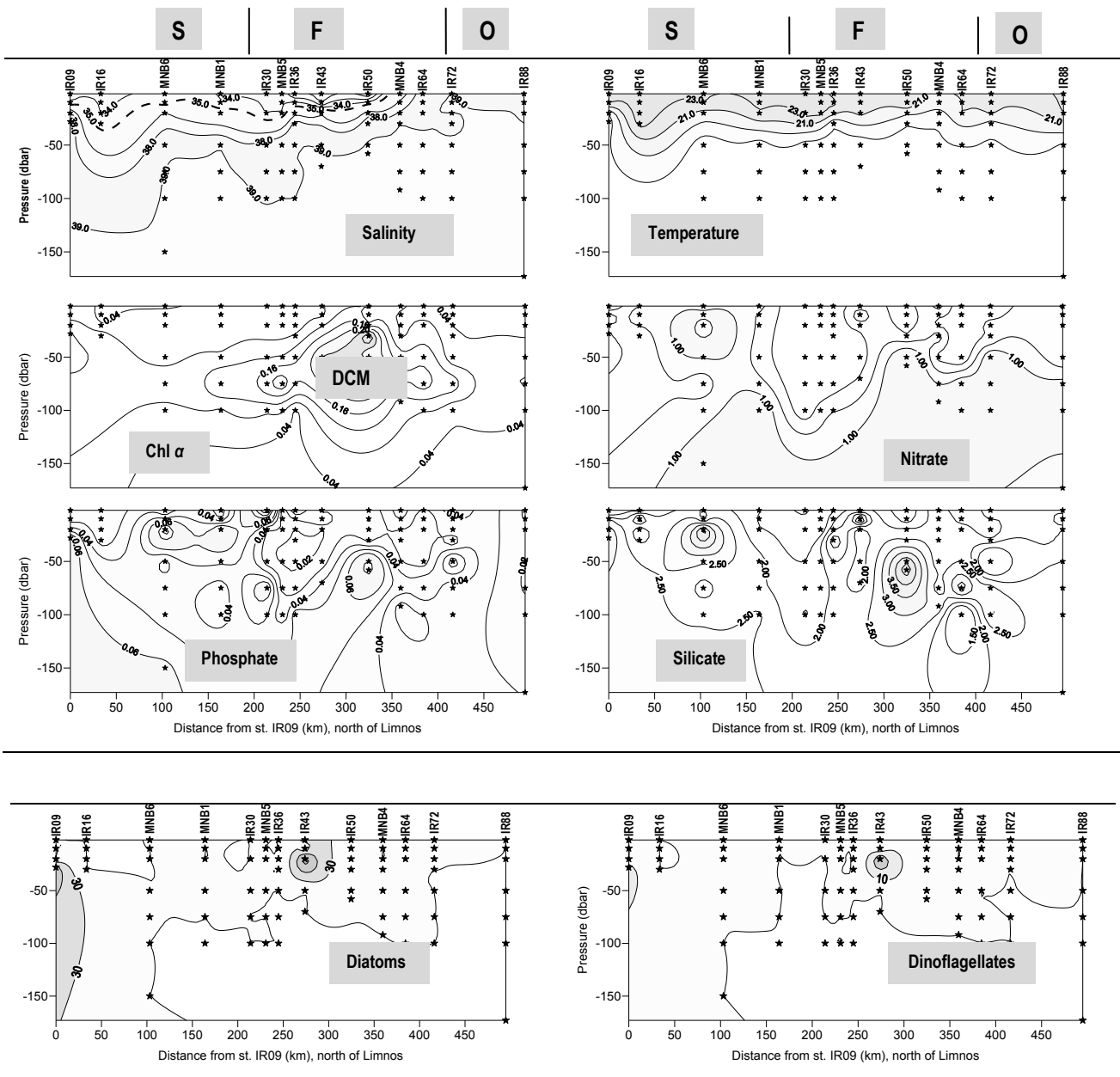


Figure 3.9.: Vertical distribution of temperature ($^{\circ}\text{C}$), salinity, phosphate, nitrate and silicate concentrations ($\mu\text{M l}^{-1}$), chlorophyll α concentration ($\mu\text{g.l}^{-1}$) and the dominant phytoplankton groups diatoms and dinoflagellates abundance ($\times 10^4 \text{ cells.l}^{-1}$) at the section east of Limnos in September 1998. (S=Shelf stations, F=Front stations and O=oceanic stations). Dashed line represents the less saline Black sea waters in the upper layer).

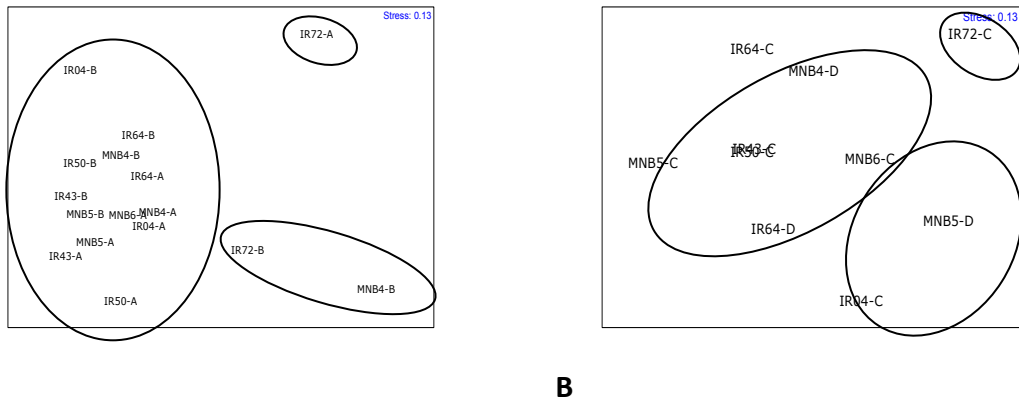


Figure 3.10.: Multi-dimensional scaling (MDS) plot of phytoplankton assemblages based on the data of numeric abundance of the species during June 1998 (A, B). Labels correspond to the station number. A-B corresponds to 2-20m layer and C-D corresponds to 50-75m layer.

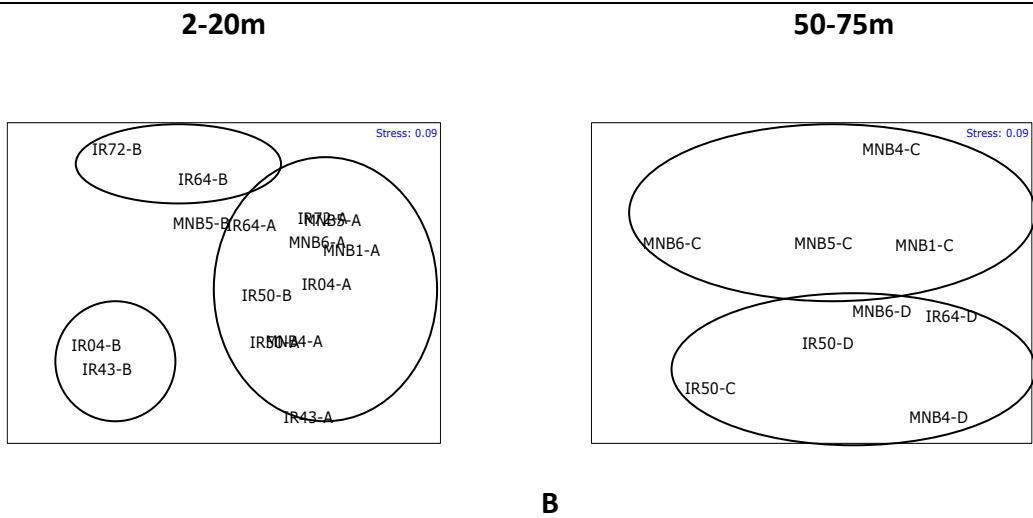


Figure 3.11.: Multi-dimensional scaling (MDS) plot of phytoplankton assemblages based on the data of numeric abundance of the species during September 1998 (A, B). Labels correspond to the station number. A-B corresponds to 2-20m layer and C-D corresponds to 50-75m layer.

CHAPTER 4: Dynamics of autotrophic picoplankton in the N. Aegean Sea

Assimakopoulou G.¹, K. Pagou.¹, Krasakopoulou, E.¹, Zervakis V.¹, Christou N., Ruser A.², Colijn, F.²

¹Institute of Oceanography, National Centre for Marine Research, P.O. Box 712, Anavyssos 19013, Greece

²Research- and Technology Centre Westcoast of Christian-Albrechts-University at Kiel, Germany

Abstract

Size-fractionated phytoplankton biomass and primary production, was studied in the oligotrophic northeastern Aegean Sea (eastern Mediterranean), which is characterized by a permanent thermohaline front. Cruises were conducted by two distinct oceanographic conditions (September 1999-late summer and April 2000-spring). The work assessed the spatial, vertical and temporal variations of size fractionated chlorophyll α , primary production (*in situ*), and the taxonomic composition of picophytoplankton. During the late summer, total chlorophyll α (Chl α) and primary production rates were in the range of 3.9-6.5 mg Chl α m⁻² and 178.55-442.37 mgCm⁻²d⁻¹, respectively, and were mainly accounted for (>60%) by the picophytoplankton size fraction (<3 μ m). In spring, total chlorophyll α (Chl α) and primary production rates were much higher 18.87-31.58 mg Chl α m⁻² and 190.84-512 mgCm⁻²d⁻¹, the pico- and nano size fractions significantly increased their contribution to total Chl α (25.50-61.60%) and primary production rates (28.00-51.20%). Throughout the study area, almost 60–70% of autotrophic biomass and primary production was performed by cells <3 μ m. A marked seasonality of the relative contribution of prokaryotes and eukaryotes was found. While cyanobacteria were generally more abundant in summer (up to 47.3 10³ cellsml⁻¹), picoeukaryotes dominated the community (up to 4.90x10³ cellsml⁻¹) in spring. Different seasonality of pigment and biomass values resulted in a clear temporal pattern of picophytoplanktonic carbon to chlorophyll α ratio, which ranged from 100 (summer) to 130 (spring). The main aim of the study was to obtain a preliminary characterization of the

autotrophic community structure of an oligotrophic basin during two contrasting seasonal conditions (stratification vs homogeneity).

Keywords: Picophytoplankton; Productivity; Biomass; Size fractionation; Eastern Mediterranean; Aegean Sea

4.1 Introduction

When two water masses with distinct properties meet, a third water mass is formed, called a front. The two adjacent water masses are essentially two separate ecosystems and the zone created by mixing along the edges is a unique ecosystem, or anecotone (Odum 1971). Enhanced phytoplankton biomass often occurs at fronts—defined as regions of strong horizontal temperature and/or salinity gradients (Franks 1992a; Franks 1992b; Laubscher *et al.* 1993; Flint and Sukhanova, 2002).

Over most continental shelves, fronts exist near the shelf break, separating low-salinity coastal water from high salinity open ocean water. Frontal zones are associated with strong horizontal gradients for physical and chemical properties (Sournia, 1994) and exhibit high variability over a broad range of spatial and temporal scales (Rodionov, 1994). The effects of frontal dynamics on phytoplankton biomass and production have been studied by Estrada (1985a, b; 1991), Margalef (1985), Estrada and Margalef (1988), Estrada and Salat (1989), and Estrada *et al.*, (1993). Shelf areas are characterized by physical processes that generate complex plankton distribution patterns (Denman and Powell, 1984; Horne and Platt, 1984; Yoder *et al.*, 1987; McClain *et al.*, 1988). Shelf slope fronts typically are narrow but can extend several hundred kilometres along the shelf edge. Physical and biological coupling in these frontal zones presents a high spatio-temporal variability as a result of both the hydrographic complexity of such systems and biological activity of the organisms. In diverse marine systems, subsurface chlorophyll maximum layers are common, and a variety of governing mechanisms such as nutrient supply, differential grazing, and cell sinking have been proposed to account for them (e.g., Bienfang *et al.*, 1983).

For these reasons the study of physical and biological coupling in frontal areas holds out great scientific interest. There is considerable evidence indicating that oceanic fronts support high levels of biotic activity across a broad range of trophic levels (Pingree *et al.*, 1975; Richardson, 1985; Le Fèvre, 1986; Olson *et al.*, 1994). The size structure of the phytoplankton community is the most relevant ecological property that controls the carbon/energy flow through the marine food web. Phytoplankton size structure depends on physical and biological factors that ultimately are influenced by local and mesoscale hydrodynamics of the system (Riegman *et al.*, 1993) such as eddies and unstable fronts (Rodriguez *et al.*, 2001).

In oligotrophic systems, as well as the open waters of the Mediterranean Sea, the phytoplankton communities are dominated by the presence of small-sized cells. A complex microbial food web favors the cycling of a significant fraction of organic carbon (DOC) within the upper layer (Chisholm *et al.*, 1988). In some areas or periods (divergence zones or short spring-blooms) the injection of nitrate in the euphotic zone by hydrodynamic forcing (such as winter mixing, upwelling or cyclonic gyres) stimulates high carbon production. In these cases the community is dominated by large phytoplankters (diatoms and nanoflagellates) and characterized by high export of fixed carbon (POC) to higher trophic levels through a short food chain (Eppley and Peterson, 1979).

Small sized phytoplankton such as picoplankton and nanoplankton are the major contributors of biomass and primary productivity in oligotrophic marine environments and appear to be an important component of microbial food web and carbon flow of such environments (Berman *et al.*, 1986; Azov, 1991). Due to its small size, picophytoplankton has an advantage to acquire nutrients in oligotrophic environments. However, under nutrient rich conditions, phytoplankton populations dominated by large cells (Jiao and Ni, 1997). Recent studies reveal that the phytoplankton smaller than $<3 \mu\text{m}$ (picoplankton) are ubiquitous and very common and this size fraction accounts for about 80-90% of the total primary productivity in some waters (Harris, 1986).

The Black Sea Water (BSW) exiting the Dardanelles is characterized by its distinctive low salinity (~ 30 in the area of the Dardanelles exit in the Aegean) and related low density. Upon

its intrusion in the Aegean Sea, BSW forms a surface layer of 20–40m thickness that overlies the more saline waters of Levantine origin (Zodiatis, 1994; Zervakis and Georgopoulos, 2002). After their exit from Dardanelles, the BSW waters follow a generally westward flow, and thus a very strong thermohaline front is formed at the southern boundary where the two major water masses meet, BSW and the northward flowing LW (Levantine waters). The out flowing Black Sea Water is enriched in dissolved organic carbon and nitrogen rather than in inorganic nutrients (nitrogen and phosphate) when compared to the Aegean Seawaters (Polat and Tugrul 1996; Sempere *et al.*, 2002; Siokou-Frangou *et al.*, 2002).

Autotrophic cells in the picoplankton size fraction (0.2 to 2 μm) have been recognized as an important component of microbial plankton communities for more than 2 decades (Stockner 1988). Marine picophytoplankton is composed of both prokaryotic and eukaryotic cells, generally represented by *Prochlorococcus* and *Synechococcus* cyanobacteria and by small flagellates. The dominant contribution of picophytoplankton to total phytoplankton standing stocks and carbon fluxes in oligotrophic warm environments is well established (Agawin *et al.*, 2000).

The seasonal vertical distribution of picophytoplankton was studied in the oligotrophic northeastern Aegean Sea (eastern Mediterranean). Hydrographic conditions in the area are characterized by strong density gradients, resulting from the inflow of low-salinity Black Sea water in the north-eastern Aegean Sea. Cruises were conducted during late summer and spring along a cross-shelf transect. Abundance distribution and cell characteristics of picophytoplankton (cell diameter 0.2-2.0 μm) were studied by flow cytometry in two regions of North Aegean Sea: the frontal region, where Black Sea and Aegean waters meet and a region outside the front, where more oligotrophic conditions prevail. The eukaryotic phytoplankton was dominated by populations of the picoplanktonic fraction (*Synechococcus*) in most samples, according also to chlorophyll α and primary production values. Picoplankton was exceeding 50% of the population in most cases, whereas nanophytoplankton contributed a significant portion of the population at stations influenced by the low-salinity Black Sea waters. *Synechococcus*, picophytoplankton and nanophytoplankton contributed significantly to the estimated total autotrophic biomass. The

seasonal vertical distribution of picophytoplankton was studied in the oligotrophic north-eastern Aegean Sea (eastern Mediterranean).

4.1.1. Study periods

The aim of the present thesis was to investigate the temporal and spatial distribution patterns of picophytoplankton species in relation to biological-physical factors. The thesis focuses on the two most important periods of the pelagic cycle in temperate areas: the spring bloom and late summer. The spring bloom represents the most intense period with new production, while the late summer is the culmination of the pelagic cycle with a peak in zooplankton biomass often co-occurring with blooms of large dinoflagellates. We assess population dynamics of picophytoplankton groups (<2 μ m diameter; *Prochlorococcus*, *Synechococcus*, and picoeukaryote).

4.2. Material and methods

4.2.1. Study area

The Aegean Sea acts as an intermediate area between the Eastern Mediterranean and the Black Sea. In the north, the important inflow of waters from the Black Sea (BSW) through the Dardanelles straits forms a surface layer of low salinity (<30). Highly saline (>38.8) waters of Levantine origin (LW), flow from the south to the north. The meeting of BSW and LW in the NE Aegean forms a major frontal system (salinity gradient >10) which is present all year round and its position is influenced by the prevailing winds. It has been proposed that hydrodynamical singularities (e.g. fronts, temporal transitions in vertical stability, etc.) can either promote or inhibit the production of large over small phytoplankton. The stations were split into three different groups representing three stages of the watermass (Table 4.1). The grouping of the stations was done based on the following parameters: physical characteristics (Zervakis *et al.*, 2000), nutrients and chl α and primary production (this paper).

4.2.2. Field sampling

The experimental work was performed at six stations (KA1, KA2, KA3, KA4, KA5, KA6) located in a transect crossing the Black Sea Water front in N. Aegean Sea (Fig. 4.1). Two

oceanographic cruises were undertaken in the north-eastern Aegean Sea area to assess the periods of (a) September 1999 with strong stratification (late summer-early autumn); and (b) April 2000 with relatively well-mixed (spring) water column conditions. The sampling strategy for phytoplankton pigments, primary production, biomass and community structure was similar for both cruises: a transect of hydrographic and biological stations perpendicular to the frontal axis provided basic information on the physical structure. During the second cruise in the northern Aegean Sea, due to weather conditions only six stations (instead of nine) were sampled. Detailed study on autotrophic picoplankton was performed at two stations of North Aegean Sea representing, the frontal region (KA6), where Black Sea and Aegean waters meet, and the region outside the front (KA1), where more oligotrophic conditions prevail. Water samples were collected from routine hydro casts using a CTD rosette sampler generally from the standard depths of 2, 10, 20, 50, 75, 100 and 120m throughout the euphotic zone. One of these depths was modified according to the DCM found from the in situ fluorometer (AQUATRACKA III) mounted on the CTD. Auxiliary measurements made at the time of sampling included temperature, salinity, nitrate, nitrite, phosphate, chlorophyll α , primary production and microplankton abundance. All stations were grouped according to their bottom depths. Stations with bottom depths <200, 200–1000 and >1000m (actually >2000 m) were designated as the shelf, slope and basin stations, respectively (Fig. 4.1; Table 4.1). In results comparing summer and winter, the shelf and slope stations were combined and designated as shelf-slope stations. During statistical analyses combining the results of four seasons, the few slope stations were omitted; the shelf stations were used only in seasonal comparisons. During each cruise two transects with chemical-biological sampling were carried out to study short-term dynamics (mesoscale) of the front. The positions were dependent on the hydrological structure. At each sampling station a CTD profile was carried out between 0 and 200m. Eight sampling depths between 0 and 100m were selected trying to collect water from the subsurface chlorophyll (SSCM) and the 37.5 salinity layers. For descriptive purposes the study area was divided into three “watermasses” types (Fig. 4.1) on the basis of distinct hydrographic properties (Table 4.1): the surface (BSW), intermediate (IW) and deep (DW) water mass. In order to investigate any influence of the water masses on picophytoplankton assemblage’s differentiation based on the T/S diagram. For the employment of the method, the composite T/S diagram for each

cruise was used. Comparison among areas of total abundance and biomass integrated values over the 0–100 m layer was tested by ANOVA.

4.2.3. Total and size fractionated chlorophyll α

Size fractionation has been used by ecologists to describe, in relative terms, the distribution and structure of marine organisms in pelagic ecosystems. Sieburth *et al.*, 1978 used this approach to sort plankton into size categories dividing numerous trophic compartments of plankton by using a spectrum of size classes. We adapted the terminology of Sieburth to our sizes classes, namely, picoplankton (0.2 to 1.2 μ m), nanoplankton (1.2 to 3 μ m), and microplankton (>3 μ m). *In situ* fluorescence was converted to chlorophyll α (Chl α) using a regression between the water column Chl α concentrations (mg Chl α m⁻³) from selected depths and *in situ* fluorescence measurements (Chl α =2.0740 \times Fluo (r^2 =+0.970, p <0.01, n =453) from and Chl α =1.7807 \times Fluo (r^2 =+0.960, p <0.01, n =466). Chl α concentrations were converted into carbon equivalents by applying the average conversion factor 50 for the all layers. The differences between the filters represent the three size classes studied. See Chapter 2 “General methods” (in this work).

4.2.4. Total and size fractionated primary production

Planktonic primary producers (phytoplankton) in oceans are responsible for approximately half of the world's annual primary production (carbon assimilation) and are thus a major component of the global carbon cycle (Field *et al.* 1998). Productivity measurements were carried out at 5 stations during 22–25 September 1999 and 1-4 April 2000. Water samples were collected from 6-7 depths (depends from station depth) within the euphotic layer (1% of surface PAR). Phytoplankton primary production was estimated using the standard ¹⁴C technique (Steemann-Nielsen, 1952) which has been modified according to (Ignatiades, 1988). Integrated chlorophyll α (Ichl α) and primary production (IPP) were calculated with trapezoidal method in the 0–100m layer. Daily production was obtained assuming a photoperiod of 12h (Bienfang *et al.*, 1984).

4.2.5. Microplankton stock measurements

Samples for the identification and enumeration of larger phytoplankton cells (>3 μm) were obtained from 3 standard depths of each station (including surface and DCM). Abundance of microplankton was determined using the Utermöhl technique (Utermöhl, 1958). Analysis was performed under inverted light microscope microscope (NIKON DIAPHOT) on 100ml of settled volumes.

4.2.6. Biomass-specific primary productivity (P/B)

The ratio ratio C:Chl α is determined from of carbon biomass against chlorophyll α concentration, and is used for converting chlorophyll α biomass into phytoplankton carbon. This ratio is expected to vary as a function of the light climate (phytoplankton cells contain less chlorophyll α in high light conditions, i.e. ratio C:Chl α is high(>100), and can be influenced by nutrients, especially N-availability. The biomass-specific primary productivity (P/B, $\mu\text{g C } (\mu\text{g Chl } \alpha)^{-1} \text{ h}^{-1}$) was calculated as the carbon fixation (P) per unit of chlorophyll α biomass (B).

4.2.7. Growth rate calculations

Growth, photosynthesis, and primary productivity are often considered synonymous and equivalent terms in phytoplankton ecology. For a single species under nutrient-saturated and steady-state growth, the relationship between growth and photosynthesis is fixed (Laws and Banister, 1980). The growth rate (μ) of phytoplankton is a fundamental biological property Smith *et al.*, 1999. The surface layer of the ocean governs the productivity, carbon transformations within the food web, nutrient utilization and export to depth. Over days to weeks, the growth of one taxon relative to another controls the species composition of the phytoplankton (in conjunction with group-dependent loss processes such as grazing), so knowledge of growth rates of individual groups within the phytoplankton as well as the phytoplankton assemblage as a whole is critical to our understanding of the biotic responses to environmental forcing. In order to estimate the specific growth rate (μ) of phytoplankton we combined the measurements of primary productivity and chlorophyll α integrated over the euphotic zone.

4.2.8. Flow cytometry

Prefiltered (100- μm mesh size net) water samples (4.5ml) were fixed with 2% paraformaldehyde and stored in liquid nitrogen until analysis. The samples were gently mixed and let sit in the dark at room temperature for 10 minutes before quick-freezing and storage in liquid nitrogen. In the laboratory the cryovials were stored at -80°C until flow cytometric analysis was performed (Trousselier *et al.*, 1995; Vaultot *et al.*, 1989). All the signals of the samples were calibrated against the same internal standard beads (2 μm Polysciences Fluoresbrite beads, cat.18604). Single cell analysis was run with a FACScan flow cytometry (Becton-Dickinson, at FTZ) equipped with argon laser (power-15mW, at 488nm). For each cell, five signals (Blanchot *et al.*, 1996) were recorded on 4-decade logarithmic scales: two light scatter (side scatter, SSC, and forward light scatter, FLS), and three fluorescences. The photomultipliers were set up to quantify: the red fluorescence (RF) from Chl α (wavelength $>650\text{nm}$), the orange fluorescence (OF) from phycoerythrin PE (564-606nm), and the green fluorescence (GF) from phycourobilin PUB (515-545nm), following Wood *et al.*, (1985) and Olson *et al.*, (1988). Each individual signal was stored in 'list mode' and analyzed with WinMidi software. The combination of fluorescence signals (phycoerythrin and chlorophyll α) with measurements of forward and side light scatter, allowed the enumeration of cyanobacteria (*Synechococcus*), prochlorophytes (*Prochlorococcus*) and eukaryotic phytoplankton. Autotrophic cells were separated into two groups of cyanobacteria (*Synechococcus* and *Prochlorococcus*) and two groups of picoeukaryotes based a their fluorescence and light scatter signal

4.2.9. Plankton conversion to biomass

The biovolumes of the planktonic organisms were calculated from the size measurements (Hillebrand *et al.*, 1999). Cell abundances were converted to biomass (carbon mg C m^{-3}) estimates using carbon-per-cell conversion factors (Menden-Deuer & Lessard 2000; Kana and Glibert, 1987; Campbell *et al.*, 1994).

4.2.10. Statistical analysis

The analysis of variance (ANOVA) was performed in order to search for significant differences in biological parameters (Chl α , picophytoplankton and nanophytoplankton cell

concentrations) among water masses. One-way ANOVA followed by Tukey's HSD, followed by *post-hoc* Student–Newman–Keuls (SNK) tests were employed to assess differences in picoplankton distribution between the three water masses considered and along the north–south gradient.

Using a Pearson correlation coefficient is was considered for testing of potential relationships between the phytoplankton stocks and production, as well as between hydrological and nutrient parameters with and picophytoplankton parameters. A positive correlation suggests that two variables vary in the same direction, while a negative correlation suggests that two variables vary in the opposite direction; *p*-values below 0.05 indicate a statistically significant correlation at the 95 percent confidence level.

4.3. Results

4.3.1 Hydrography

The distribution of the different water masses in the study area were mapped on the basis of salinity and temperature characteristics at the different layers of the water column using the criteria described detailed by Zervakis and Georgopoulos, 2002. The studied area was clearly divided by a thermohaline front which ran in a north-south direction, separating warmer and more saline waters at the southern side of the front from colder and less saline waters at the northern side (Fig. 4.1). The sampling stations were located at a frontal system, on the border between the continental shelf and continental slope. The water column is characterized (at most stations) by a thin surface layer (of 10-20 m thickness) containing water originating from the Dardanelles, i.e. modified Black Sea Water (BSW). Based on temperature and salinity data (T-S) characteristics (Fig. 4.2), three 'water masses' types can be distinguished (Table 4.2, Table 4.7): (I) the surface layer (10-20m) containing modified BSW; (II) the layer between 10 and 75m generally affected of very low salinity and appearing as a layer of mixing between the surface and the intermediate layer strongly influenced by LIW; (III) DW (deep water) highly saline water originating from the interaction of waters at these depths between the South and the North Aegean. During both seasons, the cruise covered three different water masses and one-way ANOVA results from these groups revealed statistically significant differences in the water column temperature (September:

$p < 0.05$; April: $p < 0.01$) and Salinity (September < 0.01 ; April: $p < 0.01$). Vertical profiles of temperature, salinity, nitrate and phosphate in the two contrasting hydrographical conditions are displayed in Fig. 4.3 for two representative stations (st. KA1-open station and st. KA6-front station). The southernmost station (st. KA1) is characterized by almost homogeneous vertically salinity, with high values (~ 39) characteristic of the South Aegean, while the northern part (st. KA6) exhibits low salinities (~ 33) indicating a large amount of water from the Black Sea at the surface. The deeper layers display very little horizontal variability, consisting mostly of water from the Levantine region. The presence of a frontal margin at station KA3 is indicated by the salinity and temperature distribution and suggests an upward flux of subsurface water at the front, and a stronger stratification at the shelf stations (st. KA4, KA5 and KA6). High-temperature ($> 21^{\circ}\text{C}$) and low –salinity (< 34) surface waters dominated the upper 40m of the water column at almost all the stations except for station KA1 and KA2 (Fig. 4.4). The average water column (0-100m) temperature and salinity for the study area was $18.85 \pm 0.60^{\circ}\text{C}$ and 37.85 ± 1.57 during summer (Tab. 4.3). During September cruise the three water masses differed significantly in temperature and salinity ($p < 0.05$; one-way ANOVA, $n=37$); with higher temperatures and low salinities in BSW waters and showed statistically significant differences at the 95.0% confidence level (SNK; $p < 0.05$; $\text{DW} > \text{LIW} > \text{BSW}$, salinity; $\text{BSW} > \text{LIW} > \text{DW}$, temperature). The contours of temperature and salinity are presented in Figure 4.4. We should point to the very small variation of salinity (from 38.90 to 39.01) throughout the highly stratified (due to temperature) water column. The 34 isohalin at a depth of 20m (Fig. 4.4), which is considered as an expression of the southernmost boundary of the front, delimits the maximum northward extension of BSW (Zervakis *et al.*, 2000, 2002).

During spring conditions, although salinities of surface waters across the shelf-slope and basin remained relatively consistent (31.5–35.9), surface temperature exhibited an onshore–offshore gradient ($11\text{--}14^{\circ}\text{C}$), with warmer waters offshore. The stations KA1 and KA2 (outside the front) are characterized by the absence of a thin, low-salinity surface layer of modified BSW that forms the Dardanelles plume in the North Aegean. The full height of the water column is occupied by a relatively homogeneous water column of highly saline, Levantine waters, and is away from strong horizontal fronts and the stratification is determined by temperature. Stations KA3 to KA6 (inside the front) on the other hand, within

the core of the BSW plume, and are characterized by very high stratification at the interface between low and high-salinity layers. The station KA6 in contrast to station KA1, is very highly stratified, and this stratification is salinity controlled. This is true especially for the top 20 meters, where (as seen in figure 4.4) there is cooler, less saline water lying on top of warmer water with higher salinity. The cool water at the surface has quite recently exited the Dardanelles, and has not warmed up yet due to the combined action of mixing and surface warming. Surface waters with a temperature of $<12.5^{\circ}\text{C}$ and low salinity (31-35) characterize the surface layer, between stations KA6 and KA2; these overlaid warmer ($12.5-14^{\circ}\text{C}$) and more saline (37-38.7), causing intense stratification (Fig. 4.4). Between stations KA6 and KA5, at the 15-30m depth, a core of water with temperatures of $11.6-12.2^{\circ}\text{C}$ was observed; these were lower than those of the overlying and underlying water layers. Station KA3 was the most representative frontal station. Stratification was not observed at station KA1, where the water column was well mixed. In April 2000 the average water column (0-100m) temperature and salinity was $13.53\pm 0.66^{\circ}\text{C}$, 37.52 ± 11.51 (Tab. 4.4). Like in summer, during the April cruise temperature and salinity values showed statistically significant differences between the three water masses ($p<0.05$; one-way ANOVA, $n=37$; (SNK; DW=LIW>BSW). The salinity values showed also statistically significant differences between the three water masses ($p<0.05$, SNK; DW=LIW>BSW).

4.3.2. Nutrients

In general higher nutrients values were recorded during the April cruise than in September. The vertical and seasonal distributions of the major nutrients are shown in Figure 4.4. During both seasons, the nitrate concentrations were higher inside the frontal area than outside whereas the phosphates and silicates presented a similar distribution throughout the area. Nitrate concentrations revealed statistically significant differences among sampling seasons (one-way ANOVA; $p<0.05$, $n=37$). In September surface waters showed nitrate concentrations below $\sim 2\ \mu\text{M}$ in the first 20 m of the water column (Fig. 4.4) inside frontal area (st. KA6) and relative high concentrations ($0.8\ \mu\text{M}$) at 80m depth. Outside the frontal area the nitrate concentrations remained low. The pattern of nitrate gradients along the transect was consistent with those of salinity (influence of BSW). So Pearson's correlation showed a significant relationship between salinity and nitrate (Pearson's $r = -0.43$, $p<0.05$).

April nitrate values showed high surface values ($\sim 1.5 \mu\text{M}$) at front stations (st. KA3) and a second maximum reaching $1.3 \mu\text{M}$ at 50 m (st. KA4). In general, the influence of BSW played a role in the pattern of nutrients distribution in the area during spring. Nitrate and phosphate correlated negatively with salinity (Pearson's $r = -0.41$, $r = -0.43$, respectively, $p < 0.05$). Phosphate concentrations were low and often undetectable $< 0.04 \mu\text{M}$ (detection limit at $\pm 0.02 \mu\text{M}$) in surface waters during both seasons (Fig. 4.4). The highest values ($\sim 0.07 \mu\text{M}$) were observed during September and April cruise inside the frontal area (st. KA3, KA4, KA5 and KA6) at the deeper layers (50-100m). During the September cruise, all three water masses sampled were not significantly different from one another with respect to nitrate concentrations. On the contrary in April 2000 BSW had a significantly higher content of nitrate than the LIW and DW water masses ($p < 0.05$, Kruskal–Wallis). During both cruises there were significant differences in phosphate concentrations ($p > 0.05$; one-way ANOVA) and between the three water masses. In September, the N/P ratio was higher inside the front and this difference was statistically significant (one-way ANOVA, $p < 0.05$), whereas in April the N/P ratio (Tab.4.4) was similar in inside and outside front and no statistical difference was detected (one-way ANOVA, $p > 0.05$).

4.3.3. Size-fractionated chlorophyll α

The vertical patterns of chlorophyll show two different conditions linked to hydrographical regimes. In September 1999 a well-defined DCM layer was seen at $\sim 60\text{m}$ depth. During spring the DCM layer was more at the upper layers ($\sim 40\text{m}$) with higher Chl α values. It must be reminded that there exists an almost permanent stratification throughout the year in the frontal region due to the less saline BSW inflow in the surface (0-20m). However station KA1 is characterized almost in absence of this thin less saline surface layer in both seasons. Total chl α concentration in the 0–100-m layer (Tab. 4.4) showed low mean values ($0.051 \pm 0.02 \text{ mgm}^{-3}$) in September increasing in April $0.405 \pm 0.09 \text{ mgm}^{-3}$.

In September the maximum concentration (0.105 mgm^{-3}) of surface Chl α was observed at station KA5 (frontal area). In general, the vertical distribution of Chl α was characterized by a surface maximum and a progressive decrease with depth (Fig. 4.6). Regarding the vertical distribution of the phytoplanktonic biomass (according to chlorophyll α) the most interesting

feature was a weak Deep Chlorophyll Maximum (50-75m) recorded at stations KA1, KA2 (outside or at the edges of the front), whereas at the remaining stations (inside front) the vertical distribution presented surface maxima (2-20m) and weaker DCMs, if at all with values $\sim 0.75 \mu\text{g.l}^{-1}$ (Fig. 4.6).

During spring along the transect, elevated chlorophyll- α concentrations ($>0.5 \mu\text{g l}^{-1}$) were recorded in the frontal stations (Fig. 4.5, 4.6) and all maxima were recorded in the surface layers with highest values $\sim 1.0 \mu\text{g.l}^{-1}$ (st. KA3). At stations where elevated chl α concentrations were recorded, picophytoplankton represented an important contributor ($>60\%$) to total chlorophyll concentrations (Fig. 4.6). At the regions of the elevated chl α concentrations, total chlorophyll concentrations were always dominated by the nano- and picophytoplankton size fractions, which contributed $\sim 90\%$ of the total (Tab. 4.5). However, microphytoplankton contributed up to $\sim 40\%$ of the total at most (Tab. 4.5).

Total integrated values were lowest during the summer period but frequently higher during spring. Total chlorophyll α concentration in the 0–100-m layer showed statistically significant differences in chlorophyll α concentration ($df=1$, $F= 42.13$, $p =0.0001$; one-way ANOVA, $n=37$) among sampling seasons. The chlorophyll maximum in September occurred at 50m, due of the homogenization the water column in contrast with April (stratification) DCM occurs at the upper layers (30–50 m).

The integrated $<3\mu\text{m}$ Chl α size fraction, corresponding to the nano-and picoplanktonic autotrophs, contributed much ($>60\%$) to the total Chl α concentration, was highly variable through the both seasons, but not between stations. The larger $>3\mu\text{m}$; microplankton, usually contributed only a small proportion ($\sim 30\%$) of the total Chl α .

Different size classes' contributions to the total chl α were observed during the two samplings (Tab. 4.5), characterized by an increasing dominance of pico-phytoplankton from summer ($66.40 \pm 7.60\%$, st. KA4) to spring ($61.60 \pm 2.10\%$, st. KA3). A constant contribution to total chl α is given by the nano-fraction ($29.10 \pm 5.80\%$, st. KA3 and $41.15 \pm 1.6\%$, st. KA4 in summer and spring, respectively). The large fraction (micro) accounting $31.30 \pm 2.00\%$, st. KA5 in September especially at the DCM and $39.70 \pm 0.10\%$, st. KA4 in April. Significant

correlations between fractions and chl α were found in September 1999 (nano: $r=0.60$, $p<0.05$; pico: $r=0.88$, $p<0.05$; $n=38$), except micro: $r=0.27$, $p>0.05$ and Apr (micro: $r=0.86$, $p<0.05$; nano: $r=0.37$, $p<0.05$; pico: $r=0.97$, $p<0.05$; $n=31$). Biomass showed (Fig. 4.8) highest values in spring (April 2000). Total euphotic layer integrated Chl α concentrations varied from 3.90 (st. KA5) to 6.70 (st. KA6) mg m^{-2} during the summer period and in spring ranged from 18.90 (st. KA1) to 31.60 (st. KA6) $\text{mg Chl } \alpha \text{ m}^{-2}$ (Fig. 4.8).

During summer the statistical analysis showed a weak negatively correlation with salinity ($r=-0.34$). In spring Chl α concentrations correlated negatively with salinity and temperature ($r=-0.70$, $r=-0.41$, respectively) and positively with nitrate ($r=0.36$) (Tab. 4.10).

4.3.4. Size-fractionated primary production

In summer the water column integrated phytoplankton production ranged between from $0.149\pm 0.03 \mu\text{gC l}^{-1} \text{ h}^{-1}$ in the open sea and $0.486\pm 0.05 \mu\text{gC l}^{-1} \text{ h}^{-1}$ in the frontal area. During spring, the phytoplankton production was found to be also higher in the frontal area compared with the stations in the open sea (Tab. 4.4).

Only the constitution of the micro-fraction to the total PP rates showed a statistically significant difference between the two seasons (ANOVA: micro- $F=4.37$, $p<0.05$) but not the other two fractions (pico, $p>0.05$; nano, $p>0.05$). As expected the size fractions were also correlated with the total PP in both seasons (September: pico- $r=0.98$, $p<0.05$; nano- $r=0.91$, $p<0.05$; micro- $r=0.93$, $p<0.05$; $n=38$ and April pico- $r=0.98$, $p<0.01$; nano- $r=0.95$, $p<0.05$; micro- $r=0.96$, $p<0.05$; $n=31$). Integrated daily primary production (IPP) showed in September mean integrated value of $174.95\pm 0.09 \text{mgCm}^{-2} \text{ d}^{-1}$ (st. KA1) to $442.37\pm 0.05 \text{mgCm}^{-2} \text{ d}^{-1}$ (st. KA5) and during April ranged from $190.84\pm 0.02 \text{mgCm}^{-2} \text{ d}^{-1}$ (st. KA2) and $512.04\pm 1.90 \text{mgCm}^{-2} \text{ d}^{-1}$ (st KA6) (Tab. 4.5).

The contribution of the size fractions to total PP rates was no different during the two periods the pico- and nano fractions were the dominating fractions. In September the mean contribution to total PP showed a predominance of pico- and nano-classes ($67.90\pm 9.80\%$, st. KA5 and $44.04\pm 2.70\%$, st. KA1) with respect to micro- ($29.50\pm 2.0\%$, st. KA1). In April the pico-

fraction accounted for $51\pm 20\%$ (st. KA2) and nano fraction for $38.45\pm 6.90\%$ (st. KA1) of total PP, and thus were also the dominant size classes, whereas micro-phytoplankton contributed $51.80\pm 1.30\%$ to total PP (Tab. 4.5).

The distribution of total phytoplankton biomass relative to the front along the transect provide, a context for the interpretation of productivity rates measured in spring (April) and summer (September) (Fig. 4.8). Depth-integrated primary (^{14}C) productivity exceeded $1\text{mgCm}^{-3}\text{h}^{-1}$ at two stations in the frontal region (st. KA5, KA6) and were lower in the outer shelf (st. KA1 and KA2) during both seasons. Different vertical patterns of mean PP were observed during the contrasting periods. Profiles were constructed for two representative stations in the area (Fig. 4.5). These stations were selected on the basis of their surface water properties, vertical structure and geographic location. In September homogeneous PP rates close to $0.30\text{mgCm}^{-3}\text{h}^{-1}$ were found at 0–60m, decreasing downwards to a minimum of $0.16\text{mgCm}^{-3}\text{h}^{-1}$. In April the mean PP showed a vertical pattern characterized by two peaks: maximum of $>1\text{mgCm}^{-3}\text{h}^{-1}$ at the surface and a secondary maximum at $\sim 40\text{m}$ ($0.81\text{mgCm}^{-3}\text{h}^{-1}$) and the minimum PP rate ($0.05\text{mgCm}^{-3}\text{h}^{-1}$) was observed at 80m. Phytoplanktonic primary production showed high values during both seasons, which were slightly lower during summer than spring. Surface maxima (0–20m) of primary production were recorded during both seasons (Fig. 4.7). PP showed a seasonal pattern close to that of Chl α (Fig. 4.5). In Figure 4.8 integrated daily primary production (IPP) exhibited maxima during both seasons. In September 1999 total primary production values ranged from $174.95\pm 0.09\text{mgCm}^{-2}\text{d}^{-1}$ (st. KA1) to $442.37\pm 0.05\text{mgCm}^{-2}\text{d}^{-1}$ (st. KA5) and most of the photosynthetic rate was due to the picoplankton fraction that showed a clear temporal variability. The values of primary production in April ranged from $190.84\pm 0.02\text{mgCm}^{-2}\text{d}^{-1}$ (st. KA2) and $512.04\pm 1.90\text{mgCm}^{-2}\text{d}^{-1}$ (st. KA6) (Tab. 4.5, Fig. 4.8). The statistical analysis showed a negatively correlation with salinity ($r=-0.71$) in September and a positive correlation with temperature ($r=0.63$) and a weak temporal relationship with chlorophyll α , indicating a relationship of higher phytoplankton biomass with high productivity (Tab. 4.11). In April 2000 primary production correlated negatively with salinity ($r=-0.75$) and positive with phosphate and chlorophyll α ($r=0.43$ and $r=0.58$, respectively) (Tab. 4.11).

4.3.5. Picoplankton abundances

The following groups of picophytoplankton were distinguished by flow cytometry (i.e. *Synechococcus*, *Prochlorococcus*, picoeukaryotes, and nanoeukaryotes); according to their distinctive autofluorescence and different light scatter properties. The vertical distribution of picoplankton abundances in the upper 100m of each group varied independently according to depth and location (Fig. 4.10) along the transect in North Aegean Sea during both seasons.

Changes in *Synechococcus*, *Prochlorococcus*, picoeukaryotes, and nanoeukaryotes abundance with depth in relation to chlorophyll and salinity are shown in (Fig. 4.13) for selected stations of the transect located in open sea (st. KA1) and in frontal area (st. KA6). This figure illustrates that the majority of the *Synechococcus* and picoeukaryotes cells were accumulated at the surface mixed layer.

On the offshore side of the front (st. KA1), these two groups showed also uniform distributions in the upper part of water column but tended to diminish with depth beneath the pycnocline. Picoeukaryotes and nanoeukaryotes showed slightly higher concentration in surface well-mixed waters on the offshore side across the front relative to the near shore waters, and a reduction in abundances was found beneath the pycnocline. The cyanobacteria abundances, increase at the surface in contrast with the prochlorophytes, which were observed at deeper layers. The vertical pattern of *Synechococcus* in September showed a maximum of $>120 \times 10^3 \text{ cells ml}^{-1}$ at $\sim 20\text{m}$ depth in frontal area (st. KA6) and an abrupt downwards decrease in DCM ($4 \times 10^3 \text{ cells ml}^{-1}$). The picoplankton distribution in frontal area was similar to that of *Synechococcus*, with highest mean abundances in correspondence at surface ($12 \times 10^3 \text{ cells ml}^{-1}$) and at DCM depth (80m) ($4 \times 10^3 \text{ cells ml}^{-1}$) (Fig. 4.10) and the integrated abundances ranged from $17.71 \pm 6.60 \times 10^3$ (st. KA1) to $47.31 \pm 9.60 \times 10^3 \text{ cells ml}^{-1}$ (st. KA6) (Tab. 4.6). Vertical distributions of *Synechococcus* cell concentrations demonstrated opposite patterns to those of *Prochlorococcus*, with the bulk of the cells located within the mixed layer. *Prochlorococcus* populations have in higher abundances at the southern edge of the front (st. KA1) with $23.58 \times 10^3 \text{ cells ml}^{-1}$ (st. KA1) in

50m depth, when a temperature of 17⁰C and a nitrate concentration at surface layer of 0.60μMol.

Prochlorococcus concentrations began to increase at nitracline (30m) and deeper where the highest concentrations were observed (Fig. 4.10). Subsurface maxima of picoeukaryotes at station KA1 were found just below the thermocline, at the deeper layers (at 50m depth, nitracline). Their integrated concentrations ranged between $2.91 \pm 0.95 \times 10^3$ and $3.11 \pm 0.95 \times 10^3$ cells.ml⁻¹. The appearance of these subsurface maxima of eukaryotic phytoplankton coincided with high *Prochlorococcus* concentrations in the mixed layer. Nanoeukaryotes concentrations were low in the whole water column and their concentrations uniformly distributed at both stations (KA1 and KA6) during September and April.

During September 1999 at station KA6 increased concentrations of cyanobacteria and picoplankton were observed at the surface and subsurface layer (0-20m). Prochlorophytes were distributed at the whole column, whereas cyanobacteria dominated in most samples at the surface.

During spring along the transect, picoplankton abundances as estimated by flow cytometer ranged from $1.50 \pm 0.70 \times 10^3$ (st. KA2) and $4.90 \pm 0.30 \times 10^3$ cells.ml⁻¹ (st. KA5) (Tab.4.6). Elevated picoeukaryotes abundances were recorded at surface layers (0-25m) of the frontal stations (Fig. 4.10) and gradually decrease with depth. Nanoeukaryotes concentrations were $\sim 1.5 \times 10^3$ cells.ml⁻¹ and showed maximum concentrations at 50m depth (st. KA3). *Synechococcus* and eukaryotic picophytoplankton were the numerically dominant autotrophic groups with maxima at 50m usually. *Prochlorococcus* abundances showed maximum concentrations at the upper 40m ($\sim 8.00 \times 10^3$ cells.ml⁻¹), when temperature was 15⁰C and decreased nitrate concentrations. During April station KA6 the total picoeukaryotes cell number showed an increase at the surface layer and integrated concentrations ranged between 1.50×10^3 and 4.90×10^3 cells.ml⁻¹. *Synechococcus* and eukaryotic picoplankton cells number coincided with that of chlorophyll maxima at 50m. *Synechococcus* showed low concentrations at surface layer and maximum cell abundances at 45m depth were detected below a rapid decrease with depth.

For descriptive purposes the study area was divided into three zones on the basis of distinct hydrographic properties (Tab. 4.2 and 4.8). *Synechococcus* dominated picophytoplankton in the zones under a marked influence of the low salinity BSW and reached maximum numbers in September ($90.33 \times 10^3 \text{ cells ml}^{-1}$) in the frontal area (Tab. 4.9). Their abundance remained high in spring ($10.64 \times 10^3 \text{ cells ml}^{-1}$). The presence of *Prochlorococcus* in surface waters was confined to DW with high salinity. Although it was also detected with increased values during summer in LIW waters ($9.36 \times 10^3 \text{ cells ml}^{-1}$) and it was significantly correlated with salinity ($r=0.64$, $p<0.05$). Conversely, relatively low abundances of both groups of autotrophic eukaryotes, usually below $4 \times 10^3 \text{ cells ml}^{-1}$, were found in the LIW and DW zones. The distribution patterns of small and large eukaryotes were rather similar, although an increase was observed of the both groups (pico and nano) during spring and summer in BSW water.

4.3.6. Phytoplankton community composition based on light microscopy

In September in the surface waters diatoms abundances ranged from 1.0 to $2.0 \times 10^3 \text{ cells ml}^{-1}$ along all stations of the transect and diatoms' highest counts were observed at 50m depth (st. KA2) from 2.0 to $4.0 \times 10^3 \text{ cells ml}^{-1}$. Dinoflagellates' highest counts were found in the deeper layers (60-80m) of stations KA3, KA4, KA5 and KA6 (frontal area) $\sim 5.0 \times 10^3 \text{ cells.ml}^{-1}$ (Fig. 4.9, 4.11). The highest concentrations of autotrophic flagellates ($1-1.6 \times 10^3 \text{ cells ml}^{-1}$) were noted at 60-80m at front. During summer phytoplankton community was dominated by diatoms (*Hemiaulus hauckii*, *Thalassionema mediterranea*, *Leptocylindrus danicus*, *Rhizosolenia alata*, *Chaetocerus decipiens*, *Pseudonitzschia longissima*, *Pseudonitzschia seriata*, *Rhizosolenia fragilissima*, *Skeletonema costatum*), dinoflagellates (*Torodinium robustum*, *Amphidinium sp.*, *Gymnodinium sp.*, *Peridinium excentricum*, *Gyrodinium fissum*), autotrophic nanoflagellates (*Rhabdosphaera hispida*, *Coccolithus Huxley*, *Calyptosphaera globosa*, *Chlamydomonas sp.*, *Cryptomonas acuta*).

In April 2000 phytoplankton community was dominated by diatoms (*Rhizosolenia alata*, *Rhizosolenia fragilissima*, *Rhizosolenia stegiraa*, *Skeletonema costatum*, *Thalassiothrix frauenfeldii*, *Thalassionema nitzschioides*, *Bacteriastum delicatulum*, *Leptocylindrus minimus*, *Ditylum brigetweigthi*, *Leptocylindrus danicus*), dinoflagellates (*Prorocentrum micans*,

Gymnodinium sp.), autotrophic nanoflagellates (*Pontosphaera haeckeli*, *Syracosphaera corii*, *Calyptrorphaera globosa*, *Cryptomonas acuta*).

4.3.7. Autotrophic carbon biomass

Mean carbon contents during the two cruises are reported in Table 4.7 and Figure 4.11 for the different picophytoplankton groups. In September the biomass of autotrophic picoplankton in the euphotic zone (integrated 0-100m) varied from $938.38 \pm 42.1 \text{ mgCm}^{-2}$ (st. KA1) to $1661.94 \pm 105.6 \text{ mgCm}^{-2}$ (st. KA6) in September. The mean carbon contents of large-phytoplankton cells were lower and ranged from $57.03 \pm 4.8 \text{ mgCm}^{-2}$ (st. KA1) to $249.34 \pm 10.6 \text{ mgCm}^{-2}$ (st. KA3). During spring the picophytoplankton carbon contents varied between $426.00 \pm 65.4 \text{ mgCm}^{-2}$ (st. KA2) and $1301.75 \pm 125.4 \text{ mgCm}^{-2}$ (st. KA6). The mean carbon contents large-phytoplankton were higher than in September with concentrations from $320.75 \pm 18 \text{ mgCm}^{-2}$ (st. KA1) to $735.40 \pm 65.2 \text{ mgCm}^{-2}$ (st. KA3). Biomass exceeding $>100 \text{ mgCm}^{-2}$, observed in spring, were due to higher abundances of microphytoplankton, which consisted mainly of diatoms and dinoflagellates. The contribution of picophytoplankton to autotroph biomass was high ($>50\%$) throughout both sampling periods. The major picophytoplankton taxa, such as cyanobacteria and eukaryotic picophytoplankton, were almost equal in carbon contents (Fig. 4.11). The statistical analysis (Pearson's correlation) in September showed a positive correlation between *Synechococcus* biomass with temperature ($r=0.35$; $p<0.05$). Positive correlations were found between picoeukaryotes and nanoeukaryotes biomasses with nitrate ($r=0.60$, $r=0.40$, respectively). In April picoeukaryotes and nanoeukaryotes carbon contents were correlated negatively with salinity ($r=-0.69$ and $r=-0.58$, respectively) and positively with phosphate and total chlorophyll. Statistically significant differences were observed in mean biomass (Fig. 4.14) of the different picoplankton groups between zones (ANOVA, $p<0.05$). The relative contribution of *Synechococcus* and picoeukaryotes to total picoplanktonic biomass was significantly higher in the BSW and LIW zones (ANOVA, $p<0.05$).

4.3.8. Total and size fractionated C:Chl α –ratios

We calculated C:Chl- α ratios for size fractionated Chl- α concentrations ($>3\mu\text{m}$ and $<3\mu\text{m}$) for two depths (surface and DCM) measured during the two cruises (Tab.4.10). The values were

higher at surface waters than at the DCM in all the surveys for the $>3\mu\text{m}$ fraction. On a temporal scale, lowest average C:Chl- α ratio was observed in April either at the surface or at the DCM. We calculated C:Chl- α ratios using total and size fractionated and Chl- α concentrations and phytoplankton biomass measured in both seasons. In September total C:Chl- α ratios ranged from 32 to 193 $\text{mgC mg Chl } \alpha^{-1}$ in the surface and from 44 to 106 $\text{mgC mg Chl } \alpha^{-1}$ in the DCM. Size-fractionated C:Chl- α ratios in the surface ranged between 2 and 18 for $<3\mu\text{m}$ phytoplankton, and between 32 and 193 for the $>3\mu\text{m}$. In the DCM, C:Chl- α ratios varied between 4 and 9 in the $<3\mu\text{m}$ size fraction and between 35 and 106 in the $>3\mu\text{m}$ size fraction. Averaged C:Chl- α ratios (Tab. 4.10) were significantly higher in the surface and in the DCM and in both fractions ($>3\mu\text{m}$ and $<3\mu\text{m}$). During April total C:Chl- α ratios ranged from 12 to 66 $\text{mgC mg Chl } \alpha^{-1}$ in the surface and from 22 to 76 $\text{mgC mg Chl } \alpha^{-1}$ in the DCM. Size-fractionated C:Chl- α ratios in the surface ranged between 8 and 21 for $<3\mu\text{m}$ phytoplankton, and between 9 and 123 for the $>3\mu\text{m}$. In the DCM, C:Chl- α ratios varied between 9 and 39 in the $<3\mu\text{m}$ size fraction and between 32 and 135 in the $>3\mu\text{m}$ size fraction. Averaged C:Chl- α ratios (Tab. 4.10) were significantly higher in DCM than at surface in both fractions ($>3\mu\text{m}$ and $<3\mu\text{m}$).

4.3.9. Phytoplankton growth rates

Growth rates in both fractions picophytoplankton ($>3\mu\text{m}$ and $<3\mu\text{m}$) were $\sim >0.5 \text{ d}^{-1}$ at the surface of the two stations during September. In April 2000 growth rates were higher in the $<3\mu\text{m}$ fraction at st. KA6 (frontal area). In general μ was higher at station KA6, where also the highest phytoplankton biomass was observed, than at station KA1 in summer and spring. In September total growth rates ranged from 0.03 to 0.24 d^{-1} in the surface and from 0.01 to 0.06 d^{-1} in the DCM. Size-fractionated growth rates in the surface ranged between 0.08 and 1.25 d^{-1} for $<3\mu\text{m}$ phytoplankton, and between 0.01 and 0.38 d^{-1} for the $>3\mu\text{m}$. In the DCM, growth rates varied between 0.16 and 0.66 d^{-1} in the $<3\mu\text{m}$ size fraction and between 0.001 and 0.02 d^{-1} in the $>3\mu\text{m}$ size fraction. During April total growth rates ranged from 0.08 to 0.82 d^{-1} in the surface and from 0.09 to 0.28 d^{-1} in the DCM. Size-fractionated growth rates in the surface ranged between 0.16 and 0.61 for $<3\mu\text{m}$ phytoplankton, and between 0.01 and 0.96 d^{-1} for the $>3\mu\text{m}$. In the DCM, growth rates varied between 0.01 and 0.37 d^{-1} in the $<3\mu\text{m}$ size fraction and between 0.005 and 0.06 d^{-1} in the $>3\mu\text{m}$ size fraction. Averaged

growth rates (Tab. 4.10) were significantly higher at surface than in DCM in both fractions (>3 μm and <3 μm) in summer and spring.

4.3.10. Carbon standing-stocks and production of autotrophic picophytoplankton

Figure 14 provides a description of the autotrophic planktonic food web in North Aegean Sea, based on carbon stocks (mgCm^{-2}) and production ($\text{mgCm}^{-2}\text{d}^{-1}$) during two contrasting oceanographic situations: September (late summer) and April (spring). Values presented in the figures are average values for all stations of each sampling area. During September, high rates of total pp were associated with high standing stocks, contributed mainly by the pico- and nanophytoplankton size class. In late summer, the water column integrated phytoplankton production was found higher in the frontal region ($362.50 \pm 7.90 \text{ mgC m}^{-2} \text{ day}^{-1}$) compared with the non-frontal stations ($190.20 \pm 13.00 \text{ mgC m}^{-2} \text{ day}^{-1}$). The contribution of the small fraction <3 μm to the total phytoplankton production was 84.40 ± 4.1 and $71.10 \pm 3.4\%$ for frontal and oceanic stations, respectively. In spring, the total phytoplankton production was high in both regions ($336.30 \pm 52.20 \text{ mgC m}^{-2} \text{ day}^{-1}$ frontal and $210.90 \pm 28.35 \text{ mgC m}^{-2} \text{ day}^{-1}$ oceanic). Almost 61.60 ± 9.40 and $67.30 \pm 3.60\%$ of the total phytoplankton production was due to cells <3 μm in the frontal and oceanic regions, respectively.

4.4 Discussion

4.4.1. Seasonal variability of Chl α concentration

The picoplankton abundance in the ocean, Agawin *et al.*, (2000a) account globally for 39% of the total primary production but only 24% of the total biomass. Our observations suggest that in our system picophytoplankton are quantitatively more important, both in terms of biomass (71%) and productivity (56%). The dominance of *Synechococcus* during this study supports the suggestion that *Synechococcus* is better adapted than *Prochlorococcus* to the hydrodynamical and nutrient conditions of the eastern Mediterranean. Regardless of the importance of each phytoplankton size fraction at the three stations, the overall pattern was a high percentage of small cells (picoplankton) in the upper layers of the photic zone while the largest cell sizes (nano- and microplankton) tended to increase their abundance with depth. Nutrient concentrations in the upper layers of the water column of the transect ranged from low to almost non-detectable (Fig. 4.5, 4.10, 4.11); under these conditions, as

commented above, small organisms would perform better than large ones. In this study one environmental variable – salinity – was especially well correlated with most of the measured variables (Tab. 4.11) such as nutrients, phytoplankton abundances (i.e. chl α) and the most abundant phytoplankton group (i.e., picophytoplankton), especially in surface waters. An increased biomass and abundance of phytoplankton appeared to be connected with the permanent hydrographic front. Because of its small size and relatively large surface to volume ratio, *Synechococcus* (Arin *et al.*, 2002) is able to grow at low nutrients. Motile organisms in the upper nanoflagellate size range could increase their nutrient uptake through swimming, by renewing the nutrient-depleted water surrounding the cell (Kiørboe, 1993), or by taking advantage of their motility to approach nutrient patches. Below 70m, where low irradiance would prevent significant photosynthetic activity (Moran and Estrada, 2001), high concentrations of nanoplankton and microplankton could be the consequence of sedimentation of senescent cells or of advection of water bodies entrained from shallower depths. Phytoplankton larger than 2 μm in diameter were most important in temperate zones. It is in these regions that the presence of diatoms have been shown to be significant (Marañón *et al.*, 2000). Overall, our size-fractionated chl α data support previous reports indicating that cyanobacteria and small flagellates are the dominant biomass component in the pelagic microbial communities. According to several studies, the extremely oligotrophic character of the Eastern Mediterranean Sea is mainly due to phosphorus depletion (Krom *et al.*, 1991, 1993; Kucuksezgin *et al.*, 1995) but it has also been attributed to nitrogen limitation (Ignatiades and Moschopoulou, 1988; Dugdale and Wilkerson, 1988). The levels of phosphorus and nitrogen found in this study (Tab. 4.4) are comparable to those reported above, thus confirming the poverty of both nutrients in the Aegean Sea. In this oligotrophic environment, the overall average level of chl α ranged from 0.0045 to 0.422 mg m^{-3} (Tab. 4.3) and that of primary production from 0.149 to 0.700 $\text{mgCm}^{-3} \text{h}^{-1}$ (Tab. 4.3).

These estimates approach the values given for the Eastern Mediterranean (Azov, 1986, 1991; Berman *et al.*, 1986) as well as for other oligotrophic areas of the tropical N. Atlantic (Claustre and Marty, 1995) and the equatorial Pacific (Everitt *et al.*, 1990) There are many studies on the phytoplankton composition and seasonal succession in the north-eastern Mediterranean coast of Turkey (Polat *et al.*, 2000). However, investigation on phytoplankton biomass and size distribution of phytoplankton is very scarce (Polat, 2006). Previous studies

on phytoplankton size classes in oligotrophic environments show a high contribution of small sizes to total biomass (Magazzu and Decembrini, 1995; Ignatiades *et al.*, 2002; Polat, 2006). On the contrary, in this study, the contributions of small and large size fractions to the total chlorophyll α were found to be similar. This situation is most probably due to high nutrient supply in the area since these conditions support the development of larger species as well as small ones. For a better understanding of the structure of phytoplankton communities in marine environments, more specific studies are required on the temporal and spatial distribution of small size classes. High picophytoplankton and low nanophytoplankton abundances were evident in all the water masses defined for the area (Tab. 4.9).

In general, Chl α $<3\mu\text{m}$ represented ca. 70% of total phytoplankton biomass. Furthermore, considering all data, Spearman rank correlations evidenced that Chl α was significantly ($r=0.55$; $p<0.05$) correlated with total $<3.0\mu\text{m}$ (picophytoplankton and nanophytoplankton) cell concentration. This high correlation is produced by picophytoplankton abundance ($r=0.56$; $p<0.05$), while no significant correlation was found for nanophytoplankton. So, it can be concluded that picophytoplankton dominated the total phytoplankton community at all studied stations. The dominance of *Synechococcus* of picophytoplankton fraction during this study supports the suggestion that *Synechococcus* would be more adapted than *Prochlorococcus* to the hydrodynamical and nutrient conditions of the eastern Mediterranean (Partensky *et al.*, 1999).

Differences in the C:Chl α ratio were observed in relation to depth, the nutrient gradient along the stations and the phytoplankton size class. Lower values of the ratio (for the total and the two fractions considered) were found below 30m depth, presumably as a consequence of a high Chl α concentration per cell due to photoacclimation (Jensen and Sakshaug, 1973; Latasa *et al.*, 1992) and lower carbon content of cells grown at light intensities (Thompson *et al.*, 1991). In general, in this study, the C:Chl α ratio increased with cell size. According to Malone (Malone, 1980), the existence of correlations between chlorophyll per cell and surface area and between carbon content per cell and volume should result in an increase of the C:Chl α ratio with cell size.

Phytoplankton size structure plays a major role in the carbon budget of microbial pelagic communities (Legendre and Le Fèvre, 1989). Theoretical models relate the export potential of pelagic ecosystems to their trophic structure. Typically, small-sized phytoplankton (<3µm) form the basis of the microbial food web, characterized by the recycling of organic matter within the ecosystem. In contrast, large phytoplankton (>3µm) sustain the classical food chain, which favours the export of organic matter either to adjacent systems or to upper trophic levels.

In Figure 15 we try to establish carbon flux budgets for the non-frontal and frontal stations and for both seasons with emphasis on autotrophic picophytoplankton. The size structure and distribution of picophytoplankton in the pelagic ecosystem of North Aegean Sea imply that most carbon is fixed by picoplankton during both seasons and throughout the study area. Small-sized (<3µm) primary producers dominated in the northern Aegean Sea. From few measurements of the carbon flow in the northern Aegean Sea most of the autotrophic carbon biomass (almost 80%) and primary production (75%) was due to small-sized cells (<3 µm), (Siokou *et al.*, 2002). These primary producers are not grazed efficiently by copepods, but they are consumed by nano- and micro-heterotrophs (Zervoudaki *et al.*, 2007). In both seasons, phytoplankton production of the smaller cells was sufficient to cover the carbon demand of nano- and micro-heterotrophs. This illustrates the importance of the microbial food web as a link between the carbon fixed by small autotrophs and zooplankton (Zervoudaki *et al.*, 2007).

Table 4.1.: Sampling dates, location and water depth of stations during the two cruises in Aegean Sea.

Station no.	September 1999	DCM	April 2000	DCM	Position (lat./long.)	Depth (m)
KA1	22.09.99	85m	01.04.00	35m	39 ⁰ .2572' N, 25 ⁰ .4378' E	300m
KA2	24.09.99	70m	02.04.00	20-40m	39 ⁰ .4000' N, 25 ⁰ .4500' E	120m
KA3	25.09.99	70m	03.04.00	2-10m	39 ⁰ .4667' N, 25 ⁰ .4498' E	85m
KA4	25.09.99	70m	04.04.00	20m	39 ⁰ .5120' N, 25 ⁰ .4493' E	80m
KA5	26.09.99	60m	04.04.00	50m	39 ⁰ .5419' N, 25 ⁰ .4499' E	80m
KA6	27.09.99	50m	06.04.00	45m	39 ⁰ .5855' N, 25 ⁰ .4499' E	80m

Table 4.2.: Salinity and temperature characteristics of waters masses in North Aegean Sea during the cruises (according Zervakis and Georgopoulos, 2002).

	Acronym	Density	Salinity
Black Sea Water	BSW	<28	36.00 ≤ S ≤ 33.00
Levantine Intermediate Water	LIW	>28-29.2	36.50 ≤ S ≤ 38.00
North Aegean Deep Water	NADW	>29.2	38.20 ≤ S ≤ 39.50

Table 4.3.: Summary of environmental parameters during September 1999 and April 2000.

	September 1999		April 2000	
	Open sea	Frontal area	Open sea	Frontal area
Salinity	38.96±0.03	36.74±2.70	38.59±0.70	36.45±2.80
Temperature (°C)	18.38±2.0	19.32±1.75	13.99±0.30	13.06±1.00
Density	28.20±0.51	26.33±2.70	28.928±0.60	27.62±1.86
NO ₃ (μM)	0.57±0.17	0.68±0.36	0.697±0.275	0.900±0.30
PO ₄ (μM)	0.032±0.006	0.03±0.01	0.045±0.007	0.053±0.01
N/:P	18±5	23 ±3	16±7	17±5
SiO ₄ (μM)	1.89±0.26	1.79±0.70	1.472±0.28	1.355±0.45
Chl α (μg l ⁻¹)	0.045±0.02	0.06±0.020	0.218±0.15	0.422±0.31
PP (μgC.l ⁻¹ .h ⁻¹)	0.149±0.03	0.486±0.05	0.203±0.02	0.700±0.08
Fluorescence	0.052±0.03	0.087±0.057	0.148±0.10	0.22±0.06

Table 4.4.: Spatial variations of the water column integrated salinity [ISal], temperature [ITemp] ($^{\circ}\text{C}$), primary production IPP ($\text{mgC}\cdot\text{m}^{-3}\cdot\text{h}^{-1}$), chlorophyll α (IChl α , $\text{mg}\cdot\text{mg}^{-3}$), nitrate concentration [INO₃] (μM), phosphate concentration [IPO₄], surface water salinity [Sal-s], water temperature Temp-s, chlorophyll α concentrations [Chl α -s] (mgm^{-3}), primary production PP-s ($\text{mgC}\cdot\text{m}^{-3}\cdot\text{h}^{-1}$), nitrate concentrations [NO₃-s] (μM), phosphate concentration [PO₄-s] depth of euphotic zone D_{eu} (m), station depth (m) in Aegean Sea during September 1999 and April 2000.

Stations-Seasons	Sep 1999	Apr 2000	Sep 1999	Apr 2000	Sep 1999	Apr 2000						
Variables	KA1		KA2		KA3		KA4		KA5		KA6	
Chl α -s	0.019	0.150	0.040	0.289	0.040	1.347	0.058	0.840	0.105	0.430	0.077	0.917
IChl α	0.051 \pm 0.02	0.160 \pm 0.03	0.055 \pm 0.00	0.302 \pm 0.05	0.078 \pm 0.01	0.371 \pm 0.08	0.070 \pm 0.00	0.368 \pm 0.02	0.050 \pm 0.001	0.256 \pm 0.02	0.086 \pm 0.01	0.405 \pm 0.09
IPP	0.127 \pm 0.08	0.200 \pm 0.08	0.171 \pm 0.15	0.207 \pm 0.15	0.413 \pm 0.35	0.506 \pm 0.35	nm	nm*	0.603 \pm 0.60	0.485 \pm 0.60	0.531 \pm 0.50	1.111 \pm 0.50
Sal-s	38.979	38.758	38.906	36.482	33.815	31.159	31.986	34.577	30.549	31.065	33.049	31.517
ISal	38.97 \pm 0.02	38.80 \pm 0.02	38.95 \pm 0.16	38.73 \pm 0.95	38.44 \pm 2.25	38.52 \pm 2.90	37.85 \pm 2.75	37.93 \pm 1.66	37.33 \pm 3.65	36.92 \pm 3.00	37.09 \pm 2.72	37.15 \pm 2.89
Temp-s	20.893	14.482	20.106	14.109	20.303	11.696	22.469	12.671	21.481	12.082	22.853	12.699
ITemp	17.86 \pm 2.38	13.95 \pm 0.26	17.93 \pm 1.60	13.80 \pm 0.27	18.19 \pm 1.80	13.78 \pm 0.89	18.48 \pm 2.83	13.51 \pm 0.75	18.50 \pm 3.17	12.82 \pm 1.15	19.35 \pm 3.52	13.00 \pm 1.06
NO ₃ -s	0.744	0.532	0.425	1.219	0.760	1.203	0.864	1.336	0.602	1.127	1.864	1.199
INO ₃	0.633 \pm 0.10	0.627 \pm 0.01	0.52 \pm 0.05	0.760 \pm 0.20	0.37 \pm 0.04	0.568 \pm 0.06	0.85 \pm 0.09	1.159 \pm 0.10	0.56 \pm 0.04	0.535 \pm 0.01	0.79 \pm 0.07	1.016 \pm 0.30
PO ₄ -s	0.031	0.041	0.031	0.041	0.025	0.052	0.025	0.058	0.025	0.069	0.031	0.075
IPO ₄	0.036 \pm 0.01	0.043 \pm 0.01	0.029 \pm 0.00	0.048 \pm 0.01	0.035 \pm 0.01	0.040 \pm	0.027 \pm 0.01	0.056 \pm 0.01	0.031 \pm 0.00	0.031 \pm 0.01	0.031 \pm 0.01	0.054 \pm 0.03
N:P	18	14	18	17	12	14	32	21	20	12	27	20
Deu	86,110m	35m	68,95m	20-40m	70m	10m	70m	20m	60m	50m	50m	45m
Depth	300m		120m		85m		80m		80m		80m	

Differences between regions at the 5% significance level are indicated by different superscripts (Student-Newman-Keuls test, $p < 0.05$). If the same; nm* : Not measured

Table 4.5.: Mean and integrated chlorophyll α [chl α (mgm^{-2})] and primary production [PP ($\text{mgCm}^{-2}.\text{d}^{-1}$)] observed in the Aegean Sea during September 1999 and April 2000.

St	September 1999				April 2000			
	IChl α	Micro (%)	Nano (%)	Pico (%)	IChl α	Micro (%)	Nano (%)	Pico (%)
KA1	6.10 \pm 0.02	24.70 \pm 3.15	10.40 \pm 4.80	64.90 \pm 1.80	18.90 \pm 0.13	33.40 \pm 1.50	41.15 \pm 1.60	25.50 \pm 9.00
KA2	6.50 \pm 0.02	22.45 \pm 0.50	16.60 \pm 6.40	60.90 \pm 5.50	29.60 \pm 0.15	39.50 \pm 4.48	22.90 \pm 3.00	37.60 \pm 1.90
KA3	6.50 \pm 0.02	26.10 \pm 2.80	29.10 \pm 5.80	44.70 \pm 8.05	30.80 \pm 0.10	20.90 \pm 1.60	17.50 \pm 7.10	61.60 \pm 2.10
KA4	5.45 \pm 0.01	21.70 \pm 1.60	11.90 \pm 0.90	66.40 \pm 7.60	28.70 \pm 0.20	39.70 \pm 0.10	26.50 \pm 1.00	33.70 \pm 1.40
KA5	3.90 \pm 0.03	31.30 \pm 2.00	17.35 \pm 3.70	51.35 \pm 1.60	20.00 \pm 0.14	29.50 \pm 5.40	18.20 \pm 4.20	52.30 \pm 0.20
KA6	6.70 \pm 0.02	14.20 \pm 9.10	21.80 \pm 1.50	64.00 \pm 4.50	31.60 \pm 0.20	26.50 \pm 1.00	17.00 \pm 8.30	56.40 \pm 2.50
St	IPP	Micro (%)	Nano (%)	Pico (%)	IPP	Micro (%)	Nano (%)	Pico (%)
KA1	174.95 \pm 0.09	29.50 \pm 2.00	44.00 \pm 2.70	26.50 \pm 5.70	230.90 \pm 0.01	33.50 \pm 2.40	38.45 \pm 6.90	28.00 \pm 4.50
KA2	199.90 \pm 0.05	20.10 \pm 9.70	20.40 \pm 3.80	59.50 \pm 9.60	190.80 \pm 0.02	36.30 \pm 5.70	12.40 \pm 3.00	51.20 \pm 7.90
KA3	288.90 \pm 0.05	18.75 \pm 2.30	22.20 \pm 7.80	59.10 \pm 9.20	251.57 \pm 0.07	51.80 \pm 1.30	21.10 \pm 4.70	27.10 \pm 1.00
KA5	442.40 \pm 0.05	12.20 \pm 5.30	19.90 \pm 5.30	67.90 \pm 9.80	245.50 \pm 0.06	46.20 \pm 5.00	15.40 \pm 8.20	38.30 \pm 9.20
KA6	359.60 \pm 0.04	19.20 \pm 6.50	18.70 \pm 7.80	62.10 \pm 3.60	512.00 \pm 1.90	27.85 \pm 2.80	28.90 \pm 9.30	43.25 \pm 4.30

Table 4.6.: Mean cell abundance of autotrophic picoplankton abundance $\text{cells}(\times 10^3 \text{ml}^{-1})$ at each station in September 1999 and April 2000.

Stations	Sep 1999				Apr 2000			
	Syn	Pro	Pico	Nano	Syn	Pro	Pico	Nano
KA1	17.70 \pm 6.60	7.40 \pm 0.80	2.90 \pm 0.95	0.20 \pm 0.10	13.70 \pm 0.90	1.40 \pm 0.50	3.50 \pm 0.50	0.60 \pm 0.03
KA2	0.00	0.00	0.00 \pm	0.00	3.25 \pm 1.70	0.70 \pm 0.09	1.50 \pm 0.70	0.20 \pm 0.10
KA3	0.00	0.00	0.00	0.00	13.60 \pm 2.05	5.65 \pm 0.40	3.60 \pm 0.50	1.00 \pm 0.30
KA4	0.00	0.00	0.00	0.00	8.15 \pm 4.20	1.40 \pm 0.20	4.05 \pm 0.60	0.40 \pm 0.20
KA5	0.00	0.00	0.00	0.00	8.00 \pm 2.45	2.00 \pm 0.50	4.90 \pm 0.30	0.80 \pm 0.03
KA6	47.30 \pm 9.60	8.50 \pm 5.10	3.10 \pm 0.90	0.40 \pm 0.08	8.80 \pm 1.90	0.90 \pm 0.95	3.80 \pm 0.20	1.20 \pm 0.40

Table 4.7.: Carbon content (mgCm^{-2}) of pico-phytoplankton and large-phytoplankton main groups at each station in September 1999 and April 2000.

September 1999														
St	Diatoms	%	Dinos	%	ANF	%	Syn	%	Pro	%	Pico	%	Nano	%
KA1	28.10±1.00	3.40±0.30	23.15±0.80	2.20±1.80	0.60±0.10	0.09±0.10	182.50±6.60	19.00±3.40	76.70±7.80	9.90±0.40	631.10±1.80	60.60±10.20	48.00±0.10	4.90±1.50
KA2	21.10±1.80	19.70±1.90	134.85±0.90	78.60±2.60	0.60±0.40	1.80±0.80	nm	0.00	nm	0.00	nm	0.00	nm	0.00
KA3	172.40±0.90	70.30±3.10	76.30±0.75	29.40±6.90	0.65±0.50	0.30±0.20	nm	0.00	nm	0.00	nm	0.00	nm	0.00
KA4	76.50±0.60	40.89±5.45	124.45±0.80	58.70±5.30	0.70±0.70	0.40±0.06	nm	0.00	nm	0.00	nm	0.00	nm	0.00
KA5	39.10±0.90	25.80±1.50	124.50±1.70	73.30±11.90	1.10±0.50	0.90±0.04	nm	0.00	nm	0.00	nm	0.00	nm	0.00
KA6	45.40±0.95	3.80±0.60	92.30±0.40	13.80±1.10	14.50±0.20	1.30±0.20	946.15±59.60	31.50±3.90	35.90±5.10	4.60±0.90	606.90±5.00	37.50±9.45	73.00±0.20	7.60±0.35

April 2000														
St	Diatoms	%	Dinos	%	ANF	%	Syn	%	Pro	%	Pico	%	Nano	%
KA1	189.30±0.80	13.40±3.20	107.10±0.45	9.40±6.05	24.30±0.20	1.20±0.10	342.40±2.20	21.90±3.20	7.40±0.03	0.60±0.30	727.35±5.30	45.40±3.80	109.30±0.90	8.10±0.10
KA2	246.50±2.00	25.70±5.50	236.50±2.00	24.20±8.80	27.60±0.20	3.70±1.00	103.40±0.40	10.75±0.70	4.25±0.02	0.60±0.09	275.60±0.20	29.70±5.50	42.70±2.10	5.40±0.20
KA3	378.60±7.90	16.40±6.80	240.40±0.50	7.00±4.10	116.50±0.30	3.15±0.60	788.40±1.40	21.90±6.80	56.00±0.25	1.06±0.50	1578.85±3.60	44.20±1.30	200.90±1.90	6.30±0.55
KA4	101.70±1.10	7.80±2.40	196.90±0.70	19.50±0.60	40.10±0.40	4.50±0.50	159.75±1.20	13.70±5.70	3.90±0.030	13.70±5.70	617.00±8.70	0.30±0.13	121.35±0.60	45.20±6.40
KA5	152.35±2.10	12.70±7.50	196.00±1.70	16.30±2.80	12.70±0.25	0.80±0.60	147.70±1.40	11.20±0.15	10.90±0.15	0.80±0.60	823.55±12.70	48.35±2.50	131.60±1.90	10.00±1.00
KA6	175.60±1.20	15.00±8.40	134.10±2.40	10.30±4.40	17.70±0.30	1.00±0.05	317.70±1.50	24.20±12.50	4.00±0.05	0.30±0.07	792.60±15.20	39.10±1.20	187.50±5.05	10.10±0.80

Table 4.8.: Mean values and (\pm SD) of physical, chemical and biological parameters found in the two recognized oceanographic periods at different water masses (nitrate concentration [NO_3 , μM], phosphate concentration [PO_4 , μM], chlorophyll α concentrations [$\text{Chl}\alpha$, ($\mu\text{g l}^{-1}$)] and primary production in [$\text{mg C m}^{-2} \text{d}^{-1}$].

	Summer			Spring		
	BSW	LIW	DW	BSW	LIW	DW
Salinity [ISal]	34.512 \pm 2.20	38.953 \pm 0.04	38.965 \pm 0.04	35.052 \pm 2.80	38.542 \pm 0.70	38.617 \pm 0.30
Temperature [ITemp]	21.865 \pm 1.20	18.511 \pm 1.85	16.550 \pm 0.40	12.593 \pm 1.00	13.985 \pm 0.30	13.746 \pm 0.20
Nitrate [INO_3]	0.775 \pm 0.40	0.594 \pm 0.20	0.635 \pm 0.20	0.895 \pm 0.30	0.747 \pm 0.30	0.853 \pm 0.30
Phosphate [IPO_4]	0.028 \pm 0.00	0.034 \pm 0.01	0.031 \pm 0.01	0.053 \pm 0.01	0.048 \pm 0.01	0.049 \pm 0.01
Chlorophyll [$\text{IChl } \alpha$]	0.070 \pm 0.02	0.060 \pm 0.02	0.044 \pm 0.02	0.547 \pm 0.30	0.262 \pm 0.10	0.161 \pm 0.10
Primary production [IPP]	62.50 \pm 2.00	45.40 \pm 8.70	41.40 \pm 7.30	54.70 \pm 4.40	46.60 \pm 3.80	20.60 \pm 5.30
N:P	28 \pm 14	18 \pm 7	21 \pm 7	17 \pm 5	16 \pm 7	17 \pm 6

Table 4.9.: Mean $\bar{\pm}$ SE autotrophic picoplankton abundance in the three watermasses during the cruises.

Cells ($\times 10^3 \text{ ml}^{-1}$)	Sep-99			Apr-00		
	BSW	LIW	DW	BSW	LIW	DW
Syn	90.30 \pm 6.00	9.90 \pm 8.80	16.10 \pm 7.70	10.60 \pm 4.60	8.70 \pm 5.20	5.90 \pm 1.00
Pro	4.90 \pm 0.60	9.40 \pm 0.90	0.80 \pm 0.75	2.20 \pm 0.07	1.80 \pm 0.90	1.10 \pm 1.10
Pico	6.90 \pm 0.80	3.20 \pm 1.60	0.80 \pm 0.40	7.80 \pm 0.02	2.40 \pm 1.50	1.80 \pm 0.05
Nano	0.50 \pm 0.00	0.30 \pm 0.20	0.08 \pm 0.02	1.50 \pm 0.80	0.50 \pm 0.40	0.50 \pm 0.60

Table 4.10.: Averaged values (\pm SD) of C:Chl- α ratios (mgCmgChl^{-1}) and growth rate $\mu(\text{d}^{-1})$ (in surface and in the DCM layer for each size fraction).

		Total fraction		>3 μm fraction		<3 μm fraction	
		Surface	DCM	Surface	DCM	Surface	DCM
summer	C:Chl-α ratio	112 \pm 17	79 \pm 8	109 \pm 69	77 \pm 5	10 \pm 1	6 \pm 4
	$\mu(\text{d}^{-1})$	0.085 \pm 0.006	0.031 \pm 0.003	0.018 \pm 0.002	0.008 \pm 0.009	0.665 \pm 0.029	0.412 \pm 0.056
spring	C:Chl-α ratio	32 \pm 2	46 \pm 5	50 \pm 4	69 \pm 3	14 \pm 5	24 \pm 3
	$\mu(\text{d}^{-1})$	0.424 \pm 0.030	0.092 \pm 0.001	0.267 \pm 0.097	0.024 \pm 0.025	0.378 \pm 0.060	0.107 \pm 0.020

Table 4.11.: Matrix of correlation coefficients for environmental variables including salinity, temperature (Temp, °C), nitrate, phosphate concentration (NO_3 , PO_4 , $\mu\text{Mol.l}^{-1}$), total chlorophyll α concentration ($\text{Chl}\alpha$ -tot, $\mu\text{g.l}^{-1}$), size-fractionated chlorophyll α concentration [$\text{Chl}\alpha > 3\mu\text{m}$, $\text{Chl}\alpha$ -Pico and $\text{Chl}\alpha$ -Nano], total primary production (PP-tot, $\mu\text{gC.l}^{-1} \text{h}^{-1}$), size-fractionated primary production [$\text{PP} > 3\mu\text{m}$, PP-Pico and PP-Nano], phytoplankton and picoplankton cells ($\text{ce} \times 10^3 \text{cells.ml}^{-1}$) obtained September 1999 and April 2000.

		September 1999															
	Sal	Tem	NO_3	PO_4	$\text{Chl}\alpha$ -tot	$\text{Chl}\alpha > 3$	$\text{Chl}\alpha$ -Pico	$\text{Chl}\alpha$ -Nano	PPtot	PP->3	PP-Pico	PP-Nano	ce Phy	ce Syn	ce Pro	ce Pico	
Tem	-0.75																
NO_3	-0.42	0.26															
PO_4	0.17	-0.10	0.18														
$\text{Chl}\alpha$-tot	-0.34	0.26	0.21	0.10													
$\text{Chl}\alpha > 3\mu\text{m}$	-0.10	-0.04	0.16	-0.12	0.27												
$\text{Chl}\alpha$-Pico	-0.31	0.29	0.29	0.12	0.88	0.02											
$\text{Chl}\alpha$-Nano	-0.18	0.12	-0.14	0.09	0.60	-0.11	0.30										
PP-tot	-0.71	0.63	0.34	-0.10	0.34	0.25	0.19	0.27									
PP->3μm	-0.65	0.70	0.24	-0.06	0.30	0.21	0.18	0.23	0.93								
PP-Pico	-0.73	0.57	0.37	-0.13	0.34	0.26	0.18	0.29	0.98	0.87							
PP-Nano	-0.58	0.70	0.25	0.05	0.30	0.17	0.22	0.19	0.91	0.92	0.84						
Euk. >3 μm	0.19	-0.22	-0.24	0.29	0.24	0.10	0.05	0.48	-0.07	-0.09	-0.06	-0.08					
ce Syn	-0.22	0.31	0.22	0.03	0.22	-0.07	0.25	0.13	0.23	0.28	0.17	0.34	-0.07				
ce Pro	0.13	-0.02	0.10	0.22	0.25	0.08	0.35	-0.11	-0.02	0.09	-0.08	0.12	0.15	0.25			
ce Pico	-0.17	0.21	0.62	0.22	0.10	-0.04	0.14	0.02	0.37	0.36	0.35	0.40	0.01	0.44	0.43		
ce Nano	-0.05	0.14	0.41	0.36	0.14	-0.04	0.18	0.02	0.18	0.23	0.13	0.27	0.01	0.62	0.59	0.81	

Table 4.11.: (continued)

April 2000																
	Sal	Tem	NO ₃	PO ₄	Chl α -tot	Chl α ->3	Chl α -Pico	Chl α -Nano	PPtot	PP->3	PP-Pico	PP-Nano	ce Phy	ce Syn	ce Pro	ce Pico
Tem	0.76															
NO ₃	-0.42	-0.21														
PO ₄	-0.40	-0.11	0.45													
Chl α -tot	-0.70	-0.41	0.36	0.26												
Chl α ->3 μ m	-0.58	-0.24	0.52	0.37	0.85											
Chl α -Pico	-0.72	-0.49	0.30	0.24	0.96	0.73										
Chl α -Nano	-0.08	0.09	-0.03	-0.10	0.34	0.23	0.18									
PP-tot	-0.75	-0.31	0.27	0.43	0.58	0.59	0.58	-0.02								
PP->3 μ m	-0.78	-0.37	0.32	0.38	0.67	0.66	0.65	0.04	0.96							
PP-Pico	-0.65	-0.28	0.27	0.45	0.53	0.54	0.53	-0.07	0.98	0.90						
PP-Nano	-0.62	-0.231	0.15	0.37	0.47	0.47	0.46	-0.03	0.95	0.88	0.92					
Euk. >3 μ m	-0.35	-0.22	-0.23	0.03	0.37	0.23	0.36	0.27	0.45	0.38	0.46	0.49				
ce Syn	0.04	-0.01	-0.42	-0.27	0.23	0.08	0.19	0.43	0.09	0.06	0.09	0.15	0.84			
ce Pro	-0.04	-0.13	-0.22	-0.27	0.03	-0.07	0.03	-0.01	0.05	0.03	0.05	0.05	0.45	0.29		
ce Pico	-0.67	-0.39	0.13	0.42	0.43	0.37	0.44	0.04	0.67	0.60	0.69	0.67	0.74	0.32	0.14	
ce Nano	-0.52	-0.19	0.08	0.38	0.38	0.33	0.41	-0.06	0.83	0.71	0.85	0.85	0.64	0.26	0.11	0.80

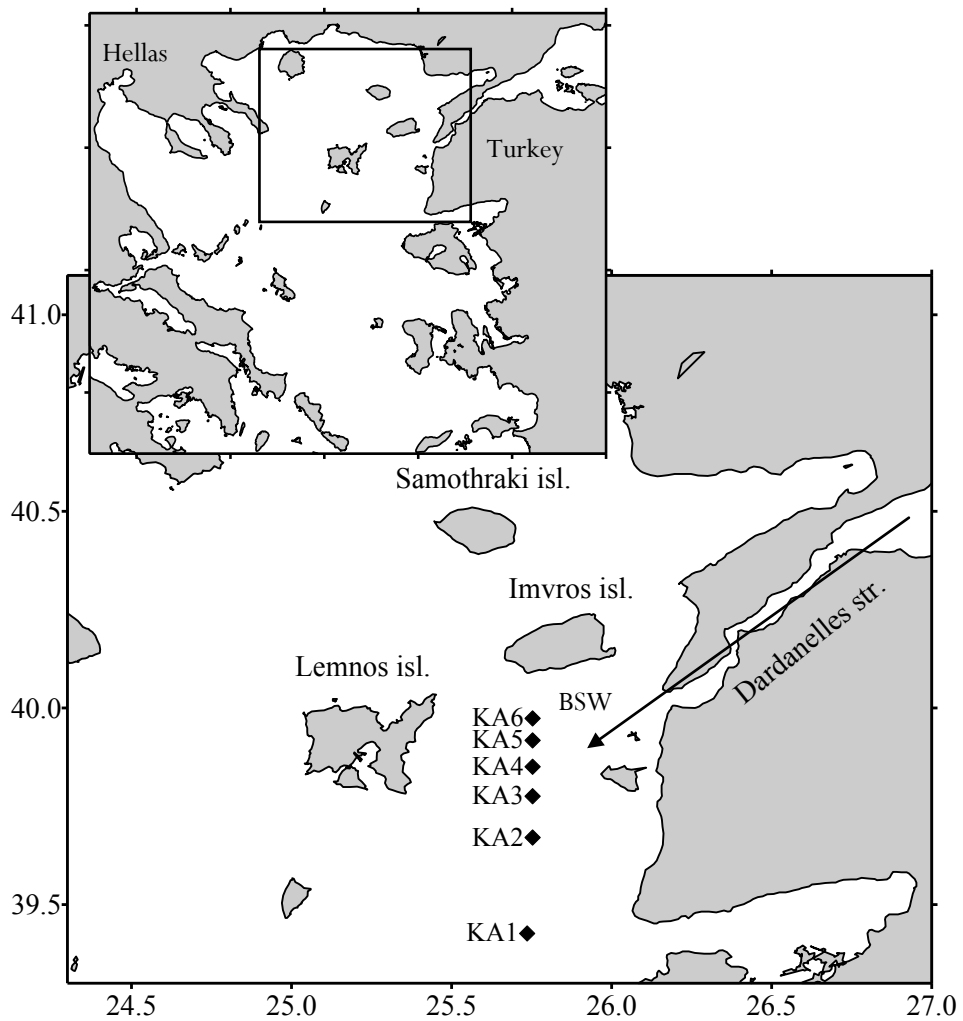


Figure 4.1.: Maps showing the locations of the stations sampled during September 1999 and April 2000 in north-eastern Aegean Sea.

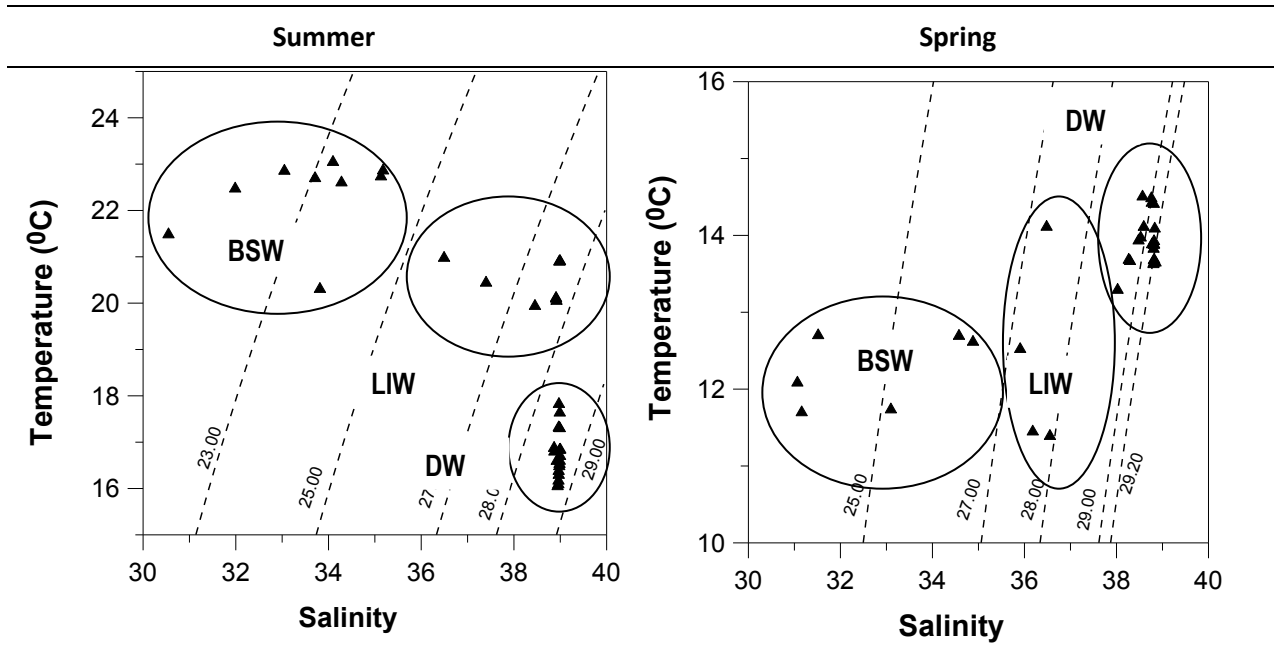


Figure 4.2.: T/S diagram showing water masses found in the study area: Black Sea Water (BSW), Levantine Intermediate Water (LIW) and North Aegean Deep Water (NADW).

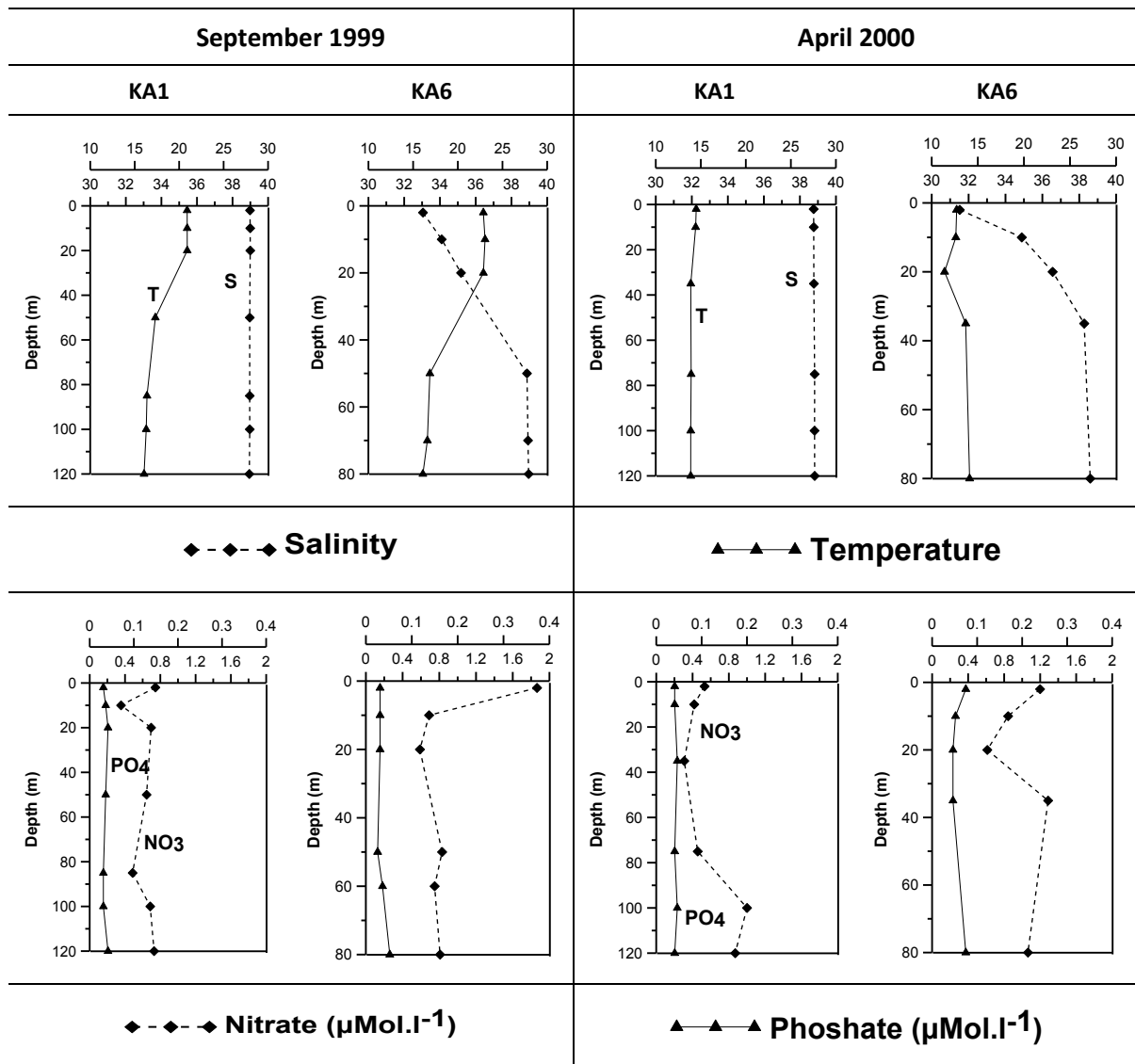


Figure 4.3.: Representative vertical profiles at stations KA1 (open station) and KA6 (front station) of salinity, temperature ($^{\circ}\text{C}$), nitrate ($\mu\text{M}\cdot\text{l}^{-1}$) and phosphate ($\mu\text{M}\cdot\text{l}^{-1}$) during September 1999 and April 2000.

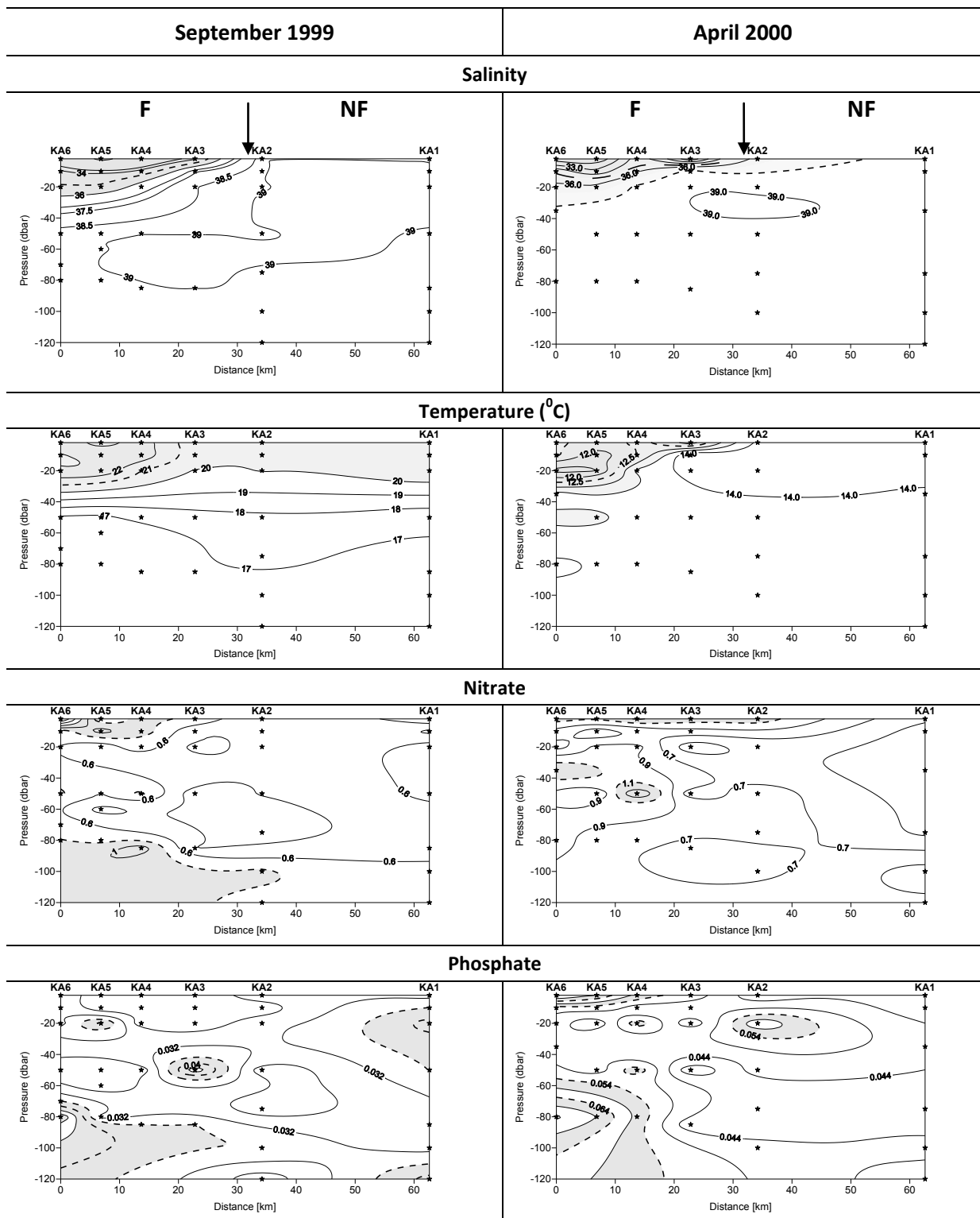


Figure 4.4.: Vertical distribution of salinity, temperature ($^{\circ}$ C), nitrate concentrations (NO_3^- , μM^{-1}) and phosphate concentrations (PO_4^- , $\mu\text{M.l}^{-1}$) along the transect during September 1999 and April 2000. The location of front is with a vertical arrow labelled. Dashed line represents thermoclines. Sampling depths are represented as dots.

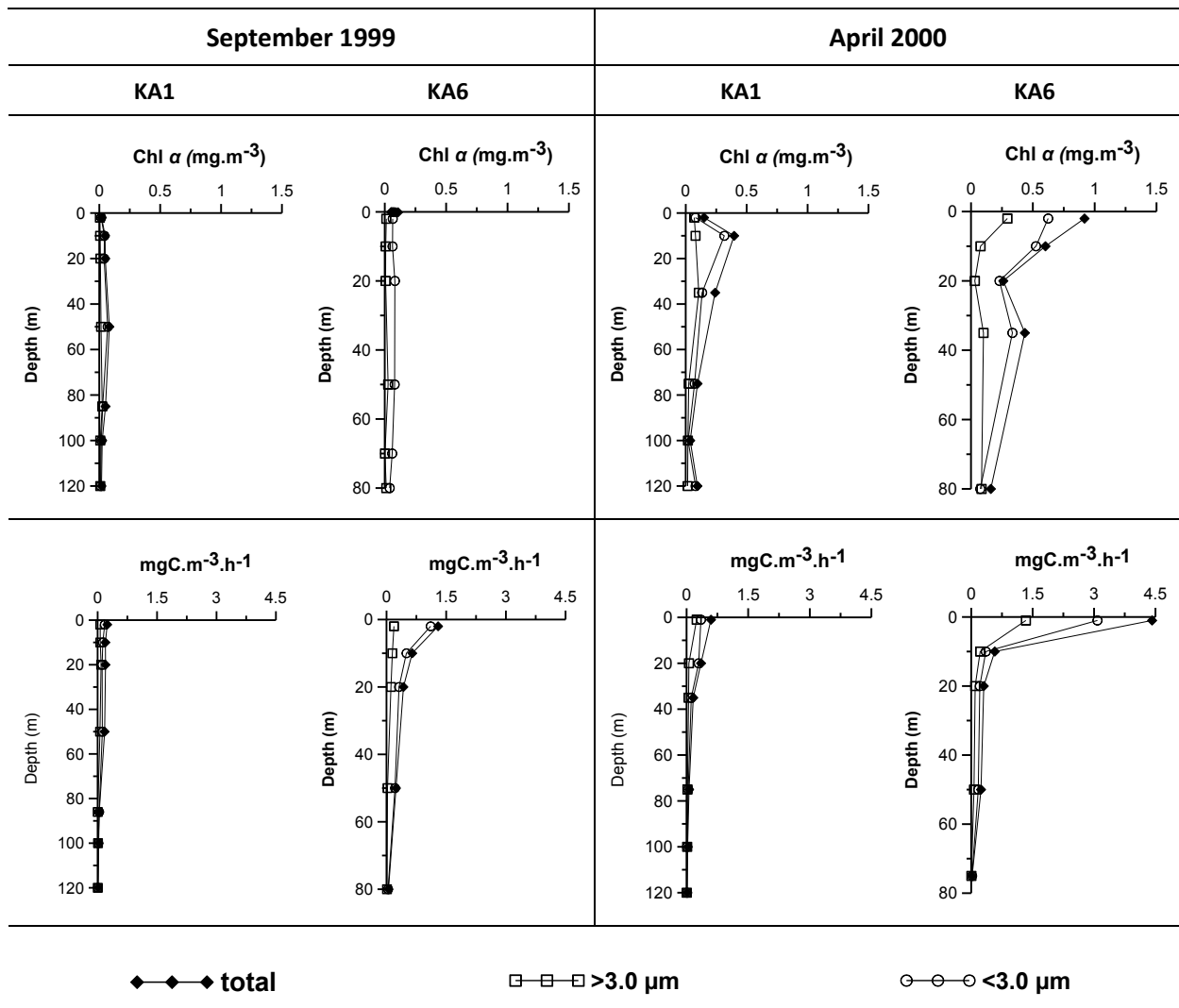


Figure 4.5.: Representative vertical profiles at stations KA1 (open station) and KA6 (front station) of chlorophyll concentrations ($\text{mg}\cdot\text{m}^{-3}$) and primary production ($\text{mg}\cdot\text{C}\cdot\text{m}^{-3}\cdot\text{d}^{-1}$), of each size class the community [total- $0.2\mu\text{m}$, pico and nanoplankton ($<3.0\mu\text{m}$) and micro- ($>3.0\mu\text{m}$)] during September 1999 and April 2000.

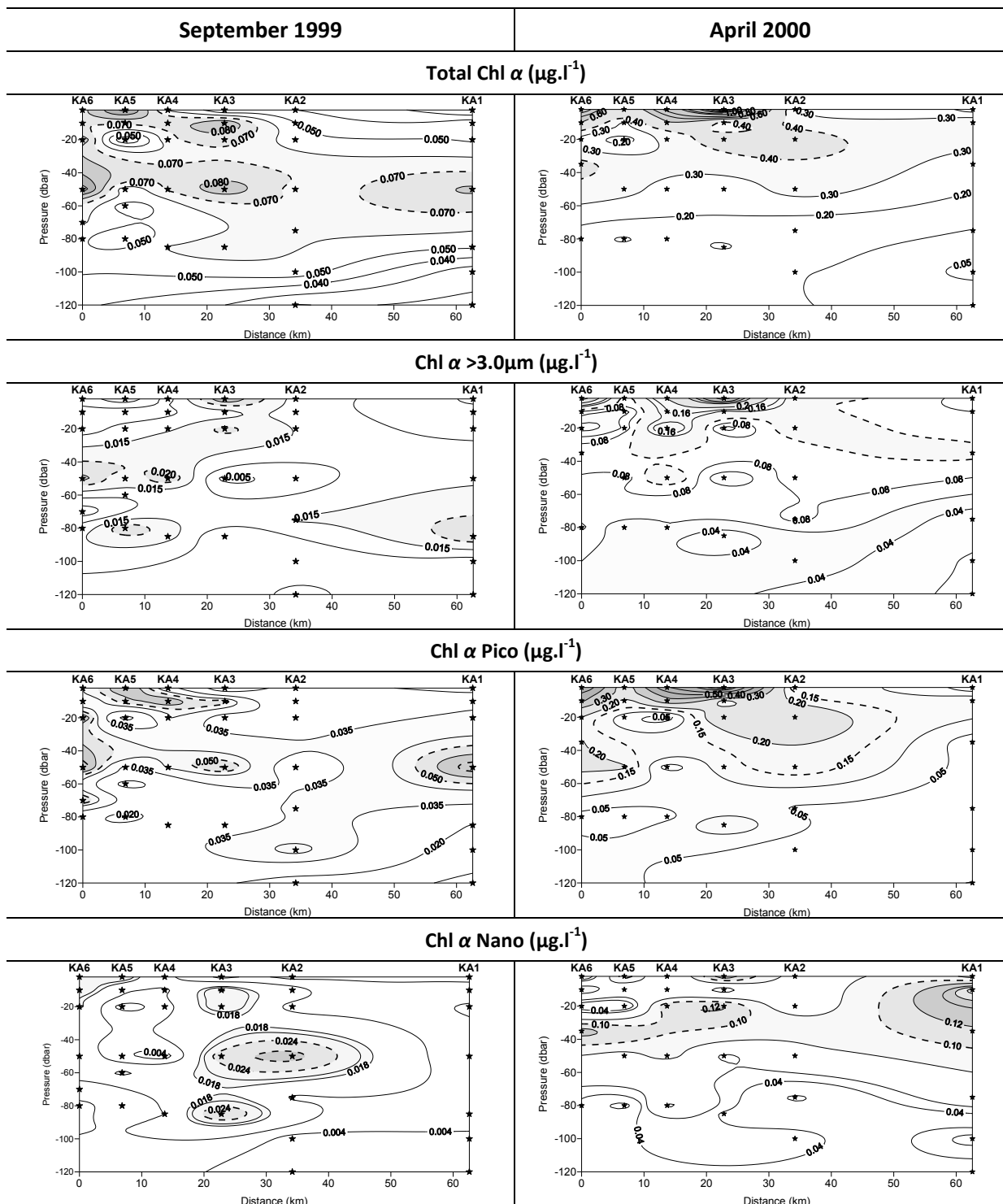


Figure 4.6.: Vertical distribution of chlorophyll α ($\mu\text{g l}^{-1}$) total and size-fractionated (>3 μm , Pico and Nano) along the transect during September 1999 and April 2000.

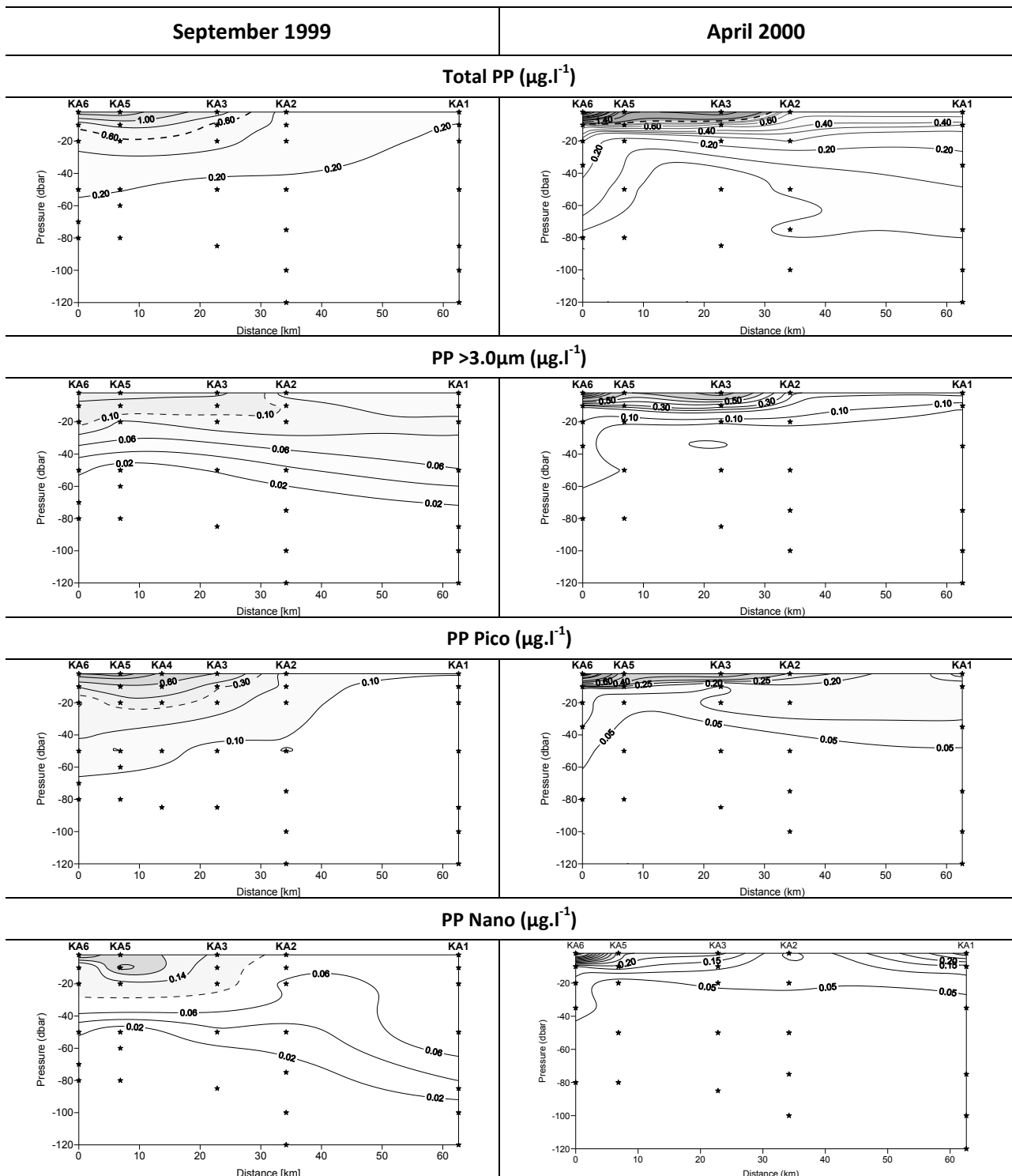


Figure 4.7.: Vertical distribution of primary production ($\text{mgC.m}^{-3} \cdot \text{h}^{-1}$) total and size-fractionated ($>3\mu\text{m}$, Pico and Nano) along the transect during September 1999 and April 2000.

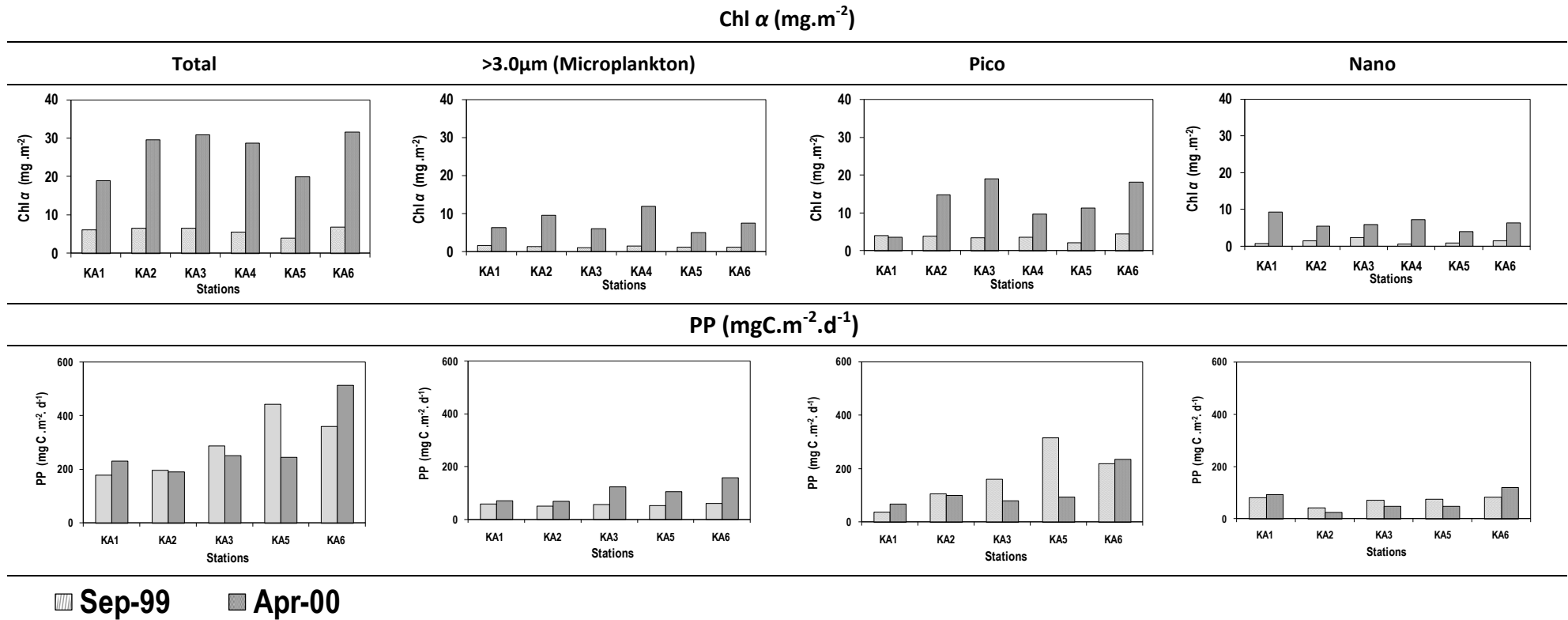


Figure 4.8.: The seasonal averages of the euphotic zone calculated integrated chlorophyll α ($\text{mg} \cdot \text{m}^{-2}$), integrated primary production (IP) primary production ($\text{mgC} \cdot \text{m}^{-2} \cdot \text{d}^{-1}$) obtained at the 6 stations on the North Aegean transect.

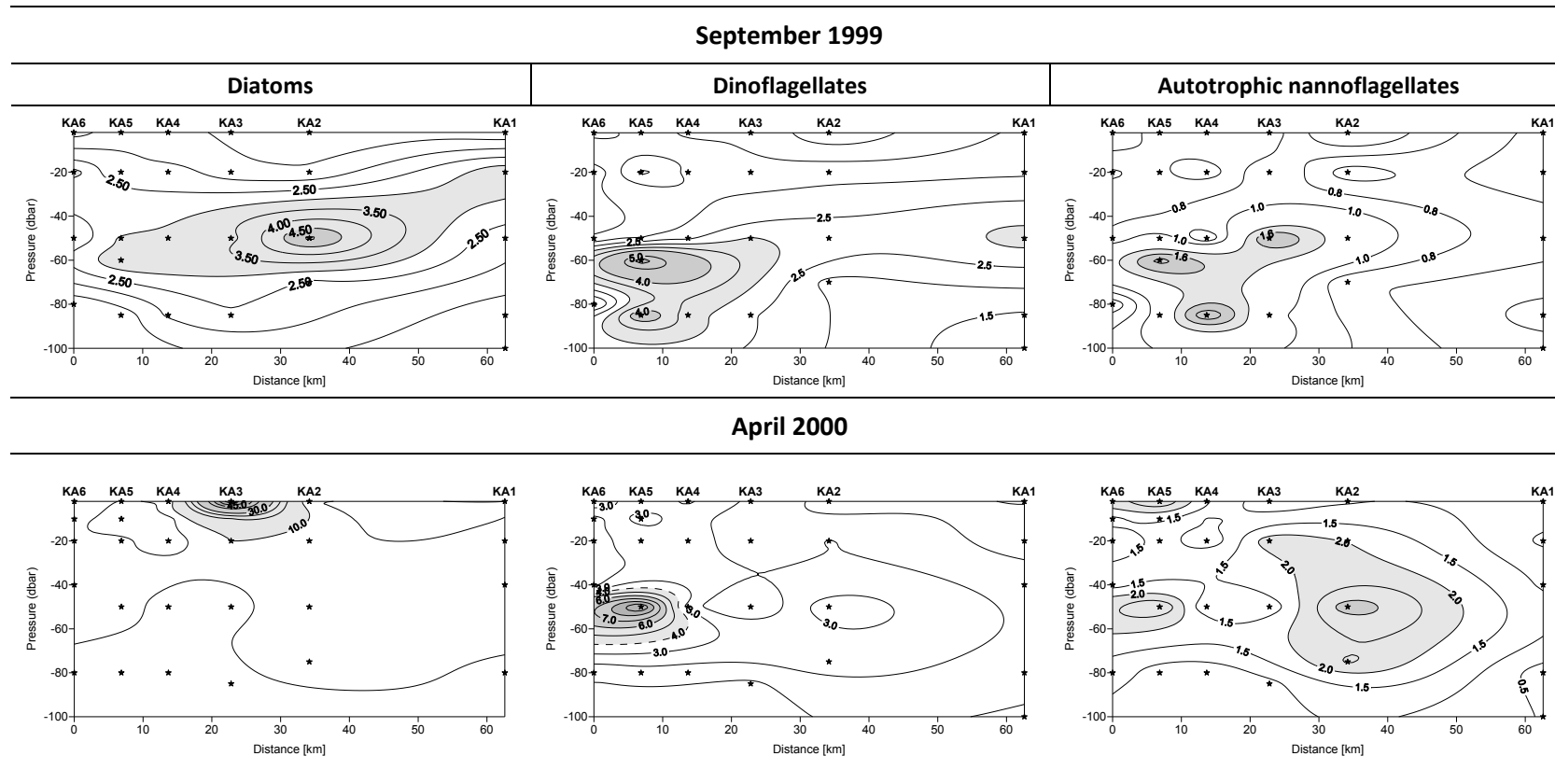
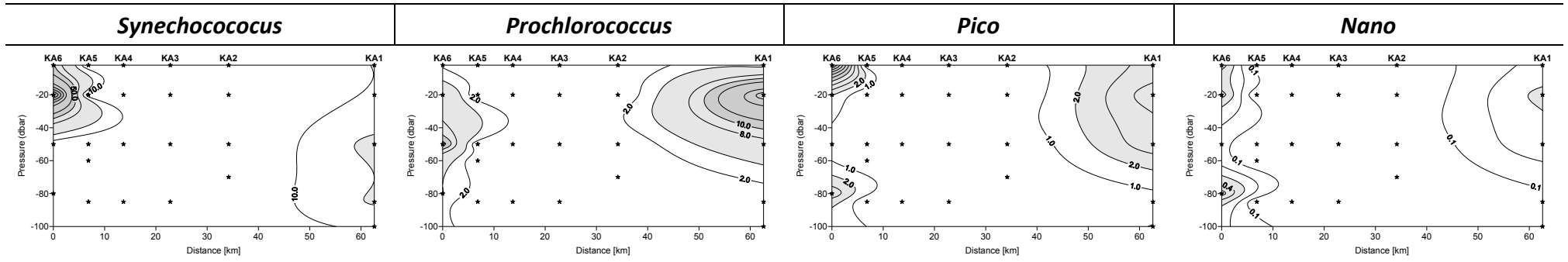


Figure 4.9.: Vertical distribution of cell abundance (cells ml⁻¹×10³) of phytoplankton (Diatoms, Dinoflagellates and autotrophic flagellates), across the transect in September 1999. Black dots correspond to actual sampling depths.

September 1999



April 2000

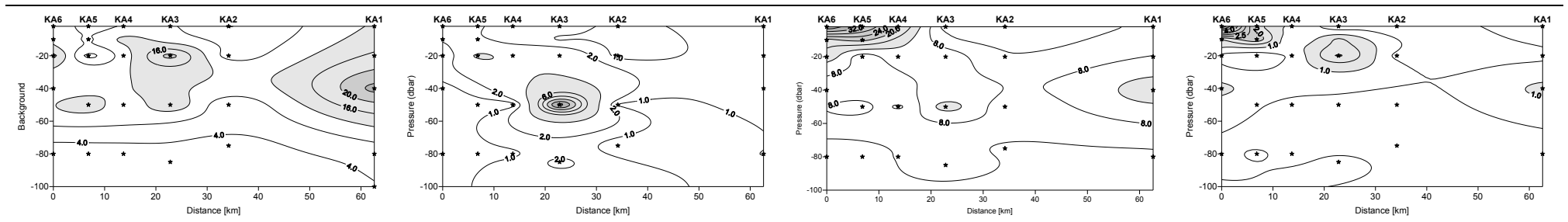
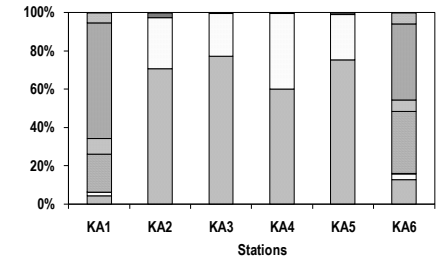
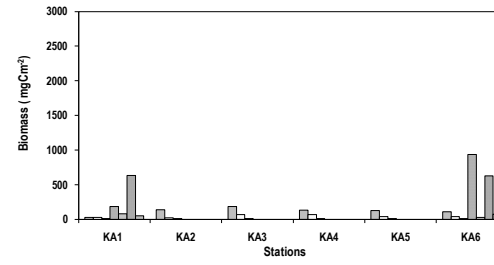
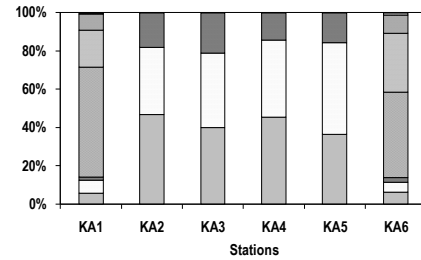
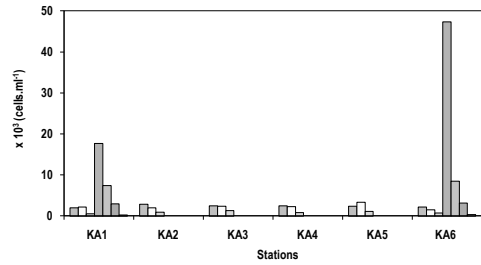


Figure 4.10.: Vertical distribution of cell abundance ($\text{cells ml}^{-1} \times 10^3$) of prokaryotic cyanobacteria (*Synechococcus* and *Prochlorococcus*) and eukaryotic picoplankton (Picoplankton and Nanoplankton) assessed by flow cytometry across the transect in September 1999 and April 2000. Black dots correspond to actual sampling depths.

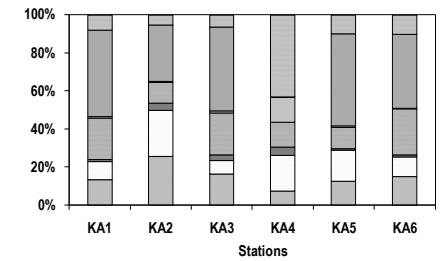
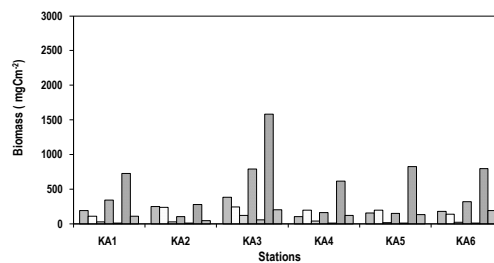
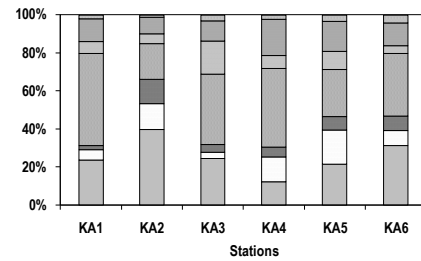
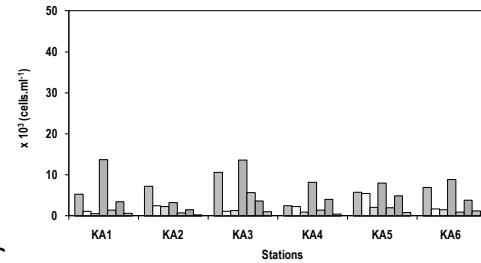
September 1999

cells

Biomass



April 2000



C

■ D □ Di ■ ANF ■ Syn ■ Pro ■ Pico ■ Nano

Figure 4.11.: Comparison of integrated (0–100 m) phyto – and picoplankton autotrophic cells ($\times 10^3 \text{ cells. ml}^{-1}$) and biomass (mgC m^{-3}) [Diatoms (D), Dinoflagellates (Di), autotrophic flagellates (ANF), *Synechococcus* (Syn), *Prochlorococcus* (Pro), Picoplankton (Pico) and Nanoplankton (Nano)], during the summer and spring cruise. Also shown is the relative contribution (%) of the different groups of picophytoplankton to total integrated autotrophic cells and biomass.

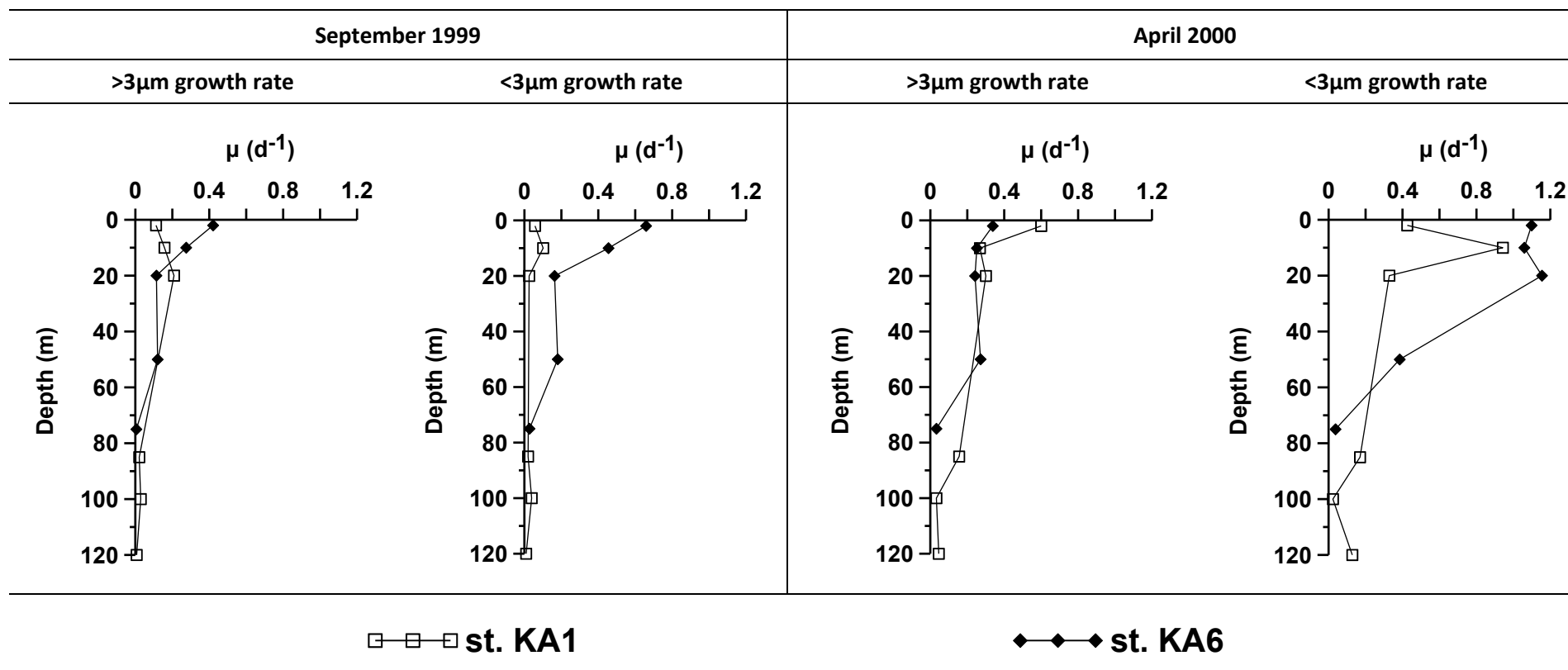


Figure 4.12.: Representative vertical profiles at stations KA1 (open station) and KA6 (front station) of phytoplankton growth rates (μ) at two size fractions (>3 μ m and <3 μ m) during September 1999 and April 2000.

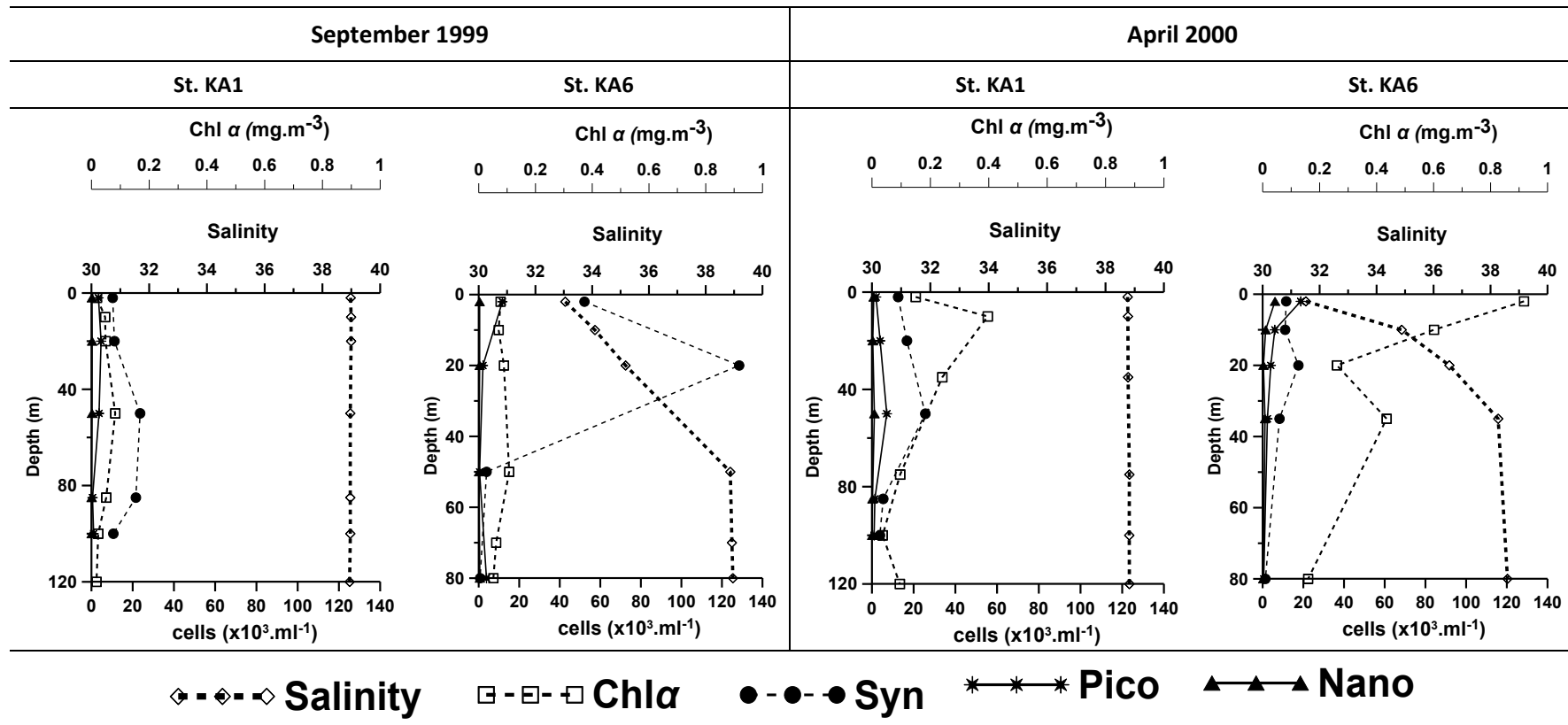


Figure 4.13.: Selected stations KA1 (open station) and KA6 (front station) representing the different sectors of the study area as defined in Fig. 4, to show the vertical distribution of salinity, nitrate ($\mu\text{M.l}^{-1}$) and cells ($\times 10^3\text{cells.ml}^{-1}$) during September 1999 and April 2000.

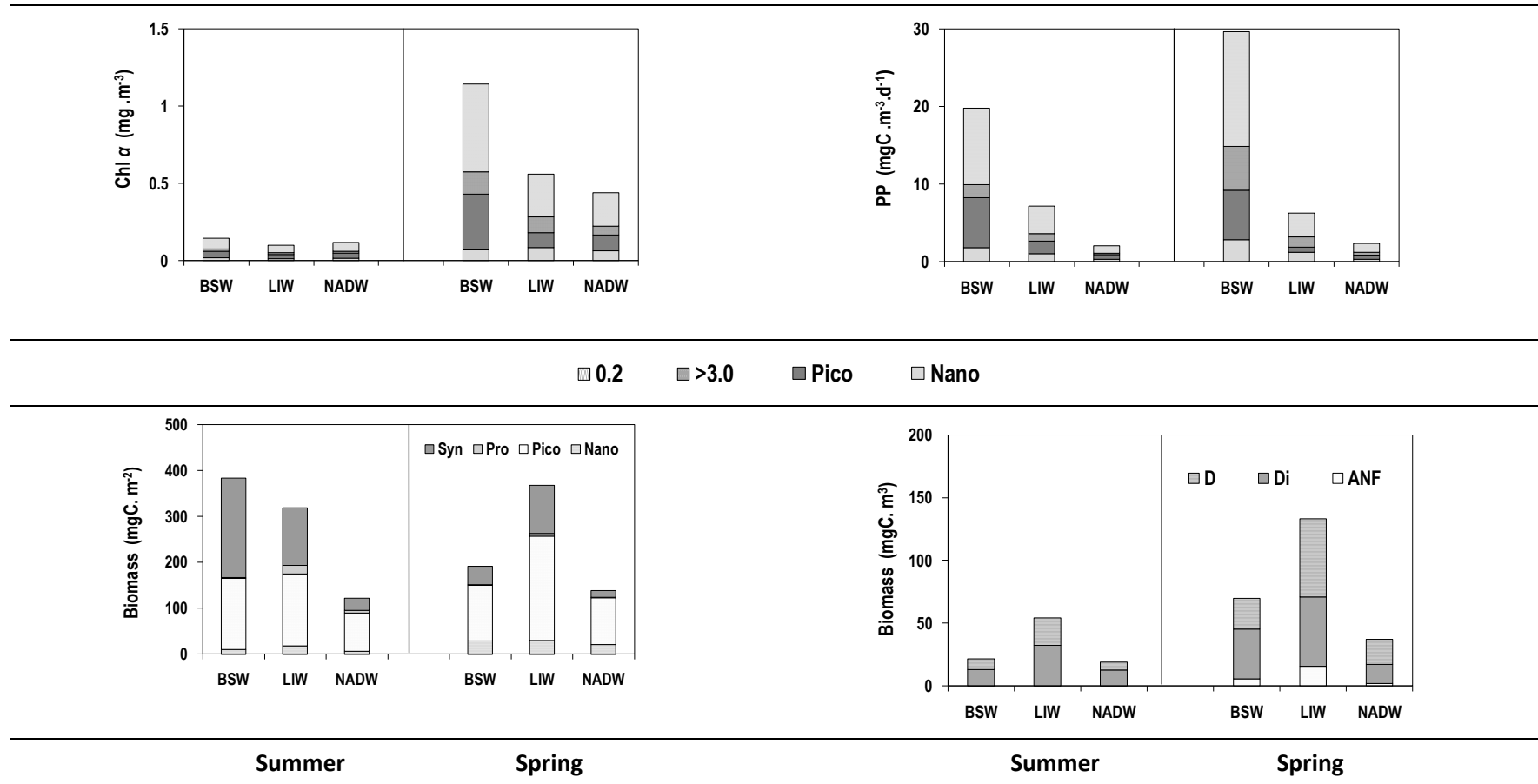


Figure 4.14: Summary of total and size-fractions ($>3.0\mu\text{m}$, Pico and Nano) of chlorophyll α (mgm^{-3}), primary production ($\text{mgC} \cdot \text{m}^{-3} \cdot \text{d}^{-1}$) and picophytoplankton biomass ($\text{mgC} \cdot \text{m}^{-3}$) in the three water masses [Black Sea Water (BSW), Levantine Intermediate Water (LIW) and North Aegean Deep Water (NADW)], during spring September 1999 and April 2000.

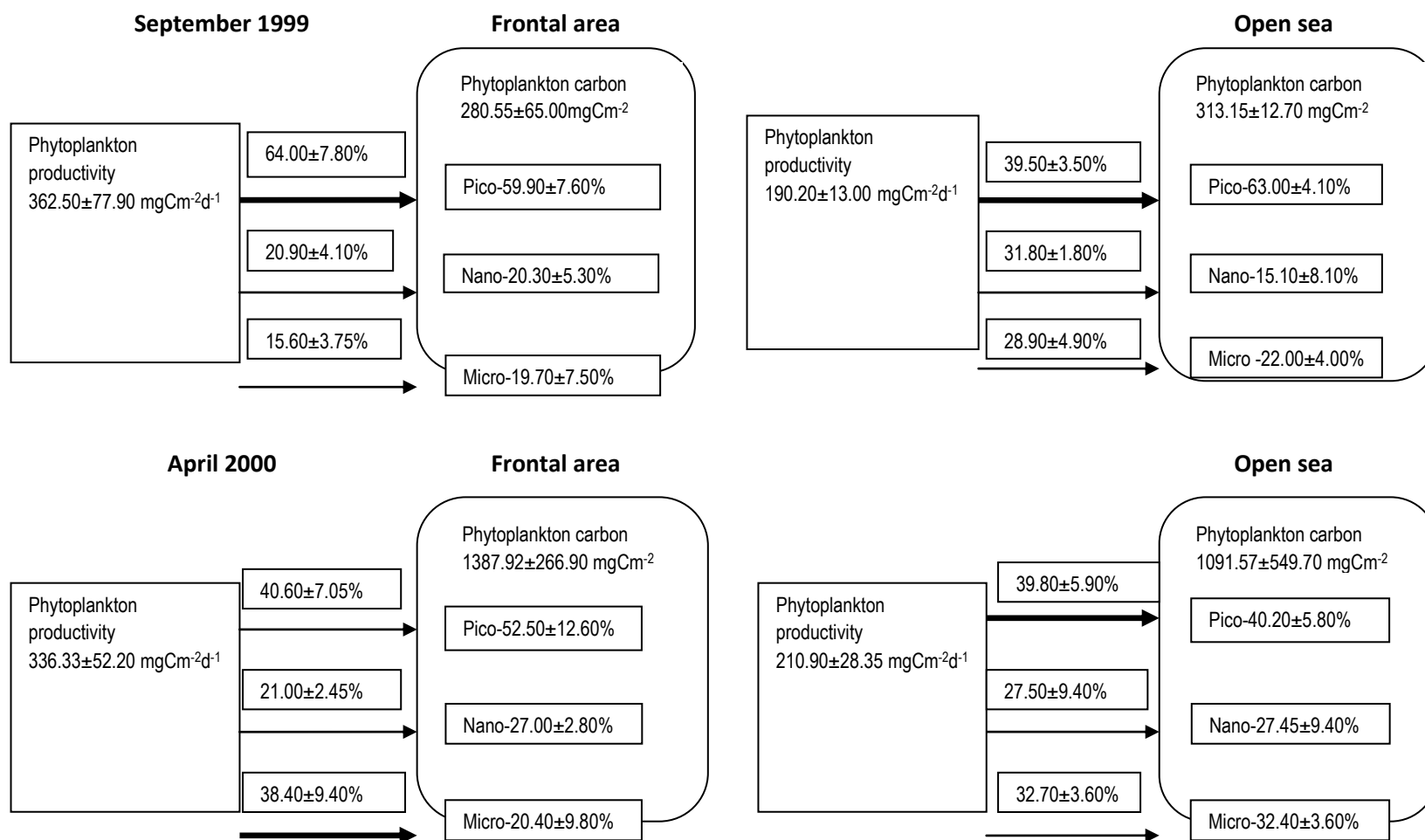


Figure 4.15.: Scheme of carbon standing-stocks and production in the two sampling conditions (September 1999 and April 2000) for the investigated area. Numbers in boxes show phytoplankton carbon biomass (mg C m^{-2}), their contribution (%) and carbon production ($\text{mgC m}^{-2} \text{ day}^{-1}$).

CHAPTER 5: Seasonal variability of autotrophic picoplankton in the Saronikos

Assimakopoulou G.¹, K. Pagou.¹, Pavlidou A.¹, Siokou I.¹, Ruser A.², Colijn, F.²

¹Institute of Oceanography, National Centre for Marine Research, P.O. Box 712, Anavyssos 19013, Greece

²Research- and Technology Centre Westcoast of Christian-Albrechts-University at Kiel, Germany

Abstract

This paper covers spatial and temporal variation in picoplankton communities and physico-chemical water properties in the Saronikos Gulf, Aegean Sea based on field measurements conducted from September 2000 to September 2001 (twelve cruises). The distribution of inorganic nutrients, and chlorophyll α (chl α) fractionated into three size classes were also investigated. Picophytoplankton chlorophyll α (chl α) amounted to a mean of 47% (19 to 72%) of euphotic-layer integrated total values. *Synechococcus* and picoeukaryotes generally were the greatest contributors to total picophytoplankton biomass (>70%) for most of the year. Picoeukaryotes and *Synechococcus sp.*, varied over time in abundance and carbon biomass, greater in summer than in winter, in range of 3.38×10^3 and 19.94×10^2 cells.ml⁻¹ in the abundance, 347.24 and 473.88 mgC.m⁻² in the carbon biomass, for *Synechococcus sp* and picoeukaryotes, respectively. Temperature and nutrients are the key controlling factors for the picophytoplankton distribution in the gulf.

Keywords: Picophytoplankton; Biomass; Size fractionation; Eastern Mediterranean; Aegean Sea, Flow cytometry.

5.1 Introduction

The increase of human activities in coastal systems affects nutrient loading and consequently the phytoplankton response (McComb, 1995 and Livingston, 2001). Point

source discharges of industrial wastewaters and sewage *effluent* into aquatic systems often introduce nutrients into the environment in quantities sufficient to noticeably accelerate the natural eutrophication process. Phytoplankton may thus serve as sensitive indicators of trophic state.

Nutrient availability could control algal growth (DiTullio *et al.*, 1993; Sakka *et al.*, 1999), biomass (Caron *et al.*, 2000) and species composition (Berdalet *et al.*, 1996; Caron *et al.*, 2000), but there is no general consensus as to which element (N or P) is limiting for phytoplankton. A few studies on the seasonal changes in the planktonic food web have been conducted in Saronikos gulf. Coastal eutrophication caused by human activities (anthropogenic eutrophication) is a problem in densely populated coastal regions throughout the world. Reports describing causes and consequences of enhanced anthropogenic nutrient emission to the coastal zone are numerous (e.g., Schiewer 1998; Colijn *et al.*, 2002). Although it has been shown beyond reasonable doubt that increased nutrient inputs increase the primary production and phytoplankton biomass, there is also evidence for an order-of-magnitude difference in biomass yield per unit of nutrient input among systems (e.g., Nixon and Pilson, 1983; Borum, 1996; Cloern, 2001), thus happening the prediction of eutrophication effects.

The picophytoplankton (0.2 μm), including the cyanobacteria *Prochlorococcus* and *Synechococcus* and the small eukaryotic algae, contribute substantially to both phytoplankton biomass and production in marine ecosystems (Li *et al.*, 1983; Campbell *et al.*, 1994; Liu *et al.*, 2004). Because their rapid growth rates are closely matched by mortality losses due to grazing by microzooplankton, they play an important role in nutrient regeneration and cycling in the ocean. Although many aspects of the ecosystem of Saronikos gulf have been studied, no information is available about the microbial components of the plankton. The ability to predict the ecological response of increased nutrient inputs, however, is still relatively poor.

Saronikos Gulf (mean depth $\sim 100\text{m}$) was impacted by untreated sewage for more than 30 years from the metropolitan Athens discharged by an outfall (in Keratsini Bay) in the surface waters of its northern part. The industrial effluents from the Elefsis Bay (a shallow semi-

enclosed area to the north of Saronikos Gulf) contributed also to the pollution of Saronikos. Elefsis Bay was the most industrialized area of Greece, where anoxic conditions near the bottom were recorded every summer. As from the summer of 1994, Saronikos Gulf receives the primary treated effluents (domestic and industrial) from the Psittalia Treatment Plant, through an outfall positioned at 60 m depth. However, according to recent data (1998-2004), minimum values (annual means) of N/P ratios (5-9) were found in areas near the sewage outfall in Saronikos Gulf. After 1995 dramatic changes occurred: no significant phytoplankton bloom has been reported since and this can be attributed to the lowering of the trophic status of the most eutrophic areas (from eutrophic to high mesotrophic) due to the operation of the new waste water treatment plants (Pagou *et al.*, 2002; 2005).

Saronikos Gulf presents a large scale of trophic conditions related to the eutrophic phenomena that had prevailed there the last decades, because of pollution mainly from urban and industrial effluents and had changed the natural oligotrophic character (Ignatiades *et al.*, 1969). In the outer Saronikos Gulf, under the influence of northerly winds, circulation is cyclonic during both winter and summer (Kontoyiannis and Papadopoulos 1999). Several impact studies that have been realized in Saronikos Gulf described the changes which occurred in relation to the phytoplanktonic populations and made reference to spatial and time variations, due to the existing pollution sources (Ignatiades *et al.*, 1985, 1986, Karydis *et al.*, 1983, Pagou *et al.*, 1996). Consequently it was proved that the trophic status of the gulf became independent of seasonality, influencing also that of phytoplankton variability along with its distribution and abundance (Ignatiades, 1981; Ignatiades & Karydis, 1982, Pagou, 1986). However the operation from 1994 onwards of the new sewage outfall of Psittalia Island has already induced some changes that is hoped finally to improve the environmental conditions of the marine receiving waters. Among the several criteria that are used for evaluating the response of phytoplankton to the changes of the trophic nature of the marine environment are indicators that utilize distribution of population size classes (Eppley & Weiler, 1979).

Many environmental studies have been performed in the Saronikos Gulf, in order to collect information on the impact of the Athens sewage outfall prior to the functioning of the sewage treatment. Ministry of Environment, Planning and Public Works, has allocated to the

HCMR the realization of a project for the Monitoring of the biological and physic-chemical parameters which was accomplished in 1987 (Panayotidis *et al.*, 1988) and in 1989 (Siokou-Frangou *et al.*, 1991). Furthermore a monitoring pollution project (MED-POL project) is performed in Saronikos Gulf since 1986 (seasonal cruises) to 1998 sponsored by UNEP. However, chl α content was not determined in the different size classes. Therefore, to better understand plankton processes in Saronikos Gulf, studies on the size structure dynamics of picophytoplankton were undertaken.

The present paper includes the scientific results and conclusions of the research project “Monitoring of the Saronikos Gulf ecosystem affected by the Psittalia Sea Outfalls”. This project is performed by the HCMR (Hellenic Centre for Marine Research) for the Special Service of Public Works/Greater Athens Area Sewerage and Sewage Treatment, Ministry of Environment, Planning and Public Works.

5.2. Material and methods

5.2.1. Study area

Saronikos Gulf practically constitutes these a border of the metropolitan city of Athens and the along shore outskirts. As shown in Fig. 5.1, the Saronikos Gulf communicates with the Aegean Sea at its south end and is bounded by the coast of Peloponnisos to the west and the coast of Attica to the north and east. The islands of Salamina and Aigina and the plateau (<100m) between them divide the Gulf into two basins. The western basin basically includes an elongated north–south trough with maximum depths of ~220 m in the north and ~450m in the south. The northern part of the eastern basin, called Inner Saronikos Gulf, is the area upon which receives the treated wastes of ~4 million people from a point source that discharges close to the bottom at ~65m water depth just south of the Psittalia island (Fig. 5.1) An approximate $800.000 \text{ m}^3 \text{ d}^{-1}$ of treated waste is discharged, carrying $\sim 100 \times 10^6 \text{ g C d}^{-1}$ (or 96 mol C s^{-1} ; $8.3 \times 10^6 \text{ mol C d}^{-1}$) of dissolved organic carbon (data from the Centre of Psittalia Sewage Treatment KELPS). Apart from the treated sewage, no other potential sources of anthropogenic organic matter exist in the area of the Inner Gulf. Two rivers, which supplied terrestrial material into the gulf, have now limited outflow, due to several human interventions and urban development.

The Saronikos Gulf is situated in the west-central region of the Aegean Sea, and covers a total surface area of 1,117 km² (Fig. 5.1). The gulf is separated into two basins by a shallow zone (inner Saronikos, depths < 100 m); the western basin has depths exceeding 400 m, the eastern basin depths around 100 and 200 m.

In the outer Saronikos Gulf, under the influence of northerly winds, circulation is cyclonic during both winter and summer (Kontoyiannis and Papadopoulou 1999). Two cyclonic structures exist; a larger cyclone in the eastern basin, and a smaller one in the outer gulf. At times of north-westerly winds, an anticyclone appears in the surface waters in the southeast, whereas a cyclone develops in the northern and western parts. In deeper waters, the cyclone progressively shrinks and the anticyclone prevails.

The gulf region exhibits very low rainfall rates throughout the year (Therianos 1974). The catchment area of the Saronikos Gulf comprises small rivers and ephemeral streams. Two rivers (Kifissos and Ilissos) discharge into the gulf a few kilometres to the east of the port of Piraeus [indicated in the map] (Fig. 5.1) (Krasakopoulou *et. al.*, 2005). These once supplied substantial amounts of terrigenous material to the gulf but today have limited outflow because of urban development.

Therefore, apart from the wastewater treatment plant (WWTP) on the Psittalia Island [indicated in the map] (Fig. 5.1), external particulate matter sources are presumably mainly atmospheric, with fine material being transported by the prevailing northerly winds (Athanasoulis and Skarsoulis 1992). Until the construction of the WWTP on the small island of Psyttaleia (Fig. 5.1), the effluents of the Athens metropolitan area (population five million; wastewater average flow rate 800,000 m³ day⁻¹) were released untreated into the gulf, leading to eutrophication in naturally oligotrophic waters. It is worth mentioning that no phytoplanktonic blooms were detected in the Inner Saronikos Gulf during the last years. Even in the most eutrophic area (Elefsis Bay, Keratsini Bay), blooms are scarce in contrast to what happened in the 80ties, where red-tides were quite often observed (Pagou, 1990).

The WWTP initiated its operation in 1994 (first stage treatment); the effluents are released into the sea by a V-shaped pipeline situated close to the bottom at ~63 m depth, southwards

of Psittalia Island. Discharged wastewater, being less dense than the seawater at the same depth, moves towards the surface. During the period of seasonal thermocline formation, the wastewater field is trapped below the thermoclinic pycnocline, and it is dispersed by the dominant currents at this depth (Siokou-Frangou *et al.*, 1999, 2000).

The eastern Keratsini channel is enriched by the industrial and shipyard area of Piraeus harbour. Until 1994, Keratsini channel was receiving the untreated domestic and industrial sewage of the Athens Metropolitan area which was discharged into the surface water layer of the channel and enriched the bay with metals, nutrients and organic matter. After 1994, the sewage of the Athens Metropolitan area was primarily treated in the Psitallia Sewage Treatment Plant and discharged into the inner Saronikos Gulf (Fig. 5.1). Additionally, by the end of 2004, the secondary stage of the Psittalia Sewage Plant became operational.

5.2.2. Field sampling

Monthly water samples were collected from September 2000 to September 2001, at two stations for a total of 12 dates in the Saronikos Gulf (Table 5.1, Fig. 5.1) with the R/V Aegaeo: Coastal station S7 (37°55'42''E, 23°35'45''N; depth: 65m) is directly affected by the waste effluents of the Psittalia sewage treatment plant and one open sea station S16 (37°47'23''E, 23°42'04''N; depth: 90m) was used as a reference station. Water samples were collected from depths of 10, 20, 30, 50 and 100m by Niskin bottles. Nitrate/nitrite, ammonium, silicate, and orthophosphate ($\text{NO}_3^- + \text{NO}_2^- = \text{NO}_3^-$, SiO_4 , PO_4^{3-}) were determined by automated colorimetric analyses using Technicon Auto Analyzers. Chlorophyll α (Chl α) was measured fluorometrically after extraction in 90% acetone [Holm-Hansen *et al.*, (1965), EPA Method 445).

5.2.3. Total and size fractionated chlorophyll α

Size fractionation has been used by ecologists to describe, in relative terms, the distribution and structure of marine organisms in pelagic ecosystems. Sieburth *et al.*, (1970) used this approach to sort plankton into size categories dividing numerous trophic compartments of plankton by using a spectrum of size classes. We adapted the terminology of Sieburth to our sizes classes, namely, picoplankton (0.2 to 1.2 μm), nanoplankton (1.2 to 5 μm), and

microplankton (>5 μm). The differences between the filters represent the three size classes studied.

5.2.4. Flow cytometry

Prefiltered (100- μm mesh size net) water samples (4.5ml) were fixed with 2% paraformaldehyde. The samples were gently mixed and kept in the dark at room temperature for 10 minutes before quick-freezing and storage in liquid nitrogen. In the laboratory the cryovials were stored at -80 $^{\circ}\text{C}$ until flow cytometric analysis was performed (Trousselier *et al.*, 1995; Vaulot *et al.*, 1989). All the signals of the samples were calibrated against the same internal standard beads (2 μm Polysciences Fluoresbrite beads, cat.18604). Single cell analysis was run with a FACScan flow cytometer (Becton-Dickinson, FTZ) equipped with argon laser (power-15mW, at 488nm). For each cell, five signals (Blanchot and Rodier, 1996) were recorded on 4-decade logarithmic scales: two light scatter (side scatter, SSC, and forward light scatter, FLS), and three fluorescences. The photomultipliers were set up to quantify: the red fluorescence (RF) from Chl α (wavelength>650nm), the orange fluorescence (OF) from phycoerythrin PE (564-606nm), and the green fluorescence (GF) from phycourobilin PUB (515-545nm), following Wood *et al.*, (1985) and Olson *et al.*, (1988). Each individual signal was stored in 'list mode' and analyzed with WinMidi software. The combination of fluorescence signals (phycoerythrin and chlorophyll α) with measurements of forward and side light scatter, allowed the enumeration of cyanobacteria (*Synechococcus*), prochlorophytes (*Prochlorococcus*) and eukaryotic phytoplankton. Autotrophic cells were separated into two groups of cyanobacteria (*Synechococcus* and *Prochlorococcus*) and two groups of picoeukaryotes based on their size and fluorescence and light scatter signal.

5.2.5. Plankton conversion to biomass

The biovolumes of the planktonic organisms were calculated from the size measurements. Cell abundances were converted to biomass (carbon mg C m $^{-3}$) estimates using carbon-per-cell conversion factors. *Prochlorococcus*, *Synechococcus*, photosynthetic eukaryotes (*Peuks*) cell numbers were directly converted to biomass with conversion factors (53 fg C cell $^{-1}$, 250 fg C cell $^{-1}$ and 2100 fg C.cell $^{-1}$, respectively) (Kana and Glibert, 1987; Campbell *et al.*, 1994).

5.2.6. Statistical analysis

The 12 cruises between September 2000 and September 2001 were divided into four seasons: fall (September–November), winter (December–March), spring (April–June), summer (July– August) and mean data of different variables in each season were obtained, which represent the average of a parameter for the whole water column.

One-way ANOVA was used to detect statistical significance for the differences between samples according to stations and with regard to seasons. Following the ANOVA, the post hoc Tukey HSD test was employed to compare samples among stations or seasons.

Pearson's correlation was used to examine the relationship between the community variables and phosphate, nitrate, salinity, temperature and chlorophyll α . The use of a Pearson correlation coefficient was considered to testing for potential relationships between hydrological and nutrient parameters with picophytoplankton parameters. The latter combination of analyses was also applied to compare the sites with each other, with respect to whole-season values (averages or sums). All the above-mentioned statistical analyses were carried out using the Statgraphics Centurion XV.

5.3. Results

5.3.1 Hydrography

The annual ranges, means and standard errors of the physical, chemical and biological parameters at all sampling stations during the study period have been calculated and summarized in Tables 5.2.

From detailed analyses of the parameters it is seen that, the dynamics of temperature are typically seasonal for temperate waters of the Mediterranean Sea, with annual means ranging from 17.86 to 18.04⁰C at station S7 and S16, respectively (Tab. 5.2). Figure 5.2 show the monthly temperature variations in the water column at both stations S7 and S16. Water temperatures at S7 were highest during September (22.68±4.70⁰C) and lowest (14.62±0.15⁰C) in March. The temperature at station S16 ranged from 22.32±4.80⁰C in September to the lowest 14.48±0.28⁰C in March 2001. Mean data of temperature and

salinity, which represent the average of a parameter over the whole water column in each season (fall, winter, spring and summer) were obtained showing the vertical variation in temperature and salinity at both stations between the four seasons from surface and bottom waters, indicating that the water column is generally well mixed throughout autumn and winter, with stratification during spring and summer. At both stations thermocline was at ~30m in spring and summer, while during autumn at station S7 was at depths >50m and S16 at 75m. Temperature of deeper waters, below 30 m, was almost constant around 15.5 °C and typically for Mediterranean waters (Fig. 5.3).

To illustrate seasonal features of the region, we divided the year into four seasons based on water column structure. The water column temperatures at st. S7 were the highest in the warm seasons; summer (18–25°C) and fall (21–25°C), relatively lower in spring (16–19°C), the transition between the cold and warm seasons and the lowest in winter (16–18°C) (Tab. 5.7). The water column temperatures at st. S16 were the highest in the warm seasons; summer (19–25°C) and fall (20–25°C), relatively lower in spring (16–19°C), the transition between the cold and warm seasons and the lowest in winter (15–18°C). Figure 5.2 shows the seasonal variations in salinity at the study stations (S7, S16). Salinity did not vary between seasons in both stations ($p > 0.05$; one-way ANOVA, $n=60$), and ranged between 38.3 and 38.7 (Tab. 5.1); with the lowest values in winter and/or spring and the highest in summer.

Fig. 5.3 shows profiles of temperature, salinity and fluorescence at the site of the plume outflow (station S7) and open sea station (S16) during four seasons (fall, winter, spring and summer). The seasonal variations of temperature and salinity from the surface to ~100m, appearing in Fig. 5.3 for station S7, are representative for the particular coastal environment of Saronikos Gulf. Winter temperatures fall near ~13–14 °C, with a complete mixing of the water column in the Inner Gulf, not though in the western basin. Thus, reported values for each sampling month were pooled and have been evaluated on seasonal scales (fall, winter, spring, summer).

5.3.2. Nutrients

Figure 5.4 shows the seasonal variations in concentrations of inorganic nutrients at the two study sites. Ammonium concentrations varied between 0.05 μM and $\sim 1\mu\text{M}$, only in August 2001 an elevated concentration of 4.0 μM was observed at S7 (Figure 5.4C). At station S7, nitrate levels were highest in January (Figure 5.4B) showed similar annual ranges in the two stations; S7 (0.57–1.86 μM), and S16 (0.31–1.40 μM). Nitrate concentrations peaked in December at station S16. The mean phosphate values (Figure 5.4A) at station S7 were clearly higher than at station S16 during the whole observation period. At both stations phosphate concentrations were higher during spring-summer but lower during winter. The lowest phosphate level of 0.117 μM occurred at station S16 in August while the highest phosphate level of 1.02 μM was recorded in station S7 in May. Nitrates had the highest values at station S7 recording the lowest level of 0.309 μM in May while the highest level of 1.589 μM was observed in January at station S7. Nitrate reaches a peak value of $\sim 2\mu\text{M}$ in winter (December). Utilisation of nitrate begins in early spring and concentrations decline from April to August (Fig. 5.4B). Minimal levels, typically $<1\mu\text{M}$, are observed throughout the rest of the summer.

Correlations among variables revealed a significant negative relationship between temperature and NO_3^- ($r = -0.68$, $p < 0.05$) and PO_4^{3-} ($r = -0.57$, $p < 0.05$), as well as salinity ($r = -0.72$, $p < 0.05$), indicating that cold, saline surface waters enriched with NO_3^- and PO_4^{3-} characterize coastal waters during winter months, whereas summer waters are warm and deficient in inorganic nutrients. There was no significant difference in ammonium concentration between st. S7 and S16 ($p > 0.05$).

5.3.3. Size-fractionated chlorophyll α

Surface chl α concentrations were significantly higher (one-ANOVA, $p < 0.05$, $n = 13$) at S7 (annual mean: $0.34 \pm 0.03 \mu\text{g l}^{-1}$, range = 0.14 to $0.84 \mu\text{g l}^{-1}$) than at S16 (annual mean: $0.15 \pm 0.02 \mu\text{g l}^{-1}$, range = 0.05 to $0.46 \mu\text{g l}^{-1}$) (Tab. 5.2). Based on size-fractionated chl α , picophytoplankton (0.2–2.0 μm) dominated phytoplankton biomass at both stations (annual mean: $31.60 \pm 9.70\%$ at S7; $46.70 \pm 10.70\%$ at S16) (Tab. 5.3) followed by microphytoplankton ($>5\mu\text{m}$) (annual mean: $21.80 \pm 9.60\%$ at S7; $27.10 \pm 6.90\%$ at S16) and nanophytoplankton (2–

5 μm) (annual mean: 18.90 \pm 7.50% at S7; 26.20 \pm 1.40% at S16). Table 5.3 shows the monthly chlorophyll α concentrations of each studied size fraction and its relative abundance to total chl α . The relative contribution of microphytoplankton Chl α to total Chl α were highest during winter (51.20 \pm 9.80%) and lowest during summer (14.90 \pm 1.15%) at station S7. In contrast picophytoplankton was the dominant size class during summer, accounting 72.10 \pm 6.10% of total Chl α (Tab. 5.3).

At station S7 the monthly changes on depth-integrated total chl α ranged from 0.842 \pm 0.33 $\mu\text{g l}^{-1}$ in March 2001 to 0.145 \pm 0.05 $\mu\text{g l}^{-1}$ in September 2001. Station S7 showed a clear seasonality, with a bimodal pattern, with high concentrations during fall and winter–spring (Figure 5.6A). The seasonal pattern of micro- and picophytoplankton Chl α was nearly the same as that for total Chl α (Figure 5.6B, 5.6C). At Station S16, total Chl α concentrations in surface water increased in October and peaked during November (Figure 5.6A). The fractions studied showed different temporal patterns (Fig. 5.6). Nanoplankton had its lowest contribution in summer and its maximum in spring (March). Picoplankton peaked in autumn (November) and spring (March) while its minimal contribution to total chl α occurred during cold months (January). At both stations (S7, S16) the mean annual chl α biomass reached maximum values in fall of 0.51 $\mu\text{g l}^{-1}$ and 0.22 $\mu\text{g l}^{-1}$, respectively (Tab. 5.7) and in summer the lowest concentrations were observed. Table 5.10 shows correlation analysis of relationships between environmental and biological at the stations S7 and S16. At st. S7 total chl α was significantly positively correlated with nitrate ($r=0.33$ $p<0.05$) and at st. S16 significantly positively correlated with ammonia ($r=0.31$ $p<0.05$).

5.3.4. Picoplankton abundances

The temporal changes in mean abundances of picophytoplankton in water column at st. S7 and S16 are illustrated in Fig. 5.8. Abundances of picophytoplankton were linearly integrated between dates, and monthly depth integrated abundances were calculated for both sampling stations for the upper water layer.

At st. S7 the pico-phytoplankton was composed of populations of *Synechococcus* sp., *Prochlorococcus* sp. pico- and nanoeukaryotes, with annual averaged abundance of

$20.80 \pm 1.10 \times 10^3$, $5.30 \pm 0.40 \times 10^3$, and $4.30 \pm 1.50 \times 10^3$, $0.10 \pm 0.01 \times 10^3$ cells ml^{-1} (Tab. 5.7). A low standing stock of *Synechococcus* ($9.10 \pm 5.30 \times 10^3$ cells ml^{-1}) was observed in the cold season (January), and in late spring (April) the *Synechococcus* abundance increased to ($21.60 \pm 2.00 \times 10^3$ cells ml^{-1}). In July (warm season) the increase continued and reached the highest intensity in September ($39.70 \pm 1.20 \times 10^3$ cells ml^{-1}) (Tab. 5.4, Fig. 5.8A). The integrated abundance of *Prochlorococcus* at st. S7 varied at a high abundance ($18.00 \pm 4.60 \times 10^3$ cells l^{-1}) occurring in summer and a low abundance in early autumn (Tab. 5.4). The *Synechococcus* population accounts for about 44 % (December)–83% (August) of total phytoplankton and the contribution of picoeukaryotes ranged from 6.5% (Aug) to 23% and ~30 % (April and December, respectively) (Fig. 5.11).

Vertical distributions of picophytoplankton cell densities for both stations are shown in Fig. 5.9. At st. S7 the cell density of *Synechococcus* and picoeukaryotes were high in the upper 50m during spring ($\sim 30 \times 10^3$ and $\sim 15 \times 10^3$ cells ml^{-1} , respectively), at a temperature of $\sim 18^\circ\text{C}$. In summer *Synechococcus* reached maximum abundances at a depth of 50m ($\sim 40 \times 10^3$ cells ml^{-1}), and an abrupt decrease with depth ($\sim 10 \times 10^3$ cells ml^{-1}). The vertical patterns of picoeukaryotes were homogeneous throughout the water column with low cell densities ($\sim 4 \times 10^3$ cells ml^{-1}). At st. S7 abundance of *Synechococcus* was negatively correlated with phosphate ($r = -0.26$, $p < 0.05$), but not with temperature and concentrations of nitrogen (Tab. 5.10). Picoeukaryotes and *Synechococcus* cell concentrations were well correlated with one another ($r = 0.67$, $p < 0.05$). No significant correlations were observed between picophytoplankton and environmental variables ($p > 0.05$) at st. S7. Correlation analyses were performed on data subsets of *Synechococcus* and picoeukaryotes delineated in terms of spring, summer, fall and winter periods of the sample year (Tab. 5.11). During the fall period negative significant correlation between abundances of *Synechococcus* and picoeukaryotes with nitrate ($r = -0.54$ and $r = -0.76$, respectively; $p < 0.05$) were recorded at st. S7. There was no correlation between *Synechococcus* and temperature (Tab. 5.11) but there was a positive significant correlation between picoeukaryotes and temperature ($r = 0.59$). During periods of vertical mixing (cold period) negative correlations between abundances of *Synechococcus* and picoeukaryotes and phosphate ($r = -0.69$ and $r = -0.55$, respectively; $p < 0.05$) were recorded.

At the open sea station (S16) the picophytoplankton was composed of populations of *Synechococcus sp.*, *Prochlorococcus sp.* pico- and nanoeukaryotes, with a year averaged abundance of $19.09 \pm 3.70 \times 10^3$, $5.27 \pm 2.40 \times 10^3$, $2.41 \pm 0.90 \times 10^3$ and $0.10 \pm 0.02 \times 10^3$ cells ml⁻¹ (Tab. 5.4). At both stations *Synechococcus sp.* tended to be more abundant than the other pico-phytoplanktonic groups. The seasonal distribution showed a distinct peak during midsummer at S16 (Fig. 5.8 A, B). At station S16 higher picoeukaryotes abundance was observed in summer $7.40 \pm 2.10 \times 10^3$ cells l⁻¹ (July) (Tab. 5.4) and a minimum of $0.66 \pm 0.20 \times 10^3$ cells l⁻¹ in September. *Synechococcus* abundance increased in the warm season to $31.16 \pm 3.70 \times 10^3$ cells ml⁻¹.

The vertical distribution of cyanobacteria and picoeukaryotes at station S16 was uniform with the exception of the bottom layer where cells numbers was somewhat lower during mixing periods and somewhat higher during stratification periods. During summer at st. S16 the cell density of *Synechococcus* abundance was high in the upper 20m high during spring ($\sim 40 \times 10^3$ cells.ml⁻¹) (Fig. 5.9). At st. S16 a statistically significant negatively correlation (Tab. 5.10) between *Synechococcus* and picoeukaryotes abundance and nitrate concentration ($r = -0.35$ and $r = -0.32$, $p < 0.05$, respectively) was observed. A statistically significant negatively correlation (Tab. 5.10) between *Synechococcus* and picoeukaryotes abundance and phosphate concentration ($r = -0.47$ and $r = -0.29$, $p < 0.05$, respectively) was observed.

A one-way ANOVA analysis showed significant differences in seasonal variation in *Synechococcus* population ($p < 0.05$) but no between stations ($p > 0.05$) (Tab. 5.11). There were no significant differences during fall between picophytoplankton and environmental parameters and summer periods at station S7. A statistically significant negatively correlation between *Synechococcus* abundance and nitrate concentration ($r = -0.54$, $p < 0.05$, $n = 18$) during fall was observed. During mixing periods (winter) there was a negative correlation between cyanobacteria cells and phosphate ($r = -0.68$, $p < 0.05$, $n = 18$) (Tab. 5.11). At station S16, *Synechococcus* abundance ranged from 8.89 ± 5.25 (December) to $31.16 \pm 3.70 \times 10^3$ cells l⁻¹ (July). Again a statistically significant negatively correlation between *Synechococcus* abundance and phosphate concentration ($r = -0.68$, $p < 0.05$, $n = 18$) in winter period measured. At both stations there was no clear seasonal variation in both temperature and population density (Fig. 5.4A and 5.4B). No statistically significant correlation was found

between *Synechococcus* cells with temperature at both stations. A one-way ANOVA showed no significant spatial differences ($p>0:05$) from winter (December) through to spring (April) but significant differences ($p<0:05$) in summer (June) and fall (September). Comparisons of ANOVA results using the LSD method showed that the average integrated abundance of *Synechococcus* at st. S7 was significantly higher than at st. S16 from summer to fall. Analysis of variance showed that picophytoplankton abundances and biomass were not statistically different between the two sampling stations.

5.3.5. Biomass distribution over size classes

At st S7 picoeukaryotes contained the largest amount of carbon biomass in the different picophytoplankton size classes (Tab. 5.6), with values ranging from 1.38 (January) to 22.59 mgC m^{-3} (April). *Synechococcus* carbon biomass ranged from 2.27 (January) to 9.93 mgC m^{-3} (September), *Prochlorococcus* from 0.06 (September) to 0.95 mgC m^{-3} (July) and nanoeukaryotes from 0.05 (January) to 1.22 mgC m^{-3} (September).

Picoeukaryotes component contained the largest fraction of carbon biomass at st S16 (open sea station) with values ranging from 1.40 (September) to 15.54 mgC m^{-3} (July). *Synechococcus* carbon biomass ranged from 2.22 mgC m^{-3} (December) to 7.79 mgC m^{-3} (July) (Tab. 5.6).

The highest autotrophic picophytoplankton biomass occurred mainly from spring to summer at both stations: in April, July and August 2001 at st. S7, from May to July 2001 at st.S16 and the lowest values were mostly recorded in winter (January 2001). Averaged over the entire sampling period, this corresponded at st. S7 to $54.14\pm 7.40\%$ of carbon biomass being picoeukaryotic, $41.63\pm 14.00\%$ from *Synechococcus*, (Tab. 5.5, Fig. 5.11). Fluctuations in carbon biomass over time (Fig. 5.8) at st. S7 and S16 were highly related to changes in cell concentration (*Prochlorococcus*, $r = 0.67$; *Synechococcus*, $r = 0.990$; picoeukaryotes, $r = 0.96$; for all, $p < 0.05$).

The abundance and biomass of *Synechococcus* were similar at both stations. On the contrary picoeukaryotes biomass was higher at st. S7 than at st. S16 (Fig. 5.8). Some characteristic features of the vertical distribution of autotrophic picophytoplankton biomass are shown in

the profiles (Fig. 5.10). During spring picoplankton biomass showed a high level of 50 mgC m^{-3} at station S7, at open sea station a deep biomass value was observed at 80m depth. Among the autotrophic picophytoplankton, *Synechococcus* and picoeukaryotes dominated autotrophic carbon biomass during most of the year, and contributed >85% of the autotrophic picoplanktonic biomass, especially in summer and fall periods.

5.4 Discussion

The biomass and size distribution of the phytoplankton community play an important role in the energy flow and food web dynamics of marine ecosystems. In general, it is accepted that, the larger phytoplankton species are associated with nutrient rich waters, whereas smaller microorganisms are dominant in the oligotrophic waters (Bec *et al.*, 2005). However, the physical and chemical properties of a given environment are very important factors controlling the size distribution. There have been many investigations on the size distribution of phytoplankton in many parts of the Mediterranean Sea and the importance of small sized phytoplankton has been described in those studies (Delgado and Estrada, 1992; Arin *et al.*, 2002; Ignatiades *et al.*, 2002).

The oligotrophy of the Mediterranean Sea supports the contribution of the small size fractions since small cells can use nutrients more effectively than larger ones under nutrient limited conditions (Harris, 1986; Kormas *et al.*, 2002). However, blooms of large sized species are observed in coastal environments of the Mediterranean due to nutrient enrichment.

In this study, reported that pico- and nanoplankton fraction constituted the most important part in the phytoplankton biomass. Chlorophyll α values ranged overall from 0.14 and 0.84 $\mu\text{g l}^{-1}$ (Tab. 5.3) in the Psittalia area (S7, sewage outfall) and from 0.46 to 0.55 $\mu\text{g l}^{-1}$ at st. S16 with an overall level of Chl α in the Aegean Sea ranging from 0.12 to 0.37 $\mu\text{g L}^{-1}$ (Ignatiades, Psarra & Zerkavis 2002). Phytoplankton biomass exhibited a bimodal cycle with fall and spring maxima at both stations (Fig. 5.6), but more pronounced at station S7. Chlorophyll α seasonality is characterized by the distinctive maxima appearing in fall (0.74 mg m^{-3}), and in early spring (March) 0.842 mg m^{-3} (Fig. 5.6). Such bimodal cycles are typical for temperate waters, where phytoplankton increase occurs in spring due to the enrichment of water

column with nutrients and increasing levels of temperature and light in this period (Delgado, 1990). Previous studies on phytoplankton size classes in oligotrophic environments show a high contribution of small sizes to total biomass. The investigated area also showed characteristics of coastal environments, in contrast to the oligotrophic Mediterranean waters in term of nutrients and biomass dynamics (Magazzu and Decembrini, 1995; Ignatiades *et al.*, 2002; Polat, 2006).

Nutrient and chlorophyll α concentrations have been determined during 2000–2001 cruises in the Saronikos gulf and compared with the similar regions in the Mediterranean Sea (Siokou *et al.*, 2002). There was significant seasonal variation between sampling periods ($p < 0.05$). In the outer bay, nutrient results were similar to the Aegean Sea (Tab. 5.2) (Siokou *et al.*, 2002). Nitrate is an essential nutrient; the nitrate values obtained are representative for an unpolluted coastal system. Under normal conditions nitrate generally occurs in trace quantities in surface water but the concentration is enhanced through inputs from other sources (rivers). Phosphate is also of great importance as an essential nutrient in aquatic system. Phosphates are generally the limiting nutrient for plant growth, and excess amounts can lead to eutrophication. The picophytoplankton community observed in the Saronikos gulf was composed by *Synechococcus* sp., *Prochlorococcus* sp., pico- and nanoeukaryotes and showed abundances comparable to those found in other Mediterranean areas (Jacquet *et al.*, 1998, Ferrier-Pages & Rassoulzadegan 1994, Vaulot *et al.*, 1990, Agawin *et al.*, 1998). The community structure of picophytoplankton was dominated by phycoerythrin-rich cyanobacteria of the *Synechococcus* type. Picoeukaryotic cells were also a quantitatively significant component of the picophytoplankton community. The numerical dominance of eukaryotic picophytoplankton is typical of the open oligotrophic waters of the Mediterranean Sea (Casotti *et al.*, 2003).

The three pico-phytoplankton groups and biomass showed important seasonality and differed in the period of peak abundance (Fig. 5.8, Tab. 5.8, Tab. 5.8), which were observed in spring, summer, and fall for *Prochlorococcus* sp., *Synechococcus* sp. and picoeukaryotes, respectively. Despite the differences found in the timing of the occurrence of peak abundance, *Prochlorococcus* and pico-eukaryote abundances were positively correlated to that of *Synechococcus* sp. ($r = 0.53$, $r = 0.52$, $p < 0.05$ respectively), as observed for

Mediterranean communities elsewhere (Vaulot *et al.*, 1990, Ribes *et al.*, 1999). This suggests that, despite differences described for growth requirements (Vaulot *et al.*, 1990), the populations were affected by similar controls in the Saronikos gulf (e.g. water temperature, nutrients availability, grazing, etc.). In conclusion, phytoplanktonic biomass distribution, as resulted from this research, appeared to be typical of the Mediterranean coastal sites (Fonda Umani *et al.*, 1992).

The seasonal trend was similar in the two stations with the annual peaks occurring in April and July, respectively. The temperature and nutrients (considered as factors controlling the occurrence of picophytoplankton in marine waters) could have been responsible for the picophytoplankton increase, as also suggested by the correlation analysis (Tab. 5.11). In addition, the small size of picophytoplankton makes it more efficient than larger autotrophs, in absorbing and using the incident light and nutrients (Agustí. *et al.*, 1994). The summer bloom of phytoplankton assemblages reduces both the light and nutrient availability, favouring smaller autotrophs. The summer increase of picophytoplankton abundances could be due to the combined effects of temperature and light/nutrients assimilation.

Independent of nutrient ratios, the general decrease in both nutrient concentrations and light availability should promote higher contributions of smaller sized cells with a higher surface to volume ratio, such as picocyanobacteria. Also, the differences recently described in the sensitivity to PAR and UVR for the different pico-phytoplankton groups, may indicate that *Synechococcus sp.* is more resistant to high solar radiation levels than *Prochlorococcus sp.* and picoeukaryotes are (Agustí, *et al.*, 2004), which could also be an advantage for *Synechococcus sp.* during the summer time. In summary, an important picophytoplankton community was present throughout the year with a dominance of *Synechococcus sp.*. This indicates that the conditions for growth during summer are more favourable for *Synechococcus sp.* than for the other groups. *Synechococcus sp.* cell division strongly increases with increased water temperature (e.g. Agawin *et al.*, 1998) and phosphorus inputs (Vaulot, 1996). The seasonal variations in picophytoplankton community structure showed the same pattern at both stations, similar to those in other temperate coastal regions. An increase for integrated *Synechococcus* abundance in summer, increase for picoeukaryotes in spring.

Table 5.1.: Sampling protocol during the study in Saronikos gulf from September 2000 to September 2001.

Sampling number	Months	Season
1	Sep-00	11 September 2000
2	Oct-00	29 September 2000
3	Nov-00	2 November 2000
4	Dec-00	18 December 2000
5	Jan-01	29 January 2001
6	Mar-01	12 March 2001
7	Apr-01	2 April 2001
8	May-01	22 May 2001
9	Jun-01	29 June 2001
10	Jul-01	26 July 2001
11	Aug-01	29 August 2001
12	Sep-01	4 October 2001

Table 5.2.: Annual Mean \pm SD of biological and physico-chemical parameters in stations S7 and S16. In the last column, results of one-way ANOVA analysis. F values: between groups mean square/within-groups mean square. *Significant difference between sampled points: (*p < 0.05, **p < 0.01, ***p < 0.001), nd: not determined.

Biological and physico-chemical parameters (Mean \pm SD)	S7	S16	F (values)	df
Physical parameters				
Salinity	38.542 \pm 0.09	38.581 \pm 0.10	0.42	(129)
Temperature ($^{\circ}$ C)	17.864 \pm 3.00	18.046 \pm 3.30	0.30	(129)
Chemical parameters				
NO ₃ ⁻ (μ mol.l ⁻¹)	1.063 \pm 0.40	0.714 \pm 0.07	6.17	(129)*
PO ₄ ³⁻ (μ mol.l ⁻¹)	0.488 \pm 0.30	0.177 \pm 0.06	4.36	(129)*
NH ₄ ⁻ (μ mol.l ⁻¹)	0.797 \pm 1.20	0.201 \pm 0.06	2.87	(129)
N/P ratio	5 \pm 6	4 \pm 1	0.06	(129)
Biological parameters				
Total Chl α (mgm ⁻³)	0.342 \pm 0.20	0.152 \pm 0.08	16.01	(129)*
Total picoplankton density (x10 ³ cells.ml ⁻¹)	30.57 \pm 4.30	26.87 \pm 1.70	1.11	(129)
Total picoplankton biomass (mgCm ⁻³)	14.95 \pm 1.50	10.32 \pm 4.00	3.51	(129)

Table 5.3.: Euphotic layer-integrated values of contribution (%) each studied size fraction to chlorophyll α total at the two stations during 2000 and 2001 in Saronikos Gulf.

Date	S7			S16		
	Pico (%)	Nano (%)	Micro (%)	Pico (%)	Nano (%)	Micro (%)
Sep-00	42.80±1.60	11.50±1.60	45.80±8.00	50.80±6.30	24.30±2.25	24.90±1.30
Oct-00	65.20±3.10	20.25±3.00	14.50±6.40	52.50±3.75	19.10±3.70	28.30±1.00
Nov-00	50.10±8.30	21.40±8.90	28.50±3.20	17.90±1.70	13.60±1.65	68.50±3.75
Dec-00	32.90±3.85	15.80±1.50	51.20±9.80	42.65±7.20	17.70±2.20	39.60±2.90
Jan-01	18.90±8.60	34.90±6.00	46.20±8.70	30.70±3.10	54.60±7.40	14.70±4.70
Mar-01	44.10±2.30	31.70±2.10	24.20±7.10	43.60±1.50	31.00±2.90	25.40±4.10
Apr-01	47.90±8.20	22.10±1.70	30.03±2.90	43.60±9.80	15.90±2.00	40.50±2.10
May-01	42.50±8.50	40.20±4.90	17.30±1.10	72.20±9.50	16.60±3.40	11.30±2.30
Jun-01	37.70±7.25	34.90±8.15	27.40±2.60	47.00±2.40	24.70±1.60	28.30±1.70
Jul-01	72.10±6.10	13.00±2.00	14.90±1.15	52.10±3.30	30.90±3.10	17.00±3.40
Aug-01	41.80±2.30	36.10±1.40	22.10±3.55	45.60±2.00	30.30±1.40	24.10±2.60
Sep-01	35.10±4.70	28.20±3.80	36.75±4.70	61.65±9.50	35.20±2.70	3.20±0.75
Mean±SD	44.30±14.70	25.80±9.10	29.90±12.10	46.70±10.70	26.16±1.40	27.14±6.90

Table 5.4.: Cells abundance ($\times 10^3$ cells ml^{-1}) of the different groups. Syn: *Synechococcus*; Proc: *Prochlorococcus*; Pico: picoeukaryotes; Nano: nanoeukaryotes. (mean±SD values).

Date	Syn		Pro		Pico		Nano	
	S7	S16	S7	S16	S7	S16	S7	S16
Sep-00	12.90±3.90	28.30±5.60	1.19±0.70	6.48±0.40	1.50±0.80	1.60±0.30	0.03±0.02	0.10±0.04
Nov-00	14.80±5.30	18.90±5.50	5.80±1.70	4.75±1.30	1.80±0.90	2.80±0.60	0.09±0.10	0.16±0.10
Dec-00	10.30±0.80	8.90±5.25	5.80±0.80	3.40±0.20	7.30±1.20	2.20±1.55	0.10±0.02	0.06±0.05
Jan-01	9.10±5.30	10.71±0.90	1.95±0.90	1.60±0.10	0.70±0.10	1.15±0.50	0.02±0.01	0.07±0.02
Apr-01	21.60±2.00	14.65±5.40	3.00±0.30	7.89±0.10	10.80±1.90	2.70±0.95	0.15±0.03	0.10±0.04
May-01		28.50±4.20		4.69±0.15		2.60±0.50		0.16±0.10
Jun-01		15.80±1.30		4.73±0.50		1.60±0.65		0.14±0.02
Jul-01	25.70±8.20	31.20±3.70	18.00±4.60	10.02±1.40	6.65±0.40	7.40±2.10	0.20±0.05	0.06±0.04
Aug-01	32.20±8.00	17.50±0.60	3.50±1.40	4.90±0.80	2.40±1.60	1.50±0.70	0.09±0.05	0.10±0.08
Sep-01	39.70±1.20	16.60±1.90	3.40±1.60	4.30±0.20	3.60±1.50	0.70±0.20	0.05±0.02	0.02±0.01
Mean±SD	20.78±1.10	19.09±3.70	5.34±0.40	5.27±2.40	4.34±1.50	2.41±0.90	0.10±0.01	0.10±0.02

Table 5.5.: Carbon biomass (mg C m^{-2}) of of the different groups. *Syn*: *Synechococcus*; *Proc*: *Prochlorococcus*; *Pico*: picoeukaryotes; *Nano*: nanoeukaryotes in each month at the two stations during 2000 and 2001 in Saronikos gulf. Annual means \pm SD are also shown.

Biomass (mg Cm^{-3})								
Date	Syn		Pro		Pico		Nano	
	S7	S16	S7	S16	S7	S16	S7	S16
Sep-00	3.20 \pm 0.50	7.10 \pm 1.90	0.06 \pm 0.04	0.34 \pm 0.02	3.20 \pm 1.80	3.30 \pm 0.90	0.05 \pm 0.05	0.20 \pm 0.09
Nov-00	3.70 \pm 1.30	4.70 \pm 0.90	0.30 \pm 0.09	0.25 \pm 0.07	3.80 \pm 0.10	5.80 \pm 1.20	0.19 \pm 0.06	0.34 \pm 0.05
Dec-00	2.60 \pm 0.20	2.20 \pm 1.30	0.30 \pm 0.04	0.18 \pm 0.06	15.40 \pm 2.45	4.60 \pm 0.60	0.27 \pm 0.04	0.13 \pm 0.01
Jan-01	2.30 \pm 1.30	2.70 \pm 0.20	0.10 \pm 0.01	0.08 \pm 0.07	1.40 \pm 0.20	2.40 \pm 0.90	0.05 \pm 0.03	0.14 \pm 0.05
Apr-01	5.40 \pm 1.00	3.70 \pm 1.30	0.20 \pm 0.08	0.42 \pm 0.06	22.60 \pm 2.95	5.60 \pm 1.90	0.32 \pm 0.07	0.21 \pm 0.08
May-01		7.10 \pm 1.55		0.25 \pm 0.06		5.40 \pm 0.80		0.33 \pm 0.09
Jun-01		3.90 \pm 0.60		0.25 \pm 0.08		3.40 \pm 0.60		0.29 \pm 0.08
Jul-01	6.40 \pm 2.10	7.80 \pm 1.50	0.95 \pm 0.04	0.53 \pm 0.01	14.00 \pm 7.15	15.50 \pm 1.60	0.50 \pm 0.30	0.13 \pm 0.05
Aug-01	8.00 \pm 4.50	4.40 \pm 0.65	0.19 \pm 0.07	0.26 \pm 0.04	5.10 \pm 1.40	3.10 \pm 1.50	0.18 \pm 0.10	0.23 \pm 0.07
Sep-01	9.90 \pm 2.30	4.10 \pm 0.90	0.18 \pm 0.08	0.03 \pm 0.01	7.50 \pm 3.20	1.40 \pm 0.85	1.22 \pm 0.60	0.04 \pm 0.01
Mean \pm SD	5.20 \pm 1.30	4.88 \pm 2.20	0.30 \pm 0.06	0.11 \pm 0.03	9.10 \pm 1.40	11.85 \pm 4.10	0.35 \pm 0.05	0.20 \pm 0.04

Table 5.6.: Annual seasonal Mean \pm SD of biological and physico-chemical parameters in stations S7 and S16.

	S7				S16			
	Fall	Winter	Spring	Summer	Fall	Winter	Spring	Summer
ISal	38.63 \pm 0.20	38.46 \pm 0.06	38.55 \pm 0.20	38.59 \pm 0.15	38.61 \pm 0.20	38.48 \pm 0.10	38.59 \pm 0.10	38.66 \pm 0.10
ITemp	21.64 \pm 3.30	16.09 \pm 1.60	16.09 \pm 1.50	18.04 \pm 3.70	20.56 \pm 4.10	15.92 \pm 1.60	16.44 \pm 1.70	19.63 \pm 5.20
INO ₃	1.30 \pm 1.40	1.93 \pm 0.50	1.13 \pm 0.60	0.79 \pm 0.07	1.16 \pm 0.80	1.25 \pm 0.50	0.50 \pm 0.03	0.66 \pm 0.02
IPO ₄	0.37 \pm 0.04	0.39 \pm 0.09	0.57 \pm 0.80	0.42 \pm 0.05	0.15 \pm 0.08	0.27 \pm 0.05	0.15 \pm 0.04	0.15 \pm 0.06
INH ₄	0.44 \pm 0.09	0.60 \pm 0.02	0.26 \pm 0.03	0.92 \pm 0.04	0.20 \pm 0.08	0.32 \pm 0.07	0.16 \pm 0.04	0.15 \pm 0.04
ICl α	0.514 \pm 0.06	0.366 \pm 0.06	0.262 \pm 0.08	0.148 \pm 0.04	0.217 \pm 0.08	0.144 \pm 0.05	0.098 \pm 0.06	0.077 \pm 0.02
Picoplankton ($\times 10^3 \cdot \text{ml}^{-1}$)	18.82 \pm 1.70	16.67 \pm 6.60	47.08 \pm 2.60	30.80 \pm 2.40	29.80 \pm 4.30	13.83 \pm 2.80	27.98 \pm 1.30	28.15 \pm 1.40

Table 5.7.: Mean of cell abundance of autotrophic picoplankton abundance cells ($\times 10^3 \text{ml}^{-1}$) and contribution (%) to total abundance measured in Saronikos Gulf (Syn: *Synechococcus*; Pro: *Prochlorococcus*; Pico: Picoeukaryotes and Nano: Nanoeukaryotes) calculated as seasonal means for winter (December, January, February), spring (March, April, May), summer (June, July, August) and fall (September, October, November) from September 2000 to September 2001.

Season	Stations	Cells ($\times 10^3 \text{ml}^{-1}$)				cells(%)			
		Syn	Pro	Pico	Nano	Syn	Pro	Pico	Nano
Fall	S7	13.89 \pm 4.40	3.30 \pm 2.60	1.56 \pm 0.15	0.07 \pm 0.01	72.28 \pm 11.10	18.07 \pm 2.10	9.35 \pm 0.45	0.31 \pm 0.02
	S16	20.78 \pm 4.00	1.79 \pm 0.80	7.12 \pm 0.10	0.11 \pm 0.02	62.27 \pm 3.90	7.65 \pm 4.70	29.69 \pm 7.50	0.39 \pm 0.01
Winter	S7	9.38 \pm 3.60	3.73 \pm 0.70	3.49 \pm 0.80	0.07 \pm 0.02	60.38 \pm 5.80	21.46 \pm 1.10	17.82 \pm 2.15	0.34 \pm 0.03
	S16	8.69 \pm 3.00	1.61 \pm 2.50	3.46 \pm 1.90	0.07 \pm 0.05	59.25 \pm 10.60	13.37 \pm 7.10	26.64 \pm 1.50	0.74 \pm 0.04
Spring	S7	23.53 \pm 8.20	16.73 \pm 4.60	6.57 \pm 3.40	0.25 \pm 0.05	49.06 \pm 5.40	36.56 \pm 9.40	13.85 \pm 5.50	0.53 \pm 0.06
	S16	19.42 \pm 2.70	1.69 \pm 1.20	6.74 \pm 0.90	0.12 \pm 0.03	69.67 \pm 5.15	5.85 \pm 0.50	23.89 \pm 4.60	0.58 \pm 0.02
Summer	S7	25.75 \pm 9.50	2.83 \pm 1.60	2.16 \pm 0.60	0.06 \pm 0.02	78.13 \pm 11.50	12.98 \pm 2.90	8.69 \pm 2.00	0.20 \pm 0.03
	S16	18.52 \pm 0.60	2.68 \pm 0.50	6.89 \pm 0.60	0.05 \pm 0.01	63.35 \pm 9.80	9.09 \pm 0.70	27.35 \pm 5.40	0.21 \pm 0.09

Table 5.8.: Mean of autotrophic picoplankton biomass (mg Cm^{-3}) and contribution (%) to total biomass measured in Saronikos Gulf (Syn: *Synechococcus*; Pro: *Prochlorococcus*; Pico: Picoeukaryotes and Nano: Nanoeukaryotes) calculated as seasonal means for winter (December, January, February), spring (March, April, May), summer (June, July, August) and fall (September, October, November) from September 2000 to September 2001.

Season	Stations	Biomass (mg Cm^{-3})				Relative Biomass (%)			
		Syn	Pro	Pico	Nano	Syn	Pro	Pico	Nano
Fall	S7	3.47 \pm 0.40	0.18 \pm 0.04	3.28 \pm 1.80	0.14 \pm 0.09	47.65 \pm 11.20	2.76 \pm 20.30	47.97 \pm 11.40	1.62 \pm 0.50
	S16	5.19 \pm 1.50	0.09 \pm 0.04	14.95 \pm 2.80	0.22 \pm 0.06	31.40 \pm 5.10	0.56 \pm 0.06	66.73 \pm 5.40	1.31 \pm 0.80
Winter	S7	2.35 \pm 0.90	0.20 \pm 0.02	7.34 \pm 0.50	0.14 \pm 0.05	36.40 \pm 3.80	2.42 \pm 1.30	59.95 \pm 3.50	1.23 \pm 0.55
	S16	2.17 \pm 0.60	0.10 \pm 0.02	6.75 \pm 6.60	0.14 \pm 0.10	29.11 \pm 4.40	1.13 \pm 0.50	67.78 \pm 4.20	1.98 \pm 0.50
Spring	S7	5.88 \pm 2.10	6.77 \pm 2.20	13.80 \pm 7.15	0.52 \pm 0.30	28.70 \pm 6.89	4.73 \pm 2.04	64.17 \pm 7.90	2.40 \pm 0.60
	S16	4.86 \pm 1.20	0.09 \pm 0.06	14.16 \pm 2.80	0.26 \pm 0.20	31.72 \pm 8.60	0.52 \pm 0.07	65.80 \pm 9.20	1.96 \pm 0.90
Summer	S7	6.44 \pm 2.90	6.59 \pm 0.90	4.55 \pm 3.35	0.41 \pm 0.04	53.40 \pm 5.90	1.85 \pm 0.40	42.64 \pm 5.80	2.12 \pm 0.30
	S16	4.63 \pm 0.20	0.22 \pm 0.09	11.26 \pm 5.80	0.11 \pm 0.01	28.02 \pm 4.30	1.31 \pm 0.70	69.93 \pm 3.85	0.74 \pm 0.06

Table 5.9.: Values of one-way analysis for environmental of environmental and biological data including temperature (Temp, °C), nitrate, phosphate concentrations (NO₃, PO₄, μMol.l⁻¹), total chlorophyll α concentration (Chlα-tot, μg.l⁻¹), size-fractionated chlorophyll α concentration [Chlα >3μm, Chlα-Pico and Chlα –Nano, μg.l⁻¹], picophytoplankton abundance (Syn-ce, Pico-ce, Nano-ce, x10³ cells.ml⁻¹), and picophytoplankton biomass (Syn-PB, Pico-PB, Nano-PB, μgC.l⁻¹) variables of variance obtained September 2000 and September 2001.

Variables	Station			Season		
	d.f.	F	p	d.f.	F	p
Salinity	129	0.42	ns	127	13.30	0.0000
Temperature (°C)	129	0.20	ns	127	19.69	0.0000
PO ₄ (μM)	129	10.73	0.0014	127	1.00	ns
NO ₃ (μM)	129	4.66	0.0326	127	0.75	ns
NH ₄ (μM)	129	3.03	ns	127	1.43	ns
Chl α (μg.l ⁻¹)	129	19.25	0.0000	127	5.28	0.0018
Chl α >3μm (μg.l ⁻¹)	129	8.37	0.0045	127	6.69	0.0003
Chl α-pico (μg.l ⁻¹)	129	14.01	0.0003	127	3.48	0.0180
Chl α-nano (μg.l ⁻¹)	129	13.77	0.0003	127	1.78	ns
Syn-ce (x10 ³ cells.ml ⁻¹)	129	0.03	ns	127	2.01	ns
Pico-ce (x10 ³ cells.ml ⁻¹)	129	5.31	0.0228	127	1.96	ns
Syn-PB (μgC.l ⁻¹)	129	0.03	ns	1277	2.01	ns
Pico- PB (μgC.l ⁻¹)	129	0.48	ns	127	1.96	ns

*P<0.05.; ns, non significant

Table 5.10.: Matrix of correlation coefficients of environmental and biological data from two stations including temperature (Temp, °C), salinity, nitrate, phosphate concentration (NO₃, PO₄, μMol.l⁻¹), total chlorophyll α concentration (Chlα-tot, μg.l⁻¹), and picophytoplankton abundance (Syn-ce, Pico-ce, Nano-ce, x10³ cells.ml⁻¹, *significant level (*p < 0.05).

	S7								S16							
	Sal	Temp	PO ₄	NH ₄	NO ₃	Chlα _{tot}	Syn ce	Pico ce	Sal	Temp	PO ₄	NH ₄	NO ₃	Chlα _{tot}	Syn ce	Pico ce
Temp	0.48*								0.21							
PO ₄	-0.50	-0.42*							-0.23	-0.29*						
NO ₃	-0.22	-0.40*	0.38*						-0.22	-0.35*	0.55*					
NH ₄	-0.38*	-0.19	0.45	0.04					-0.23	0.02	0.56*	0.32*				
Chlα _{tot}	-0.37*	0.01	0.16	0.05	0.33*				-0.37*	-0.21	0.14	0.31*	0.15			
Syn-ce	0.08	0.07	-0.26*	-0.25	0.02	-0.12			0.02	0.06	-0.47*	-0.30	-0.35*	-0.20		
Pico-ce	-0.06	0.02	-0.17	-0.05	-0.14	-0.01	0.67*		-0.11	0.01	-0.29*	-0.12	-0.32*	-0.05	0.71*	
Nano-ce	-0.08	0.06	0.10	0.03	-0.13	0.20	-0.66*	-0.11	-0.10	-0.02	0.41*	0.05	0.44*	0.37*	-0.68*	-0.49*

Table 5.11.: *Pearson's* correlations between pico-, nano- and microplankton abundance and physical – chemical parameters and Chl α . (r = *Pearson's* correlation coefficient, $n=18$) during 4 different seasons (F=fall, W=winter, SP=spring and S=summer, **significant level* ($*p < 0.05$)).

Parameter	S7				S16			
	F	W	SP	SU	F	W	SP	SU
	r	r	r	r	r	r	r	r
<i>Synechococcus</i> -Salinity	-0.02	0.09	-0.18	0.06	-0.06	-0.17	0.18	0.07
<i>Synechococcus</i> -Temperature	-0.06	0.26	-0.38	0.24	0.20	0.33	0.12	0.18
<i>Synechococcus</i> -Nitrate	-0.54*	0.41	-0.04	-0.22	-0.10	-0.03	-0.33	-0.30
<i>Synechococcus</i> -Phosphate	-0.29	-0.69*	-0.24	-0.13	-0.46	-0.68*	-0.39	-0.40
<i>Synechococcus</i> -Chl α	0.21	-0.58*	0.24	0.23	0.12	0.18	-0.01	-0.64*
Picoplankton-Salinity	-0.11	0.20	-0.13	0.37	0.06	-0.44	-0.19	0.23
Picoplankton-Temperature	0.59*	0.40	-0.37	0.39	-0.27	0.19	0.16	0.48*
Picoplankton-Nitrate	-0.76*	0.30	-0.04	-0.25	0.35	-0.19	-0.15	-0.54*
Picoplankton-Phosphate	-0.22	-0.55*	-0.24	-0.35	-0.25	-0.69*	-0.18	-0.54*
Picoplankton-Chl α	0.45	-0.44	0.22	0.07	-0.05	0.47*	0.15	-0.52
Chl α - Salinity	-0.48	-0.47	-0.19	-0.31	-0.41	-0.65*	-0.19	-0.37
Chl α - Temperature	0.30	-0.46	-0.57*	0.03	0.19	-0.30	-0.55*	-0.63*
Chl α -Nitrate	-0.09	-0.70*	0.06	-0.12	0.05	-0.60*	0.53*	0.36
Chl α -Phosphate	-0.09	0.77*	0.11	0.33	-0.15	-0.223	0.49*	0.54*

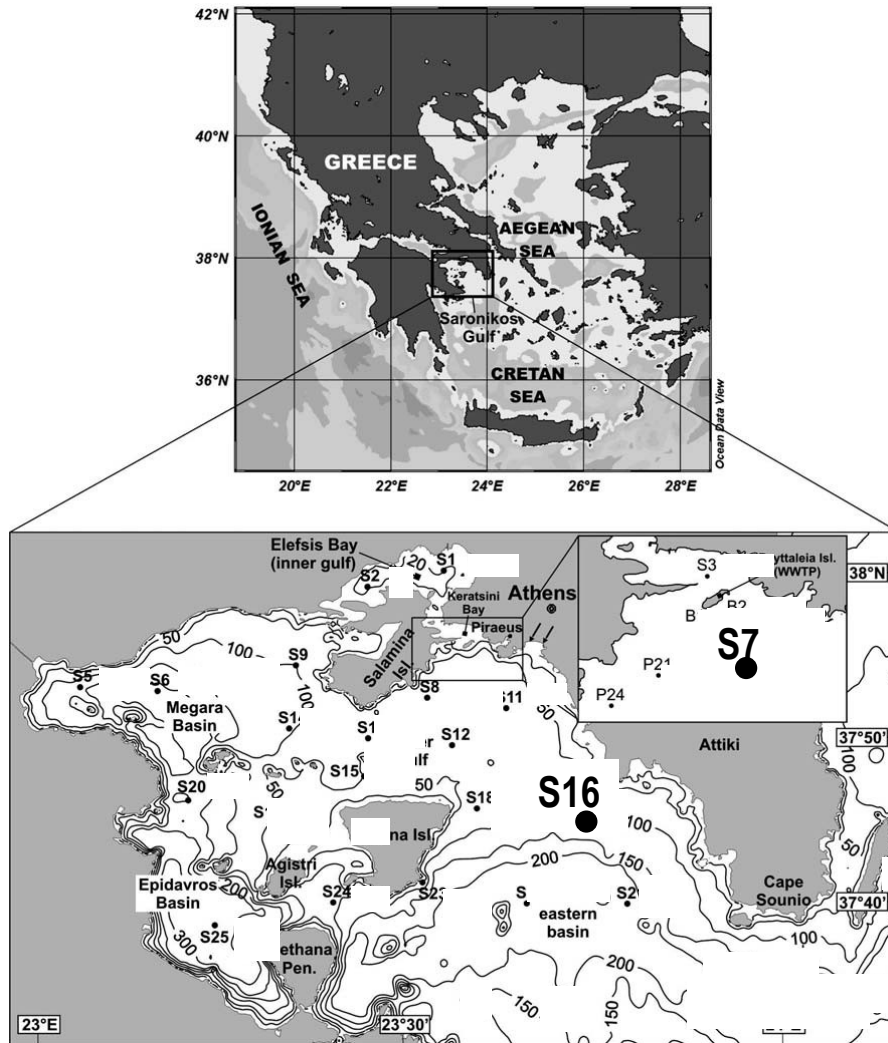
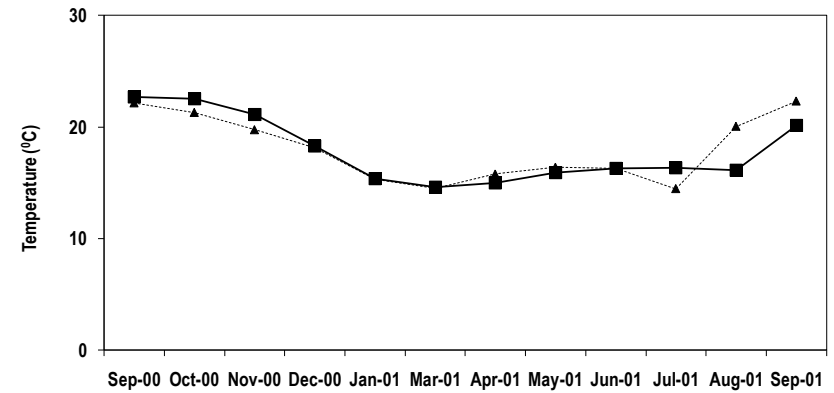
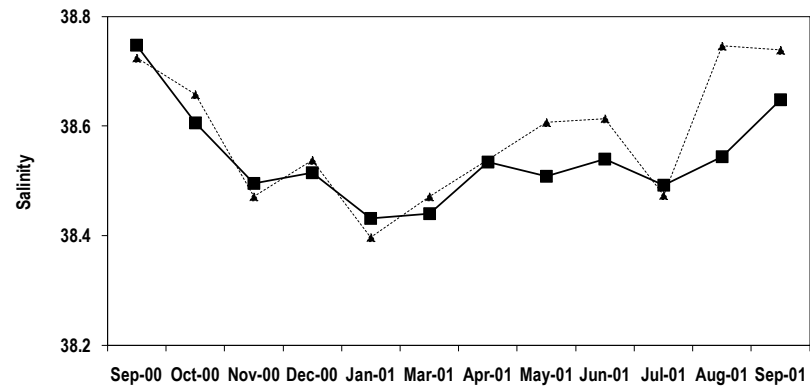


Fig. 5.1.: Map of the study area showing the bathymetry (contours in m) and the location of the two sampling stations. (S7, S16). Arrows indicate the location of the Kifissos River (west) and the Ilissos River (east) mouths. The WWTP is located on the Psyttalia Island, and the sewage outfall (inset) (according Evangelia Krasakopoulou & Aristomenis P. Karageorgis, *Geo-Mar Lett*, 2005)



■ S7

▲ S16

Figure 5.2.: Comparison of hydrographic parameters between station S7 and S16. (A) temperature, (B) salinity, from September 2000 to September 2001 in Saronikos gulf.

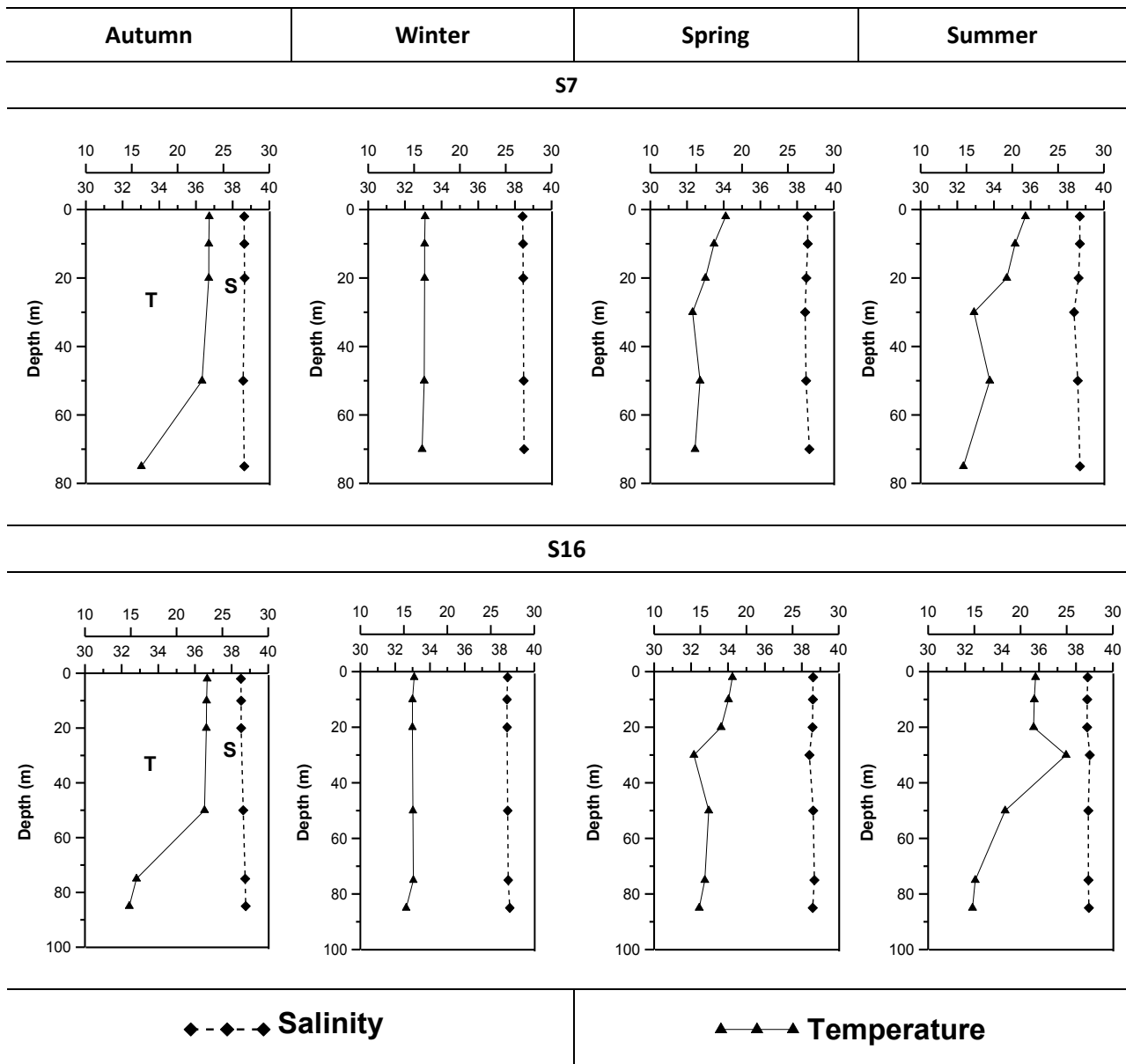


Figure 5.3.: Vertical profiles at stations S7 (sewage outfall) and S16 (open sea station) of salinity, temperature ($^{\circ}\text{C}$) calculated as seasonal means for autumn (September, October, November), winter (December, January, March), spring (April, May, June) summer (July, August, September), in Saronikos gulf from September 2000 to September 2001.

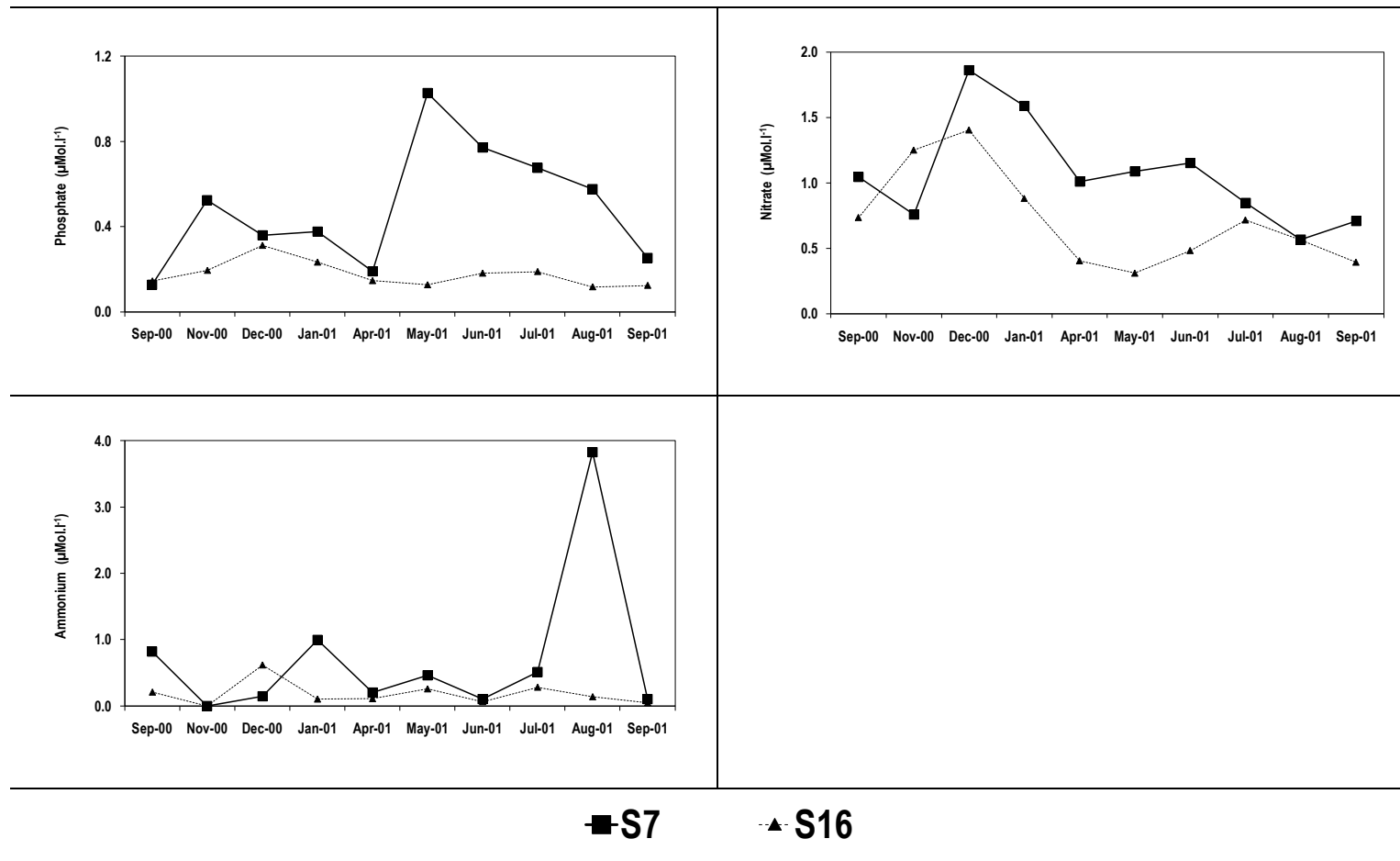


Figure 5.4.: Temporal and spatial variation of phosphate, nitrate, and ammonium ($\mu\text{Mol.l}^{-1}$) at the two stations (S7, S16) in Saronikos Gulf.

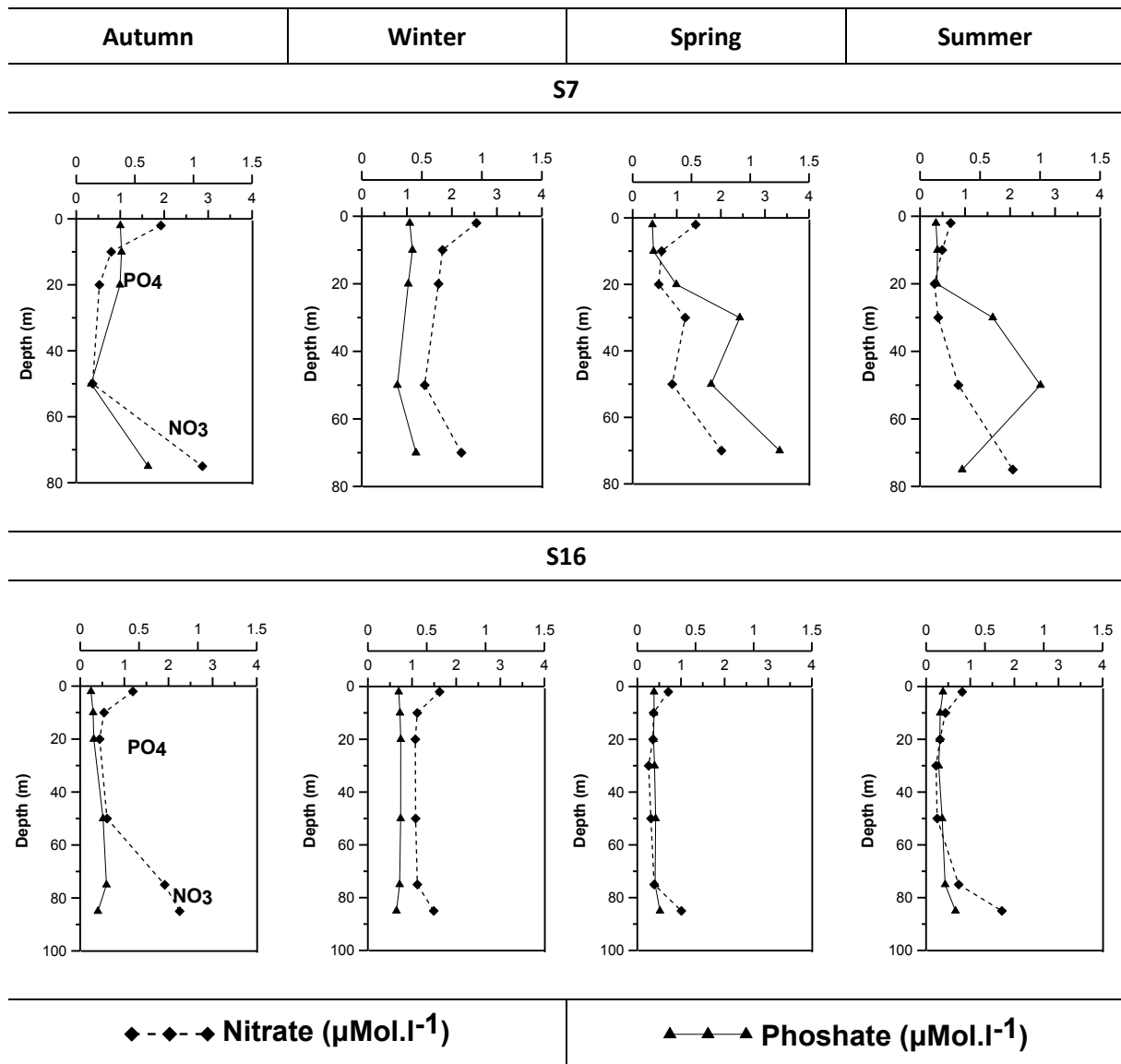


Figure 5.5.: Vertical profiles at stations S7 (sewage outfall) and S16 (open sea station) of nitrate ($\mu\text{M.l}^{-1}$) and phosphate ($\mu\text{M.l}^{-1}$) calculated as seasonal means for autumn (September, October, November), winter (December, January, March), spring (April, May, June) summer (July, August, September), from September 2000 to September 2001.

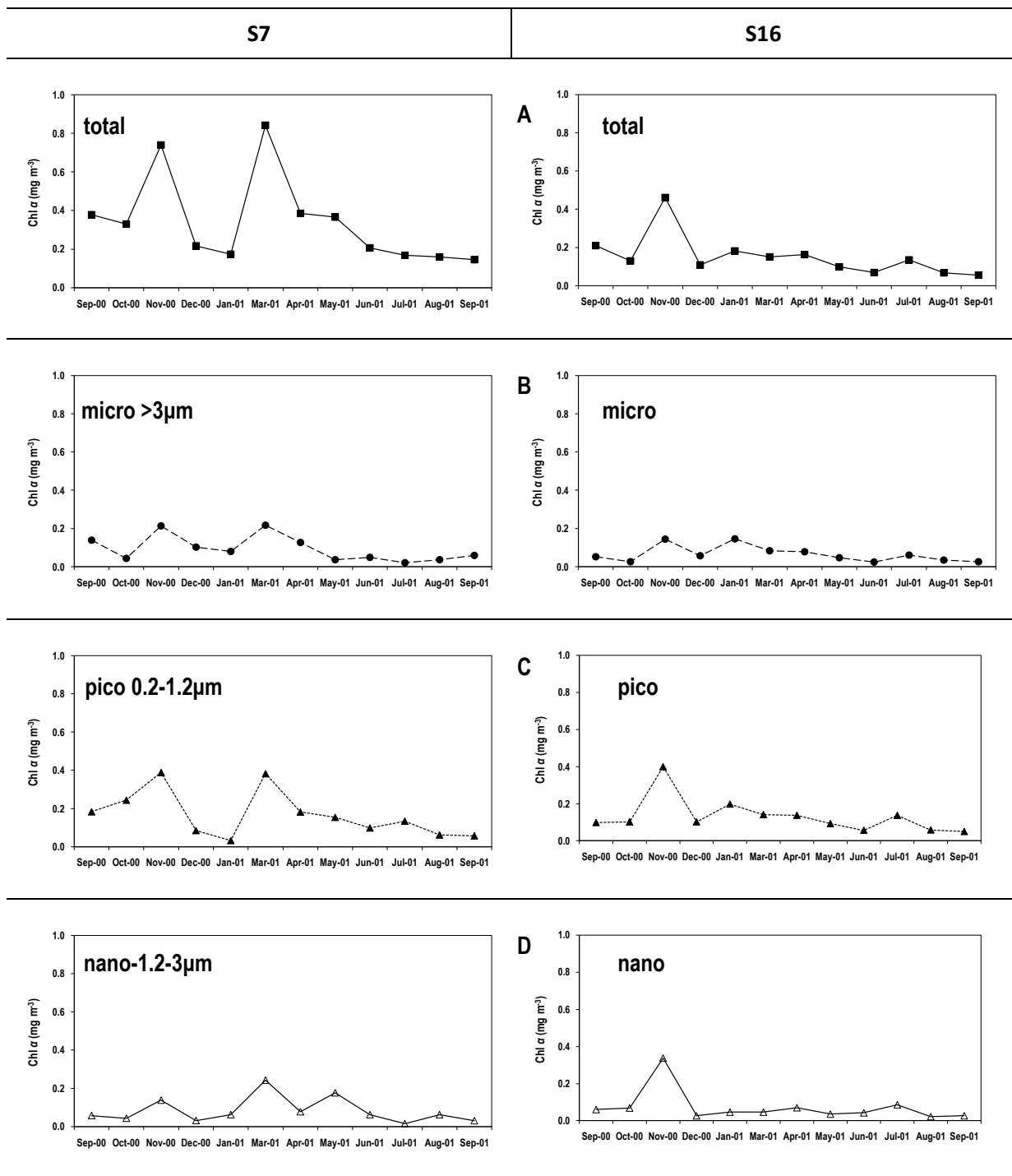


Figure 5.6.: Temporal and spatial variations in size fractionated chlorophyll a ($\text{mg}\cdot\text{m}^{-3}$). (A) total-Chl a , (B) microplankton-Chl $a > 3\mu\text{m}$, (C) picoplankton-Chl a , (D) nanoplankton-Chl a , at stations S7 and S16 in Saronikos Gulf during September 2000 to September 2001.

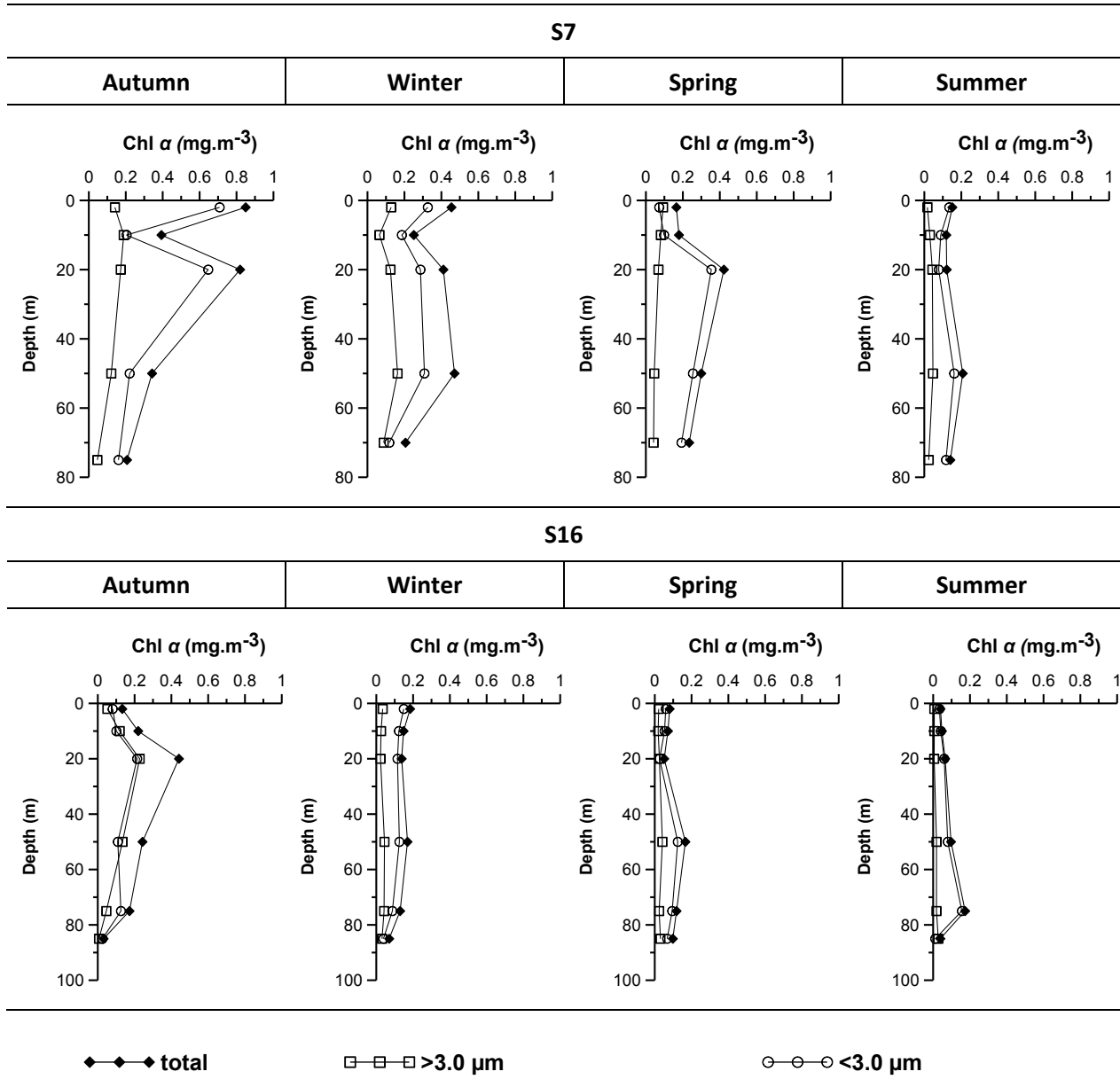


Figure 5.7.: Vertical profiles of chlorophyll concentrations (mgm^{-3}) at stations S7 (sewage outfall) and S16 (open sea station) calculated as seasonal means for autumn (September, October, November), winter (December, January, March), spring (April, May, June) summer (July, August, September), from September 2000 to September 2001 of each size class the community [total-0.2 μm , pico and nanoplankton (<3.0 μm) and micro- (>3.0 μm)] from September 2000 and September 2001.

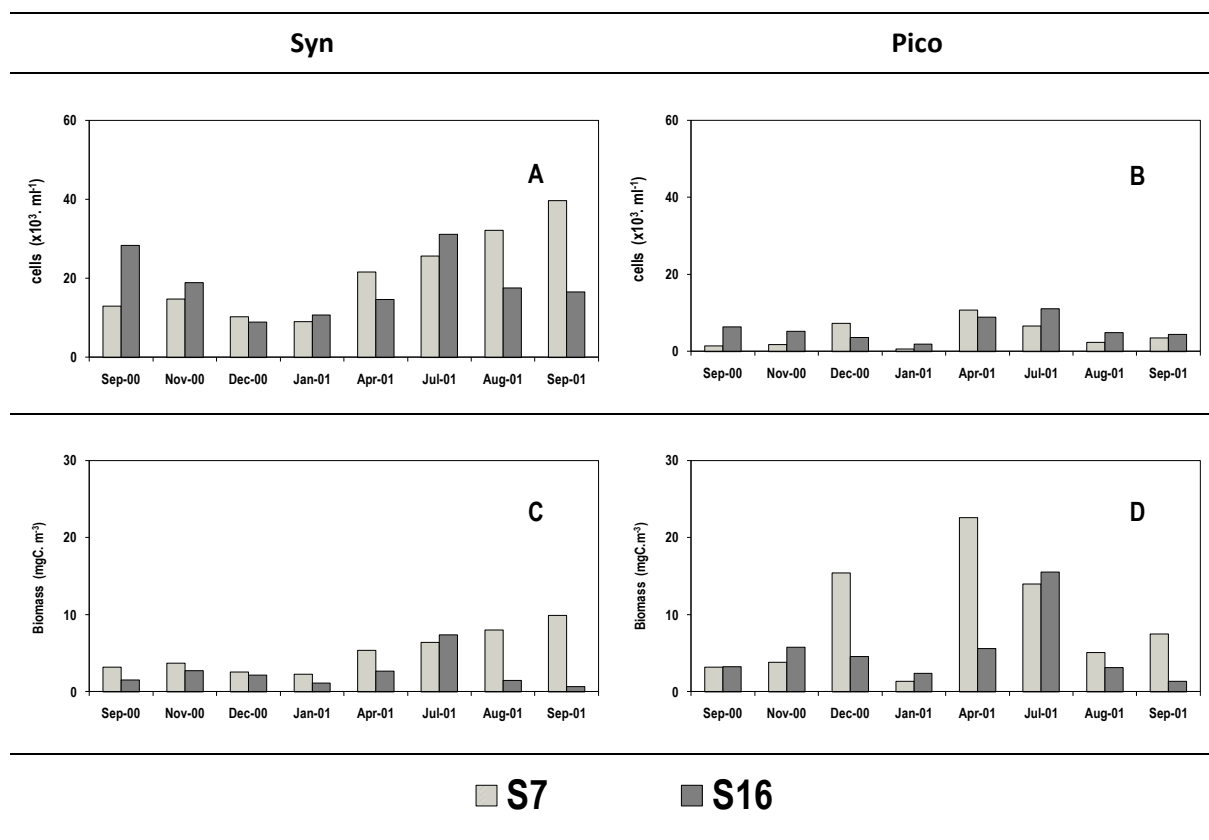


Figure 5.8.: Temporal and spatial variation in integrated (0–100 m) abundance ($\times 10^3 \text{ cells ml}^{-1}$) of *Synechococcus* (Syn) and picoeukaryotes (Pico) (A and B) and biomass (mgC.m^{-3}) (C and D) at stations S7, S16 from September 2000 to September 2001.

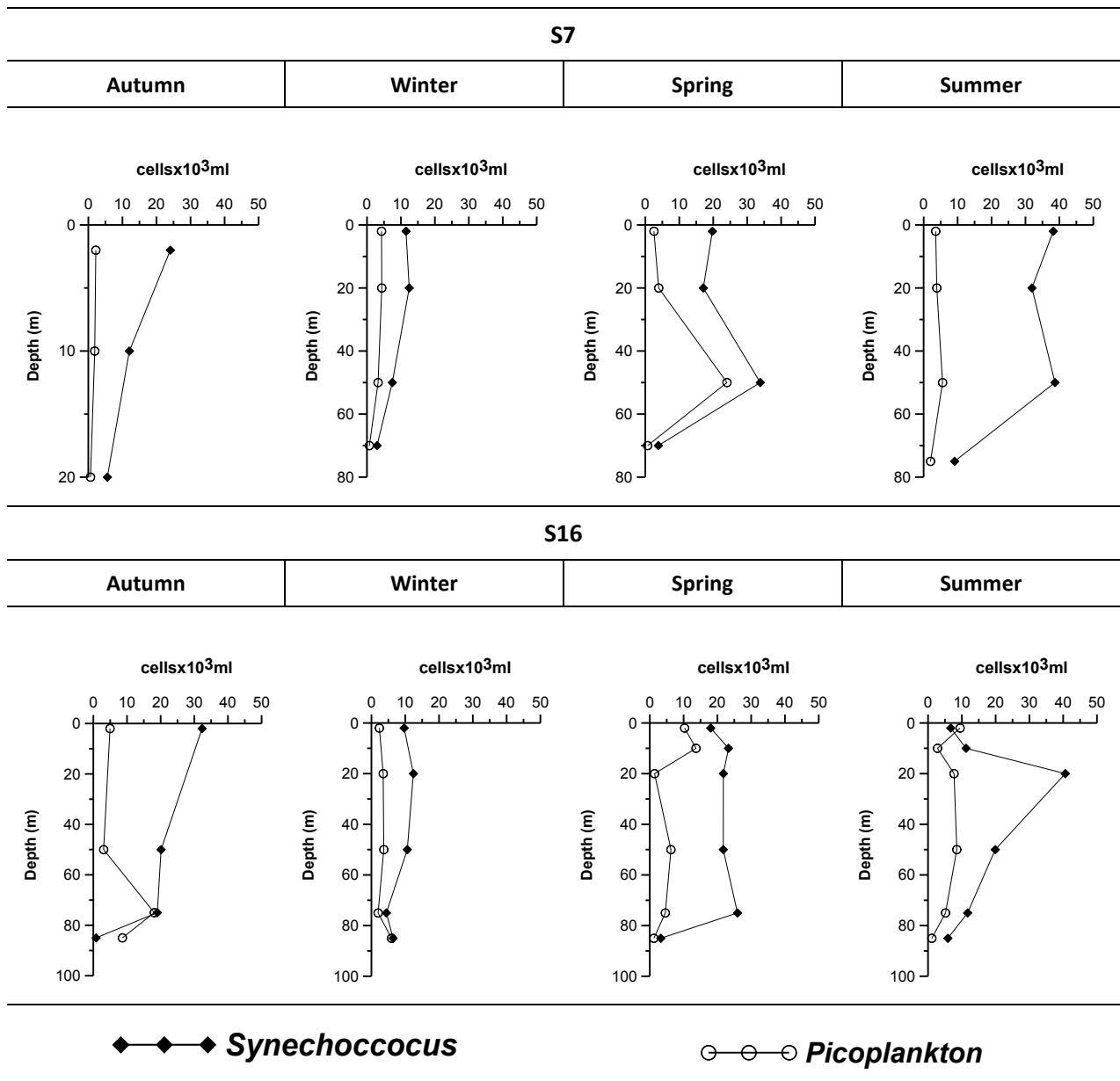


Figure 5.9.: Vertical profiles at stations S7 (sewage outfall) and S16 (open station) of *Synechococcus* and picoplankton abundances ($\times 10^3$ cells ml^{-1}), calculated as seasonal means for autumn (September, October, November), winter (December, January, March), spring (April, May, June) summer (July, August, September), from September 2000 to September 2001.

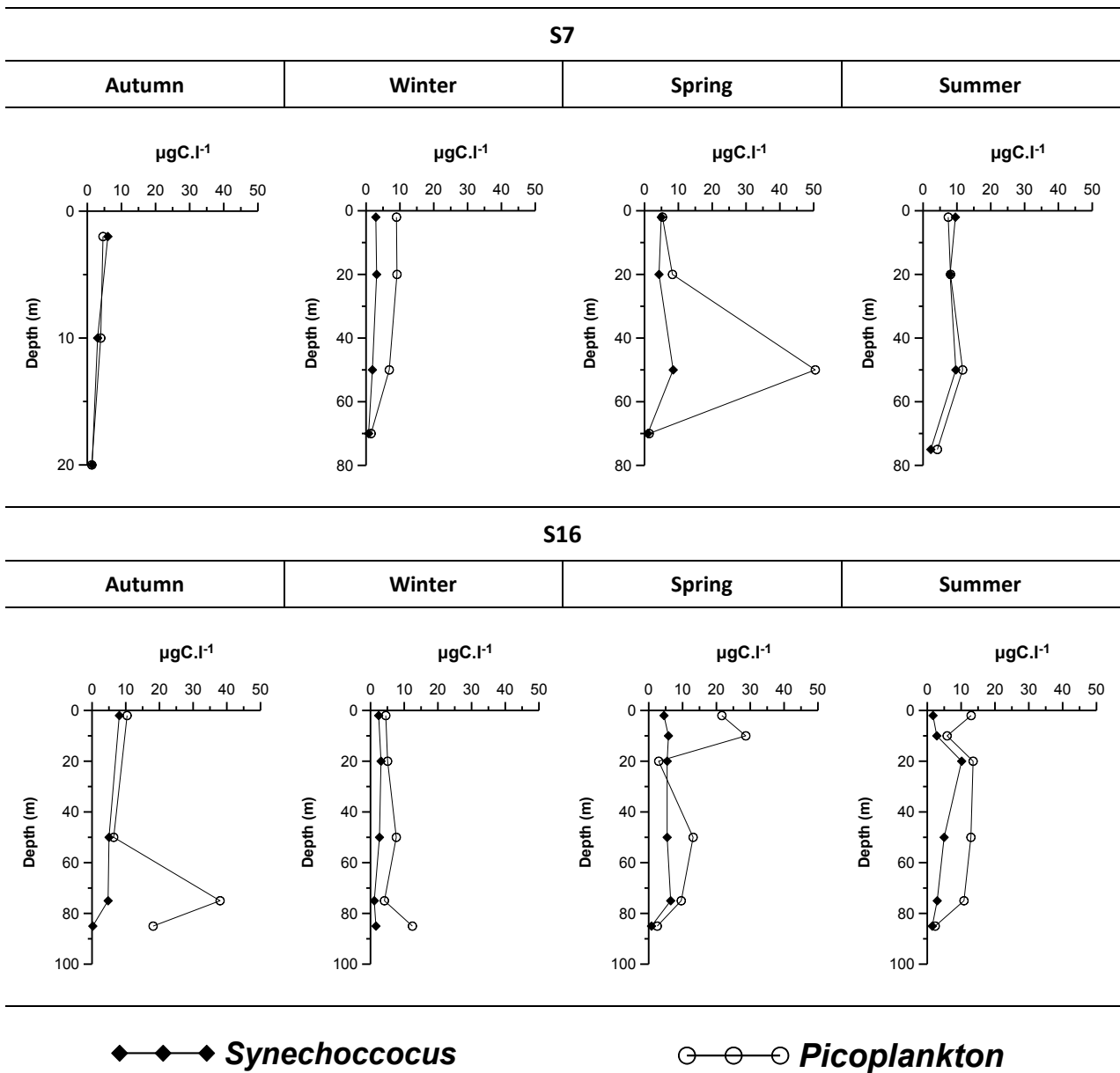


Figure 5.10.: Vertical profiles at stations S7 (sewage outfall) and S16 (open station) of *Synechococcus* and picoplankton biomass ($\mu\text{gC.l}^{-1}$), calculated as seasonal means for autumn (September, October, November), winter (December, January, March), spring (April, May, June) summer (July, August, September), from September 2000 to September 2001.

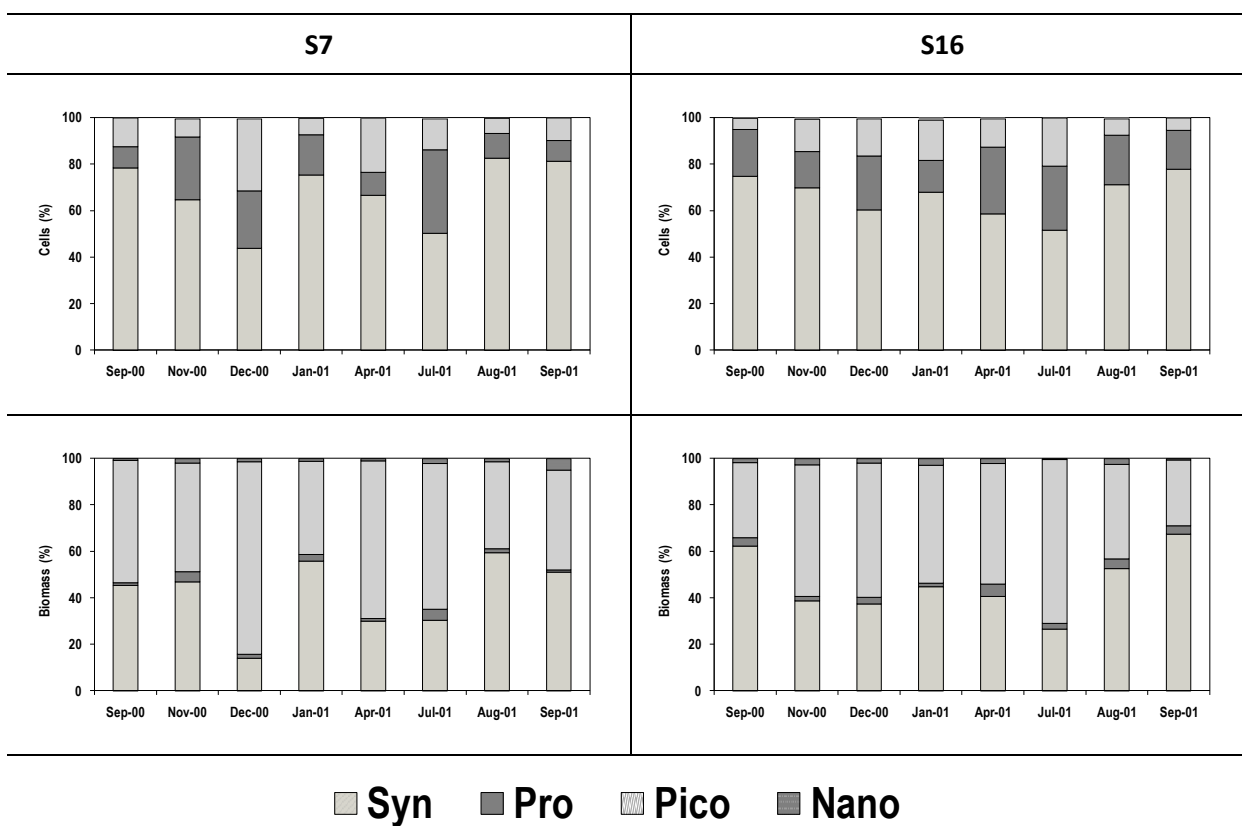


Figure 5.11.: Seasonal changes of prokaryotes (Syn: *Synechococcus* and Pro: *Prochlorococcus*), pico- and nanophytoplankton (pico and nano) contribution (%) to total autotrophic p at the two stations in Saronikos gulf (Sep2000-Sep2001).

CHAPTER 6: Conclusions

The similarities and differences in phytoplankton response to anthropogenic nutrient enrichment were studied in an open system (North Aegean Sea) and a coastal site of Saronikos gulf and in the Eastern Mediterranean. Although by physico-chemical parameters two different environments have been compared, the two regions exhibited similar features. The analysis of the data provides information on the contribution of each size class to the total autotrophic biomass and how nutrients and hydrographical variability of the water column affects the picophytoplankton assemblage composition. Phytoplankton size structure depends on a variety of factors, which ultimately are controlled by hydrodynamics of the system (Riegman *et al.*, 1993). In general, the food web structure is also dependent on the nutrient availability. At low nutrient concentration, the picophytoplankton is supposed to be the relatively most important group, whereas under extensive nutrient supply larger size fractions dominate the phytoplankton. These larger organisms can be eaten directly by the mesozooplankton, which is the main component of the diet of the planktivorous fish. Picophytoplankton is not directly consumed by the mesozooplankton but is mainly consumed by protists. Some authors have pointed out that stability-instability conditions in the water column play a major role in controlling phytoplankton size structure. On one hand, hydrodynamical forcing controls nutrient supply to the euphotic layer. High nutrient concentrations cause an increase in the biomass and primary production of larger phytoplankton (Chisholm, 1992; Agawin *et al.*, 2000). On the other hand, water column stability determines the size-differential residence time of phytoplankton cells within the euphotic layer, either favouring large-sized phytoplankton losses by passive sinking or accumulating them through the effect of vertical motion (Margalef, 1985; Malone, 1980; Rodrigues *et al.*, 2001).

In **Chapter 3** the spatial and temporal variations in chlorophyll α distribution and phytoplankton composition were studied, during a series of seasonal oceanographic cruises in the North Aegean Sea. The water-column structure of the N. Aegean represents the transition zone of different water masses. The enhanced biomass and abundance of phytoplankton appeared to be connected with a permanent hydrographic front. Nutrient levels fell within the range characteristic of oligotrophic environments, and concentrations were often below detection limits. In general higher nutrient values were recorded during spring in comparison with the summer period. Our analysis of nutrient depth profiles clearly shows that of the three macronutrients (nitrate, phosphate and silicate) utilized by phytoplankton in these waters, nitrate was the most limiting nutrient in the euphotic zone. The winter mixing brings up nitrogen from the deep layers mainly as nitrate. In the spring, as the water stratifies, and as phytoplankton grows, it depletes the surface layer of nitrate, which drops to low levels. It can be assumed that the chlorophyll and phytoplankton dynamics with an increase of phytoplankton in the area are mainly driven by the presence of Black Sea Waters. The vertical stability in summer, with inorganic nutrient depletion in the upper warmer layer which leads to low phytoplankton biomass and the summer DCM formation at the nutricline (75 or 100m depth) typical of an oligotrophic system. The results clearly demonstrate a link between phytoplankton abundance and composition and physical features of their environment such as a hydrographic heterogeneity, extension of the continental shelf and the presence of a hydrographic front. However, long-term multidisciplinary studies are required to fully understand the interaction between physical and biological processes in the N. Aegean Sea.

Our observations during two seasons (spring, summer) in N. Aegean Sea (**Chapter 4**) suggest that in our system picophytoplankton are quantitatively more important, both in terms of biomass (71%) and productivity (56%) than microphytoplankton (30%). As discriminated by flow cytometry, the picophytoplankton community was dominated by the prokaryote *Synechococcus* and *Prochlorococcus* and as well as at least eukaryotic pico- and nanoplankton. The dominance of *Synechococcus* in terms of abundance and biomass during the study supports the hypothesis that *Synechococcus* is better adapted than *Prochlorococcus* to the hydrodynamical and nutrient conditions of the eastern Mediterranean. Regardless of the importance of each phytoplankton size fraction at the

three stations, the overall pattern was a high percentage of small cells (picoplankton) in the upper layers of the photic zone while the largest cell sizes (nano- and microplankton) tended to increase their abundance with depth. Nutrient concentrations in the upper layers of the water column in the study area ranged from very low to (almost) non-detectable (ranges 0.02-0.9 μ M). An increased biomass and abundance of phytoplankton appeared to be connected with a permanent hydrographic front. Below 70m, where low irradiance would prevent significant photosynthetic activity (Moran and Estrada, 2001), high concentrations of nanoplankton and microplankton could be the consequence of sedimentation of senescent cells or of advection of water bodies entrained from shallower depths. So, it can be concluded that picophytoplankton dominated the total phytoplankton community at all studied stations. The size structure and distribution of picophytoplankton in the pelagic ecosystem of North Aegean Sea imply that most carbon is fixed by picoplankton during both seasons and throughout the study area. In both seasons, phytoplankton production of the smaller cells was sufficient to cover the carbon demand of nano- and micro-heterotrophs. This illustrates the importance of the microbial food web as a link between the carbon fixed by small autotrophs and (micro-) zooplankton (Zervoudaki *et al.*, 2007).

The Saronikos Gulf (**Chapter 5**) represents in many ways an excellent case for investigations of the effects of urban waste disposal into an oligotrophic marine environment. The background nutrient values and primary production are among the lowest found anywhere in the world oceans, providing a situation of great contrast between the ambient oligotrophic Aegean water and the eutrophic waters created by the Athens waste disposal. The phytoplankton abundance, composition and size structure in coastal and shelf waters are generally characterized by a high degree of spatial and temporal variability. Nutrient and chlorophyll α concentrations have been determined during cruises in the Saronikos gulf 2000–2001 and compared with similar regions in the Mediterranean Sea (Siokou *et al.*, 2002). Chlorophyll α seasonality is characterized by maxima appearing in fall and in early spring, typical for temperate waters, where phytoplankton increase occurs in spring due to the enrichment of water column with nutrients and increasing levels of temperature and light in this period (Delgado, 1990). In summary, an important picophytoplankton community was present throughout the year with a dominance of *Synechococcus sp.*, with increased abundance in summer.

CHAPTER 7: References

- [1] **Agawin S.R. Nona and Susana Agustí, 1997.** Abundance, frequency of dividing cells and growth rates of *Synechococcus* sp. (cyanobacteria) in the stratified Northwest Mediterranean Sea, *J. Plankton Res.* Vol.19 no II, pp.1599-1615).
- [2] **Agawin S.R. Nona, Duarte, M. Carlos, Agustí, Susana, 1998.** Growth and abundance of *Synechococcus* sp. in a Mediterranean Bay: seasonality and relationship with temperature. *Mar. Ecol. Progr. Ser.*, Vol. 170: 45-53.
- [3] **Agawin, N.S.R, Duarte C.M, Agustí, S., 2000.** Response of Mediterranean *Synechococcus* growth and loss rates to experimental nutrient inputs. *Mar. Ecol. Progr. Ser.* 206: 97-106.
- [4] **Agawin, S.R. Nona, Carlos M. Duarte, Susana Agustí, 2000.** Nutrient and temperature control of the contribution of picoplankton to phytoplankton biomass and production. *Limnol. Oceanogr.* 45 (3), 591-600.
- [5] **Agustí, S., M.P. Satta and M. P.. Mura, 2004.** Summer community metabolism in upper surface Antarctic waters. *Aquat. Microb. Ecol.* 35: 197-205.
- [6] **Angel, M.V., 1994.** Biodiversity of the pelagic ocean. *Conserv. Biol.*, 7, 760-772.
- [7] **Athanasoulis G.A, Skarsoulis, E.K., 1992.** Wind and wave atlas of the Mediterranean Sea. Hellenic Navy General Staff, Athens.
- [8] **Algarra and Vaque, 1989.** Cyanobacteria distribution across the Western Mediterranean divergence: A proof of pigment adaptation in different light conditions. *Sci. Mar.*, 53, 197-202.
- [9] **Angel, M.V. 1994.** Spatial distribution of marine organisms: patterns and processes. In Large-scale ecology and conservation biology (ed. P. J. Edwards, R. M. May & N. R. Webb), pp. 59-109. Oxford, UK: Blackwell Scientific Publications.
- [10] **Arin, Laura, Xosé Anxelu G. Morán and Marta Estrada, 2002.** Phytoplankton size distribution and growth rates in the Alboran Sea (SW Mediterranean): short term variability related to mesoscale hydrodynamics. *J. Plankton Res.*, Volume 24, Number 10, pages 1019-1033.
- [11] **Azam, F., Fenchel T., Field J.G., 1983.**The ecological role of water column microbes in the sea. *Mar. Ecol. Progr. Ser.* 10:257-263.
- [12] **Azov, Y., 1986.** Seasonal patterns of phytoplankton productivity and abundance in nearshore oligotrophic waters of the Levant Basin (Mediterranean). *J. Plankton Res.*, 8: 41-53.
- [13] **Azov, Y., 1991.** Eastern Mediterranean — a marine desert? *Mar. Pollut. Bull.*, 23, 225-232.
- [14] **Banse, K., 2002.** Should we continue to measure ¹⁴C-uptake by phytoplankton for another 50 years? *Limnology and Oceanography Bulletin* 11 (3): 45-46.
- [15] **Bec Béatrice, Julie Hussein-Ratrema, Yves Collos, Philippe Souchu and André Vaquer, 2005.** Phytoplankton seasonal dynamics in a Mediterranean coastal lagoon: emphasis on the picoeukaryote community. *J. Plankton Res.*, (9): 881-894.

-
- [16] **Berdalet, E., Arin, L., Marràse, C., Cruzado, A., and M. Estrada, 1996.** Limiting nutrients and biochemical composition of natural microbial communities in the NW Mediterranean. 2nd Workshop of the Mediterranean Targeted Project. 5EMMS, Crete.
- [17] **Bethoux, J.P., 1989.** Oxygen consumption, new production, vertical advection and environmental evolution in the Mediterranean Sea. *Deep-Sea Research*, 36, 769–781.
- [18] **Beers, J.R., Reid F.M.H. and Stewart G.L., 1982.** Seasonal abundance of the microplankton population in the North Pacific central gyre. *Deep Sea Res.*, 29: 227-245.
- [19] **Bendschneider & Robinson, 1952.** A new spectrophotometric method for the determination of nitrite in sea water. *J. Mar. Res.*, 11: 87-96.
- [20] **Berland, B.R., Bonin D.J., Maestrini S.Y., 1980.** Azote ou phosphore? Considerations sur le «paradoxe nutritionnel». *Oceanol. Acta* 3, 135-1142.
- [21] **Berman, T., Townsend D.W., El Sayed, S.Z., Trees C.C. & Azov Y., 1984.** Optical transparency, chlorophyll and primary productivity in the Eastern Mediterranean near the Israeli coast, *Oceanol. Acta* 7, 367-372.
- [22] **Berman, T., Azov Y., Scneller A., Walline P., and Townsend D.W. 1986.** Extent transparency, and phytoplankton distribution of the neritic waters chlorophyll and primary productivity in the Eastern Mediterranean near the Israeli Coast shelf. *Oceanol. Acta*, 9: 439-447.
- [23] **Béthoux, J. P., 1979.** Budgets of the Mediterranean Sea, their dependence on the local climate and on the characteristics of the Atlantic waters. *Oceanol. Acta* 2: 157-163.
- [24] **Bienfang, P.K. and Takahashi M., 1983.** Ultraplankton growth rates in a subtropical ecosystem. *Mar. Biol.*, 76, 213-218.
- [25] **Bienfang, P.K., Szyper, J.P., Okamoto, M.Y., Noda, E.K., 1984.** Temporal and spatial variability of phytoplankton in a subtropical ecosystem. *Limnol. Oceanogr.* 29, 527– 539.
- [26] **Blanchot, J., Rodier M., 1996.** Picophytoplankton abundance and biomass in the western tropical Pacific Ocean during the 1992 El Niño year: results from flow cytometry. *Deep-Sea Res.* 16, 877-895.
- [27] **Bode, A., Suzana Barquero, Manuel Varela, Jose G. Braun, Demetrio de Armas, 2001.** Pelagic bacteria and phytoplankton in oceanic waters near the Canary Islands in summer. *Mar. Ecol. Prog. Ser.*, Vol. 209.
- [28] **Borum, J., 1996.** Shallow waters and land/sea boundaries, p. 179-203. In B. B. Jørgensen and K. Richardson [eds.], Eutrophication in coastal marine ecosystems. *American Geophysical Union*.
- [29] **Bowman, M.J., Iverson R.L. , 1978.** Estuarine and plume fronts. In: Bowman, M. J., Esaias, W. E. (eds.) Oceanic fronts in coastal processes. Springer-Verlag, New York, p. 87-104.
- [30] **Bradford-Grieve, J.,M., Chang, F.H., Gall, M., Pickmere, S., Richards, F., 1997.** Size-fractionated phytoplankton standing stocks and primary production during austral winter and spring 1993 in the Subtropical Convergence region near New Zealand. *N. Z. J. Mar. Freshw. Res.* 31, 201-224.
- [31] **Boucher, J., Ibanez, F., Prieur, L., 1987.** Daily and seasonal variations in the spatial distribution of zooplankton populations in relation to the physical structure in the Ligurian Sea front. *J. Mar. Res.* 45: 133-173
- [32] **Buck K.R., F.P. Chavez, L. Campbell, 1996.** Basin-wide distributions of living carbon components and the inverted trophic pyramid of the central gyre of the North Atlantic Ocean, summer 1993. *Aquat Microb Ecol*, Vol. 10: 283-298.
-

- [33] **Bustillos-Guzman, J., H. Claustre, and J. C. Marty, 1995.** Specific phytoplankton signatures and their relationships to hydrographic conditions in the coastal northwestern Mediterranean Sea, *Mar. Ecol. Prog. Ser.*, 124, 247-258.
- [34] **Campbell, L., Nolla, H.A. and D. Vault, 1994.** The importance of *Prochlorococcus* to community structure in the Central North Pacific Ocean. *Limnol. Oceanogr.* 39(4): 954-961.
- [35] **Caron, D.A., E.E Lin Lim, Robert W. Sanders, Mark R. Denett, Ulrike-G Berninger, 2000.** Response of bacterioplankton and phytoplankton to organic carbon and inorganic nutrient additions in contrasting oceanic ecosystems. *Aquat. Microb. Ecol.*, Vol. 22: 175-184.
- [36] **Casotti, R., A. Landolfi, C. Brunet, F. D'Ortenzio, O. Mangoni, M.R. d'Alcala & M. Denis, 2003.** Composition and dynamics of the phytoplankton of the Ionian Sea (eastern Mediterranean). *J. Geophys. Res.* Vol. 108, 9.
- [37] **Chisholm, S.W., Olson, R.J., Zettler, E.R., Goericke, R., Waterbury, J. B., Welschmeyer, N.A., 1988.** A novel free-living prochlorophyte abundant in the oceanic euphotic zone. *Nature* 334, 340-343.
- [38] **Chisholm S.W, Olson, R.J., Palenik, B., Waterbury, J.B., Wesr-Johnsrud, L., Zettler, E.R., 1992.** *Prochlorococcus marinus* nov. Gen. Nov. Sp.: an oxiphototrophic marine prokaryote containing divinyl chlorophyll α and b. *Arch. Microbiol.* 157: 297-300.
- [39] **Christaki, U., Giannakourou, A., Van Wambeke, F., Gregori, G., 2001.** Nannoflagellate predation on auto- and heterotrophic picoplankton in the oligotrophic Mediterranean Sea. *J. Plankton Res.* 23, 1297-1310.
- [40] **Claustre, H., Kethervé P., Marty J.C, Prieur L., Hecq J.H, 1994.** Phytoplankton distribution associated with a geostrophic front: ecological and biogeochemical implications. *J. Mar. Res.*52: 711-742.
- [41] **Claustre, H., and J.-C. Marty, 1995.** Specific phytoplankton biomasses and their relation to primary production in the tropical North Atlantic, *Deep Sea Res. I*, 42, 1475-1493.
- [42] **Claustre, H., 1994.** The trophic status of various oceanic provinces as revealed by phytoplankton pigment signatures. *Limnol. Oceanogr.* 39: 1207-1211.
- [43] **Cloern, J. E., 1984.** Temporal dynamics and ecological significance of salinity stratification in an estuary (south San Francisco Bay, USA). *Oceanol. Acta*, v. 7, p: 137-141.
- [44] **Cloern, J. E. 2001.** Our evolving conceptual model of the coastal eutrophication problem. *Mar. Ecol. Prog. Ser.* 210: 223-253.
- [45] **Coachman L.K. and Hopkins, T.S., 1975.** Description analysis and conclusions on water masses in the Saronikos Gulf. In: *Interim Technical Report 2*, Envir. Pollut. Cont. Proj., Athens, Greece.
- [46] **Coachman, L. K., Aagaard, K. & Tripp, R.B., 1976:** *Bering Strait: The Regional Physical Oceanography*. Univ. of Washington Press, Seattle. 186pp.
- [47] **Colijn, F., K. J. Hesse, N. Ladwig, and U. Tillmann, 2002.** Effects of the large-scale uncontrolled fertilization process along the continental coastal North Sea. *Hydrobiologia* 484: 133-148.
- [48] **Conan, P., Pujo-Pay M, Raimbault P, Leveau M., 1998.** Variabilité hydrologique et biologique au sein du Courant Nord Méditerranéen à l'entrée du golfe du Lion. I. Bilan annuelles transports en azote et productivité potentielle. *Oceanol Acta* 21:751-765.
- [49] **Cullen, J.J., 1982.** The deep chlorophyll maximum: comparing vertical profiles of chlorophyll α . *Can. J. Fish. Aquat. Sci.*, 39: 791-803.

-
- [50] **Cunha, M. A., A. Alemida and F. Alcantara, 2000.** Patterns of variation of ectoenzymatic and heterotrophic bacterial activities along a salinity gradient in a Shallow tidal estuarine. *Mar. Ecol. Prog. Ser.*, 204: 1-12.
- [51] **Delgado, M., M. Latasa and M. Estrada, 1992.** Variability in the size-fractionated distribution of the phytoplankton across the Catalan front of the north-west Mediterranean. *Journal of Plankton Res.*, Vol. 14, no 5, pp. 753-771.
- [52] **Delgado, M., 1990.** Phytoplankton distribution along the Spanish coast of the Alborán Sea. *Sci. Mar.*, 54, 169-178.
- [53] **Denman, K. L. and T. M. Powell, 1984.** Effects of physical processes on planktonic ecosystems in the coastal ocean. *Oceanogr. Mar. Biol. Ann. Rev.*, 22, 125-168.
- [54] **Dickson, M. L. and P. A. Wheeler, 1995.** Nitrogen uptake rates in a coastal upwelling regime: A comparison of PN-specific, absolute and Chl a specific rates. *Limnol. Oceanogr.* 40, 533-543.
- [55] **DiTullio R. Giacomo, David A. Hutchins, Kenneth W. Bruland, 1993.** Interaction of iron and major nutrients controls phytoplankton growth and species composition in the tropical North Pacific Ocean. *Limnol. Oceanogr.*, 38(3), 495-508.
- [56] **de Young, Brad, Mike Heath, Francisco Werner, Fei Chai, Bernard Megrey and Patrick Monfray, 2004.** Challenges of Modeling Ocean Basin Ecosystems. *Science* 4. Vol. 304 no. 5676 pp. 1463-1466.
- [57] **Dolan, J.R., 2000.** Tintinnid ciliate diversity in the Mediterranean Sea: longitudinal patterns related to water column structure in late spring-early summer. *Aquat. Microb. Ecol.* 22, 69-78.
- [58] **Dowidar, N. M., 1984.** Phytoplankton biomass and primary productivity of the south-eastern Mediterranean. *Deep-Sea Res.*, 31, 983-1000.
- [59] **Ducklow, H.W., 2000.** Bacterial production and biomass in the oceans, p. 85-120. In D.L. Kirchman [ed.], *Microbial ecology of the oceans*. Wiley-Liss.
- [60] **Dugdale, R. C., & Wilkerson F. P., 1988.** Nutrient sources and primary production in the Eastern Mediterranean. *Oceanol. Acta*, 9, 179-184.
- [61] **DuRand, M.D., Olson, R.J., 1998.** Diel patterns in optical properties of the chlorophyte *Nannochloris sp.*: Relating individual-cell to bulk measurements. *Limnol. Oceanogr.* 43, 1107-1118.
- [62] **DuRand, M.D., 1995.** Phytoplankton growth and diel variations in beam attenuation through individual cell analysis. Massachusetts Institute of Technology/Woods Hole Oceanographic Institution, 267pp.
- [63] **Ediger & Yilmaz, A., 1996.** Characteristics of deep chlorophyll maximum in the Northeastern Mediterranean with respect to environmental conditions. *J. Mar. Syst.*, 9, 291-303.
- [64] **Edler, L. [Ed.], 1979.** Phytoplankton and Chlorophyll: Recommendations on Methods for Marine Biological Studies in the Baltic Sea. *Baltic Marine Biologists Publication No. 5*, 38pp.
- [65] **EPA Method 445:** "Methods for the determination of chemical substances in Marine and Estuarine Environmental Samples". (EPA website at: www.epa.gov).
- [66] **Epifanio, C. E., 1987.** The role of tidal fronts. In maintaining patches of brachyuran zoeae in estuarine waters. *J. Crust. Biol.* 7: 513-517
- [67] **Eppley, R.W., & Weiler C.S., 1979.** The dominance of nanoplankton as an indicator of marine pollution: a critique. *Oceanol. Acta* 2: 241 - 245.
- [68] **Eppley, R.W. and B. J. Peterson, 1979.** Particulate organic matter flux and planktonic new production in the deep ocean. *Nature*, 282: 677-680.
-

- [69] **Eppley, R.W., Swift E., Redalje D.G., Landry M. R., Haas L.W., 1988.** Subsurface chlorophyll maximum in August-September 1985 in the CLIMAX area of the North Pacific. *Mar. Ecol. Prog. Ser.* 42: 289-301.
- [70] **Eppley, R.W., 1972.** Temperature and phytoplankton growth in the sea. *Fish. Bull.* 70: 1063-1085.
- [71] **Estrada, M., Margalef R., 1988.** Supply of nutrients to the Mediterranean photic zone across a persistent front. *Oceanol. Acta* Special Issue 9: 133-142.
- [72] **Estrada, M., Salat J., 1989.** Phytoplankton assemblages of deep and surface water layers in a Mediterranean frontal zone. *Sci. Mar.* 53: 203-214.
- [73] **Estrada, M., 1991.** Phytoplankton assemblages across a NW Mediterranean front: changes from winter mixing to spring stratification. In: Ros, J D., Prat, N. (eds.) Homage to Ramon Margalef; or, Why there is such pleasure in studying nature. *Oecologia Aquatica* 10: 157-185.
- [74] **Estrada, M., Marrasé, C., Latasa M., Berdalet E., and Delgado M., and Riera, T., 1993:** Variability of deep chlorophyll maximum characteristics in the Northwestern Mediterranean, *Mar. Ecol.-Prog.Ser.*, 92, 289-300.
- [75] **Estrada, M., 1985a.** Deep phytoplankton and chlorophyll maxima in the Western Mediterranean. In: Moraitou-Apostolopoulou, M, Kiortsis, V. (eds.) *Mediterranean marine ecosystems*. Plenum Press, New York. p. 247-277.
- [76] **Estrada, M., 1985b.** Primary production at the deep chlorophyll maximum in the Western Mediterranean. In: Gibbs, P. E. (ed.) *Proc. 19th Eur. Mar. Biol. Symp.* Cambridge University Press, Cambridge, p. 109-121.
- [77] **Everitt, D. A., Wright, S. W., Volkman. J. K., Thomas, D. P, Lindstrom, E. J., 1990.** Phytoplankton community compositions in the western equatorial Pacific determined from chlorophyll and carotenoid pigment distributions. *Deep Sea Res.* 37: 975-997.
- [78] **Fahnenstiel, G.L., Chandler, J.F., Carrick, H.J., Scavia, D., 1989.** Photosynthetic characteristics of phytoplankton communities in lakes Huron and Michigan: P-I parameters and end-products. *J. Great Lakes Res.* 15, 394-407.
- [79] **Falkowski, P.G., Z. Dubinsky and K. Wyman, 1985.** Growth irradiance relationships in phytoplankton. *Limnol. Oceanogr.* 30: 311-321.
- [80] **Fedorov, K.N. and Ginsburg, A. I., 1986.** "Mushroom-like" currents (vortex dipoles) in the ocean and in laboratory tank. *Annales Geophysicae*, B5: 507-516.
- [81] **Fernández, M., Bianchi, M., Van Wambeke, F., 1994.** Bacterial biomass, heterotrophic production and utilization of dissolved organic matter photosynthetically produced in the Almeria-Oran front. *J. Mar. Syst.* 5, 313-325.
- [82] **Ferrier-Pages, C, Rassoulzadegan F., 1994.** Seasonal impact of the protozooplankton on pico- and nanoplankton growth rates in the northwest Mediterranean Sea. *Mar. Ecol. Prog. Ser.* 108: 283-294.
- [83] **Fiala, M., M. Semeneh, L. Oriol, 1998.** Size-fractionated phytoplankton biomass and species composition in the Indian sector of the Southern Ocean during austral summer. *J. Mar. Syst.* 17, 179-194.
- [84] **Field, C.B., M.J. Behrenfeld, J.T. Randerson and P.G. Falkowski, 1998.** Primary production of the biosphere: Integrating terrestrial and oceanic components. *Science.* 281: 237-240.
- [85] **Fiocca, F., Lugliè, A., Sechi N., 1996.** The phytoplankton of S' Ena Arrubia Lagoon (centre-western Sardinia) between 1990 and 1995. *Giornale Botanico Italiano* 130, 1016-1031.

-
- [86] **Flint, V. Mikhail, Irina N. Sukhanova, Alexander I. Kopylow, Sergei G. Polyarkov, Terry E. Whitledge, 2002.** Plankton distribution associated with frontal zones in the vicinity of the Pribilof Islands. *Deep-Sea Res. II* 49, 6069-6093.
- [87] **Floodgate, G. D., G. E. Fogg, D.A. Jones K. Lochte and C. M. Turley, 1981.** Microbiological and zooplankton activity at affront in Liverpool Bay. *Nature*, 290, 133-136.
- [88] **Fonda Umani, S., Franco, P., Ghirardelli, E. and Malej, A.1992.** Outline of oceanography and the plankton of the Adriatic Sea. *In Marine Eutrophication and Population Dynamics*, pp. 347–365. Ed. by G. Colombo, I. Ferrari, V. U. Ceccherelli, and R. Rossi. Olsen & Olsen, Fredensborg, Denmark.
- [89] **Franks, P.J.S., 1992a.** Phytoplankton blooms at fronts: patterns, scales and physical forcing mechanisms. *Rev Aquat Sci* 6:121-137.
- [90] **Franks, P.J.S., 1992b.** Sink or swim: accumulation of biomass at fronts. *Mar Ecol Prog Ser* 82: 1-12.
- [91] **Friligos, N., 1984a.** Nutrients of the Saronikos Gulf in relation to environmental characteristics (1973-1976). *Hydrobiologia* 112: 17-25.
- [92] **Froneman, P. W., McQuaid, C. D. and Laubscher, R. K., 1999.** Size-fractionated primary production studies in the vicinity of the Subtropical Front and an adjacent warm-core eddy south of Africa in austral winter. *J Plankton Res.*, 21, 2019–2035.
- [93] **Gasol, J. M., and del Giorgio P. A., 2000.** Using flow cytometry for counting natural planktonic bacteria and understanding the structure of planktonic bacterial communities, *Sci. Mar.*, 64, 197-224.
- [94] **Gasol, M. Josep, del Giorgio Paul A. and Carlos M. Duarte, 1997.** Biomass distribution in marine planktonic communities. *Limnol. Oceanogr.*, 42 (6), 1353-1363.
- [95] **Geider, R.J., 1987.** Light and temperature dependence of the carbon to chlorophyll a ratio in microalgae and cyanobacteria: implications for physiology and growth of phytoplankton. *New Phytol.* 106, 1-34.
- [96] **Georgopoulos, D., Salusti, E. and Theocharis, A., 1992.** Dense water formation processes in the North Aegean Sea (Eastern Mediterranean). Eastern Mediterranean Sea. *Proc. Of the UNESCO/IOC 2d POEM Scientific.*
- [97] **Gieskes, J.M., Lawrence, J.R., and Galleisky, G., 1978.** Interstitial water studies, Leg 38. *In* Talwani, M., Udintsev, G., et al., *Initial Reports of the Deep Sea Drilling Project*, v. 38 Supplement: Washington (U.S. Government Printing Office), p. 121-135.
- [98] **Glover, E. Hilary, Andrew E. Smith and Lyna Shapiro, 1985.** Diurnal variations in photosynthetic rates: comparisons of ultraphytoplankton with a larger phytoplankton size fraction. *J. Plankton Res.*, Vol. 7, no. 4, pp. 519-535.
- [99] **Gómes, R. Do Helga, Joaquim I. Goes and A. H. Parelekar, 1992.** Size-fractionated biomass, photosynthesis and dark CO₂ fixation in a tropical oceanic environment. *J. Plankton Res.* Vol. 14, no. 9, pp. 1307-1329.
- [100] **Gotsis-Skretas, O., Pagou, K., Christaki, O. & Akepsimaidis, K., 1993a.** The chlorophyll α distribution in the oligotrophic waters of Aegean, Levantine and Ionian seas. *In Proceedings of 4th National Symposium in Oceanography and Fisheries* (pp. 73-76). Athens, Greece: NCMR (in Greek).
- [101] **Gotsis-Skretas, Olympia, Kalliopi Pagou Maria Moraitou-Apostolopoulou, Lydia Ignatiades, 1999.** Seasonal horizontal and vertical variability in primary production and standing stocks of
-

- phytoplankton and zooplankton in the Cretan Sea and the Straits of the Cretan Arc (March 1994-January 1995). *Prog. Oceanogr.* 44, 625-649.
- [102] **Green, R.E., H.M. Sosik, and R.J. Olson, 2003.** Contributions of phytoplankton and other particles to inherent optical properties in continental shelf waters. *Limnol. Oceanogr.* 48: 2377-2391.
- [103] **Harris, G.P., 1986.** Phytoplankton Ecology: Structure, Function and Fluctuation. Chapman and Hall, London.
- [104] **Heiskanen, A.S. and Kononen, K. 1994.** Sedimentation of vernal and late summer phytoplankton communities in the coastal Baltic Sea. *Arch. Hydrobiol.*, 131, 175-198.
- [105] **Herbland and Voituriez, 1979** .Hydrological structure analysis for estimating the primary production in the tropical Atlantic Ocean. *J. Mar. Res.* 37: 87-101.
- [106] **Hess, W.R., Partensky F., Van der Staay, G.W.M., Garcia-Fernandez, J. M., Börner, T., Vault, D., 1996.** Coexistence of phycoerythrin and a chlorophyll a/b antenna in a marine prokaryote. *Proc. Nat. Acad. Sci. USA* 93, 11126-11130.
- [107] **Hewes, C.D., Sakshaug, E., Reid, F.M.H. and Holm-Hansen, O., 1990.** Microbial autotrophic and heterotrophic eucaryotes in Antarctic waters: relationships between biomass and chlorophyll, adenosine triphosphate and particulate organic carbon. *Mar. Ecol. Prog. Ser.*, 63, 27-35.
- [108] **Hillebrand Helmut, Claus-Dieter Dürselen, David Kirschtel Utsa Pollingher and Tamar Zohary, 1999.** Biovolume calculation for pelagic calculation for pelagic and benthic microalgae. *J. Phycol.* 35, 403-424.
- [109] **Hitchcock, G. L., A. J. Mariano, and T. Rossby, 1993.** Mesoscale pigment fields in the Gulf Stream: Observations in a meander crest and trough, *J. Geophys. Res.*, 98, 8425-8445, 1993.
- [110] **Holligan, P.M., R. P. Harris, R. C. Newell, D.S. Newell, D.S. Harbour, R. N. Head, E.A. S. Linley, M. I. Lucas, P. R. G. Tranter and C. M. Weekly, 1984a.** Vertical distribution and partitioning of organic carbon in mixed, frontal and stratified waters of the English Channel. *Mar. Ecol. Prog. Ser.*, 14, 111-127.
- [111] **Holligan P.M., 1981.** Biological implications of fronts on the north-west European continental shelf. *Philosophical Transactions of the Royal Society of London, Series A*, 302, 547-562.
- [112] **Holm-Hansen, O., Lorenzen C.J., Hormes R.N. and J.D.H. Strickland, 1965:** Fluorometric determination of chlorophyll. *J. Cons. Perm. Int. Explor. Mer*, 30: 3-15.
- [113] **Hood, R. R., M. R. Abbott, and A. Huyer, 1991.** Phytoplankton and photosynthetic light response in the coastal transition zone of northern California in June 1987. *J. Geophys. Res.* 96: 14,769-14,780.
- [114] **Hood, R.R., H.V. Wang, J.E. Purcell, E.D. Houde, and L.W. Harding, Jr., 1999.** Modeling particles and pelagic organisms in Chesapeake Bay: Convergent features control plankton distributions, *J. Geophys. Res.*, 104, 1223-1243, 1999.
- [115] **Hopkins, T.S. & L.K. Coachman, 1975.** Circulation patterns in the Saronikos gulf in relation to the winds. *Interim. techn. Rep. env. Poll. Cont. Proj.* Athens, vol III: 223-279.
- [116] **Horne, P.W, Platt T, 1984.** The dominant space and time scales of variability in the physical and biological fields on continental shelves. *Rapp PV Reun Cons Int Explor Mer* 183:8-19.
- [117] **Houghton, R. W. and J. Marra, 1983:** Physical Biological Structure and Exchange across the Thermohaline Shelf Slope Front in the New-York Bight. *J. Geophys. Res.-Oceans and Atmospheres*, 88 (NC7): 4467-4481.

- [118] **Jacquet, S., J.-F. Lennon and D. Vaultot, 1998.** Application of a compact automatic sea water sampler to high frequency picoplankton studies. *Aquat Microb Ecol.* 14: 309-314.
- [119] **Ignatiades, L., M. Karydis, and N. Moschopoulou, 1981.** Phytoplankton ecology of the Saronikos Gulf, Aegean Sea. Data Report-Year 1980, Part 1: Hydrography, Greek Atomic Energy Commission, Nuclear Research Center 'Democritus', Athens.
- [120] **Ignatiades, L., Vassiliou A., & Karydis, M., 1985.** A comparison of phytoplankton biomass parameters and their interrelation with nutrients in Saronikos Gulf (Greece). *Hydrobiologia*: 128: 201 - 206.
- [121] **Ignatiades, L., Pagou K. & Vassiliou, A., 1986.** Long term response of six diatom species to eutrophication. *Oceanol. Acta*: 9(4): 449-456.
- [122] **Ignatiades, L. and Moschopoulou, N., 1988.** Nitrogen as a factor affecting algal growth potential of an oligotrophic coastal environment of Eastern Mediterranean Sea. *Int. Rev. Gesamten Hydrobiol.* 73, 457-464.
- [123] **Ignatiades, L., M. Karydis & P. Vounatsou 1992:** A possible method for evaluating oligotrophy and eutrophication based on nutrient concentration scales. *Mar. Poll. Bull.*, 25 238-243.
- [124] **Ignatiades L., Psarra S., Zervakis V., Pagou K., Souvermezoglou E., Assimakopoulou, G. & Gotsis-Skretas, O., 2002.** Phytoplankton size-based dynamics in the Aegean Sea (Eastern Mediterranean). *J. Mar. Syst.* 36: 11-28.
- [125] **Ignatiades, L., 1969.** Annual cycle species diversity and succession of phytoplankton in lower Saronikos bay. Aegean Sea. *Mar. Biol.* 3 (3): 196 - 200.
- [126] **IOC, 1994.** Manual on sea-level measurement and interpretation. Volume 2 - Emerging Technologies. *Intergovernmental Oceanographic Commission Manuals and Guides No. 14.* IOC, Paris, 72pp.
- [127] **Iverson, R. L., T. E. Whitledge and J. J. Goering, 1979.** Chlorophyll and nitrate fine structure in the southeastern Bering Sea shelf-break front, *Nature*, 281, 644-666.
- [128] **Jacquet, S., J.-E Lennon and D. Vaultot, 1998.** Application of a compact automatic sea water sampler to high frequency picoplankton studies. *Aquat. Microbial. Ecol.* 14: 309-3 14.
- [129] **Johnson and Sieburth, 1979.** Chroococcoid cyanobacteria in the sea: a ubiquitous and diverse phototrophic biomass. *Limnol. Oceanogr.* 24, 928-935.
- [130] **Kana, T. and Glibert, P.M. 1987.** Effect of irradiances up to $2000 \mu\text{Em}^{-2} \text{s}^{-1}$ on marine *Synechococcus* WH 7803-I. Growth, pigmentation and cell composition. *Deep Sea Res.* 34:479-516.
- [131] **Karydis, M., Moschopoulou N. & Ignatiades L., 1983.** Carotenoid / Chlorophyll α ratio in relation to nutrient distributions. *Rapp. Comm. Int. Mer Medit.*: 28: 69 - 71.
- [132] **Kimor, B., Berman T., Schneller A., 1987.** Phytoplankton assemblages in the deep chlorophyll maximum layers off the Mediterranean Coast of Israel. *J. Plankton Res.* 9, 433-443.
- [133] **Kimor, B., 1990.** Microplankton of the Red Sea, the Gulf of Suez and the Levantine Basin of the Mediterranean. *Institut Oceanographique. Bulletin* 19.
- [134] **Kjørboe, T., H. Kaas, B. Kruse, F. Møhlenberg, P. Tiselius & G. Ærtebjerg, 1990.** The structure of the pelagic food web in relation to water column structure in the Skagerrak. *Mar. Ecol. Prog. Ser.* 59: 19-32.
- [135] **Kjørboe, T., 1993.** Turbulence, phytoplankton cell size, and the structure of pelagic food webs. *Adv. Mar. Biol.*, 29: 1-72.

- [136] **Kirchman, D. L. 2002.** Calculating microbial growth rates from data on production and standing stocks. *Mar. Ecol. Prog. Ser.* 233: 303-306.
- [137] **Kontoyiannis, H., Papadopoulos V., 1999.** Hydrography and circulation. In: Monitoring of the Saronikos Gulf ecosystem affected by the Psittalia sea outfall. NCMR, October 1999, Final Report, pp 21-64.
- [138] **Kormas A. Konstantinos, Vasiliki Garametsi, Artemis Nicolaidou, 2002.** Size-fractionated phytoplankton chlorophyll in an Eastern Mediterranean coastal system (Maliakos Gulf, Greece). *Helgol Mar Res*, 56: 125–133.
- [139] **Koroleff, F., 1983.** Simultaneous oxidation of nitrogen and phosphorus compounds by persulphate. In Grashoff, K., Enrhardt, M. and Kremling, K. (eds), *Methods of Seawater Analysis*. pp. 168-169.
- [140] **Krasakopoulou, Evangelia, Karageorgis P., Aristomenis 2005.** Spatial and temporal distribution patterns of suspended particulate matter and particulate organic carbon in the Saronikos Gulf (eastern Mediterranean, Greece). *Geo-Mar Lett.* 25: 343-359.
- [141] **Krom, M.D., Kress N., Brenner S., Gordon L.I., 1991.** Phosphorus limitation of primary productivity limitation in the eastern Mediterranean. *Limnol. Oceanogr.* 36 (3), 424-432.
- [142] **Krom, M.D., Brenner S., Kress N., Neori, A., Gordon L.I., 1992.** Nutrient dynamics and new production in a warm-core eddy from the E Mediterranean. *Deep-Sea Res.* 39, 467-480.
- [143] **Krom, M.D., Brenner, S., Kress N., Neori A., & Gordon L.I., 1993.** Nutrient distribution during an annual cycle across a warm-core eddy from the Eastern Mediterranean Sea. *Deep-Sea Res.*, 40, 805-825.
- [144] **Krom, M.D., S. Groom, and T. Zohary, 2003.** The Eastern Mediterranean, p. 91–126. In K.D.S.G.B. Black [ed.], *The biogeochemistry of marine systems*. Blackwell.
- [145] **Krom, M.D., E.M.S. Woodward, B. Herut, N. Kress, P. Carbo, R.F.C. Mantoura, G. Spyrese, T.F. Thingsted, P. Wassmann C. Wexels-Riser, V. Kitidis, C. Law, G. Zodiatis, 2005.** Nutrient cycling in the south east Levantine basin of the eastern Mediterranean: Results from a phosphorus starved system. *Deep-Sea Res. II* 52, 2879-2896.
- [146] **Kucuksezgin, Filiz, Ahmet Balci, Aynur Kontas and Oyya Altay, 1995.** Distribution of nutrients and chlorophyll α in the Aegean Sea. *Oceanol. Acta*, Vol. 18-No 3.
- [147] **Latasa, Mikel, Marta Estrada, Maximino Delgado, 1992.** Plankton-pigment relationships in the Northwestern Mediterranean during stratification. *Mar. Ecol. Prog. Ser.*, Vol. 88: 61-73.
- [148] **Laubsher, R.K., Perissinoto R., McQuaid C.D., 1993.** Phytoplankton production and biomass at frontal zones in the Atlantic sector of the Southern Ocean. *Polar Biol.* 13, 471-481.
- [149] **Laws, E. A., and T. T. Banister, 1980.** Nutrient and light-limited growth of *Thalassiosira fluviatilis* in continuous culture, with implications for phytoplankton growth in the ocean. *Limnol. Oceanogr* 25: 457-473.
- [150] **Le Borgne, R., R.T. Barber, T. Delcroix, H.Y Inoue, D.J. Mackey, M. Rodier, 2002.** Pacific warm pool and divergence: temporal and zonal variations on the equator and their effects on the biological pump. *Deep -Sea Res. II* 49: 2471-2512.
- [151] **Leaman, K. D., and F. Schott, 1991:** Hydrographic structure of the convection regime in the Gulf of Lions: Winter 1987. *J. Phys. Oceanogr.*, 21, 573–596.
- [152] **Lefèvre, N., 1986.** Aspects of biology of frontal systems. In: Blaxter JHS, Southward AJ (eds) *Advances in marine biology*, Vol 23. Academic Press, London, p 1-385.

- [153] **Legendre, L., M. Rochet and S. Demers, 1986.** Sea ice microalgae to test the hypothesis of photosynthetic adaptation to high frequency light fluctuations. *J. Exp. Mar. Biol. Ecol.* 97: 321-326.
- [154] **Legendre, L., Le Fèvre, J., 1989.** Hydrodynamical singularities as controls of recycled versus export production in oceans. In: Berger, W. H., Smetacek, V.S., Wefer, G. (Eds.), *Productivity of the Ocean: Present and Past*. John Wiley and Sons Limited, New-York.
- [155] **Legendre, L., and F. Rassoulzadegan, 1995.** Plankton and nutrient dynamics in marine waters, *Ophelia*, 41, 153-172.
- [156] **Lehman, P.W. 1992.** Environmental factors associated with long-term changes in chlorophyll concentration in the Sacramento-San Joaquin delta and Suisun bay, California. *Estuaries*, 15:335-348.
- [157] **Letelier, R.M. and M.R. Abbott. 1996.** An analysis of chlorophyll fluorescence algorithms for the Moderate Resolution Imaging Spectrometer (MODIS). *Rem. Sens. Environ.* 58: 215-223.
- [158] **Levin, S.A., 1990.** Physical and biological scales and the modeling of predator-prey interactions in large marine ecosystems. pp. 179-187. In (K. Sherman, L.M. Alexander, and B.D. Gold eds.) *Large Marine Ecosystems-Patterns, Processes, and Yields*. AAAS Selected Symposium. Publ. No. 90-305, American Association for the Advancement of Science, Washington, D.C.
- [159] **Li, W.K.W., Subba Rao D. Vv., Harrison W.G., Smith J.C., Cullen J.J., Irwin B., Platt, T., 1983.** Autotrophic picoplankton in the tropical ocean. *Science*, 219, 292-295.
- [160] **Li, W.K.W, Platt, T., 1987.** Photosynthetic picoplankton in the ocean. *Sci Prog* 71:117-132.
- [161] **Li, W. K. W., Dickie, P.M., Irwin, B.D. and Wood, A.M., 1992a.** Biomass of bacteria, cyanobacteria, prochlorophytes and photosynthetic eukaryotes in the Sargasso Sea. *Deep-Sea Res.*, 39: 501-519.
- [162] **Li, W. K. W., Zohary, T., Yacobi, Y. Z. and Wood, A. M., 1993.** Ultraphytoplankton in the eastern Mediterranean Sea: towards deriving phytoplankton biomass from flow cytometric measurements of abundance, fluorescence and light scatter. *Mar. Ecol. Prog. Ser.*, 102, 79-87.
- [163] **Li, W.K.W. and Harrison, W. G., 2001.** Chlorophyll bacteria and picophytoplankton in ecological provinces of the North Atlantic. *Deep-Sea Res. II.*, 48, 2271-2293.
- [164] **Lipschultz, F., 1995.** Nitrogen specific uptake rates of marine phytoplankton isolated from natural populations of particles by flow cytometry. *Mar. Ecol. Prog. Ser.* 123: 245-258.
- [165] **Liu, Hongbin, Koji Suzuki and Hiroaki Saito, 2004.** Community Structure and dynamics of phytoplankton in the Western Subarctic Pacific Ocean: A Synthesis. *J. Oceanogr.*, Vol. 60, pp. 119 to 137.
- [166] **Livingston, R. J., 2001.** Eutrophication Processes in Coastal Systems. *CRC Press*, Boca Raton.
- [167] **Loder J. W., Platt, T., 1984.** Physical controls on phytoplankton production at tidal fronts. In: Gibbs, P. E. (ed.) 19th EMBS: Plymouth, England. Cambridge University Press, Cambridge, p. 16-21.
- [168] **Lohrenz, S.E., 1993.** Estimation of primary production by the simulated in situ method. *ICES Mar. Sci. Symp.* 197:159-171.
- [169] **Longhurst, A. 1998.** Ecological geography of the sea. Academic Press, London.
- [170] **Mackey D.J., J. Blanchot, H.W. Higgins, J. Neveux, 2002.** Phytoplankton abundances and community structure in the equatorial Pacific. *Deep-Sea Res. II* 49, 2561-2582.
- [171] **Magazzu, G. and Decembrini, F., 1995.** Primary production, biomass and abundance of phototrophic picoplankton in the Mediterranean Sea: a review. *Aquat. Microb. Ecol.*, 9, 97-104.

- [172] **Malone, T.C., 1980.** Algal size. In Morris, I. (ed.): The Physiological Ecology of Phytoplankton. Blackwell, Oxford, pp. 433-463.
- [173] **Malone, T.C., E.M. Kemp, H.W. Ducklow, W.R. Boynton, J.H.T. Uttle and R.B. Jonas, 1986.** Lateral variation in the production and fate of phytoplankton in a partially stratified estuary. *Mar. Ecol. Prog. Ser.*, 32: 149-160.
- [174] **Malone, T.C., S. E. Pike, and D. J. Conley, 1993.** Transient variations in phytoplankton productivity at the JGOFS Bermuda time series station. *Deep-Sea Res. I* 40: 903-924.
- [175] **Marañón, Emilio, Patrick M. Holligan, Manuel Varela, Beatriz Mouriño, Anthony J. Bale, 2000.** Basin-scale variability of phytoplankton biomass, production and growth in the Atlantic Ocean. *Deep-Sea Res. I* 47, 825-857.
- [176] **Marañon, Emilio, Pedro Cermeño, Valesca Pérez, 2005.** Continuity in the photosynthetic production of dissolved organic carbon from eutrophic to oligotrophic waters. *Mar Ecol Prog Ser*, Vol. 299: 7-17.
- [177] **Marie, D., Simon, N. & Vaultot, D. 2005.** Phytoplankton cell counting by flow cytometry, p. 253-267. In Andersen, R. A. [ed.], *Algal Culturing Techniques*. Academic Press.
- [178] **Margalef, R., 1985.** Environmental control of the mesoscale distribution of primary producers and its bearing to primary production in the Western Mediterranean. In M. Moraitou-Apostolopoulou, & V. Kiortsis, *Mediterranean marine ecosystems* (p. 8). *Ecology, series 1*. NY, USA: Plenum Press.
- [179] **Marty, J.C, Chiaverini J., Pizay MD & Avril B., 2002.** Seasonal and interannual dynamics of nutrients and phytoplankton pigments in the Western Mediterranean Sea at the DYFAMED time-series station (1991-1999). *Deep-Sea Res. II*, 49, 2017-2030.
- [180] **Menden-Deuer, Susanne and Evelyn J. Lessard, 2000.** Carbon to volume relationships for dinoflagellates, diatoms, and other protest plankton. *Limnol. Oceanogr.* 45 (3), 569-579.
- [181] **McComb, W. D, 1995.** Theory of turbulence. *Rep. Prog. Phys.* 58, No 10, 1117.
- [182] **McClain, W.D, J.A. Yoder, L.P. Atkinson, J. O. Blanton, T. N. Lee, J. J. Singer and F. Mueller-Karger, 1988.** Variability of surface pigment concentration in the South Atlantic Bight. *J. Geophys. Res.*, 93, 10,675-10,697.
- [183] **McGillicuddy, D. J., Jr, A. R. Robinson, D. A. Siegel, H. W. Jannasch, R. Johnson, T. D. Dickey, J. McNeil, A. F. Michaels & A. H. Knap, 1998.** Influence of mesoscale eddies on new production in the Sargasso Sea. *Nature* 394, 263-266.
- [184] **Minas, H.J., Minas M, Coste B, Gostan J, Nival P, Bonin M.C., 1988.** Production de base et de recyclage; une revue de la problematique en Mdditerrande nord-occidentale. *Oceanol Acta* SP 9:155-162.
- [185] **Mitchell, B.G., Brody, E.A., Holm-Hansen, O., McClain, C.R. and J. Bishop, 1991.** Light limitation of phytoplankton biomass and macronutrient utilization in the Southern Ocean. *Limnol. Oceanog.*, 36, 1662-1677.
- [186] **Montagnes, D.J.S., Berges, J. A., Harrison, P.J., 1994.** Estimating carbon, nitrogen, protein and chlorophyll a from Volume in marine phytoplankton. *Limnol. Oceanog.*, 39, 1044-1060.
- [187] **Morán, G. Xosé Anxelu, Marta Estrada, 2001.** Short-term variability of photosynthetic parameters and particulate and dissolved primary production in the Alboran Sea (SW Mediterranean). *Mar Ecol Prog Ser*, Vol. 212: 2., 53-67.

- [188] **Morán, G. Xosé Anxelu, 2007.** Annual cycle of picophytoplankton photosynthesis and growth rates in a temperate coastal ecosystem: a major contribution to carbon fluxes. *Aquat Microb Ecol*, Vol. 49: 267-279.
- [189] **Moreira-Turcq, P.F., Cauwet, G. & Martin, J. M. 2001.** Contribution of flow cytometry to estimate picoplankton biomass in estuarine systems, *Hydrobiologia*, vol. 462, pp. 157-169.
- [190] **Morel, A., 1991:** Light and marine photosynthesis: a spectral model with geochemical and climatological implications. *Prog. Oceanogr.*, 26, 263-306.
- [191] **Morris, I. [editor], 1980.** The Physiological Ecology of Phytoplankton. Blackwell. A collection of reviews.
- [192] **Moutin, T., and P. Raimbault, 2002.** Primary production, carbon export and nutrients availability in western and eastern Mediterranean Sea in early summer 1996. *J. Mar. Syst.* (MATER spec. issue) 33/34: 273–288.
- [193] **Mullin, N.J.B., Riley, J.P., 1955.** The colorimetric determination of silicate with special reference to sea and natural waters. *Anal. Chim. Acta* 12, 162-176.
- [194] **Murphy, J., Riley, J.P., 1962.** A modified solution method for determination of phosphate in natural waters. *Anal. Chim. Acta* 27, 31-36.
- [195] **Murphy, L.S., and E.M. Haugen. 1985.** The distribution and abundance of phototrophic ultraplankton in the North Atlantic. *Limnol. Oceanogr.* 30: 47-58.
- [196] **Murphy, E.J, Morris, D. J., Watkins, J. L. & Priddle, J., 1988.** Scales of interaction between Antarctic krill and the environment. In Antarctic Ocean and resources variability (ed. D. Sahrhage D. (ed), *Antarctic Ocean and Resources Variability*. Springer-Verlag, New:York, pp 120-30.
- [197] **Najjar, R.G., 1999.** The water balance of the Susquehanna River Basin and its response to climate change. *Journal of Hydrology* 219, 7–19.
- [198] **Nixon, S. W, and M. E. Q. Pilson, 1983.** Nitrogen in estuarine and coastal marine ecosystems, p. 565-648. In E. J. Carpenter, and D. G. Capone [eds.], Nitrogen in the marine environment. New York: Academic Press, pp. 565-648.
- [199] **Olson, R.J., Chisholm S.W., Zettler, E.R., Armbrust, E.V., 1988.** Analysis of *Synechococcus* pigment types in the sea using single and dual beam flow cytometry. *Deep-Sea Res. I* 35,425-440.
- [200] **Olson, R.J., Zettler, E.R., Anderson, O.K., 1989.** Discrimination of eukaryotic phytoplankton cell types from light scatter and autofluorescence properties measured by flow cytometry. *Cytometry* 10, 636-643.
- [201] **Olson, R.J., Chisholm S.W., Zettler E.R., Armbrust E.V., 1990.** Pigments, size, and distribution of *Synechococcus* in the north Atlantic and Pacific Oceans. *Limnol. Oceanogr.* 35, 45- 58.
- [202] **Olson, D.B., Hitchcock G.L., Mariano, A.J., Ashjian C.J., Peng G., Nero R.W., Podesta H, G.P., 1994.** Life on the edge: marine life and fronts. *Oceanography* 7, 52-60.
- [203] **Öszo, E., Hecht A., & Únlúata U., 1989.** Circulation and hydrography of the Levantine Basin. Results of POEM coordinated experiments 1985-1986. *Progr. Oceanogr.*, 22: 125-170.
- [204] **O'Reilly, J.E. and C. Evans-Zetlin, 1998.** Ocean color chlorophyll algorithms for SeaWiFS. *J. Geophys. Res.* 103: 24,937-24,953.
- [205] **Pagou, K., & Ignatiades L., 1988.** Phytoplankton seasonality patterns in eutrophic marine coastal waters. *Biol. Ocean.* 5: 229-241.

- [206] **Pagou, K. & Gotsis-Skretas, O., 1989.** Phytoplankton. In: *Pollution research and monitoring programme in the Aegean and Ionian Seas*, A. Bousoulengas & A.V. Catsiki (eds). National Centre for Marine Research, Athens, Hellas, Technical Report (1986-87), 128-156.
- [207] **Pagou, K. & O. Gotsis-Skretas, 1990.** A comparative study of phytoplankton in S. Aegean, Levantine and Ionian Seas during March-April 1986. *Thalassografica*, 13(1): 13-18.
- [208] **Pagou, K., Siokou-Frangou I., Christianidis. S., Friligos N. & Psyllidou-Giouranovits, 1996.** Pollution effects on plankton composition and spatial distribution near the sewage outfall of Athens. *MAP Technical Reports Series*. 96: 1-100.
- [209] **Pagou, K., Assimakopoulou G., Krasakopoulou E., Pavlidou A. & A. Giannakourou, 1998.** Biological production variability in relation to nutrients input and dispersion in a Mediterranean marine coastal environment (Thermaikos Gulf, NW Aegean Sea). *Proc., 2nd Annual Scientific ELOISE Conference*, Huelva (Spain), 30 September-3 October 1998, pp. 105-106.
- [210] **Pagou, K, Assimakopoulou G., 1999.** Phytoplankton. In: Monitoring of the Saronikos Gulf ecosystem affected by the Psittalia sea outfall. NCMR, November 1999, Final Report.
- [211] **Pagou, K., A. Giannakourou & G. Assimakopoulou, 2000.** Planktonic biomass, production and community structure along a trophic gradient in a North Eastern Mediterranean shelf ecosystem. *Dynamics of matter transfer and biogeochemical cycles: their modelling in coastal systems of the Mediterranean Sea: Final Scientific Report*, Vol. 1, 11: 82-89.
- [212] **Pagou, K., Giannakourou A., Assimakopoulou G., Christaki U., Krasakopoulou E., Karayanni H. & Zeri Ch., 2002.** Small pulses of nutrients-poor environments favour the development of small cells. Case study: N. Aegean Sea. In: *Proc., 2nd Int.Conf. On Oceanography of the Eastern Mediterranean and Black Sea: Similarities and differences of two interconnected basins*. 14-18 Oct. 2002, Ankara, Turkey, p. 285.
- [213] **Pagou, K., 1986.** The effect of pollution on the phytoplankton species diversity. *Rapp. Comm. int. Mer Medit.*, 30 (2): 191.
- [214] **Panayotidis, P. & K. Pagou, 1990.** Algal blooms and nutrient conditions in the Greek seas. *Water Pollution Research Reports*, 12: 225-232.
- [215] **Pancucci-Papadopoulou, Maria-Antonietta, Ioanna Siokou, Alexander Theocharis and Dimitris Georgopoulos, 1992.** Zooplankton vertical distribution in relation to the hydrology in the NW Levantine and the SE Aegean Seas (spring 1986). *Oceanol. Acta*, Vol. 15, No 4, 365-381.
- [216] **Parsons, T.R., Maita, Y., Lalli C.M., 1984.** A manual of chemical and biological methods for seawater analysis. Pergamon Press, Oxford, 173 pp.
- [217] **Partensky, F., W.R. Hess and D. Vulot, 1999.** *Prochlorococcus*, a marine photosynthetic prokaryote of global significance. *Microbiology and Molecular Biology Reviews* 63: 106-27.
- [218] **Pennock, J.R., 1987.** Temporal and spatial variability in phytoplankton ammonium and nitrate uptake in the Delaware estuary. *Estuar. Coast. Shelf Sci.* 24, 841-857.
- [219] **Pingree, R.D., P.R. Pugh, P.M. Holligan and G.R. Forster, 1975.** Summer phytoplankton blooms and red tides along tidal fronts in the approaches to the English Channel. *Nature*, 258, 672-677.
- [220] **Pingree, R.D., Holligan P.M., Mardell G.T., 1978.** The effects of vertical stability on phytoplankton distributions in the summer on the northwest European Shelf, *Deep-sea Res.*, 25, 101 1-1028.
- [221] **Pitta, Paraskevi, Antonia Giannakourou, 2000.** Planktonic ciliates in the oligotrophic Eastern Mediterranean: vertical, spatial distribution and mixotrophy. *Mar Ecol Prog Ser*, Vol. 194: 269-282.

- [222] **Prieur and Sournia, 1994.** "Almofront-1" (April-May 1991): an interdisciplinary study of the Almeria-Oran geostrophic front, SW Mediterranean Sea. *J. Mar. Syst.*, Volume 5, Issues 3-5.
- [223] **Polat, C., Turgul S., 1996.** Chemical exchange between the Mediterranean and the Black Sea via the Turkish straits. *Bulletin de l' Institut oceanographique*, Monaco, no special 17, CIEM Science Series no. 2, pp. 167-186.
- [224] **Polat, S., E. Sarihan and T. Koray, 2000.** Seasonal changes in the phytoplankton of the northeastern Mediterranean (Bay of Iskenderun), *Turk J Bot*, 24: 1-12.
- [225] **Polat, S., 2006.** Size fractionated distribution of the phytoplankton biomass in the Iskenderun Bay, Northeastern Mediterranean Sea, *Fresh. Env. Bull.* 15:417-423.
- [226] **Poulos, S.E., Drakopoulos P.G. and Collins M.B., 1997.** Seasonal variability in sea surface oceanographic conditions in the Aegean Sea (Eastern Mediterranean): an overview. *J. Mar. Syst.*, 13: 225-244.
- [227] **PRIMER5 (Plymouth Routines in Multivariate Ecological Research)** the Plymouth Marine Laboratory.
- [228] **Psarra, S., A. Tselepides, L. Ignatiades, 2000.** Primary productivity in the oligotrophic Cretan Sea (NE Mediterranean): seasonal and interannual variability. *Prog. Oceanogr.* 46, 187-204.
- [229] **Quevedo, M., and R. Anadón, 2001.** Protist control of phytoplankton growth in the subtropical north-east Atlantic. *Mar.Ecol. Prog. Ser.* 221: 29-38.
- [230] **Raimbault, P., Coste, B., Boulhadid M., and Boudjellal B., 1993:** Origin of high phytoplankton concentration in deep chlorophyll maximum (DCM) in a frontal region of the southwestern Mediterranean Sea (Algerian Current), *Deep-Sea Res. I*, 40, 791-804.
- [231] **Reckermann, Markus, Marcel J. W. Veldhuis, 1997.** Trophic interactions between picophytoplankton and micro-and nanozooplankton in the western Arabian Sea during NE monsoon 1993. *Aquat Microb Ecol*, Vol. 12: 263-273.
- [232] **Reckermann, M., 2000:** Flow sorting in aquatic ecology. In *Aquatic flow cytometry: Achievements and Prospects*, Reckermann M. and Colijn F. (eds.), *Sci. Mar.*, 64 (2): Pages 235-246.
- [233] **Redfield, A.C., Ketchum, B.H., Richards, A., 1963:** The influence of organisms on the consumption of sea water. In Hill, M.N. (Ed.): *The Sea*, Vol., 2. Interscience, New York, pp. 26-77.
- [234] **Ribes, M. Marta, Rafel Coma and Josep-Maria Gili, 1999.** Seasonal variation of particulate organic carbon dissolved organic carbon and the contribution of microbial communities to the live particulate organic carbon in a shallow near-bottom ecosystem at the North-western Mediterranean Sea. *J. Plankton Res.*, Vol. 21, no. 6, pp. 1077-1100.
- [235] **Richardson, K., 1985.** Plankton distribution and activity in the North Sea/Skagerrak-Kattegat frontal area in April 1984. *Mar Ecol Prog Ser* 26: 233-244.
- [236] **Riegman, R, Kuipers BR, Noordeloos AMM, Witte H.J., 1993.** Size-differential control of phytoplankton and the structure of plankton communities. *Neth J Sea Res*, 31:255-265.
- [237] **Riemann Bo, Helene Munk Sørensen, Peter Koefoed Bjornsen, Steen Jesper Horsted, Lars Møller Jensen, Torkel Gissel Nilesen, Morten Søndergaard, 1990.** Carbon budgets of the microbial food web in estuarine enclosures. *Mar. Ecol. Prog. Ser.*, Vol. 65, 159-170.
- [238] **Riley, G.A., 1957:** Phytoplankton of the North Central Sargasso Sea, 1950-52. *Limnol. Oceanogr.*, 2: 252-270.

- [239] **Rodionov, S.N., 1994.** Global and Regional Climate Interactions: The Caspian Sea Experience, Kluwer Academic Pub., Dordrecht, The Netherlands.
- [240] **Rodríguez, J., Tintoré J., Allen J. T., 2001.** Mesoscale vertical motion and the size structure of phytoplankton in the ocean. *Nature* 410:360-363.
- [241] **Sakka, Asma, Louis Legendre, Michel Gosselin, Natalie Niquil and Bruno Delesalle, 2002.** Carbon budget of the planktonic food web in an atoll lagoon (Takapoto, French Polynesia). *J. Plankton Res.*, Volume 24, Number 4, pages 301-320.
- [242] **Salihoglu, I., Saydam, C., Bastrurk O, Yilmaz K., Gocmen D., Hatipoglu E. & Yilmaz A., 1990.** Transport and distribution of nutrients and chlorophyll- α by mesoscale eddies in the Northeastern Mediterranean. *Mar. Chem.* 29, 375-390.
- [243] **Schiewer, U. 1998.** 30 years' eutrophication in shallow brackish waters—lessons to be learned. *Hydrobiologia* 363: 73-79.
- [244] **Schlitzer, R., W. Roether, H. Oster, H.-G. Junghans, H. Johnsen, and A. Michelato, 1991:** Chlorofluoromethane and oxygen in the eastern Mediterranean. *Deep-Sea Res.*, 38, 1531–1551.
- [245] **Sempere, R. et al. 2002.** Mesoscale distribution and bacterial cycling of total organic carbon in North Atlantic Ocean (Pomme area). International meeting, European Geochemical Society (EGS) Nice, March 22-26.
- [246] **Shapiro, L.P. and Guillard, R.R.L., 1987.** Physiology and ecology of the marine eukaryotic ultraplankton. In Platt, T. and Li, W.K.W. (eds), *Photosynthetic Picoplankton. Can. Bull. Fish. Aquat. Sci.*, 214, 371–389.
- [247] **Sieburth, J. McN, V. Smetacek and J. Lenz, 1978.** Pelagic ecosystem structure: Heterotrophic compartments of the plankton and their relationship to plankton size fractions. *Limnol Oceanogr.* 23: 1256-1263.
- [248] **Siokou-Frangou, I., Gotsis-Skretas, O., Christou, E.D. & Pagou K., 1999.** Plankton characteristics in the NW Levantine Sea and the adjacent areas. In: Malanotte-Rizzoli P. and Eremeev V.N. (eds) *The Eastern Mediterranean as a laboratory basin for the assessment of contrasting ecosystems.* Kluwer Academic publishers, pp. 205-223.
- [249] **Siokou-Frangou, I., Assimakopoulou G, Georgakopoulou-GregoriadouE, Zenetos A, Zeri C., 2000.** Changes in Saronikos Gulf ecosystem after the functioning of the Psittalia Sewage Treatment Centre. In: *Proceedings of the Sixth Hellenic Symposium on Oceanography and Fisheries*, vol 1, pp 2-6.
- [250] **Siokou-Frangou I., M. Bianchi, U. Christaki, E.D. Christou, A. Giannakourou, O. Gotsis, L. Ignatiades, K. Pagou, P. Pitta, S. Psarra, E. Souvermezoglou, F. Van Wambeke, V. Zervakis, 2002.** Carbon flow in the planktonic food web along a gradient of oligotrophy in the Aegean Sea (Mediterranean Sea). *J. Mar. Syst.* 33-34, 335-353.
- [251] **Small, L. F., and D. W. Menzies, 1981.** Patterns of primary productivity and biomass in a coastal upwelling region. *Deep-Sea Res.* 28:123-149
- [252] **Smetacek, V.S., 1985.** Role of sinking in diatoms life-history cycles: ecological, evolutionary and geological significance. *Mar. Biol.*, 84, 239-251.
- [253] **Smetacek, V., 2002.** Microbial food webs. The ocean's veil. *Nature* 419 (6907):565.
- [254] **Smith, W. O., and D. M. Nelson, 1986.** Importance of ice edge phytoplankton blooms in the Southern Ocean. *Bioscience* 36: 251-257.
- [255] **Smith, S.L., Roman, M., Prusova, I., Wishner, K., Gowing, M., Codispoti, L.A., Barber, R., Marra, J., Flagg, C., 1998.** Seasonal response of zooplankton to monsoonal reversals in the Arabian Sea. *Deep-Sea Res. II* 45, 2369-2403.

- [256] Sokal, R.R. & Rohlf F.J., 1995. Biometry, 3rd Edition. W.H. Freeman and Company, New York, 887pp.
- [257] Sommer, U., 1994. The impact of light intensity and day length on silicate and nitrate competition among marine phytoplankton. *Limnol. Oceanogr.*, 39, 1680-1688.
- [258] Sournia, A., 1994. Pelagic biogeography and fronts. *Progress in Oceanography* 34, 109–120.
- [259] Souvermezoglou, E., Pavlidou, A., & Georgakopoulou, E. 1996. Distribution of nutrients and oxygen in the straits of the Cretan Arc and the Cretan Sea. In *CEC/MAST-Mediterranean Targeted Project, sub-project "PELAGOS", Hydrodynamics and Biogeochemical fluxes in the Straits of the Cretan Arc (Aegean Sea, Eastern Mediterranean Basin)*, (pp. 177-199). 2nd Annual Progress Report, September 1994-August 1995. Athens, Greece: NCMR.
- [260] Souvermezoglou, K. & Krasakopoulou, E., 1999. Evolution of oxygen and nutrient concentrations in the deep layers of the North Aegean Sea (eastern Mediterranean). *Mediterranean Marine Science*, Vol. 3, Number 1, June 2002.
- [261] Souvermezoglou, E., 1989. Distribution of nutrients and oxygen in the eastern Mediterranean Sea. In: Proceedings of the UNESCO/IOC second POEM workshop (pp. 85-102). Trieste, Italy, 1988. POEM Scientific Reports, no. 3, Cambridge, Massachusetts, 1989.
- [262] Steemann-Nielsen, E., 1952. The use of radioactive carbon (¹⁴C) for measuring organic production in the sea. *Journal du Conseil Permanent International pour l' Exploration de la Mer* 18, 117-140.
- [263] Stockner, J.G., 1988. Phototrophic picoplankton: an overview from marine and freshwater ecosystems. *Limnol. Oceanogr.* 33, 765-775.
- [264] Strass, V.H., Grabato, A.C.N., Pollard R.T., Fischer, H.I., Hense, I., Allen J.T, Read, J.F., Leach, H., Smetacek, V., 2002. Mesoscale frontal dynamics: shaping the environment of primary production in the Atlantic Circum-polar Current. *Deep-Sea Res.* 49: 3735-3769.
- [265] Strickland, J.D.H., Parsons T. R., 1968. A practical handbook of sea water analysis. *Bull. Fish. Res. Board Can.* 167, 310pp.
- [266] Thompson, P.A., Harrison, P.J., Parslow, J.S., 1991. Influence of irradiance on cell volume and carbon quota for ten species of marine phytoplankton. *J. Phycol.* 27: 351-360.
- [267] Traganza, E.D., D.G. Redalje and R.W. Garwood, 1987. Chemical flux, mixed layer entrainment and phytoplankton blooms at upwelling fronts in the California coastal zone. *Cont. Shelf Res.*, 7, 89-105.
- [268] Theocharis, A., Georgopoulos, D., 1993. Dense water formation over the Samothraki and Lemnos plateau in the North Aegean Sea (Eastern Mediterranean Sea). *Cont. Shelf Res.* 13 (8/9), 919-939.
- [269] Theocharis, A., 1992. Deep water formation and circulation in the Aegean Sea. In: Winds and currents of the Mediterranean basin, *Proceedings of the Workshop held at Santa Teresa, La Spezia, Italy, NATO Advanced Science Institute (ASI): Atmospheric and Oceanic Circulation in the Mediterranean Basin, 7-14 September (1983, H. Charnock)*, Harvard University Report in Meteorology and Oceanography 41, 1, 335-359.
- [270] Therianos, AD., 1974. Water regime and geographical distribution of the river yield in Greece (in Greek). *Bull Geol Soc, Greece* 11:28-58
- [271] Tomas, C. (Editor), 1997. Identifying Marine Phytoplankton. Academic Press, San Diego. 858 pages.
- [272] Trotter Joe (1993-1998). WinMDI 2.8 Free Software for Flow Cytometry. Purdue University, Cytometry Laboratories.

- [273] **Traganza, E.D., D.G. Redalje and R.W. Garwood, 1987.** Chemical flux, mixed layer entrainment and phytoplankton blooms at upwelling fronts in the California coastal zone. *Cont. Shelf Res.*, 7, 89-105.
- [274] **Troussellier, M., C. Courties & S. Zettelmaier, 1995.** Flow cytometric analysis of coastal lagoon bacterioplankton and picophyto- plankton: fixation and storage effects. *Estuar. Coast. Shelf Sci.* 40: 621–633.
- [275] **Tselepidis, A., Zervakis V., Polychronaki T., Danovaro R. & Chronis G., 2000.** Distribution of nutrients and POM in relation to the prevailing hydrographic features of the Cretan Sea (NE Mediterranean). *Prog. Oceanogr.*, vol. 46, (2-4), 113-142.
- [276] **Tyler, M.A., D.W. Coats and D.M. Anderson, 1982.** Encystment in a dynamic environment: deposition of dinoflagellate cysts by a frontal convergence. *Mar. Ecol. Prog. Ser.*, 7: 163-178.
- [277] **Underwood and Kromkamp, 1999** Primary production by phytoplankton and microphytobenthos in estuaries. *Adv. Ecol. Res.*, Vol 29 (journal), p93-153.
- [278] **Utermöhl, H., 1958.** Zur Vervollkommung der quantitativen *Phytoplankton-Methodik*. *Mitt. Int. Ver. Theor. Angew. Limnol.*, 9:1-38.
- [279] **Vadstein, A. Jensen, Y. Olsen, and H. Reinertsen, 1988.** Growth and phosphorus status of limnetic phytoplankton and bacteria. *Limnol. Oceanogr.* 33: 489-503.
- [280] **Van Wambeke, F., Christaki, U., Giannakourou, A., Moutin, T., Souvermezoglou, K., 2002.** Longitudinal and vertical trends of bacterial limitation by phosphorus and carbon in the Mediterranean Sea. *Microb. Ecol.* 43, 119-133.
- [281] **Varela, M. & Costas, E. 1987.** Distribución del tamaño de las especies en un área de afloramiento. *Investigación Pesquera* 51, 97-105.
- [282] **Vaulot, D., Courties C., Partensky F., 1989.** A simple method to preserve oceanic phytoplankton for flow cytometric analyses. *Cytometry* 10: 629-635.
- [283] **Vaulot, D, Partensky F, Neveux J, Mantoura RFC, Llewellyn C. A., 1990.** Winter presence of prochlorophytes in surface waters of the north-western Mediterranean Sea. *Limnol Oceanogr* 35: 1156-1164.
- [284] **Vaulot, D. , N. LeBot, D. Marie, and E. Fukai, 1996.** Effect of phosphorus on the *Synechococcus* cell cycle in surface in Mediterranean waters during summer. *Appl. Environ. Microbiol.* 132. 265-274.
- [285] **Veldhuis, M.J.W., Kraay G.W., 1990.** Vertical distribution and pigment composition of a picoplanktonic prochlorophyte in the subtropical north Atlantic: a combined study of HPLC-analysis of pigments and flow cytometry. *Mar. Ecol. Prog. Ser.* 68, 121-127.
- [286] **Veldhuis, M.J.W., Kraay G.W., 2000.** Application of flow cytometry in marine phytoplankton research: current applications and future perspectives. *Sci. Mar.* 64, 121-134.
- [287] **Verity, G. Peter, Diane K. Stoecker, Michael E. Sieracki and James R. Nelson, 1996.** Microzooplankton grazing of primary production at 140°W in the equatorial Pacific *Deep Sea Res II*, Volume 43, Issues 4-6, Pages 1227-1255.
- [288] **Vidussi, Francesca, Hervé Claustre, Beniamino B. Manca, Anna Luchetta and Jean-Claude Marty, 2001.** Phytoplankton pigment distribution in relation to upper thermocline circulation in the Eastern Mediterranean Sea during winter. *J Geophys Res*, Vol. 106, No C9, pages 19939-19956.
- [289] **Vlasenko, V.L., V.A. Ivanov, I.G. Krasin and A.D. Lisichenok, 1996,** Study of intensive internal waves in the shelf zone of Morocco, *Physical Oceanography*, Volume 7, No. 4, pp. 281- 298.

- [290] Washburn, L., Kadko, D., Jones, B., Hayward, T., Kosro, P., Stanton, T., Ramp, S. and Cowles, T., 1991. Water mass subduction and the transport of phytoplankton in a coastal upwelling system. *J. Geophys Res* 96(C8):
- [291] Wassmann, P., 1993. Regulation of vertical export of particulate organic matter from the euphotic zone by planktonic heterotrophs in eutrophicated aquatic environments. *Mar. Pollut. Bull.* 26: 636-643.
- [292] Waterbury, J. B., Watson, S. W., Guillard, R. R. L. and Brand, L. E., 1979. Widespread occurrence of a unicellular, marine, planktonic cyanobacterium. *Nature*, 277, 293-294.
- [293] Welschmeyer and Lorenzen, 1984. Carbon-14 labelling in phytoplankton carbon and chlorophyll a carbon: Determination of specific growth rates. *Limnol. Oceanogr.* 29: 135-145.
- [294] Wilkinson, C.R., 1993. Coraql reefs of the world are facing widespread devastation: can we prevent this through sustainable management practices? *Proc 7th Int Symp Coral Reefs* 1: 11-21.
- [295] Wood, A.M., Horan, P.K., Muirhead K., Phinney D.A., Yentsch C.M. and Waterbury J.B., 1985. Discrimination between types of pigments in marine *Synechococcus spp.* by scanning spectroscopy, epi-fluorescence microscopy, and flow cytometry. *Limnol. Oceanogr.*, 30,1303-1315.
- [296] Yacobi, Y.Z., T. Zohary, N. Kress, A. Hecht, R.D. Robarts, M. Waiser, A.M. Wood & W.K.W. Li, 1995. Chlorophyll distribution throughout the southeastern Mediterranean in relation to the physical structure of the water mass. *J. Mar. Syst.*, Vol. 6, 66: 179-190.
- [297] Yentsch, C.S., 1974 Some aspects of the environmental physiology of marine phytoplankton: A second look. *Oceanogr. Mar. Biol. Annu. Rev.* 12: 41-75.
- [298] Yoder, J.A., McClain, C.R., Blanton, J.O., Oey, L.Y., 1987. Spatial scales in CZCS-chlorophyll imagery of the southeastern US continental shelf. *Limnol. Oceanogr.* 32, 929-941.
- [299] Yoder, J.A., C.R. McClain, G. C. Feldman and W.E. Esaias, 1993. Annual cycles of phytoplankton chlorophyll concentrations in the global ocean: A satellite view, *Global Biogeochem. Cycles*, 7, 181-194.
- [300] Zervakis, V. & Georgopoulos, D., 1998. High frequency variability in the North Aegean water column. P. 76-78. In: 3rd MTP-II-MATER Workshop on the Variability of the Mediterranean Sea, Rhodes, Greece, 15-17 October 1998.
- [301] Zervakis, V., Georgopoulos, D., Drakopoulos, P.G., 2000. The role of the North Aegean in triggering the recent Eastern Mediterranean climatic changes. *J. Geophys. Res.* 105 (C11), 26103-26116.
- [302] Zervakis, V. & Georgopoulos, D., 2002. Hydrology and circulation in the North Aegean (eastern Mediterranean) throughout 1997 and 1998. *Medit. Mar. Sci.*, Vol.3/1, 2002, 05-19.
- [303] Zervoudaki, S., Zervakis V., Krasakopoulou E., Assimakopoulou G., Pagou K., Souvermezoglou E. and E. Christou, 1999. Hydrobiological observations at the meeting area of the Mediterranean and the Black seas. In: E. Th. Balopoulos *et al.* (eds). *Proceedings of the International Conference Oceanography of the Eastern Mediterranean and Black*, 23-26 February 1999, Athens, Greece. p.:129-130.
- [304] Zervoudaki, S., E.D. Christou, T.G. Nielsen, I. Siokou-Frangou, G. Assimakopoulou, A. Giannakourou, M. Maar, K. Pagou, E. Krasakopoulou, U. Christaki and M. Moraitou-Apostolopoulou, 2007. The importance of small-sized copepods in a frontal area of the Aegean Sea. *J. Plankton Res.* 29 (4), 317-338.

- [305] **Zodiatis, G., 1994.** Advection of the Black Sea water in the North Aegean Sea. *The Global Atmosphere and Ocean System*, Vol. 2, pp. 41-60.

CHAPTER 8: Zusammenfassung

Ähnlichkeiten und Unterschiede wie Phytoplankton auf anthropogenische Nährstoffanreicherung reagiert wurden in einem offenen System (Nord Aegean) und einem Küstengebiet (Saronischer Golf) im östlichen Mittelmeer untersucht. Obwohl durch die physikalisch-chemischen Parameter zwei unterschiedliche Umgebungen verglichen worden sind, zeigten beiden Regionen ähnliche Merkmale. Die Analyse der Daten liefert Informationen über den Anteil der einzelnen Größenklassen, an der totalen autotrophen Biomasse und wie sich Nährstoffe und hydrographische Variabilität der Wassersäule auf die Zusammensetzung des Picophytoplankton wirken. Phytoplanktongröße hängt von einer Vielzahl von Faktoren ab, die letztlich von der Hydrodynamik des Systems (Riegman *et al.*, 1993) gesteuert werden. Im Allgemeinen, hängt die Struktur des Nahrungsnetzes auch von der Verfügbarkeit von Nährstoffen ab. Bei niedrigem Nährstoffgehalt ist Picophytoplankton die wichtigste Gruppe, während bei umfangreichen Nährstoffversorgung Microphytoplankton dominiert. Das kann direkt von Mesozooplankton, Hauptbestandteil der Ernährung der planktivorous Fische, gefressen werden. Picophytoplankton wird nicht direkt von der Mesozooplankton, sondern vor allem von Protisten verbraucht.

Einige Autoren haben herausgefunden, dass die Stabilitäts-/Instabilitäts-Bedingungen in der Wassersäule bei der Steuerung des Phytoplanktongröße eine wichtige Rolle spielen. Auf der einen Seite steuern hydrodynamische Wirkungen die Nährstoffversorgung der euphotischen Schicht. Hohe Nährstoffkonzentrationen rufen einen Zuwachs in Biomasse und Primärproduktion des Microplanktons (Chisholm, 1992; Agawin *et al.*, 2000) hervor. Auf der anderen Seite bestimmt die Wassersäulestabilität der Verweilzeit von Phytoplanktonzellen innerhalb der euphotischen Schicht, entweder durch Begünstigung von Verlusten von grossen Phytoplankton durch passive Versenkung oder durch deren

Akkumulation durch die Wirkung der vertikalen Bewegung (Margalef, 1978; Malone, 1980, Rodrigues *et al.*, 2001).

In **Kapitel 3** wurden die räumlichen und zeitlichen Variationen in Chlorophyll α Distribution- und Phytoplanktonzusammensetzung untersucht, während einer Reihe von saisonalen ozeanographischen Kreuzfahrten in der Nord Aegaeis. Die Wassersäule der N. Aegaeis stellt die Übergangzone von verschiedenen Wassermassen dar. Die erhöhte Biomasse und Abundanz von Phytoplankton erschien mit einer permanent hydrographischen Front zusammenzuhaengen. Nährstoffgehalte waren charakteristisch für oligotrophen Meeresgebieten und die Konzentrationen lagen häufig unter der Nachweisgrenze. In der Regel wurden im Frühjahr höhere Nährstoffwerte im Vergleich zu Sommer beobachtet. Nach unserer Analyse wurde deutlich, dass von den drei Makronährstoffen (Nitrat, Phosphat und Silikat), die vom Phytoplankton verwendet werden. Nitrat derjenige limitierende Nährstoff in der euphotischen Zone war. Die Vermischung während des Winters bringt Stickstoff aus den tiefen Schichten an die Oberfläche, als Nitrat, auf. Im Frühjahr, wenn die Wassersäule schichtet, und Phytoplankton wächst, wird Nitrat an der Oberflächenschicht verbraucht, so das es auf ein niedriges Niveau sinkt. Es ist anzunehmen, dass hohes Chlorophyllgehalt und erhöhte Phytoplanktonzellen hauptsaechlich durch SchwarzMeerWasser angetrieben werden. Die vertikale Stabilität im Sommer, mit anorganischer Nährstoffverarmung in der oberen wärmeren Schicht, führt zu niedriger Phytoplanktonbiomasse und Bildung des Tiefenchlorophyllmaximum (TCM) in Wasssrtiefen zwischen 75 und 100m, typisch für ein oligotrophes System. Die Ergebnisse zeigen deutlich einen Zusammenhang zwischen Abundanz und Zusammensetzung des Phytoplanktons und den physikalischen Eigenschaften ihrer Umgebung, wie die hydrographische Heterogenie, die Erweiterung des Kontinentalssockels und die Anwesenheit einer hydrographischen Front. Allerdings sind für das Verständnis der Wechselwirkung zwischen physikalischen und biologischen Prozesse in der N. Aegaeis langfristige multidisziplinäre Studien erforderlich.

Unsere Beobachtungen während zwei Jahreszeiten (Frühjahr, Sommer) in Nord Aegean (**Kapitel 4**) deuten an, dass in unserem System Picophytoplankton quantitativ noch wichtiger, in Bezug auf Biomasse (71%) und Produktivität (56%) als in Bezug auf

Microphytoplankton (30%) sind. Mit Hilfe der Durchflusszytometrie wurden die Picophytoplanktongruppen unterschieden. Die Dominanz der *Synechococcus* in Bezug auf die Abundanz und Biomasse im Verlauf der Studie unterstützt die Hypothese, dass *Synechococcus* besser als *Prochlorococcus* an die Hydrodynamischen- und Nährstoffbedingungen des östlichen Mittelmeers angepasst ist. Das Gesamtbild der Picophytoplanktondistribution war, dass die kleinen Zellen (Pikoplankton) überwiegend in den Oberflächenschichten anwesend waren wobei sie mit zunehmender Tiefe durch Nano- und Mikroplankton ersetzt wurden. Nährstoffkonzentrationen in den oberen Schichten der Wassersäule im Untersuchungsgebiet reichten sehr niedrigen bis (fast) nicht nachweisbar Werten (0.02-0.9 μ M). Eine erhöhte Biomasse und hohe Phytoplankton Abundanz schien mit einer permanenten hydrographischen Front verbunden zu sein. Unterhalb 70m Tiefe, wo die niedrige Einstrahlung die photosynthetische Aktivität verhindert (Moran und Estrada, 2001), könnten hohe Nanoplankton- und Mikroplanktonkonzentrationen als Folge der Sedimentation von alternden Zellen oder Gewässernadvektion aus geringeren Tiefen sein. So kommt man zur Schlussfolgerung, dass Picophytoplanktonpopulationen in allen untersuchten Stationen dominieren. Die Größe und die Distribution des Picophytoplankton im pelagischen Ökosystem der Nord Aegaeis deuten an, dass Kohlenstoff meistens durch Pikoplankton während beider Jahreszeiten und im ganzen Untersuchungsgebiet fixiert wird. Während der beiden Jahreszeiten reicht die Produktion der kleineren Zellen aus, um den Kohlenstoffbedarf den Nano- und Mikroheterotrophs zu decken. Dies illustriert die Bedeutung der mikrobiellen Nahrungsnetzes als Bindeglied zwischen den Kohlenstoff fixiert durch kleine autotrophs und (Mikro-) Zooplankton (Zervoudaki *et al.*, 2007).

Der Saronische Golf (**Kapitel 5**) stellt in vielerlei Hinsicht ein ausgezeichnetes Beispiel für die Untersuchungen der Auswirkungen einer Kläranlage in einer oligotrophischen Umwelt. Die Hintergrund Nährstoff- und Primärproduktionswerte gehören zu den niedrigsten der Welt und bieten einen Kontrast zwischen dem oligotrophen Aegaeiswasser und eutrophen Gewässern durch die Athenerkläranlage. Die Abundanz, die Zusammensetzung und die Größe des Phytoplanktons in Küsten- und Schelfgewässern sind in der Regel durch eine räumliche und zeitliche Variabilität gekennzeichnet. Nährstoff- und Chlorophyll α -Konzentrationen wurden, während der Kreuzfahrten in den Saronischen Golf 2000-2001 ermittelt und mit ähnlichen Gebieten im Mittelmeer verglichen (Siokou *et al.*, 2002).

Chlorophyll α Variabilität ist durch Maxima im Herbst und im fruehen Frühjahr gekennzeichnet. Dies ist typisch für gemäßigte Gewässern, wo Phytoplanktonwachstum im Frühjahr durch die Anreicherung des Wassers mit Nährstoffen und steigende Temperatur und Licht in dieser Zeit (Delgado, 1990) erfolgt. Zusammenfassend kann man folgern, dass eine wichtige picophytoplankton Gesellschaft über das ganze Jahr hinweg anwesend ist mit einer erhoehten Abundanz von *Synechococcus sp.*, insbesondere während des Sommers.

CURRICULUM VITAE

EDUCATION AND TRAINING

1992-1993, MSc in Marine Biology, Institute of Ecology and Zoology, Section of Biology, FU Berlin, Germany.

1992, Diplom in Biology, Institute of Ecology and Zoology, Section of Biology, FU Berlin, Germany.

SCIENTIFIC IDENTITY

2001-today: Research scientist, *Biological Oceanography, Institute of Oceanography, HCMR, Athens, Greece*

1995-2001: Research scientist with contract, *Biological Oceanography, Institute of Oceanography, HCMR, Athens, Greece*

PARTICIPATION IN RESEARCH PROJECTS (SINCE 2000)

2006-today: Southern European Seas: Assessing and Modelling Ecosystem changes (SESAME)/EC,

Phytoplankton study in NE Aegean Sea, in Black Sea , in Turkish Straits and in Marmara Sea as well as study of production rates of key phytoplankton species in the above areas

2007-today: Study of the long term effect of the Sea Diamond oil spill in Caldera/Santorini area/ Ministry of Mercantile Marine. Effects of phytoplankton community

2006-2007: "Study of the environmental conditions in Antikira Bay"/ Greek Aluminium, Study of phytoplankton community in Antikira Bay

2005-2006: Fluxes in the Aegean of Carbon and Thorium Study. Collaboration HCMR with Graduate School of Oceanography, University of Rhode Island. Phytoplankton study and primary production rates in Cretan Sea, in W. Mediterranean and Atlantic.

2004-2005: Transfer and Fate of Harmful Algal Bloom (HAB) toxins in European Marine Waters (FATE)/EC, Study of toxic phytoplankton in Thermaikos Gulf.

2005-today: Monitoring of Messiniakos Gulf for the period 2006-2010, Seasonal variation of phytoplankton in Messiniakos Gulf.

2001-2003: «Impact of natural and trawling events on re-suspension, dispersion and fate of pollutants» (INTERPOL)/EC, Study of phytoplankton community and primary production rates in Thermaikos Bay.

1998-2001: «Key coastal processes in the mesotrophic Skagerrak and the oligotrophic Northern Aegean: a comparative study» (KEYCOP)/(EU-MAST-III), Phytoplankton pigments, populations and primary production in North Eastern Aegean Sea as well as study of study of pelagic food web and estimation of the carbon flux in NE Aegean Sea.

2000-today: Monitoring of Thermaikos Gulf/Seasonal and inter annual variation of phytoplankton in Thermaikos Gulf.

SELECTED RESEARCH PUBLICATIONS (MAGAZINES, NEWSPAPERS, BOOKS, SPECIAL EDITIONS ETC)

Zervoudaki S., Christou E.D., **Assimakopoulou G.**, Gucu A.C., Örek H. Terbiyik T., Ycel N., Giannakourou A., Moutsopoulos T., Pagou K., Pitta P., Psarra S., Ozsoy E., Papathanassiou E., 2010. Composition, production and grazing of copepods in the Turkish Straits System and the adjacent northern Aegean Sea. *Journal of Plankton Research*, p. 1-36.

Pavlidou A., H. Kontoyiannis, Ch. Anagnostou, I. Siokou-Frangou, K. Pagou, E. Krasakopoulou, **G. Assimakopoulou**, S. Zervoudaki, Ch. Zeri, J.Chatzianestis and R. Psylidou, 2010. Biogeochemical Characteristics in the Elefsis Bay (Aegean Sea, Eastern Mediterranean) in relation to anoxia and climate changes. In: E.V. Yakushev (ed.), *Chemical Structure of Pelagic Redox Interfaces: Observation and Modeling*, Hdb Env Chem, DOI 10.1007/698_2010_55, Springer Verlag Berlin Heidelberg 2010

Lepore K., S.B.Moran, A.B.Burd, G.A.Jackson, J.N.Smith, R.P.Kelly, H.Kaberi, S. Stavrakakis, **G.Assimakopoulou**, 2009. Sediment trap-and-in-situ pump size-fractionated POC/²³⁴Th ratios in the Mediterranean Sea and Northwest Atlantic: Implications for POC export. *Deep-Sea Research I* 56, 599-613.

Zervoudaki, S., E. D. Christou, T. G. Nielsen, I. Siokou-Frangou, **G. Assimakopoulou**, A. Giannakourou, M. Maar, K. Pagou, E. Krasakopoulou, U. Christaki and M. Moraitou-Apostolopoulou (2007). The importance of small-sized copepods in a frontal area of the Aegean Sea. *Journal of Plankton Research* 29(4), 317-338.

Giannakourou A., Orlova T., **Assimakopoulou G.**, Pagou K., 2005. Dinoflagellate cysts in Recent Marine Sediments from Thermaikos Gulf, Greece: Effects of resuspension events on vertical cyst distribution. *Continental Shelf Research* 25, 2585-2596.

Price N.B., A.P. Karageorgis, H. Kaberi, C. Zeri, E. Krasakopoulou, F. Voutsinou-Taliadouri, F. Lindsay, Assimakopoulou G., K. Pagou, 2005. Temporal and spatial variations in the geochemistry of major and minor particulate and selected dissolved elements of Thermaikos Gulf, Northwestern Aegean Sea. *Continental Shelf Research* 25, 228-2455.

Price N.B., Karageorgis A.P., Kaberi H., Zeri C., Krasakopoulou E., Voutsinou-Taliadouri F., Lindsay F., **Assimakopoulou G.** & Pagou K. (2005). Temporal and spatial variations in the geochemistry of major and minor particulate and selected dissolved elements of the Thermaikos Gulf, northwestern Aegean Sea. *Continental Shelf Research*, 25(19-20): 2428-2455.

Assimakopoulou G., Reckermann M., Pagou K., Krasakopoulou E., Colijn F., 2004. Dynamics of photosynthetic picoplankton in North Aegean Sea (Eastern Mediterranean) using flow cytometric analysis. *Poster presented during the MARBEF (= Marine Biodiversity and Ecosystem Functioning – EU Network of Excellence) Advanced Course in Flow Cytometry: “The role of Flow Cytometry in Marine Biodiversity and Ecosystem Functioning” Stazione Zoologica Anton Dohrn, Napoli, Italy, 3-6 November 2004* (available at www.marbef.org).

Kontoyiannis H, Balopoulos E, Gotsis-Skretas O, Pavlidou A, **Assimakopoulou G**, Papageorgiou E., 2004. The hydrology and biochemistry of the Cretan Straits (Antikithira and Kassos Straits) revisited in the period June 1997-May 1998. *Journal of Marine Systems* 53 (1-4): 37-57.

Ignatiades, L., Psarra, S., Zervakis, V., Pagou, K., Souvermezoglou, E., **Assimakopoulou, G.**, Gotsis-Skretas, O. Phytoplankton size-based dynamics in the Aegean Sea (Eastern Mediterranean). *J. Mar. Sys.* 36 (2002) 11-28.

Siokou-Frangou I., S. Zervoudaki, E.D. Christou, **Assimakopoulou G.** Mesozooplankton distribution and grazing in a frontal area of the Eastern Mediterranean Sea. *GLOBEC 2nd Open Science Meeting, Qingdao, PR China, 15-18 October 2002*. Book of abstracts pp 135

Christaki U., Van Wambeke F., Pagou K., Gotsis Skretas O., **Assimakopoulou G.**, Pitta P., Giannakourou A., Siokou-Frangou I., Christou E.D., Zervoudaki S., Gregori G., Lykoussis V. Planktonic food web structure and dynamics in the Mediterranean-Longitudinal trends. 8th Symposium on Aquatic Microbial Ecology. Taormina, Italy, 25-30 October 2002.

Pagou K., Christaki U., **Assimakopoulou G.**, Zervoudaki S., Christou E.D., Siokou-Frangou I. Do “episodic” near bottom nutrient flux have a significant impact on phytoplankton, bacteria and zooplankton production and biomass? *INTERPOL Workshop, Athens Greece 21-23, November 2002*.

Pagou K., Krasakopoulou E., Pavlidou A., **Assimakopoulou G.**, Kontoyiannis H. & Anagnostou Ch. (2001). Inner Thermaikos Gulf (NW Aegean Sea, E. Mediterranean): a preliminary approach. In: Dupra V. *et al.* (eds) "Coastal and Black Sea regions: carbon, nitrogen and phosphorous fluxes" *LOICZ Reports and Studies*, No 19, i+101 pages, LOICZ, Texel, The Netherlands, pp.: 6 -11. (http://data.ecology.su.se/mnode/Europe/Med_Aegean_BlackSea/Greece/InnerThermaikos/thermaikosbud.htm)

Pagou, K., **Assimakopoulou, G.**, Krasakopoulou, E., Pavlidou, A., & Giannakourou, A. (2000). Biological production variability in relation to nutrients input and dispersion in a Mediterranean marine coastal environment (Thermaikos Gulf, NW Aegean Sea). *Final Scientific Report of the EU - MAST-III ELOISE Project METRO-MED: "Dynamics of Matter Transfer and Biogeochemical Cycles: Their Modelling in Coastal systems of the Mediterranean Sea (CT 960049), Part B: Specific topics"*, November 2000, p.: 127-131.

Pagou K., **Assimakopoulou, G.** (2000). Phytoplankton biomass and production in N. Aegean Sea, during September 1999. *Mid-Term Scientific report in the frame of the Key coastal processes in the Mesotrophic Skagerrak and oligotrophic Northern Aegean: A comparative study (KEYCOP)*.

Pagou K., **Assimakopoulou, G.** (2000). Distribution and variability of the phytoplankton biomass and primary production in Thermaikos Gulf. *Final Scientific Report of METRO - MED Project, Dynamics of Matter Transfer and Biogeochemical Cycles. A MAST - III ELOISE European Union Project.*

Zervoudaki, S., Christou, E.D, Gucu, A.C., **Assimakopoulou, G.**, Örek, H., Terbiyik, T., Moutsopoulos, T., Pagou,, K., Ozsoy, E., Papathanassiou,E. (2009). Community structure, production and grazing of copepods in the Bosphorus and Dardanelles straits and adjacent seas (NE AegeanSea, Marmara Sea). *ASLO Aquatic Sciences Meeting 2009 (Session: 064 - Signals of Change in the Mediterranean and Black Seas: Multi-Lateral Initiatives)*, 25-30 January 2009, Nice, France (oral).

Papathanassiou E., Pagou K., Giannakourou A., Krasakopoulou, E., Galinou-Mitsoudi S., **Assimakopoulou G.**, Anagnostou Ch., Krestenitis I.,Drakopoulou P., Zervoudaki S., Stroglyoudi E. & Pavlidou A. (2007). Mussel cultures and the eutrophic marine environment in Thermaikos Gulf – NW Aegean Sea, Greece. *"10th International Conference on Shellfish Restoration (ICSR) 2007"*, November 12-16, 2007, Vlissingen, TheNetherlands. Book of Abstracts, p.: 40-41.

RESEARCH INTERESTS

Ecology and structure of marine phytoplankton populations in coastal waters shelf and open seas, influence of environmental parameters, interrelationships between phytoplankton and biological-environmental parameters, biological processes in the water column, primary production rates, growth rates of phytoplankton, structure and dynamic of pelagic food web, and carbon budget through food webs.

ACKNOWLEDGEMENTS

I would like to extend my great appreciation to Prof. Dr. Franciscus Colijn, the supervisor of my thesis, for his scientific and organisational support and, particularly, for his patience and commitment to fully assisting me during the writing process.

I would also like to thank Dr. Marcus Reckermann, who welcomed me to the Research and Technology Centre (FTZ) and trained me to analyze and evaluate my samples. I truly appreciate his thoroughness, patience and fruitful discussions. Also, I would like to give many thanks to Dr. Andreas Ruser for his great help in sample analysis and assistance to my every need – and for the beautiful music during the measurements!

I would like to extend many warm thanks to all my colleagues at the Research and Technology Centre (FTZ) for their hospitality and exceptional help during my stay in Büsum. In particular, I would like to thank Ms. Cornelia Reineke (†), a kind person, who generously gave me her help and friendship.

Many thanks to Prof Dr. Ullrich Sommer, Prof Dr., Arne Körtzinger, and Prof. Dr. Kai Wirtz, who accepted to participate to the examination committee of my thesis.

I am also deeply appreciative to my colleagues Dr. Epaminondas Christou, Dr. Popi Pagou, Dr. Ionanna Siokou and Dr. Alexandra Pavildou for their cooperation within programmes, which gave me the opportunity to write this thesis. In particular, I would like to thank two physicians, Dr. Vassilis Zervakis and Dr. Dimitris Georgopoulos who helped me understand the “beauty” of the Aegean Sea through the “movements” of the water masses. Many thanks to Dr. Evangelos Papathanasiou for his moral support and encouragement to pursue my goal.

And, of course, I would like to thank my friend, Dr. Eva Krasakopoulou, who was always there to listen and for the perfect maps she helped me create. Many thanks, also, to my friend, Angeliki Konstantinopoulou, for her energy, enthusiasm and companionship.

Last but not least, I want to thank my sister, Tassia Assimakopoulou and my brother-in-law, Kostas Konstantinidis, for their support, love, and inimitable manner to motivate me sometimes and for their continuous encouragement and optimism. I thank my mother who has always supported me with her love. Finally, I dedicate this dissertation to my father (†).

ERKLÄRUNG

Hiermit erkläre ich, dass ich die vorliegende Dissertation selbständig verfasst und keine anderen als die angegebenen Hilfsmittel und Quellen verwendet habe. Ich habe bisher keinen anderen Promotionsversuch unternommen und diese Arbeit hat weder ganz noch teilweise im Rahmen eines anderen Prüfungsverfahrens teilgenommen.

....., den, 2011